

Sheffield Hallam University

The mechanisms of moisture ingress & migration in rammed earth walls.

HALL, Matthew Robert.

Available from the Sheffield Hallam University Research Archive (SHURA) at:

<http://shura.shu.ac.uk/19744/>

A Sheffield Hallam University thesis

This thesis is protected by copyright which belongs to the author.

The content must not be changed in any way or sold commercially in any format or medium without the formal permission of the author.

When referring to this work, full bibliographic details including the author, title, awarding institution and date of the thesis must be given.

Please visit <http://shura.shu.ac.uk/19744/> and <http://shura.shu.ac.uk/information.html> for further details about copyright and re-use permissions.

SHEFFIELD HALLAM UNIVERSITY
LEARNING CENTRE
CITY CAMPUS, POND STREET,
SHEFFIELD S1 1WB.

101 788 527 3



23101

Fines are charged at 50p per hour

1/12/05 *4hr*

06 JUL 2006

SPM

12 SEP 2006

SPM

10 NOV 2006

SPM

REFERENCE

ProQuest Number: 10697046

All rights reserved

INFORMATION TO ALL USERS

The quality of this reproduction is dependent upon the quality of the copy submitted.

In the unlikely event that the author did not send a complete manuscript and there are missing pages, these will be noted. Also, if material had to be removed, a note will indicate the deletion.



ProQuest 10697046

Published by ProQuest LLC (2017). Copyright of the Dissertation is held by the Author.

All rights reserved.

This work is protected against unauthorized copying under Title 17, United States Code
Microform Edition © ProQuest LLC.

ProQuest LLC.
789 East Eisenhower Parkway
P.O. Box 1346
Ann Arbor, MI 48106 – 1346

**THE MECHANISMS OF MOISTURE INGRESS &
MIGRATION IN RAMMED EARTH WALLS**

Matthew Robert Hall

A thesis submitted in partial fulfilment of the requirements of
Sheffield Hallam University
for the degree of Doctor of Philosophy



July 2004

ABSTRACT

The ingress and migration of moisture in rammed earth walls can be a particular problem for contractors and property owners. To date there have been no comprehensive research projects aimed at understanding moisture ingress in rammed earth materials. A much more detailed understanding of how soil-grading parameters affects the moisture ingress performance of rammed earth walls is required along with appropriate suggestions for optimising soil mix designs. Quarry materials have been blended to produce a variety of rammed earth soil mix recipes with accurately controlled grading characteristics. Ten different un stabilised mix recipes were established and tested, followed by three mix recipes that were tested with different levels of cement stabilisation. Rammed earth cube samples were used for laboratory experiments that determined capillary suction and pressure-driven moisture ingress properties, and full-scale test walls were used in the SHU climatic simulation chamber. The experimental data was analysed and found to be in good agreement with existing theories on non-saturated flow theory.

Moisture ingress in rammed earth is generally very low and typically equal to or less than that of vibration-compacted C30 concrete. A positive relationship exists between the rate of capillary suction and the volume fraction porosity (f) of rammed earth. The mass of absorbed water (m_w) increases linearly against the square root of elapsed time ($t^{0.5}$). The extended Darcy equation can be used to describe capillary moisture ingress in rammed earth and so the gradient of the slope $m/t^{0.5}$ is used to define the parameter S , known as sorptivity. Static pressure-driven moisture ingress occurs at a rate that is significantly higher than S , and it does not obey the extended Darcy equation. The effective hydraulic pore radius (r) of rammed earth is typically very small which indicates high levels of constriction and tortuosity within the pore structure. The surface inflow velocity (u_o) of capillary moisture ingress decreases linearly against $t^{0.01}$. The gradient of the slope $u_o/t^{0.01}$ can be used to provide a value for the parameter o , defined here as the surface receptiveness. The value o effectively quantifies the surface finish of the material. When r is increased, the sorptivity (S) and surface receptiveness (o) also increase, but the rate of decline in S becomes greater due to a more rapid water logging of the façade, i.e. the 'overcoat' effect.

The ratio between the total specific surface area (SSA_t) of the soil aggregate fraction in a mix, and the relative clay content (CC), expressed as a proportion of the total soil mass, is defined here as the SSA_t/CC ratio. A positive relationship exists between the SSA_t/CC ratio and r of a given mix recipe. Where r is less than 0.65 nm a mix recipe should have optimised moisture ingress resistance. The ratio between the mass of soil particles in a mix whose diameter is greater than 3.35mm, and those whose diameter is less than 3.35mm, is defined here as the 3.35 ratio. When the 3.35 ratio of a mix recipe is 5 or less, and the clay content (CC) is approximately 0.1, the mix recipe appears to be optimised for low sorptivity (S) and small effective hydraulic pore radius (r). The climatic simulation of pressure-driven rainfall applied to stabilised rammed earth walls gives a calculated sorptivity (S) of approximately zero, and a very low initial surface absorption that appears to be independent of soil grading.

A correctly graded soil mix recipe can make the capillary and pressure-driven moisture ingress resistance of rammed earth significantly exceed that of vibration-compacted C30 concrete without the need for chemical admixtures or surface treatments. This is the most sustainable and potentially cost effective approach to enhancing the moisture ingress resistance of rammed earth materials. Rainfall penetration in rammed earth walls may not be a problem due to the low levels of absorption from run-off water. However, capillary ingress through basal dampness or faulty rainwater goods/plumbing could be a significant cause of damp ingress. This research provides guidance on how to optimise the moisture ingress resistance in a rammed earth mix recipe, which can be specified according to the level and nature of exposure the wall is likely to encounter.

TABLE OF CONTENTS

ABSTRACT	2
TABLE OF CONTENTS.....	3
ACKNOWLEDGEMENTS.....	6
LIST OF FIGURES	7
LIST OF TABLES	11
LIST OF NOTATIONS	12
1.0 INTRODUCTION.....	16
1.1 OVERVIEW	16
1.2 THE PROBLEMS	18
1.3 AIMS & OBJECTIVES	19
2.0 LITERATURE REVIEW	21
2.1 INTRODUCTION	21
2.2 RAMMED EARTH STRUCTURES.....	21
2.2.1 <i>Soil Suitability, Mixing & Blending</i>	22
2.2.2 <i>Stabilisation</i>	26
2.2.2.1 Overview	26
2.2.2.2 Advantages & Disadvantages of Stabilisation.....	27
2.2.3 <i>Formwork</i>	28
2.2.4 <i>Compaction</i>	29
2.2.5 <i>Dampness in Rammed Earth Walls</i>	32
2.2.6 <i>Deleterious Effects of Dampness</i>	34
2.2.7 <i>Existing Solutions for Rammed Earth Structures</i>	36
2.2.7.1 Building Design	36
2.2.7.2 Admixtures	38
2.2.7.3 Surface Treatments	40
2.3 MOISTURE INGRESS MECHANISMS IN BUILDINGS.....	44
2.3.1 <i>Gravity</i>	45
2.3.2 <i>Capillary Action</i>	45
2.3.3 <i>Kinetic Energy</i>	50
2.3.4 <i>Hydrostatic Pressure</i>	51
2.3.5 <i>Air Currents & Pressure Differential</i>	51
2.3.6 <i>Other Contributory Factors</i>	53
2.4 FUNDAMENTALS OF MOISTURE INGRESS THEORY	54
2.4.1 <i>Porous Building Materials</i>	54
2.4.2 <i>Reference Moisture Content</i>	57
2.4.3 <i>Moisture Transfer Process</i>	58
2.4.4 <i>Soil Structure and Particle Association</i>	61
2.4.4.1 Elementary Particle Arrangements.....	62
2.4.4.2 Particle Assemblages	63
2.4.4.3 Pores (Voids).....	65
2.5 MOISTURE TRANSPORT MECHANISMS.....	67
2.5.1 <i>Pressure Differential</i>	68
2.5.2 <i>Diffusion</i>	70
2.5.3 <i>Non-Saturated Flow Theory</i>	72
2.6 SUMMARY	77
CHAPTER 3 - SAMPLE PREPARATION & PHYSICAL PROPERTIES.....	79
3.1 SOIL GRADING & PREPARATION	79
3.1.1 <i>Mix Blending</i>	79
3.1.2 <i>Classification</i>	81
3.1.3 <i>Cement Stabilisation</i>	84
3.2 CUBE SAMPLE PRODUCTION	85
3.2.1 <i>Apparatus</i>	85
3.2.2 <i>Compaction Procedure</i>	86
3.2.3 <i>Catalogue of Cube Samples Produced</i>	88
3.2.4 <i>Curing</i>	90
3.3 EFFICIENCY OF PNEUMATIC COMPACTION.....	92

3.3.1	<i>Equipment & Test Wall Construction</i>	92
3.3.2	<i>Suspended Wall Mass Determination</i>	94
3.3.3	<i>Analysis of Results</i>	96
3.4	PHYSICAL PROPERTIES	97
3.4.1	<i>Dry Density</i>	97
3.4.2	<i>Dimensional Stability</i>	100
3.4.3	<i>Particle Density</i>	107
3.5	COMPRESSIVE STRENGTH	107
3.5.1	<i>Apparatus & Calibration</i>	107
3.5.2	<i>Testing Procedure</i>	108
3.5.3	<i>Shear Plane Failure of Soil Specimens</i>	110
3.5.4	<i>Results & Discussion: Unstabilised Rammed Earth</i>	112
3.5.5	<i>Results & Discussion: Cement-Stabilised Rammed Earth</i>	113
3.6	SUMMARY	115
4.0	INITIAL RATE OF SUCTION (IRS)	117
4.1	METHODOLOGY	117
4.1.1	<i>The BS3921 IRS Test</i>	117
4.1.2	<i>The IRS ‘wick’ Test</i>	118
4.1.2.1	<i>Validity of IRS ‘wick’ Test</i>	120
4.1.2.2	<i>Moisture Dissipation Test</i>	123
4.1.3	<i>Test Procedure</i>	123
4.1.3.1	<i>Unstabilised Rammed Earth</i>	124
4.1.3.2	<i>Cement-Stabilised Rammed Earth</i>	124
4.2	RESULTS & DISCUSSION	125
4.2.1	<i>IRS – Rammed Earth vs. Conventional Masonry Materials</i>	125
4.2.2	<i>IRS Testing of Unstabilised Rammed Earth</i>	128
4.2.2.1	<i>5-minute IRS ‘wick’ Test Results</i>	128
4.2.2.2	<i>60-minute IRS ‘wick’ Test Results</i>	128
4.2.2.3	<i>3-Dimensional Moisture Migration</i>	130
4.2.2.4	<i>Repeat-testing of Inflow Surfaces</i>	131
4.2.2.5	<i>The Effect of Surface Finish</i>	132
4.2.2.6	<i>Non-saturated Flow Theory</i>	134
4.2.3	<i>IRS Testing of Cement-Stabilised Rammed Earth (SRE)</i>	135
4.2.3.1	<i>5-minute IRS ‘wick’ Test Results</i>	135
4.2.3.2	<i>Clay/Cement Interaction</i>	137
4.2.3.3	<i>Non-saturated Flow Theory</i>	138
4.3	SUMMARY	139
5.0	INITIAL SURFACE ABSORPTION (ISA)	141
5.1	METHODOLOGY	141
5.1.1	<i>The BS 1881-208 ISA Test</i>	141
5.1.2	<i>The Modified ISA Test</i>	143
5.1.3	<i>Calibration of the Modified ISA Test</i>	145
5.1.4	<i>Test Methodology</i>	146
5.2	RESULTS & DISCUSSION	147
5.2.1	<i>Rammed Earth vs. Conventional Masonry Materials</i>	148
5.2.2	<i>ISA Testing of Unstabilised Rammed Earth</i>	150
5.2.3	<i>ISA Testing of Cement-Stabilised Rammed Earth</i>	152
5.2.4	<i>Analysis of the ISA Test Methodology</i>	155
5.3	SUMMARY	156
6.0	CLIMATE SIMULATION CHAMBER	157
6.1	APPARATUS & METHODOLOGY	157
6.1.1	<i>SHU Climatic Simulation Chamber</i>	157
6.1.1.1	<i>The ‘Design’ Side</i>	158
6.1.1.2	<i>The ‘Climate’ Side</i>	159
6.1.2	<i>Stabilised Rammed Earth (SRE) Test Walls</i>	160
6.1.3	<i>Static Pressure-Driven Rainfall Simulation</i>	169
6.1.3.1	<i>Low-Pressure Sparge Pipes – Test Run #1</i>	170
6.1.3.2	<i>High-Pressure Spray Nozzles – Test Run #2</i>	175
6.1.3.3	<i>Test Procedure</i>	177
6.1.4	<i>Embedded Sensor Apparatus – Test Run #3</i>	180
6.1.4.1	<i>Thermocouples (Temperature Sensors)</i>	182
6.1.4.2	<i>Relative Humidity (RH) Probes</i>	183
6.1.4.3	<i>Resistance-Type (Ω) Moisture Content Sensors</i>	184

6.1.5 <i>Fixed-Climate Differentials – Test Run #4</i>	187
6.2 RESULTS & DISCUSSION	188
6.2.1 <i>Test Run #1: Low-Pressure Sparge Pipes</i>	188
6.2.1.1 Observations.....	188
6.2.2 <i>Test Run #2: High-Pressure Spray Nozzles</i>	189
6.2.2.1 Analysis of Results	189
6.2.2.2 Additional Observations	197
6.2.3 <i>Test Run #3: Embedded Electronic Sensors</i>	199
6.2.4 <i>Test Run #4: Temperature Differential</i>	202
6.3 SUMMARY	203
7.0 SOIL GRADING OPTIMISATION	205
7.1 SORPTIVITY (S).....	205
7.2 MAXIMUM SURFACE INFLOW VELOCITY (U_0)	209
7.3 SOIL GRADING OPTIMISATION THEORY	213
7.3.1 <i>Total Specific Surface Area (SSA)</i>	213
7.3.2 <i>The 3.35 Ratio</i>	214
7.3.3 <i>The Effective Hydraulic Pore Radius (r)</i>	221
7.4 SUMMARY	226
8.0 CONCLUSIONS & FUTURE WORK.....	229
8.1 OUTCOMES OF THE STUDY	229
8.2 RECOMMENDATIONS FOR FURTHER RESEARCH	232
8.2.1 <i>Thermal Performance of Rammed Earth Materials</i>	233
8.2.2 <i>SEM Analysis of the Pore Structure in Rammed Earth Materials</i>	233
REFERENCES	234
BIBLIOGRAPHY.....	239
APPENDIX 1: THE STORY OF RAMMED EARTH.....	250
A1.1 PAST, PRESENT & FUTURE	250
A1.1.1 <i>Ancient and Historic Buildings</i>	250
A1.1.2 <i>The Modern Rammed Earth Renaissance</i>	259
A1.1.3 <i>The Future for Rammed Earth in Great Britain</i>	267
A1.2 WHY BUILD WITH EARTH?	268
A1.2.1 <i>Government Incentives</i>	268
A1.2.2 <i>Environmental Qualities</i>	269
A1.2.3 <i>Contractors</i>	270
A1.2.4 <i>Physical Properties</i>	272
A1.2.5 <i>Thermal Properties</i>	273
A1.2.6 <i>What Happens when it Rains?</i>	276
APPENDIX 2 - CONSTRUCTION TECHNIQUES	278
A2.1 FORMWORK.....	278
A2.1.1 <i>Gantry-Type Formwork</i>	278
A2.1.2 <i>Modern Proprietary Concrete Shuttering</i>	279
A2.1.3 <i>Australian Formwork - Stabilform™</i>	280
A2.1.4 <i>REW Formwork</i>	282
A2.2 MIXING AND BLENDING	284
A2.2.1 <i>Mixing Techniques</i>	284
A2.2.2 <i>Compaction</i>	289
A2.2.2.1 <i>Hand Rammers</i>	290
A2.2.2.2 <i>Pneumatic Rammers</i>	290
A2.2.2.3 <i>Form Filling</i>	292
A2.2.3 <i>Lintels, Wall Plates and Fixings</i>	294
APPENDIX 3: CUBE SAMPLES GALLERY	297

ACKNOWLEDGEMENTS

I wish to acknowledge the following people for their assistance with this research project:

- **Dr Youcef Djerbib** (*Sheffield Hallam University*) for consistently giving me his guidance, supervision and encouragement throughout this project
- **Mr Stephen Dobson** (*RAMTEC Pty Ltd., Western Australia*) for sharing his experience and contributing helpful discussions and advice
- **Mr Stephen Hetherington and the other technical staff** (*Sheffield Hallam University*) for their technical assistance, advice, knowledge and experience
- **Professor Pal Mangat, Dr Elizabeth Laycock and Dr Kevin Spence** (*Sheffield Hallam University*) for giving me support and guidance when it was needed
- **Paul Scholey** (Rotherham Sand & Gravel Ltd) for the generous donation of raw materials and technical data pertaining to them
- **Tom Craven, Mark Tuck, James Turner, Ben Sissons, and Stephen Narey** (*Sheffield Hallam University*) for their efforts and contributions
- **Darel Henman** for his translation of Japanese research papers, useful information and pictures of rammed earth buildings and structures
- To all my colleagues both in Great Britain and overseas for their dialogue and helpful discussions in relation to research and rammed earth wall construction
- To my mother, father, sister and the rest of my family for their support and patience towards me throughout my project

LIST OF FIGURES

Figure 1 particle-size distribution chart showing recommended rammed earth grading parameters (chart: adapted from BSI, 1990 ₂).....	24
Figure 2 reference diagrams for determining the optimum moisture content using the drop test (diagram adapted from Standards New Zealand, 1998).....	31
Figure 3 Illustrations to describe the ‘overcoat’ effect and the impervious skin on masonry walls.	33
Figure 4 a cross-section of the foundation details for Brimington bowls pavilion	37
Figure 5 the parameters of water droplet formation due to the forces of surface tension (adapted from Bowles, 1984)	46
Figure 6 capillary rise of water in a glass vessel.....	47
Figure 7 illustration of prevailing wind affecting incident rainfall angle and creating a pressure differential within the external walls of a building.....	52
Figure 8 illustration of the volume fraction porosity (f) in a rammed earth cube sample oven-dried to constant mass.....	56
Figure 9 Reference moisture contents in porous building materials (Diagram: adapted from de Freitas <i>et al</i> , 1996).....	57
Figure 10 illustration of the process by which moisture ingress and movement occurs in the pore space of an initially dry permeable material (Diagram: adapted from Rose, 1965)	59
Figure 11 an illustration of the relationship between porosity and permeability (Diagram: Concrete Society, 1988)	60
Figure 12 elementary particle arrangements (adapted from Mitchell, 1976).....	62
Figure 13 examples of typical particle assemblages in sub-soils (adapted from Mitchell, 1976)	64
Figure 14 an illustration of the different pore spaces that can form inside sub-soils (adapted from Mitchell, 1976)	66
Figure 15 an SEM micrograph of the micro-soil structure in freshwater alluvial silty clay (adapted from Mitchell, 1976)	67
Figure 16 specimens of the silty clay, grit sand and pea gravel that were used to create the rammed earth soil mixes for this study.....	80
Figure 17 Rammed earth soil mix recipe 523	81
Figure 18 BS 1377 particle-size distribution chart displaying the CRATerre parameters for rammed earth soils, and the PSD curves for the ten rammed earth mix recipes	82
Figure 19 rammed earth mix recipes with their corresponding SSA_i/CC ratio.....	83
Figure 20 a 6.5 kg steel hand rammer that conforms to NZS 4298: 1998.....	85
Figure 21 (above left) hand-rammed cube sample making apparatus	86
Figure 22 (above right) the view inside the guide collar and cube mould assembly.....	86
Figure 23 completed rammed earth cube samples made using the unstabilised 613 soil mix recipe	88
Figure 24 a large collection of rammed earth cube samples being stored in a curing chamber under controlled conditions	91
Figure 25 a pneumatic rammer attached to an air compressor	93
Figure 26 a miniature rammed earth test wall built on a metal base	94
Figure 27 the SHU suspended wall mass-measuring apparatus in operation	95
Figure 28 an illustration of the points on a sample at which to determine the sample dimensions	103
Figure 29 the Mayes SH250 compressive strength test machine.....	108
Figure 30 shear plane failure of a rammed earth specimen in an unconfined compressive strength test	111
Figure 31 the relationship between f'_{cu} and ρ_d for different unstabilised soil mix recipes	112
Figure 32 a comparison between the 28-day f'_{cu} for different soil mix recipes with varying percentage of cement stabilisation	114
Figure 33 the relative effect of varying levels of cement stabilisation on the 28-day f'_{cu} increase in different soil mix recipes	115
Figure 34 a diagram to illustrate the modified IRS ‘wick’ test.....	119
Figure 35 the various stages of the IRS ‘wick’ test in operation.....	120
Figure 36 a comparison between the BS3921 and the IRS ‘wick’ test results obtained for conventional materials.....	121
Figure 37 a comparison between the IRS ‘wick’ test results (5-minute regime) for various unstabilised rammed earth mix recipes and a small selection of conventional masonry materials.....	127

Figure 38 a comparison between the IRS of different unstabilised rammed earth mix recipes under the 60-minute (repeat) IRS 'wick' test regime.....	129
Figure 39 a comparison between the geometry of IRS test methodologies.....	130
Figure 40 the variation of IRS in different rammed earth mix recipes samples due to single repeat-testing of the sample face.....	131
Figure 41 the relationship between the total mass of sorbed water and the square root of elapsed time for different unstabilised rammed earth mix recipes.....	134
Figure 42 the relative effects of varying cement content on the 1-minute IRS value of three stabilised rammed earth mix recipes	136
Figure 43 Relationship between mass of sorbed water and square root of elapsed time for cement stabilised rammed earth	139
Figure 44 an illustration of the Initial Surface Absorption (ISA) test apparatus.....	141
Figure 45 Modified ISA test apparatus ready for use including all peripheral equipment	143
Figure 46 an illustration of the procedures for assembling the modified ISA test apparatus for use with rammed earth cube samples	144
Figure 47 the view through the water-filled glass inspection dome during a modified ISA test....	145
Figure 48 a comparison between the ISA rates of various conventional masonry materials and unstabilised rammed earth made with a selection of different mix recipes	149
Figure 49 a direct comparison between the ISA over elapsed time for various unstabilised rammed earth samples made using different mix recipes.....	150
Figure 50 (above left) Unstabilised rammed earth sample face <i>before</i> ISA test.....	151
Figure 51 (above right) Slaking effect of water penetration <i>after</i> 1hr ISA test.....	151
Figure 52 (above left) Unstabilised rammed earth – structural collapse of high-moisture ingress soil types during an ISA test.....	152
Figure 53 (above right) Cement stabilised rammed earth – the same high-moisture ingress soil types do not slake or disintegrate when stabilised	152
Figure 54 the comparative effect of cement content on the ISA of selected rammed earth mix recipes	153
Figure 55 the effect of increasing cement stabilisation on ISA value of different rammed earth mix recipes	154
Figure 56 a schematic diagram of the SHU climatic simulation chamber (adapted: Taylor-Firth & Flatt, 1991).....	158
Figure 57 the concrete plinth under construction	161
Figure 58 cross-sectional diagram of test wall construction detail at foundation level.....	162
Figure 59 stud wall end boards fixed to the concrete plinth to act as spacers between test walls ..	163
Figure 60 a miniature version of the REW formwork system that was used for the mini test walls	164
Figure 61 compaction of earth using Atlas Copco RAM 30 pneumatic rammer	167
Figure 62 the four rammed earth test walls as seen from the design side of the climate chamber.	168
Figure 63 the mini test walls (viewed from the climate side) after being framed and sealed, with the top half of climate chamber closed off and sealed.....	169
Figure 64 a 15mm sparge pipe with skirting attachment delivering rainfall run-off down the face of a mini rammed earth test wall	171
Figure 65 the header tank positioned on the roof of the climate chamber	172
Figure 66 a schematic diagram for the constant head low-pressure water delivery system	173
Figure 67 a test wall in calibration mode (above left).....	174
Figure 68 surface run-off collection and decantation (above right).....	174
Figure 69 Lechler 120° flat spray nozzles providing high-velocity rainfall run-off simulation	175
Figure 70 schematic diagram for the mains powered high-pressure water delivery system	176
Figure 71 a view of the mini test walls from the climate side during the pressure-driven rain phase (6hr) of the test procedure using the low-pressure sparge pipe delivery system.....	178
Figure 72 rainfall run-off collection device and equipment	179
Figure 73 the design side of a test wall showing a fully fitted embedded sensor array	181
Figure 74 type-T thermocouple	183
Figure 75 armoured thermocouple	183
Figure 76 Rotronic relative humidity & temperature embedment probe	184
Figure 77 twenty four custom-made resistance probes	185
Figure 78 gold-plated sensor tips	185
Figure 79 the bridge circuit array with sensor wiring configuration	186
Figure 80 the water run-off collected at each time interval of Monday on Test Run 2.....	191
Figure 81 the rate of surface run-off water collected over the entire 5-day test period of Run 2...	192

Figure 82 mean water absorption in stabilised rammed earth test walls over the entire 5-day period of Run 2.....	193
Figure 83 the calculated rate of water absorption per unit inflow surface area for each test wall on the first day of Test Run 2.....	194
Figure 84 the initial surface absorption (ISA) for each test wall over the entire 5-day test period of Run 2.....	194
Figure 85 comparison between ISA values for cube samples and test walls - 433 mix recipe + 6% cement.....	195
Figure 86 comparison between ISA values for cube samples and test walls - 613 mix recipe + 6% cement.....	195
Figure 87 comparison between ISA values for cube samples and test walls - 703 mix recipe + 6% cement.....	196
Figure 88 the initial stages of the pressure-driven rainfall applications for Test Run 2; much of the surface run-off pours down the wall face without being absorbed.....	198
Figure 89 the later stages of the pressure-driven rainfall applications for Test Run 2; the test wall surfaces have become visibly wet and the 'overcoat' effect appears to repel further ingress.....	199
Figure 90 a typical example of a wall temperature depth profile chart for wall 1 on Monday (day 1) of Run 3.....	200
Figure 91 a typical temperature depth profile chart for wall 1 over the entire 5-day regime of Run 3.....	201
Figure 92 the temperature depth profile of wall 1 during the entire four-day test regime of Run 4.....	203
Figure 93 graphical illustration of the sorptivity (S) range for unstabilised rammed earth, cement-stabilised rammed earth and conventional masonry materials.....	208
Figure 94 the surface inflow velocity (u_o) over elapsed time (t) for different unstabilised rammed earth mix recipes.....	210
Figure 95 relationship between surface inflow velocity (u_o) and the hundredth root of elapsed time ($t^{0.01}$).....	211
Figure 96 relationship between the effective hydraulic pore radius (r) and the surface receptiveness (o) of different unstabilised rammed earth mix recipes.....	212
Figure 97 a graphic illustration of the total Specific Surface Area (SSA_t) to clay ratio theory.....	214
Figure 98 relationship between particle-size mass retained and the average IRS value for different unstabilised rammed earth mix recipes with a CC of 0.066 (2 parts silty clay).....	215
Figure 99 relationship between particle-size mass retained and the average IRS value for different unstabilised rammed earth mix recipes with a CC of 0.099 (3 parts silty clay).....	216
Figure 100 relationship between the IRS value and the 3.35 ratio for unstabilised rammed earth mix recipes.....	217
Figure 101 the relationship between 3.35 ratio and Sorptivity (S) both for poor rammed earth mix recipes and for the same recipes but with granular stabilisation enhancement.....	219
Figure 102 percentage water retained against elapsed time for both poor and modified mix recipes.....	220
Figure 103 exponential relationship between S and f for unstabilised rammed earth mix recipes.....	221
Figure 104 relationship between the effective hydraulic pore radius (r) and sorptivity (S) for unstabilised rammed earth mix recipes.....	223
Figure 105 relationship between sorptivity (S) and the effective hydraulic pore radius (r) for different stabilised rammed earth mix recipes using varying amounts of cement.....	224
Figure 106 relationship between Sorptivity (S) and surface receptiveness (o) for unstabilised rammed earth mix recipes.....	226
Figure 107 picture found inside an Egyptian tomb depicting the manufacture of mud bricks (courtesy: C Frederick).....	251
Figure 108 the rammed earth perimeter wall that surrounds Horyuji temple, Japan (photo: courtesy Darel Henman ©2002).....	252
Figure 109 Taikoubei rammed earth wall – note the raised stone plinth, drainage channel and large eaves overhang on the roof (Photo: courtesy Darel Henman ©2002).....	254
Figure 110 Oonerihei - note the degree of weathering and surface erosion on some of the wall sections is only minor for a wall that is over 500 years old (Photo: courtesy Darel Henman ©2002).....	255
Figure 111 (above left) a typical selection of 19th century rammed earth buildings on BahnhofstraBe, Weilburg an der Lahn, Germany (Photo: courtesy Weilberg Lahn, 2004).	257
Figure 112 (above right) a seven storey rammed earth building on Heinallee, Weilburg an der Lahn, Germany that is around 150 years old (Photo: courtesy Weilberg Lahn, 2004).....	257

Figure 113 five storey rammed chalk building in Winchester, Hampshire (Photo: courtesy Maniatidis & Walker © 2003).....	259
Figure 114 Thomas Moore R.C. church (Photo: courtesy RAMTEC Pty Ltd. ©2002)	261
Figure 115 a passive solar design rammed earth house (Photo: courtesy RAMTEC Pty Ltd. ©2002)	262
Figure 116 a rammed earth holiday home in the tropical setting of Broome, Western Australia (Photo: courtesy RAMTEC Pty Ltd ©2002).....	263
Figure 117 stables at The Manor in Northamptonshire, built by Earth Structures (Europe) Ltd. (2001).....	265
Figure 118 Brimington bowls pavilion at Chesterfield, Derbyshire - built by Matthew Hall and Chesterfield Borough Council (July 2003).....	266
Figure 119 traditional style of gantry-type formwork employed by the Chinese (Photo: courtesy C Frederick, 2002).....	279
Figure 120 Stabilform™ being used by Earth Structures (Europe) Ltd. to construct the stables building in Northamptonshire (Photo: courtesy Maniatidis & Walker, 2003)	281
Figure 121 the modified REW formwork that was used on the 24-hour challenge build for the Brimington bowls pavilion (Photo: courtesy M. Heseltine ©2003).....	283
Figure 122 skid steer loader delivering a fresh mix of rammed earth to the formwork on the Brimington bowls pavilion project (Photo: courtesy Brimington Bowls Club 2003).....	286
Figure 123 typical forced action paddle mixer (Photo: courtesy Refina Ltd. ©2003).....	287
Figure 124 tractor-mounted tillers can mix large amounts of rammed earth soil very quickly (Photo: courtesy J Tingle ©2003).....	288
Figure 125 small, rapid batch mixing with a diesel-engine Rotavator.....	289
Figure 126 high-production pneumatic ramming on the Brimington bowls pavilion project (photo: courtesy M Heseltine ©2003).....	291
Figure 127 construction detail for the lintel and wallplate of the Brimington bowls pavilion (Drawing: courtesy Hall, Damms & Djerbib, 2004).....	295
Figure 128 construction detail for horizontal positive fixing of veranda.....	296

LIST OF TABLES

Table 1 a summary of the entire scheme for rammed earth cube sample production	90
Table 2 dry density values for pneumatically compacted rammed earth walls.....	96
Table 3 an example of the data recorded from a typical cube sample production run.....	98
Table 4 a comparison between the dry densities obtained for different rammed earth soil types with varying degrees of cement stabilisation	100
Table 5 an example of the dimensional data obtained from a typical rammed earth test specimen	104
Table 6 test results for the dimensional stability assessment of rammed earth specimens	105
Table 7 the average amount of sorbed water during a 5-minute IRS 'wick' test.....	126
Table 8 the assessment results for calibration of the modified ISA test, illustrating the suitability and repeatability of the methodology	146
Table 9 an example data set for water run-off collection during Test Run 2.....	190
Table 10 the sorptivity and related properties for a variety of conventional masonry materials, unstabilised rammed earth, and cement-stabilised rammed earth.....	206
Table 11 granular stabilisation of high moisture ingress mix recipes.....	218

LIST OF NOTATIONS

p = total pressure (Pascals)

θ = angle (degrees)

p_i = internal pressure (i.e. inside a water droplet)

p_o = external pressure (i.e. atmospheric pressure)

T_s = surface tension (dynes/cm)

R = radius of curvature (cm)

h_c = maximum height of capillary rise (cm)

α = angle of concavity (degrees)

γ = unit weight of a fluid (kN/m³)

d = tube diameter (cm)

f = volume fraction porosity (decimal)

f_{ap} = apparent porosity (decimal)

τ_f = maximum shear strength (N/mm²)

c' = cohesion parameter

σ' = confining stress (N/mm²)

φ' = angle of friction

u_x = mean flow velocity (mm/s)

$\delta h/\delta x$ = pressure gradient

K = coefficient of permeability (m/s)

ΔQ = volumetric flow rate (m³/s)

ΔA = total cross-sectional area perpendicular to the x -direction (m²)

ΔP = pressure head (m)

l = length of flow path (m)

P = transfer rate of the liquid/gas per unit area normal to the x -direction

$\delta C/\delta x$ = gradient of material concentration

D = the diffusivity constant (m^2/s)

q = vector flow velocity (mm/s)

$\delta \Psi/\delta x$ = gradient of capillary potential (suction)

$K(\theta)$ = moisture content-dependent hydraulic conductivity

m_s = total mass of a solid (kg)

m_w = total mass of water (kg)

v_T = total volume of a specimen (Litres)

v_a = total volume of air in a soil (Litres)

v_s = total volume of solids in a soil (Litres)

w = specific moisture content

w_0 = moisture-free state, i.e. oven dried to constant mass

w_h = minimum adsorbed moisture content under natural conditions

w_{cr} = minimum absorbed moisture content under natural conditions

w_{sat} = point of saturation under natural conditions

w_{max} = maximum moisture content under vacuum conditions

w_a = minimum specific moisture content

w_b = maximum specific moisture content

θ = dimensionless water content

S = Sorptivity ($mm \text{ min}^{-0.5}$)

t = elapsed time (min, or s)

A = cross-sectional area of the inflow test face (mm^2)

ρ_w = density of water (0.988 g/ml @ 20°C)

ρ_d = dry density (kg/m^3)

ρ_s = particle density (kg/m^3)

i = cumulative volume of absorbed water per unit inflow surface area (mm)

di = small increase in i

dt = small increase in t

u_o = maximum surface inflow velocity in x -direction where $x = 0$ (mm/min)

η = viscosity (mN s m⁻²)

s = intrinsic sorptivity (m s^{-0.5} E⁻⁵)

r = effective hydraulic pore radius (nm)

o = surface receptiveness (mm/min. min^{0.01})

SSA = specific surface area (mm²/g)

SSA_t = total specific surface area of granular soil particles (mm²/g)

CC = clay content (decimal) as a proportion of total dry mass of soil [m_d]

m_{ret} = mass retained as a proportion of original total mass

%LS = linear shrinkage of a soil (during drying) expressed as a percentage (%)

L_o = original length of specimen (mm)

L_D = length of specimen after linear shrinkage has occurred (mm)

f'_{cu} = characteristic unconfined compressive strength [uniaxial] (N/mm²)

X_s = standard deviation in a series

X_a = mean average in a series

X_l = lowest value in a series

RH = relative humidity (%)

y = height of test specimen (mm)

x_1 = diameter of top half of test specimen (mm)

x_2 = diameter of bottom half of test specimen (mm)

y_{avg} = mean average height of a series of test specimens (mm)

x_{avg} = mean average diameter of a series of test specimens (mm)

y_{LS} = mean linear vertical shrinkage of a series of test specimens (%)

x_{LS} = mean linear lateral shrinkage of a series of test specimens (%)

$k = \text{thermal conductivity (W/m}^2\text{)}$

1.0 INTRODUCTION

1.1 OVERVIEW

Rammed earth walls comprise dynamically compacted sub-soil that has been monolithically formed inside removable formwork. Through the application of modern building technologies, this ancient technique of wall construction is being successfully reintroduced as a highly sustainable alternative building material for the future (Hall, 2002). A renaissance of modern rammed earth construction has been taking place for over 25 years in developed countries throughout the world such as the USA, Canada, New Zealand, Germany, France, and Australia where in some regions it accounts for up to 20% of all new build (Easton, 1996_a). The rammed earth renaissance began during the mid-nineteen seventies during the energy crisis, when both the demand and the desire for sustainable alternatives were very high.

The technique of rammed earth (sometimes known as *Pisé*) is in fact ancient and has been practised for many thousands of years in areas such as North Africa, China and Europe. The introduction of rammed earth to Great Britain is comparatively recent and has only been practised for approximately 200 years. During the past ten years or so, its revival as a modern masonry material has inspired a Government DTi-funded Partners in Innovation project to develop modern rammed earth construction for UK housing (Maniatidis & Walker, 2003). The incentive behind this decision stems from the Governments policies and commitments to the principles of sustainable development by investigating novel ways in which to reduce CO₂ emissions. Recent projects of significance include the Eden Project visitor's centre, the ATEIC building at the Centre for Alternative Technology (CAT), and Brimington Bowling Pavilion in Chesterfield,

Derbyshire that was built by the author for a BBC-commissioned television programme in 2003.

The potential problems relating to moisture ingress and durability are the area that attracts the most concern from the public (Heathcote, 1995). Moisture movement is an important consideration for much earth based construction and so limits on moisture movement are necessary to prevent cracking of finished walls, damage to renderings, and protection from rainfall (Walker, 1996). For the damp temperate climate of the Great Britain, research is essential in order to determine the suitability of rammed earth for the construction industry. Given the absence of mechanical damage it has long been recognised that water absorbed into porous building materials is the greatest threat to the durability of masonry construction materials in the United Kingdom (Bryan, 1988).

1.2 THE PROBLEMS

At the Project Terra Research Meeting in 2000 a group of internationally renowned earth construction experts were gathered including CRA Terre-EAG, Getty conservation, ICCROM and English Heritage. They concluded that the kinetics (absorption, adsorption, migration) of moisture movement both in the pore structure and on the surface of earth walls are 'close to unknown' (Project Terra, 2000). There have been no comprehensive research projects examining the mechanisms and migration of moisture ingress in rammed earth materials. Rainfall alone is not particularly damaging if it is able to evaporate; but if moisture is allowed to build up, it can cause material deterioration due to swelling and lead to significant reduction in strength (Walker & Standards Australia, 2002). This could also cause accelerated erosion of the wall material externally, or areas of damp accumulation at the interior leading to health

concerns and damaged furnishings. As rammed earth walls are monolithic, the capillary ingress and migration of moisture within them can be a particular problem because there are no chemically dosed layers of mortar to suppress it (Dobson, 2001, *pers comm.*). Initial rate of absorption testing for compressed earth materials is recommended, although clearly further work is needed in this area (Walker, 1996).

Many commercial admixtures are available to retard moisture ingress in rammed earth. However, these are generally very expensive, difficult to mix, are sometimes only partially effective and have no supplier warranty. Stephen Dobson is a building engineer and rammed earth contractor with over 27 years experience. Apparently, he has '*...tried many things before regarding admixtures for damp ingress - all too expensive or unreliable. Does adding clay make it better or worse? Does removing clay (e.g. by washing) make it better or worse? Does lessening clay content (e.g. by adding washed sand) make it better or worse? These are real questions*' (Dobson, 2001, *pers comm.*). A greater understanding of the factors affecting the moisture ingress performance of rammed earth mix designs is required so that soil, which performs poorly, could potentially be improved simply by affecting the particle-size distribution or relative clay content.

1.3 AIMS & OBJECTIVES

The overall aim of this research project is as follows:

To investigate, through experimentation and the application of current theory, the ingress and movement mechanisms of moisture in unstabilised and stabilised rammed earth

The project will aim to present a thorough literature review of current practices and knowledge in modern rammed earth construction, as well as the application of scientific theories to the ingress of moisture in porous building materials. The current knowledge of rammed earth contractors and researchers allows them to vary soil mix constituents in order to alter appearance and strength. The focus of this research is to investigate the effect of rammed earth mix parameters on the moisture ingress performance. Past research by highly-regarded academics such as Professor Christopher Hall (formerly of the University of Manchester Institute for Science & Technology - UMIST) has allowed the application of non-saturated flow theories to be successfully adapted for use with porous building materials, since the moisture content is generally at a level below saturation (Hall 1977). The mechanisms of moisture ingress and migration are often strongly dependent upon whether the source of water is, for example, due to basal damp, wind-driven rain, surface run-off, or leaking rainwater services.

The main objectives of this research project are summarised below:

-
- Devise suitable test methodologies for measuring the amount of water sorption and the rate of ingress in rammed earth due to both capillary suction and static pressure differential
 - Investigate the ingress and migration of moisture in rammed earth materials through experimentation and the application of non-saturated flow theory
 - Determine the effect of soil grading in rammed earth mix recipes on the amount of moisture ingress and investigate methods for optimisation of the grading
 - Discover the effect of varying amounts of cement stabilisation on moisture ingress in rammed earth and the interrelation between particle size distribution and cement content to find an optimum moisture ingress resistant mix
 - Compare the studied properties of rammed earth with those of conventional masonry materials such as concrete and fired clay bricks
 - Determine the scale effect of using small representative samples compared to full-scale rammed earth walls in order to verify the appropriateness and accuracy of the laboratory tests devised

2.0 LITERATURE REVIEW

2.1 INTRODUCTION

A detailed review of the story of rammed earth - past, present & future - can be found in Appendix 1. This chapter begins by addressing the fundamental principles of rammed earth construction. The overall subject of moisture interaction with rammed earth walls is addressed. Conventional test methodologies for durability and erosion are described along with some research findings. The deleterious effects of dampness in buildings are discussed, along with the ways in which this may relate to rammed earth walls. The various moisture ingress mechanisms that are typical in the UK are, at length, described and illustrated. The notion of reference moisture content is discussed, along with the various states in which this moisture can exist. The various ways in which the phase and concentration of moisture can affect the mechanisms of transfer are described. Movement and migration of moisture only occurs where there is an external force to motivate it. As such, the three transport mechanisms that are responsible for inducing moisture movement are described in detail.

2.2 RAMMED EARTH STRUCTURES

Modern rammed earth construction utilises a combination of established ancient techniques combined with modern technology to provide an alternative, masonry building material that is both sustainable and practicable. The resultant walls offer a greater level of interior comfort and healthier living conditions than most conventional building materials, and yet they are also strong, durable and affordable.

2.2.1 Soil Suitability, Mixing & Blending

There is no simple or direct reply to the question ‘is this soil suitable for construction?’, (Houben & Guillaud, 1996). A philosophical approach to this problem is provided by David Easton who simply believes that the combination of knowledge and experience is slow to accumulate but eventually provides the most informed answer:

‘Soil is so diverse, its properties and reactions so widely variable, that to fully understand its uses and limitations, and to build with it successfully, takes years of study and experience. Civil engineers understand density and moisture content. Agronomists comprehend porosity and tilth. Geologists speak of composition and classification... Earth builders must know it all. Take your time’ (Easton, 1996_a).

The ‘earth’ used for making rammed earth generally refers to a sandy loam sub-soil of a suitable grading that allows it to be dynamically compacted. Topsoil is unsuitable due mainly to the significant amount of organic matter present that biodegrades, absorbs water, and is highly compressible. It must be limited to 1 or 2 percent of the total mass, if allowed at all (King, 1996).

The grading of a soil refers to the particle-size distribution of the soil grains and is determined using two conventional techniques: sieve analysis for the larger particles and sedimentation for the smaller particles. It is the size of a soil particle that is used to determine both its type and corresponding name, e.g. gravel, sand, silt, or clay. The specific sizes used for this process vary slightly depending upon the nationality of the standard. The standard used in this instance is British Standard 1377: 1990 Methods of Tests for Soils for Civil Engineering Purposes – Part 2 Classification (BSI, 1990₂). In

this standard, sieve analysis applies to granular soil particles, i.e. those with a diameter greater than 0.063mm (sand and gravel). The technique essentially involves passing the soil through a nest of different sized sieves to measure the amount of material retained on each one. This allows one to plot a graph illustrating the percentage of material passing each different sieve size. When a full series of points are plotted on this graph the resultant line is referred to as a particle-size distribution (PSD) curve. Sedimentation is a technique for determining the size distribution of cohesive particles with a diameter smaller than 0.063mm (i.e. silt and clay [fines]) by measuring the amount of material presently suspended in water at a given depth after a given time. The principle is reliant upon Stokes' law where larger particles suspended in water are assumed to settle more quickly than smaller ones due to the effect of gravity.

CRATerre-EAG (a French organisation) recommends non-prescriptive parameters for a suitable rammed earth particle-size distribution curve. These parameters are essentially upper and lower limits and have been superimposed onto the British Standard BS1377 particle-size distribution chart illustrated in Figure 1.

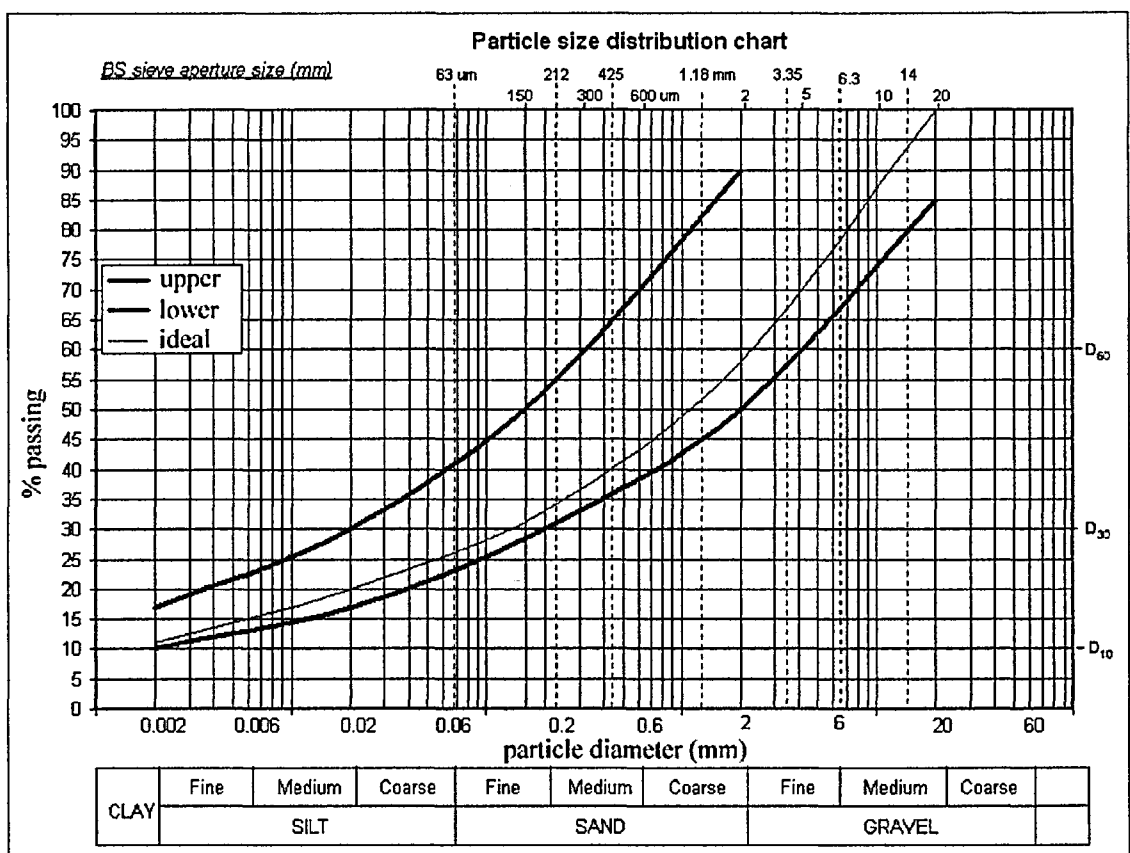


Figure 1 particle-size distribution chart showing recommended rammed earth grading parameters (chart: adapted from BSI, 1990₂)

Note that soils are a natural material and can vary considerably over a very short distance. A selection of representative soil samples should be gathered from the proposed site, perhaps in the order of at least three amounts of 25 kg from separate trial pits. It often happens that a sub-soil with the correct grading for rammed earth will not be found underfoot on a given building site. Building with soil, therefore, implies a choice between one of three approaches in terms of soil suitability (Houben & Guillaud, 1996):

1. Using the soil available on-site in its natural state, except for the removal of large rocks and artefacts etc

-
2. Importing a soil from another site that is more suitable than the soil available on-site, e.g. soil excavated from another site, quarry waste, or recycled aggregates such as crushed hardcore.
 3. Modify and enhance the soil available on-site by granular stabilisation techniques so that its grading is better suited to the requirements of the project. This can include the addition of sands and/or gravels, the addition of fines (silt or clay), or even the removal of fines through washing.

For the present, it is recommended that the earth wall designer should generate a tentative approach to mix design. By using the accepted soil classification and investigation methods described above one can generate as much useful data and information about the soil as possible in order to make the most informed decision as possible. Creating test samples from the mixes should then provide experimental evidence of the properties of the rammed earth material, e.g. compressive strength, durability etc. The two critical factors to be determined in rammed earth soil mix recipes are particle-size distribution (grading), and optimum moisture content for dynamic compaction. These factors were investigated as part of the experimental work for this project and have been described in more detail later in the thesis.

As previously discussed, the particle-size distribution of the available soil may not be suitable in its natural state and so requires the addition of other soils to enhance the grading. Blending a clay-rich soil with additional sand or gravel to improve the grading is a common practice and should be done at the mixing stage if necessary. It may also be necessary to add some fine sand or silty soil to a mix that is prone to sticking (Dobson, 2002). The addition of gravel has a similar effect on reducing stickiness in a difficult mix; although it can make the surface finish much more pebbled which can be

aesthetically very different to the original soil. This observation was further qualified during the experimental work in this project where variations in the surface finish of rammed earth materials were found to significantly alter the physical properties in terms of water absorption.

2.2.2 Stabilisation

2.2.2.1 Overview

A stabiliser is an additive that improves the strength, durability or other properties of the earth walls. Some people are in favour of stabilisation techniques to enhance the material performance, and some believe that rammed earth should not be stabilised with materials like cement as this undermines its sustainability credentials. However, as Walker & Standards Australia (2002) state, the amount of energy required to process earth is less than that required for most other building materials. Clay bricks, a comparatively low energy material, consume between 1.0 and 7.0 GJ per tonne of units produced, of which 80% to 90% is used in drying and firing. By replacing firing with cement stabilisation, the energy consumed in masonry unit production can be reduced by at least 50% (Walker & Standards Australia, 2002).

Many of the modern rammed earth construction companies in Australia and the USA stabilise their soil with admixtures to enhance the strength and durability characteristics of the material. Possibly the most common form of stabilisation in rammed earth is Ordinary Portland Cement (OPC) and is normally used only in small quantities of around 6% by mass. This amount of stabilisation is the equivalent cement content to a very lean concrete mix of around 10:1 or 12:1 (i.e. ballast: cement ratio). Other

stabilisation admixtures include lime, bituminous emulsion and proprietary chemical admixtures, e.g. TechDry KR2TM.

Some people often dismiss modern Australian rammed earth as 'brown concrete' due to the inclusion of cement. This observation is rather cynical because it chooses to ignore the fact that over the past 27 years hundreds of modern rammed earth buildings have been constructed in Australia. This has, to some degree, secured the place of modern rammed earth in their main-stream modern construction industry and in the domain of fashionable architecture. This great achievement for earth building is unrivalled anywhere else in the world, and at the time the only way of gaining statutory approval for rammed earth was through cement stabilisation (Watson, 1997).

2.2.2.2 Advantages & Disadvantages of Stabilisation

Soil stabilisation is not an exact science and there is no 'miracle' stabiliser that can be applied indiscriminately to ensure good results (Houben & Guillaud, 1996). Stabilised earth walls, however, may be built more thinly and there may be no need for the application of expensive surface treatments to improve durability and water tightness. In terms of durability, cement-stabilised materials such as rammed earth rarely have problems meeting the requirements of even the most severe tests (Walker & Standards Australia, 2002). A 'modern' building often results from the use of stabilised soils, which can be distinguished from 'traditional' earth materials, and can have higher status in certain regions such as developing countries (Keable, 1996). The decision to stabilise the soil mix should only be made after consideration of the following advantages and disadvantages:

Advantages

- Speeds up the building process as the required wall thickness is generally smaller and so less material and labour is required
- Improves durability and strength, particularly where the locally available soil is poor
- May reduce or eliminate the need for expensive surface treatment or rendering
- A 'modern' building results that can be distinguished from 'traditional' materials and may have higher social/technical status in developed countries

Disadvantages

- Costs are increased - soil is free/low cost and cement is relatively expensive
- The stabilisation materials needed may not be readily available in some countries or may be expensive to transport
- The processes of mixing and building can become more complicated depending upon the type of stabiliser that is chosen. This can increase the chance of problems occurring thus affecting time/budget
- Potential environmental impact - e.g. cement and lime; both have a high embodied energy content and are responsible for significant levels of CO₂ emissions
- Health & safety - cement and lime are both hazardous materials that can cause burns to the skin and eyes, some chemical additives contain volatile organic compounds (VOCs)

2.2.3 Formwork

The formwork used for rammed earth is rather like that used for concrete: it is essentially a mould that shapes and contains the rammed earth whilst it is being constructed. For this reason, it is the accuracy and dimensions of the formwork that

largely determines the quality and alignment of the finished wall. The use of good formwork is essential in rammed earth in order to prevent bulging or misalignment during compaction, and to ensure a high quality finish that is durable and aesthetically pleasing. The basic components of any formwork are usually the side shutters, end boards, and tie rods to hold everything together.

Many traditional types of formwork have been used since ancient times, some variants of which are still practised today such as gantry-type formwork. However, in recent times there have been significant advancements in modern rammed earth formwork technology, many of which are highly innovative and efficient. Perhaps the most notable of these examples include the REW formwork system developed by Rammed Earth Works Inc. in the USA, and the StabilformTM system patented by the Affiliated Stabilised Earth Group (asEg) in Australia. A detailed review of rammed earth formwork technology can be seen in Appendix 2 - Section A2.1.

2.2.4 Compaction

The moisture content of a rammed earth soil is critical because it has to be dynamically compacted as part of the construction process. The soil is at suitable moisture content for compaction when it is just moist, and if it can be formed into a ball when squeezed tightly in the palm of the hand. If the level of moisture is not correct during compaction then the completed rammed earth wall may not achieve the correct density to be as strong or durable as it should be.

The presence of moisture acts as a lubricant between the soil grains. If too little water is added then the soil cannot achieve the same level of compaction due to the greater

degree of friction between the soil particles. More water increases the lubrication between soil particles and so allows a higher degree of density, strength and durability to be achieved. However, an excess amount of added water can occupy the pore spaces between soil grains, thus preventing the compacted soil from achieving the correct density and exacerbating the level of porosity in the finished wall when it has cured. The optimum moisture content (OMC) of a soil, therefore, is the amount of water that allows it to be compacted to its optimum density giving the highest possible strength, durability and quality of product.

The most accurate way of determining the optimum moisture content for a given soil type is using an internationally-recognised standard laboratory experiment called the Proctor test. Once the OMC has been determined, it is expressed as a percentage of the soils dry mass. For correctly graded rammed earth soils this value is usually somewhere between 8% and 15%. However, the on-site quality control of optimum moisture content in a soil demands a more pragmatic method of testing that can be carried out by competent builders. The Proctor Test is the industry standard for determining the optimum moisture content of a soil that is to be dynamically compacted. The procedure conveniently mirrors the rammed earth production process but in a more standardised form whereby a rammer of known weight (2.5 or 4.5 kg) falls onto a specimen of moist soil from a known height (300mm or 450mm) for a known number of drops (27 times). The soil is compacted inside a 1 litre cylindrical mould in three (or sometimes five) even layers. The test is repeated several times with the soil at different moisture contents in order to determine the point at which maximum density through dynamic compaction can be achieved. This point is called the optimum moisture content (OMC), as discussed previously, and can be accurately determined by using a graph; plotting the results for dry density against moisture content for a range of values.

One highly established field test that is often used during rammed earth construction is the drop test. It is contained within the Australian codes of practice and is mandatory under the official New Zealand Standards for earth building (Standards New Zealand, 1998). The procedure is to take a small handful of the moist mix and tightly squeeze it in the palm of the hand to form a ball that is approximately 40mm in diameter. Hold the arm out straight at approximately 1.5m height (shoulder height) and drop the ball onto a smooth clean piece of plywood (min. 12mm (1/2”) thick). According to the CSIRO the ball should not shatter into tiny fragments nor should it crack in two, but somewhere in between (CSIRO, 1987). If the ball breaks into only a few pieces, typically 5 to 6, it is close to the OMC and suitable for use (Keable, 1996). In this project, the author has observed that the soil breaks apart leaving a sharp peak of soil in the middle when it is at the correct moisture content (UKTV, 2003). The diagram in Figure 2 is adapted from NZS 4298: 1998 and represents the different stages of a drop test indicating the OMC for a given soil type.

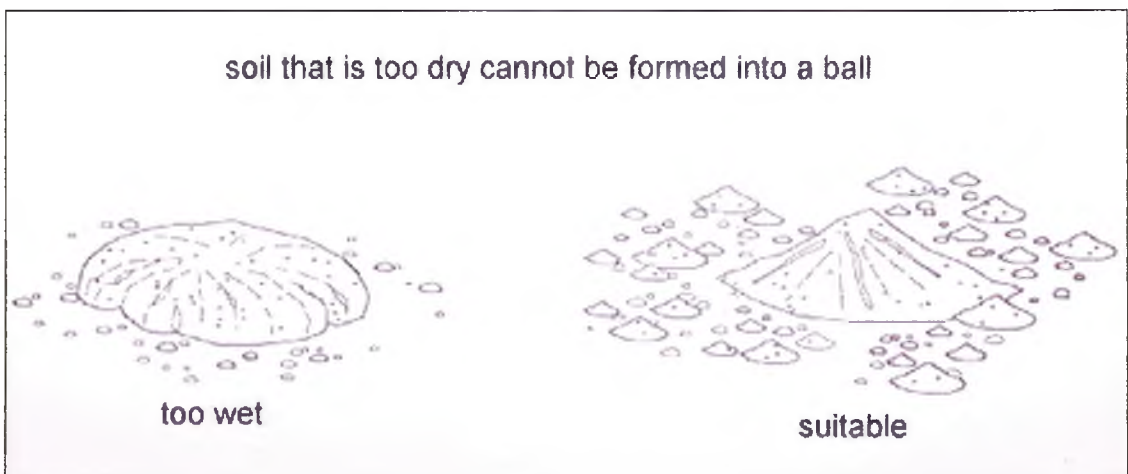


Figure 2 reference diagrams for determining the optimum moisture content using the drop test (diagram adapted from Standards New Zealand, 1998)

The practice of regular drop testing during construction ensures that quality levels in building are maintained. The test has been proven, to the satisfaction of the author, to be accurate to within approximately 1% of the actual OMC with reference to the BS1377 Part 4 Proctor test (BSI, 1990₄).

2.2.5 Dampness in Rammed Earth Walls

Before water can penetrate a building enclosure three conditions must exist simultaneously; there must be water on the wall, a route for it to travel on, and a force to move it (Killip & Cheetham, 1984). The entry of moisture into the external envelope of a rammed earth building can be caused by a number of different mechanisms primarily wind-driven rainfall, condensation (dew), infiltration & absorption from the surrounding ground, and from general building use (Walker & Standards Australia, 2002). Moisture ingress can occur in rammed earth walls due to capillary suction, as with any porous building material. Mechanisms such as gravity, surface tension, and hydrostatic pressure can also induce moisture ingress, although the key to water-infiltration resistant design is an understanding of the effect of pressure differential on and within buildings (Oliver *et al*, 1997).

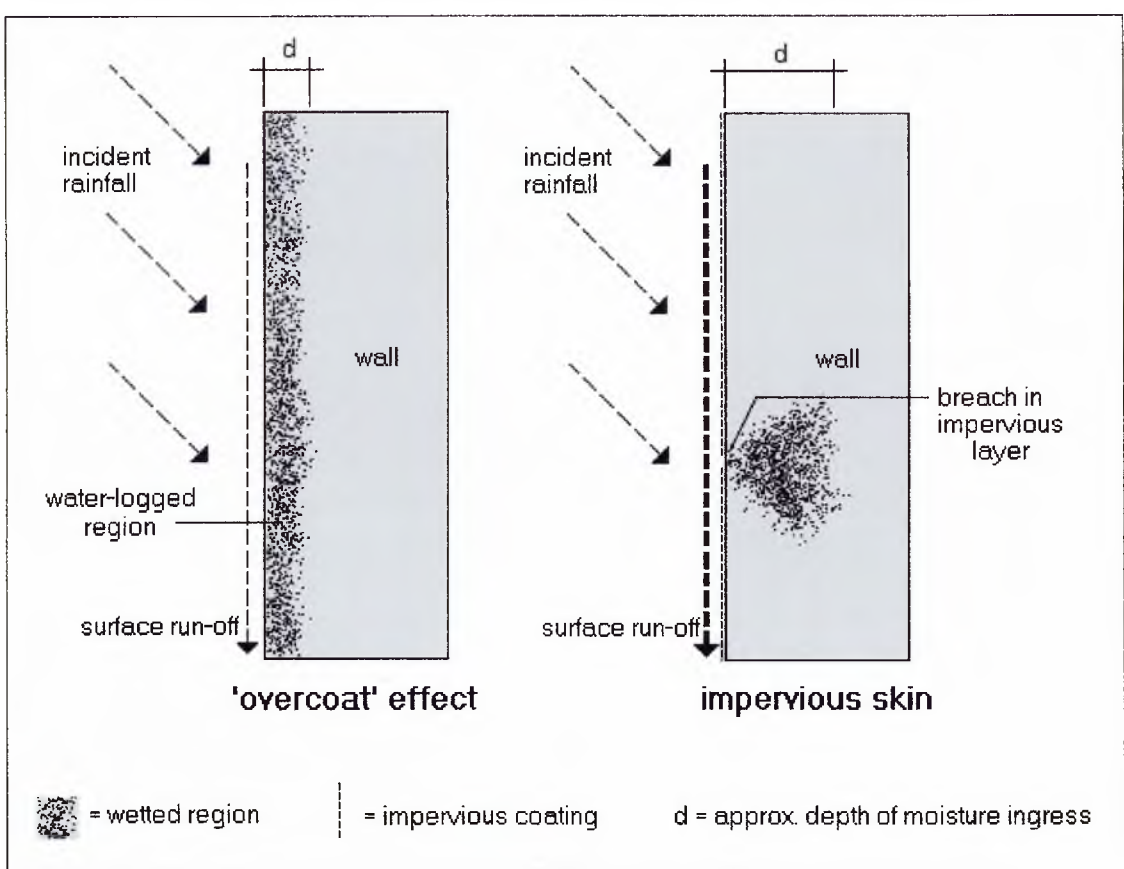


Figure 3 Illustrations to describe the ‘overcoat’ effect and the impervious skin on masonry walls

A solid (non-cavity) masonry wall naturally relies upon what is commonly referred to as the ‘overcoat’ effect to resist moisture penetration, as illustrated by Figure 3. This is when the region towards the exterior façade becomes saturated (i.e. waterlogged) to a certain depth such that little or no water can further penetrate beyond this wetted region. In the case of rainfall, the volume of surface run-off increases because the incident moisture can no longer be absorbed by the already saturated wall surface layer.

An alternative situation is the ‘impervious skin’ whereby the outer surface layer of the material is made completely impervious to water penetration (see: Figure 3). This can be achieved on porous masonry façades by, for example, treatment with a silicone-based emulsion, oil-based masonry paint, bituminous paint, or a similar suppressive treatment. However, it relies upon the durability of the thin impervious layer together with non-interruptions of it by appropriate construction detailing at joints etc. Any zone of

weakness in the impervious layer can result in the concentration of moisture penetration in this region. This effect is often exacerbated significantly with the combined effect of a pressure differential. The same volume of moisture may not have presented a problem on an untreated wall where it can be dissipated across the entire wall face through the absorption qualities associated with the overcoat effect.

A problem that often occurs with the impervious layer is in the fact that it inhibits dissipation of moisture held within the wall and, in this scenario, can cause spalling of the façade due to the accumulation of confined water pressure and/or salt crystallisation. A new breed of commercially available ‘impervious skin’ products are described as micro-porous and have significantly reduced some of the problems identified above due to their improved ‘breathe ability’ that allows the passage of moisture vapour.

2.2.6 Deleterious Effects of Dampness

Rammed earth is porous, as are many other masonry construction materials, and as such the sorption and desorption of moisture and its subsequent movement lie at the root of a number of engineering problems in construction materials. Penetrating damp is a particular problem in the United Kingdom where it is estimated that the volume of penetrating damp accounts for by far the largest amount of unwanted moisture that affects buildings (Oliver *et al*, 1997). The maximum water absorption of bricks has been specified for colder climates to limit frost damage (Walker, 1996).

Airborne moisture, both in the form of vapour and precipitation, is the largest cause of penetrating dampness due to the sheer quantity of water under consideration (e.g. total average annual rainfall). Absorbent units can significantly increase the dead loading of

external walls, but this is unlikely to be a problem in most earth construction (Walker, 1996). However, inherent difficulties exist in making the external envelope of buildings watertight using construction materials that are porous. The large volumes of water under consideration often result in extensive damage and numerous deleterious effects. Some of the various physical and chemical aspects of these effects are listed below (Oliver *et al*, 1997):

Physical:

- Water staining on wall interiors (e.g. tidemarks)
- Internal finishes damaged (e.g. wallpaper)
- Damage caused by cyclic wetting & drying – blistering and cracking instigated by dimensional fluctuations
- Freeze/thaw damage of damp masonry materials
- Rotting of timber, e.g. lintels, door frames etc
- Decreased thermal performance/efficiency of insulation material
- Uncomfortable and unhealthy ambient air conditions inside the affected building
- Electrical installations damaged and/or rendered unsafe for use

Chemical:

- Some loss of adhesion between binding agents and aggregates in the earth material, particularly when unstabilised
- Potential for sulphate attack of Ordinary Portland Cement (OPC) where used, e.g. in cement stabilised soils
- Efflorescence (re-crystallisation of soluble salt species as surface deposits)
- Corrosion of metal(s) – where present, e.g. steel reinforcement, conduit

2.2.7 Existing Solutions for Rammed Earth Structures

Various solutions currently exist whereby the resistance of rammed earth walls to moisture ingress & migration can be increased. These include elements of building design, particularly at the levels of both foundations and roof eaves. In addition, various admixtures are available to blend with rammed earth soils prior to compaction that can be used to enhance their moisture resistance. Finally, a variety of different surface treatments or render applications are available to enhance the durability and moisture ingress resistance of rammed earth wall façades.

2.2.7.1 Building Design

The foundations for a rammed earth wall, in conventional terms, are no different to those that would normally be constructed for any other type of masonry wall. It is quite common, however, to construct the sub-damp proof level section either from concrete, brick or a similar more durable material. The construction detail for this applies to cement-stabilised rammed earth only and complies with the Building Regulations (2002) for England & Wales as shown in Figure 4 (Hall, Damms & Djerbib, 2004).

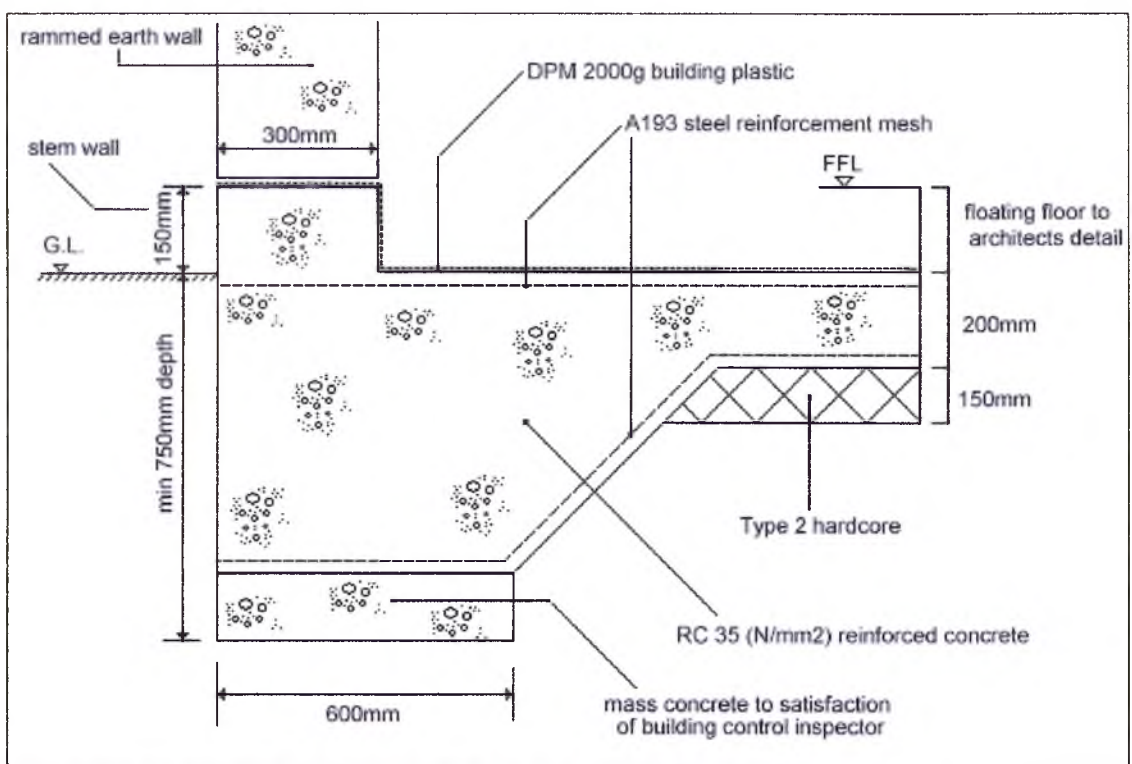


Figure 4 a cross-section of the foundation details for Brimington bowls pavilion

The main purpose of the stem wall protruding above ground is to provide a point on which to clamp the first course of formwork. In countries such as Great Britain where conditions such as basal dampness, rainfall splash back and even temporary flooding are likely to occur, the concrete stem wall (or kicker) should project a minimum of 150mm above ground level. This protects the rammed earth from prolonged wetting and excessive erosion and demonstrates compliance with Approved Document C of the Building Regulations (2000). The 2000g DPC and DPM were specified in order to ensure that the building was fully protected from the potential of penetration by Radon gas. Where there is the threat of Radon this design also necessitates the provision of sealing rings around any holes in the DPM where, for example, service risers (e.g. water, waste, telecomm. etc) enter the building through the floor slab.

The DPC is laid on top of the stem wall and then securely clamped in place with the formwork to enable the rammed earth wall to be built on top. The DPC should be a

thick bituminous-type material if possible to resist puncturing or indents from pebbles being rammed into it. It can also be tied in with the damp proof membrane from a solid floor slab construction as normal. If a different aesthetic is required then an alternative approach would be to cast the concrete foundations to ground level and build the 150mm stem wall out of engineering bricks or stone. Where potential concerns exist relating to moisture accumulation at the base of the wall, the threat of moisture ingress may occur due to the phenomenon of capillarity. The resistance of the wall material to capillary moisture absorption can be accurately assessed using the initial rate of suction (IRS) test.

A common detail used for surrounding the foundations of earth buildings is to provide a French drain. This typically consists of 600mm deep backfill of pea gravel or limestone chippings that allows any rainwater or basal flooding to percolate through the ground drain. In addition to a raised stem wall, this further reduces the risk of erosion or water accumulation around the base of an earth structure. For the Brimington project, a perforated tube was buried inside the French drain and connected to the rain water sewer pipe. Another common design feature of rammed earth buildings is in the roof design. The roof overhang at eaves height is typically greater than 200mm, which is slightly more than generally used with conventional buildings. Although the guttering will catch rainfall run-off the additional overhang protects the earth walls from the erosive effects of wind-driven rain.

2.2.7.2 Admixtures

A number of proprietary admixtures can be used with rammed earth to enhance its physical and engineering properties. It is possible to make the soil more impervious to water penetration by filling the pore structure, as well as any cracks, with a water-

repellent agent such as bitumen. Bituminous emulsion has been effectively used to make waterproof adobe, or sun-dried mud brick (commonly termed 'Bitudobe' in the USA). However, bituminous emulsion is difficult to mix with rammed earth because of the low moisture content required for rammed earth soils and the viscous nature of the bitumen. It also has other disadvantages in that it is black and can look unattractive as parts of a 'natural' rammed earth wall. According to CSIRO (1987), results from American tests suggest that bituminous stabilisation neither increases nor decreases the strength of the earth material when it is dried. It mixes quite readily with soils of moderate to high clay content where an even and complete distribution of the bitumen is obtainable if the soil is first made very wet.

Another technique is to disperse a material in the soil mix that expands upon contact with water to fill the voids and cracks when needed, e.g. bentonite. This is thought to be a very good method for use in very sandy soils due to their high degree of porosity. Conversely, it is also thought to be a poor choice for silty clays due to the high specific surface area of soil particles (Houben & Guillaud, 1996). Bentonite is essentially a natural clay-based material that is often used for tanking in basement situations.

The commercial suppliers of performance enhancing additives in Australia has responded to the entry of earth buildings into the mainstream construction industry by providing a range of products designed to suit these materials. Emulsion KR2 is a solvent-free aqueous silicone emulsion from the Tech-Dry® brand by Building Protection Systems Pty Ltd (Australia). It is designed for use as an admixture to be used with pressed/dry concrete or rammed earth materials. It is a milky white liquid that is miscible in water and significantly reduces permeability and efflorescence when used in only small quantities of between 0.25 and 1.0 litre per 1000 kg of dry mix ingredients.

Research has concluded that this product can reduce water absorption by up to 80% in pressed earth materials, and also has the effect of increasing compressive strength (Kebao *et al*, 1997).

2.2.7.3 Surface Treatments

Polyvinyl acetate (PVA) is soluble in water and can be easily diluted to form a sealing wash that can be applied to the surface of the wall either by brush or by spray. The PVA glue is normally diluted with between four and five parts water. It is often used by interior plasterers as a primer/sealing coat prior to painting. As with the stabilising admixtures, many commercial manufacturers in Australia and the USA have responded to the entry of modern rammed earth into their mainstream construction industry by supplying a number of patented surface treatments. The use of either raw or boiled linseed oil is sometimes recommended as a rammed earth wall treatment (Minke, 2000). Linseed oil, when applied to rammed earth, reduces dusting and enhances moisture resistance although the amount of oil required may prove to be expensive.

Proprietary masonry paints can be used on either interior or exterior rammed earth walls to create the desired appearance and finish. These are typically water-based paints with low toxicity but can suffer from blisters and peeling when trapped moisture cannot escape from within the substrate (wall). It is a cheap form of wall decoration but is one that requires regular maintenance. Water glass is a water-soluble substance consisting of sodium silicate ($\text{Na}_2\text{O}\cdot x\text{SiO}_2$) and is available commercially and is normally found as a stony powder or as a thick, syrupy liquid. It is typically used as a cement/adhesive and can be dissolved in solution and applied to the interior/exterior of rammed earth walls to act as a protective coating that enhances durability and water-tightness. It has been used experimentally with extremely limited success by some rammed earth contractors,

mainly due to the typical problems associated with non-breathable sealants, e.g. cracking, spalling and localised water ingress/erosion.

Lime wash is traditional surface treatment and basically consists of slaked lime that has been mixed to a thin slurry (or wash) and then applied to the wall with a brush. It is normally used in addition to a traditional lime render and, owing to its low durability, needs biennial renewal and can rub off onto clothing. The process of glazing a rammed earth wall is similar to the traditional technique once applied to pottery. A glaze was applied to the exterior façade of the rammed earth walls on the Brimington project. It was made from pulverised clay mixed, fine sand and cement then mixed with water to produce a thick paint and applied by brush. It can be used to give a more uniform, earthy tone to the wall finish that can hide the layers of compaction and conceal any patch repairs.

2.2.7.4 Renders

Sand/cement renders are generally the most common form of exterior render used in modern construction. They are very strong and durable, and are relatively cheap due to the low cost of cement and availability of a skilled workforce that are available to do the work to a high standard. Sand/cement renders can typically be applied in successive coats using a float, or they can be applied as a pebbledash or Tyrolean finish. If the render is applied by floating, the golden rule is the undercoat should be stronger than the top coat to reduce the chance of shrinkage cracking and delamination. Typical mix proportions are sharp sand to cement ratios of 6:1 for the floating coat, followed by builders sand/cement at 8:1 for the finish coat. The floating coat must always be scarified with a devil float or similar, prior to the application of the finish coat, in order to provide a key. The finish coat can be floated smooth or it can be textured with a wet

sponge to give a more rough-textured surface finish and this helps to reduce the risk of cracking as it cures. A pebble dash can either be achieved by ‘dashing’ the wet render with clean pebbles or by mixing the pebbles with the render and applying it as a textured coating. A Tyrolean gun is basically a hopper with paddles inside that flick the wet mix through a spout onto the wall, and this produces a distinct texture similar in appearance to that of porridge.

Although stucco was once the term applied to fine interior plasterwork, it is now also understood to be a very smooth, plastic exterior render that is composed of sand, lime and cement. A stucco render must be applied in the same way as a dagga in that it requires a good key to allow it to adhere, and a dampened wall surface to prevent premature drying out of the render during curing. This type of render can be floated to provide a smooth surface, or sponged as required. If the surface of the render is required to be very hard then this can be achieved by building up the render using several thin layers, each with increasing levels of cement content. Stucco renders are often whitewashed or painted white to accentuate the clean finish and smooth texture.

Lime renders are much more suitable than a cement render for an unstabilised earth wall because they are more permeable and allow moisture trapped within the wall to escape through evaporation. This characteristic of lime renders is often termed ‘breathe ability’ although more precisely it is simply a high degree of permeability. It is recommended that lime putty render should only be used indoors due to lack of durability and the fact that it will not cure in the presence of moisture, unless it is stabilised with a little cement or some form of pozzolan, e.g. brick dust (Bleaklow, 2003). To illustrate this point, unlike cement a lime render can be ‘knocked up’ and reworked even when it has been

mixed and stored for some time. This is because carbonation is such a slow process and no hydration reaction takes place unless cement or a pozzolan has been added.

NHL (naturally hydraulic limes) can be used for exterior render, and are commonly used with natural fibres (e.g. goat's hair) as a reinforcement to prevent cracking during drying, although it is often very difficult to mix. The floating coat is normally proportioned using grit sand to NHL ratios of 3:1 with some natural fibres added. The top coat is normally mixed using builder's sand/NHL at 1:1 and can be floated smooth. Unlike a cement render, the top coat is considerably richer than the float coat. Unless a great deal of aftercare is used with lime renders they are very prone to cracking, crazing and delamination. Aftercare involves covering the render with a tarpaulin or damp sheet and even necessitates regular spraying with a water trigger gun to prevent excessive cracking occurring as the render dries and cures. It is the length of time invested in aftercare (2-3 days), along with the slow production rates, that can make lime renders economically unattractive to the majority of modern contractors.

Dagga (sometimes referred to as Dogga) is essentially a traditional earth render that is popular in Africa and typically comprises three parts fine sand to one part clay (Williams-Ellis, 1999). If the weather is very hot and dry, particularly with full sunshine, the fresh render may need to be covered by a tarpaulin or damp Hessian sacking to prevent it from cracking. Dagga renders will not withstand driving rain and require further surface treatment if they are to be exposed to these conditions. The main advantages of a dagga are in its low cost and low embodied energy. Any render that falls away from the wall in subsequent years due to weathering can be collected and reapplied as part of the building's maintenance programme; an advantage that is particularly suitable for developing countries.

Traditional dagga render can be enhanced with the addition of a stabiliser in order to make it significantly more durable and to make it a more suitable technique for modern earth buildings in the developed world. Cement stabilisation is perhaps the most obvious way of enhancing a dagga render, although the strength of the mix should be limited to one part cement to every four parts of dagga components, e.g. 1: 3: 1 (cement: sand: clay). The problems of rapid drying are also increased for cement-stabilised dagga as water is consumed in the cement hydration reaction, and the material is more prone to shrinkage cracking due to its increased stiffness.

2.3 MOISTURE INGRESS MECHANISMS IN BUILDINGS

Due to the relatively high profile of issues such as rising damp and condensation in the United Kingdom, it is easy to overlook the third and most significant source of moisture ingress: penetrating damp. It is a particular problem in the United Kingdom where it is estimated that the largest amount of unwanted moisture that affects buildings is that which has somehow penetrated the external envelope (Oliver *et al*, 1997).

Traditional masonry wall construction materials, such as brick, stone and earth, have complex pore structures that can provide a number of tortuous routes for moisture to migrate through. The initial penetration of moisture through the external envelope of a building, and the subsequent migration of this moisture, can be caused by a number of different mechanisms. These mechanisms can either work independently, collectively, or perhaps even cyclically with one another. Some mechanisms are more dominant than others, in that their effects are significantly pronounced or represent the secondary effects of an event that is more common.

2.3.1 Gravity

Excluding other influences, rainwater that lands on the exterior surfaces of a building will be induced towards the ground due to the force of gravity. When the force due to gravity acts upon water that is on the wall surface or in large capillaries it may tend to pull it through any passages that lead downwards and inwards (Killip & Cheetham, 1984). This is apparent in the case of surface run-off, although the influence of gravity upon this water will always guide it along the route that conserves the largest amount of energy (i.e. the easiest route). If there is a crack in the wall or there is defective pointing, then the water could flow down these routes and expose the weakness by penetrating the external envelope of the building element. The water will only penetrate, and continue to move within the material (due to gravity) if the defect has a downward gradient and only if the path offers less resistance to flow than its current one.

2.3.2 Capillary Action

The internal molecular forces of a material may be termed cohesion, and the forces of attraction that exist between the molecules of dissimilar materials may be termed adhesion. Water has very little cohesion, and so if the adhesion forces between water and a dissimilar solid (e.g. glass) are greater than the intermolecular forces within the water, then the surface of the glass becomes “wet” (Bowles, 1984). A given quantity of water behaves as though the surface was a tightly stretched skin. This is a phenomenon known as surface tension and is the reason why discreet quantities of water that are in contact with the atmosphere form droplets, as illustrated by Figure 5.

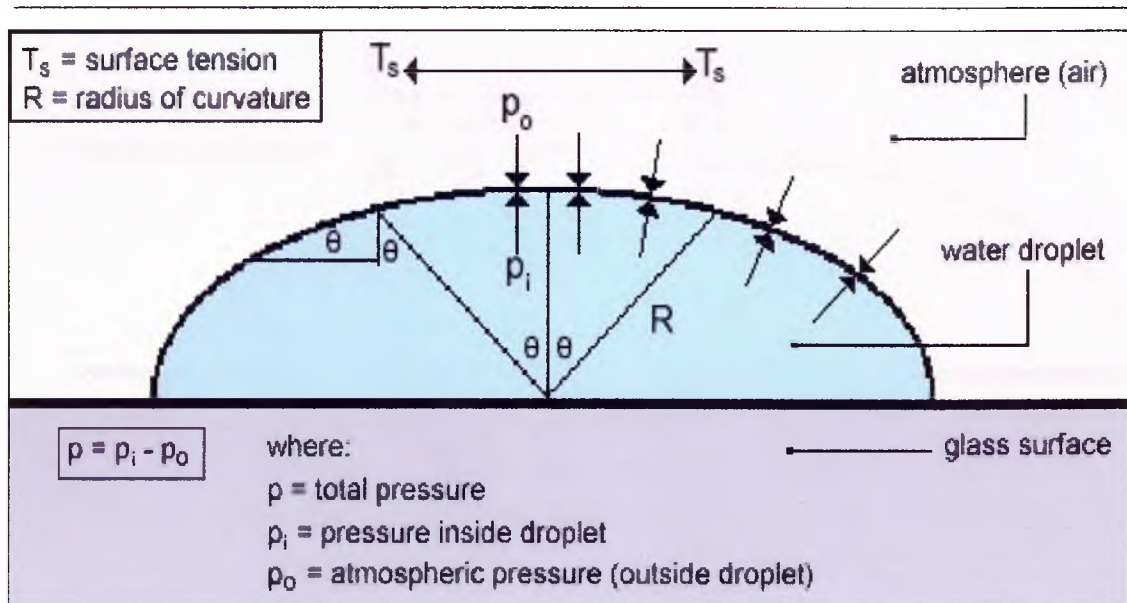


Figure 5 the parameters of water droplet formation due to the forces of surface tension (adapted from Bowles, 1984)

The formation of droplets occurs because the internal intermolecular forces of the water are in equilibrium with the atmospheric pressure of the surrounding air. Since the thickness of the surface tension 'skin' is molecular, it follows that the unit surface tension is force/length (Bowles, 1984). The internal/external pressure difference, known as p (where: $p = p_i - p_o$), inside the curved surface of the droplet is directly proportional to the surface tension T_s , and therefore inversely proportional to the radius of curvature R (see: Figure 5). This is shown by the equation below where:

$$p = \frac{2T_s}{R} \quad \text{Equation 1}$$

Capillarity (or capillary action) can be defined, therefore, as being the movement and/or retention of a liquid inside a vessel (e.g. a pore) due to the attractive forces of surface tension that exist between the two dissimilar materials, e.g. water and glass. The classic example used to illustrate this effect is that of a hollow open-ended glass tube into a container of water (see: Figure 6).

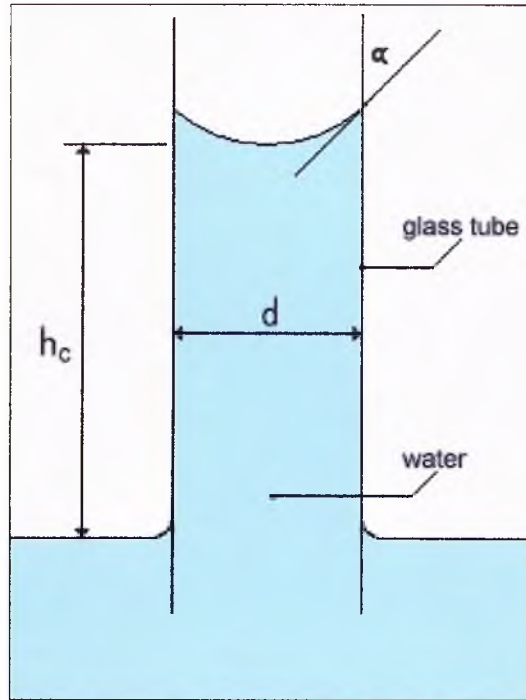


Figure 6 capillary rise of water in a glass vessel

Due to the effects of surface tension, the water climbs up the inside of the tube, unless impeded, to a maximum height (h_c). The top of the liquid forms a concave meniscus due to the more localised effects of T_s on the region of water closest to the tube. The angle of concavity (α) in the surface between the surface film of the meniscus and the tube walls is assumed zero for water, although it has been exaggerated in Figure 6 for the purposes of illustration. The maximum height of capillary rise (h_c) can be calculated in centimetres using:

$$h_c = \frac{4T_s \cos \alpha}{\gamma d} \quad \text{Equation 2}$$

Where:

T_s = surface tension (dynes/cm)

γ = unit weight of fluid (kN/m^3)

d = tube diameter (cm)

For water at 20°C: $T_s \cong 72.8$ dynes/cm, $\gamma = 9.7896$ kN/m³, and so the following simplified expression is obtained:

$$h_c = \frac{0.29746}{d} \qquad \text{Equation 3}$$

To illustrate the process of moisture ingress in porous building materials by capillary suction Hall (1977) used the classic example of a dry brick that has been placed in a shallow tray containing clean water (i.e. the initial rate of suction test). From the moment this is done water is absorbed into the brick by capillary action, and then it attempts to distribute itself throughout the pore network of the brick itself. The imbibed water partially displaces the air that previously occupied the dry pores, whilst at the surfaces that are not immersed the process of evaporation has begun to occur. At this point, equilibrium can be achieved between capillary water absorption and evaporative loss.

Evaporation entails cooling at the boundary surfaces, which results in a heat flow process being generated inside the brick. The resultant heat gradient modifies the rate of flow of moisture inside the brick through what is essentially a thermal pumping effect. Soluble salts are often dissolved and re-deposited at the surface where evaporation is occurring; the resultant crystalline deposits are referred to as efflorescence. As the pore structure of a material approaches saturation, the capillary suction begins to approach zero (Killip & Cheetham, 1984). The only exception to this occurs where the capillary pressure is simply counteracted by the pressure of entrapped air in a duct that is sealed and has no outlet.

Vos & Tammes (1968) performed various experiments on the capillary movement of water and concluded that, amongst other things, water moving through a porous material by capillarity could travel twice as far in a horizontal direction than in an upward direction. This is because the direction of flow is perpendicular to the force of gravity and so its effect in opposing the flow is at a minimum. If a temperature gradient exists along a capillary, the flow of water within that capillary will occur in the direction of the lower temperature (Vos & Tammes, 1968). This is because the surface tension of the capillary wall material is a monotonously decreasing function of temperature. This occurs because of the principles surrounding the conservation of energy in a system. A typical example of this is a pocket of water that is held within a hypothetical capillary of uniform diameter. If one end of the capillary is heated, the water moves towards the colder end in order to conserve its own energy.

Similarly, water that is held within a capillary of uniform temperature, but that has a tapering diameter, will tend to flow towards the narrower end of the capillary due to the 'effective' increase in surface tension. The actual amount of surface tension in the walls of the capillary is the same, but it has a greater effect when the diameter of the vessel is narrower because the volume of water that it acts upon is decreased. Consequently, if two capillaries communicate with one another, moisture transfer will occur between the materials with larger pore diameter towards those with the smaller pore diameter. This occurs until the gradient of unequal surface tension between them has been resolved through equilibrium (Vos & Tammes, 1969).

Obviously where large volumes of rain are incident upon wall façades, and when surface run-off occurs, the water meets with the entrances to a vast number of

capillaries and pores in the substrate material, e.g. rammed earth. The surface tension of the porous material draws the moisture into these vessels and the result is the absorption of moisture by the wall material. This same mechanism can operate in reverse to expel water from the pore network if a temperature gradient is created, for example. The forces exerted on the water vary considerably depending upon the diameter of the pore into which it is drawn.

2.3.3 Kinetic Energy

In the presence of air currents, and especially in severe windy weather, rain can be driven onto the façade of a wall at very high velocity causing erosion of the surface material. The maximum release of kinetic energy occurs at an angle of 90° (i.e. perpendicular to the wall surface), but the removal of particles from the wall may be increased by an angle lesser than this which effectively results in a ‘prising’ or chipping force (Heathcote, 1995).

Where defects exist in the wall face, or are created by the erosive forces of the wind-driven rain, water can be forcefully propelled into the material(s) simply by means of the kinetic energy it holds. If the openings in the wall remain small, however, the raindrops will be shattered upon impact and only the smaller droplets may continue to ingress (Killip & Cheetham, 1984). The combined erosive potential of wind-driven rain serves to exacerbate any weaknesses in the wall that allow moisture penetration such that they can be further exploited. However, it should be emphasised that if a through-path in the external envelope does not exist then water cannot pass through a wall solely under the influence of kinetic energy (Killip & Cheetham, 1984).

2.3.4 Hydrostatic Pressure

Hydrostatic pressure is exerted by, or existing within, the body of a liquid that is at rest with respect to adjacent bodies (Gove, 1993). Problems can occur where there is a significant, localised accumulation of moisture in or around porous building materials. A typical example of this would be a localised pocket of melt water or blocked guttering that effectively acts as a reservoir. The hydrostatic pressure exerted by the mass of the accumulated water body can result in percolation of moisture through nearby porous masonry materials (Oliver *et al*, 1997). In addition, the volume of moisture can continue to expand until it exposes another defect that would not exist under normal weather conditions, e.g. underneath flashing and overlapping tile joints at the eaves. If the source of water is at any point above the height of the point of ingress, then the difference between these points is translated as a constant head of pressure.

2.3.5 Air Currents & Pressure Differential

The volume of rainwater that falls upon a wall is much less significant in instigating penetrating damp than is an applied pressure differential (Oliver *et al*, 1997). If the material of the external wall is porous then the wall may become very damp in the presence of wind driven rain. This creates a cooling effect at the outer face of the wall and, more significantly, a pressure differential between the inside and the outside of the building. Assuming that the wind cannot pass directly through the fabric of the wall and affect the interior, some of the air becomes displaced in a turbulent flow and is redirected around the perimeter of the wall. This can often create a negative pressure zone on the sheltered elevation of the building (Oliver *et al*, 1997). It may also be possible for a suction force to be developed within the fabric of solid porous masonry walls when they are subjected to a pressure differential. These are very significant

factors in determining the penetration of moisture through masonry walls, as illustrated in Figure 7.

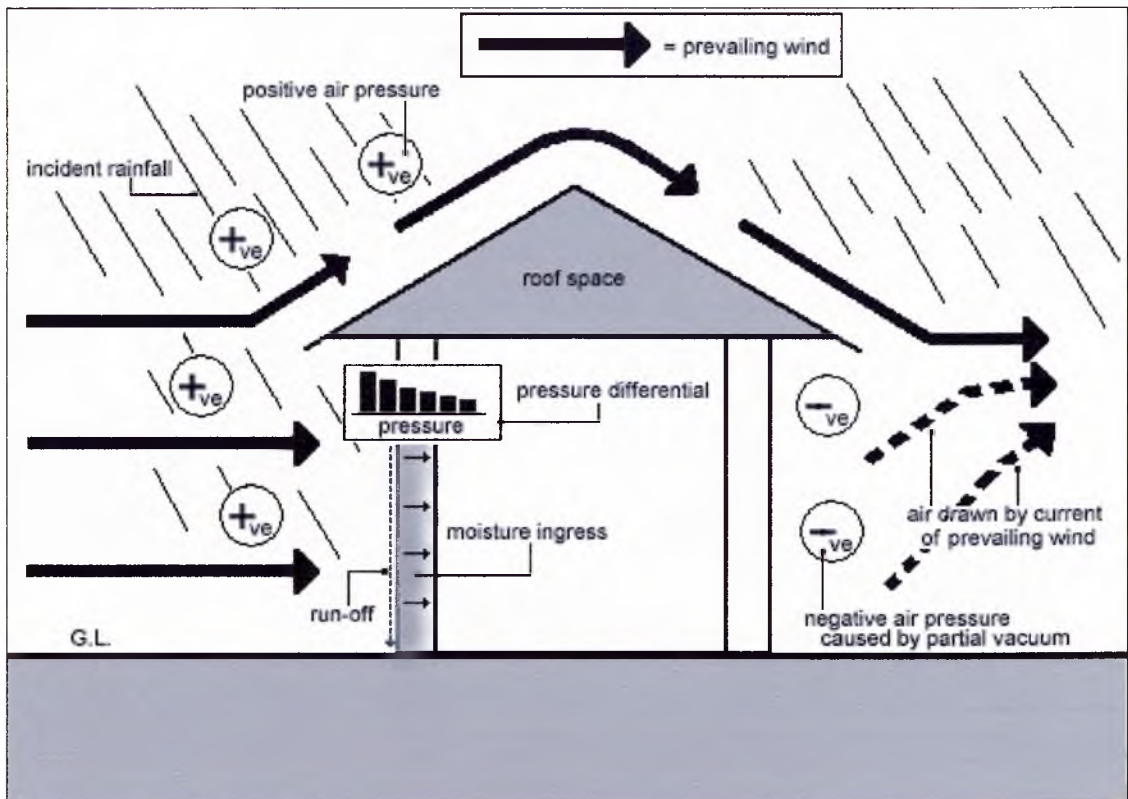


Figure 7 illustration of prevailing wind affecting incident rainfall angle and creating a pressure differential within the external walls of a building

External air pressures can become very large on the outside of a building because the incident winds exert a force on the walls by actually pushing the air up against them. The subsequent accumulation of this force results in a localised increase of the air pressure in this region. Since the air pressure at the interior of the building remains constant a pressure differential has effectively been established between the interior and the exterior face of the wall. The air pressure can easily induce moisture to penetrate and migrate through the external envelope of a building. According to the laws of thermodynamics it will prefer to move in the direction of least pressure (i.e. the interior) in order to conserve the maximum amount of energy in the system.

A wall subjected to a slight mist could still develop significant leaks if exposed to a large pressure differential, whereas a wall that is affected by a torrential downpour may not leak at all if there is little or no pressure differential. Proof of this theory exists in the form of tall buildings (e.g. skyscrapers) where the upper floors are much more susceptible to water leaks than the lower floors. This is due to the greater pressure differential that exists between the interior and the exterior of the building at higher altitudes (Oliver *et al*, 1997). This occurs because there is less shelter provided by surrounding buildings and the wind velocity is much greater. There are much fewer moisture ingress problems in the lower floors of these buildings in spite of the fact that rainfall surface run-off water at this point has much greater volume and velocity due to the effects of gravity.

2.3.6 Other Contributory Factors

The mechanisms with which moisture penetrates the external envelopes of buildings that have been discussed above are also affected, and often assisted by, other contributory factors. These factors can relate to issues within the context of the building itself as well as certain human factors that influence the building both during the course of its construction and during its life span. The location of the building, for example, is highly significant because it determines the ambient weather conditions to which it is subjected. The macroclimate of a building site in the UK can vary greatly in terms of the degree of exposure, average annual rainfall, and even mean seasonal temperatures. The site could vary from being coastal or inland, up on a hill or down in a valley, and can even enjoy significant benefits of the unusually mild weather conditions provided by the Gulf stream (e.g. the Western Isles).

Within the context of the United Kingdom, it is fair to say that a building constructed in the north-east of Scotland will, on average, be subjected to much higher velocity winds than the same building constructed in Cornwall in the south-west of England. However, the microclimate of the site on which the building is constructed will determine the level and frequency at which the macro-climatic effects will interact with the building. If the example building in the north of Scotland is built in a sheltered location behind a steep incline under a localised rain shadow it is quite likely that it suffers less detrimental exposure to certain weather conditions than the same building in Cornwall built on a completely exposed site. The microclimate of the building site can also be altered and enhanced by using careful choices regarding landscaping and tree planting. The careful positioning of slatted fencing can shelter the building from the full effects of prevailing winds.

2.4 FUNDAMENTALS OF MOISTURE INGRESS THEORY

Moisture can enter, and move within, the fabric of porous construction materials by a variety of different processes. The generic term ‘sorptions’ encapsulates the occurrence of both absorption and adsorption. Absorption literally means ‘to swallow up’, and in this context occurs when moisture is taken into the body of a porous material e.g. by capillary action (Gove, 1993). In comparison, adsorption in this case is where the moisture is taken up by (or attracted to) the surface of a porous material due to the phenomenon of surface tension.

2.4.1 Porous Building Materials

Porous materials are often permeable by air and moisture because they contain a network of open channels. According to the Building Research Establishment Digest

269, there are two classifications for these channels dependent upon their diameter. A channel with a nominal diameter of 5 microns or above is classed as a *pore* whereas a channel with a nominal diameter of less than this value is classed as a *capillary* or a *micropore* (BRE, 1983). It should be noted that pores and capillaries are not cylindrical but in fact often exhibit a high level of tortuosity (Laycock, 1997). They may also be interlinked; the extent of which largely determines the permeability of a porous material.

Analysing the movement of moisture inside a porous structure can become extremely complicated due to the multitude of different factors that can be considered. However, Hall (1977) observed that for the purposes of study we can simplify matters considerably by hypothetically assuming the solid material of a porous building material to be assumed inert (i.e. no mass transfer occurs), and that specific boundary effects and dissolved atmospheric gases in the water are ignored. The role of the solid porous material is then reduced to acting simply as a network of pores and capillaries that partially constrain the boundary surfaces of the water phases. The system then contains a single material – water – that may exist in any combination of solid, liquid or gaseous form (Hall, 1977).

The volume fraction porosity (f) can be defined as the total void space in a porous solid, including isolated pores/capillaries and those that are non-continuous (i.e. dead ends). The actual void space that is accessible to a penetrating liquid/gas has been defined here as the apparent porosity (f_{ap}). The values of f and f_{ap} are not necessarily the same for the simple reason that not all pores are permeable. The most accurate way of determining apparent porosity (f_{ap}) may be through separate weight determinations of a specimen both when dry and when fully vacuum saturated. Assuming that the bulk porosity is

already known, this test measures the amount of permeable pore space in a material by determining w_{sat} . The conventional way for determining f is illustrated by the diagram in Figure 8.

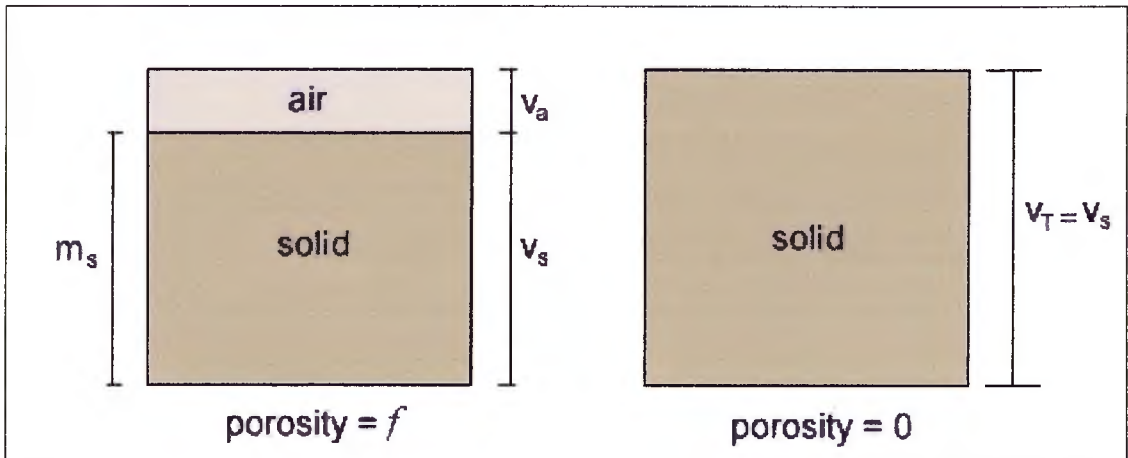


Figure 8 illustration of the volume fraction porosity (f) in a rammed earth cube sample oven-dried to constant mass

In rammed earth cube sample that has been oven dried to constant mass, the dry mass (m_d) is equal to the mass of the solid components (m_s) since the air in the sample is assumed to have zero mass. The volume of air (v_a) is equal to the total cube volume (v_T), where for a cube sample $v_T = 1$ litre, minus the volume of the solid (v_s). Figure 8 demonstrates that in a theoretical 1 litre cube sample with zero porosity ($v_a = 0$), the total mass is equal in value to the particle density (ρ_s) of the solid soil components ($m_s = \rho_s \cdot 1$). Consequently, the volume fraction porosity (f) of a cube sample can be expressed as:

$$f = \frac{1}{\rho_s}((\rho_s \cdot 1) - m_s) \quad \text{where: } 0 < f < 1 \quad \text{Equation 4}$$

2.4.2 Reference Moisture Content

The specific moisture content w of the idealised porous solid (defined above) can be determined using the following simple equation where m_w denotes the mass of water and m_s the mass of the dry solid:

$$w = \frac{m_w}{m_s} \quad \text{Equation 5}$$

In practice, the value of m_w is determined gravimetrically as the difference between the total mass of the sample when it is oven dried to a constant mass at 105°C, and when it is wet.

In simple terms, the conventional description for the specific moisture content of a porous material comprises two states: ‘hygroscopic’ moisture that is adsorbed to the pore’s interior surfaces and ‘capillary’ moisture that is absorbed into the pore cavity itself. The value for the specific moisture content ranges from w_0 ($w = 0$) up to w_{max} ($w = \text{maximum}$). Its position between these two points falls within a certain domain, which tells us the predominant state of the water at this value. This description has been illustrated by the diagram in Figure 9.

w_0	w_h	w_{cr}	w_{sat}
Artificial drying	Hygroscopic domain	Capillary domain	Pressure wetting

Figure 9 Reference moisture contents in porous building materials (Diagram: adapted from de Freitas *et al*, 1996)

A water content that exists somewhere within the hygroscopic domain (between w_h and w_{cr}) predominantly exists in the form of moisture vapour or condensed moisture that has been adsorbed by the surfaces of pores. The transition from the hygroscopic domain to the capillary domain (between w_{cr} and w_{sat}) occurs where liquid water is present within the pore spaces due to absorption and/or sufficient accumulation of condensed hygroscopic water vapour. w_{sat} is the point at which the porous solid has absorbed the maximum possible amount of liquid water due to capillary suction under normal atmospheric conditions, i.e. saturation. The theoretical point of maximum moisture content (w_{max}) is rarely achieved under natural conditions, except through prolonged vacuum saturation of the specimen to ensure that all permeable pore spaces are occupied by water. Indeed, a degree of vacuum saturation is normally required to achieve any moisture content above the value w_{sat} . In contrast to this, a completely water-free state (w_0) is only achievable through prolonged oven drying of the specimen at 105°C until constant mass is achieved. In the nominal dry state (between w_0 and w_h) a small degree of hygroscopic water remains.

2.4.3 Moisture Transfer Process

The moisture transfer process within a porous material depends upon the climatic conditions (e.g. relative humidity) and the moisture content of the material itself. The transition from hygroscopic water to capillary water, for example, is part of the mass transfer process. The six different stages of reference moisture content that control the moisture transfer process are illustrated by Figure 10.

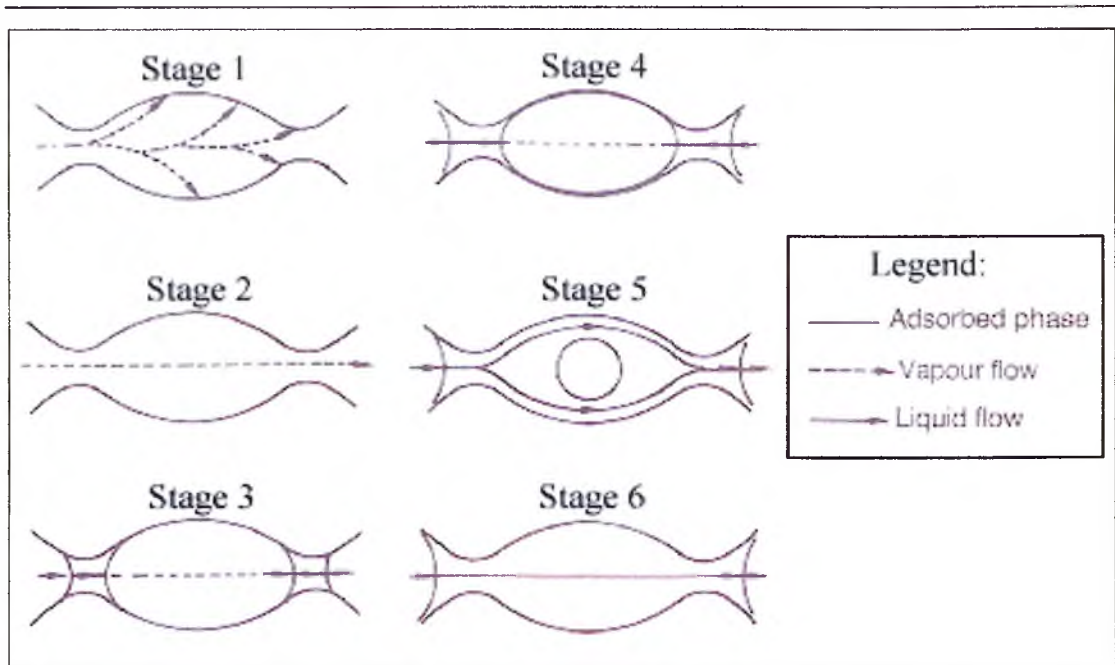


Figure 10 illustration of the process by which moisture ingress and movement occurs in the pore space of an initially dry permeable material (Diagram: adapted from Rose, 1965)

Moisture transfer depends on the degree of saturation inside the pore space(s), the six stages of which are defined here (adapted from Domone, 1994_c):

- Stage 1** Very low humidities; the moisture is in vapour state and is adsorbed to the interior surface of the pore space.
- Stage 2** The pore walls have fully adsorbed as much water vapour as possible and vapour flow through the pore space can occur when it is motivated, e.g. by a pressure differential or temperature gradient.
- Stage 3** The humidity within the pore space increases to the point where condensation occurs at the restricted part of the pore (e.g. at the neck, in the case of the diagram above). This shortens the distance that the moisture vapour must travel and so flow rates are increased.
- Stage 4** The areas of condensed water begin to expand and the flow is augmented by flow within the adsorbed moisture layers.

Stage 5 Liquid flow begins to occur in a non-saturated state and the pore space begins to fill with liquid moisture.

Stage 6 The pore space is completely saturated and full liquid flow occurs when a motivational force is applied, e.g. a pressure differential.

Movement of moisture in masonry walls is controlled both by the wall fabric and by discontinuities (e.g. fracturing) within the material (Laycock, 1997). In terms of the mechanisms of moisture movement we are dealing with a single fundamental process, the movement of water through a permeable material whose water content is non-uniform and generally less than saturation (Hall, 1977). All permeable materials are porous but not all porous materials are permeable, as clearly illustrated by the diagram in Figure 11:

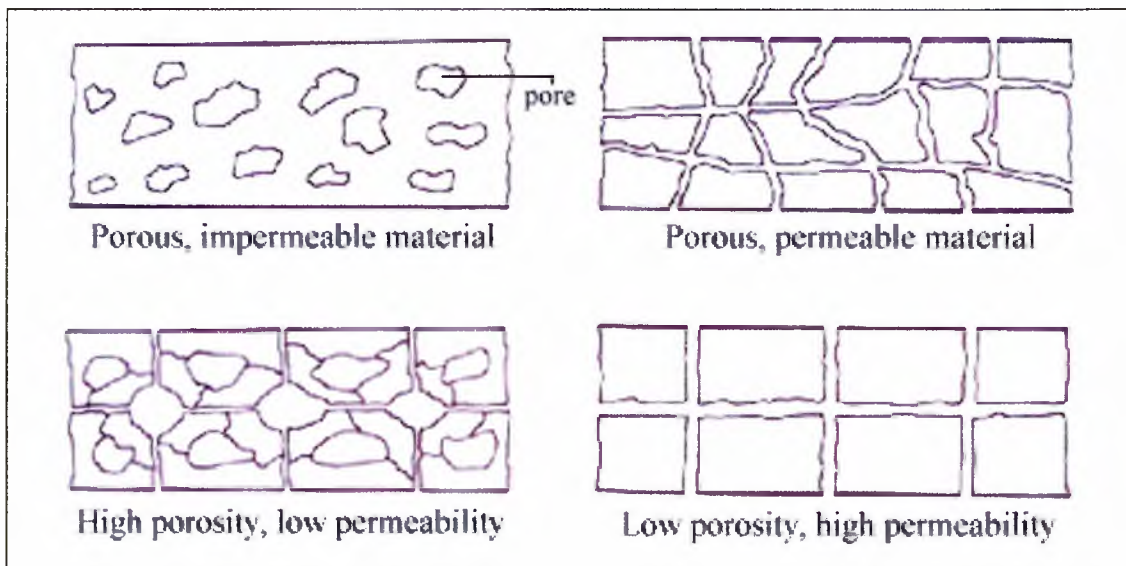


Figure 11 an illustration of the relationship between porosity and permeability (Diagram: Concrete Society, 1988)

Porosity simply refers to the amount of void space within the matrix of a material, whereas the permeability is determined by the accessibility and interconnection of these voids. Moisture can move through the network of channels in porous building materials

if they are accessible, i.e. permeable. This moisture can in turn be affected by a number of different climatic factors.

The moisture itself is simultaneously transferred in one of two basic forms - vapour and liquid. There exists a continuous phase exchange between these two forms due to the processes of condensation and evaporation. Thus, the transfer of moisture through porous building materials is strongly temperature dependent. The ambient conditions of temperature, relative humidity, rainfall, solar radiation and wind pressure define the conditions on both the inside and the outside of a wall and are inherently time-variable. When considering the global movement of moisture within porous building materials the action of gravity and pressure differentials complicate matters further in terms of experimental research.

2.4.4 Soil Structure and Particle Association

We have previously considered that, for engineering purposes, sub-soils are largely composed of particles of weathered rock that are grouped together in a fabric. The structure of this soil fabric can be considered as the combined effects of particle arrangement, composition, and inter-particle forces (Mitchell, 1976). Apparently, the volume fraction porosity (f) of a properly compacted rammed earth soil can be mainly attributed to the particle-size distribution. However, the permeability of a given soil is not simply a function of f . It is a property that varies according to the level of accessible, continuous pore space within the soil structure that can allow the ingress and passage of water.

The accessibility and continuity of pores is mainly dependent upon the inter- and intra-particle associations within the soil structure. The ways in which soil particles associate

with one another are numerous and can generally be classified as elementary particle arrangements, particle assemblages, or pore spaces (voids). These three main classifications have been described and illustrated in more detail over the following subsections.

2.4.4.1 Elementary Particle Arrangements

These are singular forms of particle interaction at the level of individual clay, silt, sand or gravel particles. Schematic representations of the typical features encountered in elementary particle arrangements are shown in Figure 12.

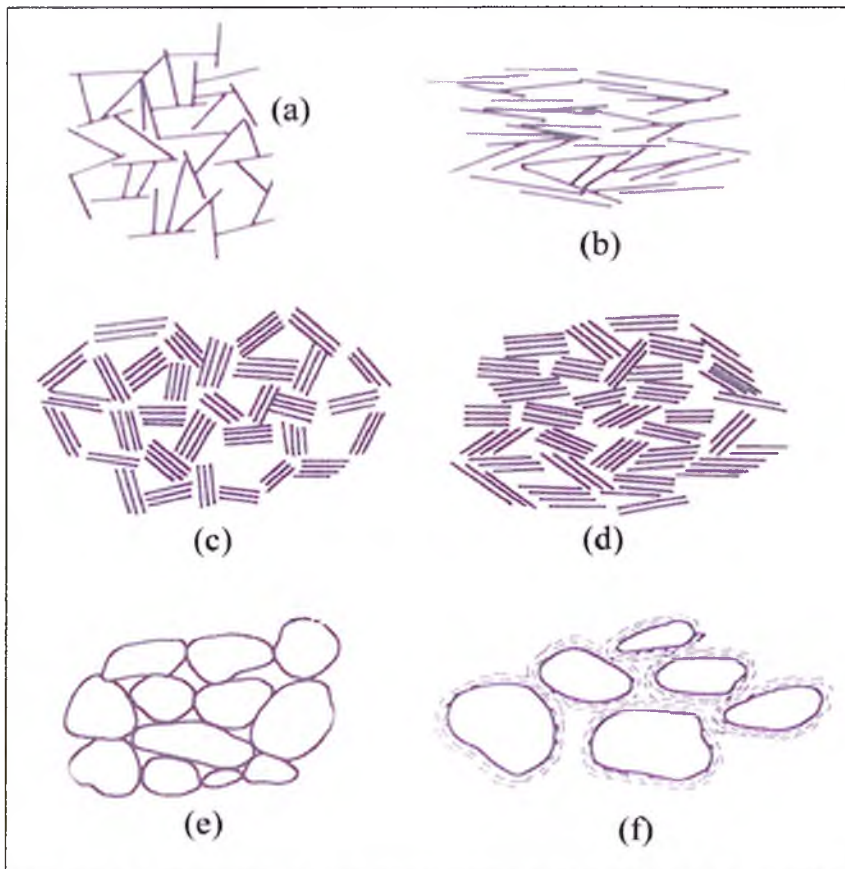


Figure 12 elementary particle arrangements (adapted from Mitchell, 1976)

Clay minerals are the product of decomposed igneous and metamorphic rocks. The crystalline, plate-like particles (platelets) have electrically charged surfaces along the

faces and edges and are scientifically classified as being $\leq 2\mu\text{m}$ in diameter (Barnes, 2000). In the diagram above, examples (a) and (b) represent two contrasting forms of interaction between individual clay platelets, whereas examples (c) and (d) illustrate clay platelet group (or aggregation) interactions. The following classifications are used to describe the particle associations between clay particles (Mitchell, 1976):

- **Dispersed.** No face-to-face association of clay particles.
- **Aggregated.** Some face-to-face association of several clay particles.
- **Flocculated.** Edge-to-edge or edge-to-face association of aggregated clays.
- **Deflocculated.** No association between aggregates.

The example (e) illustrates the typical granular interaction found between individual silt, sand or gravel particles. This formation is sometimes augmented when the granular particles become coated with cohesive soils, such as the example of interaction between clay-clothed silt particles shown by example (f) in Figure 12.

2.4.4.2 Particle Assemblages

These are simply units of particle organisation that have definable physical boundaries and that possess a specific mechanical function (Mitchell, 1976). Particle assemblages normally contain of one or more forms of elementary particle arrangements that have been presented above. An illustration of the typical particle assemblages that occur in sub-soils is provided by the schematic representations in Figure 13.

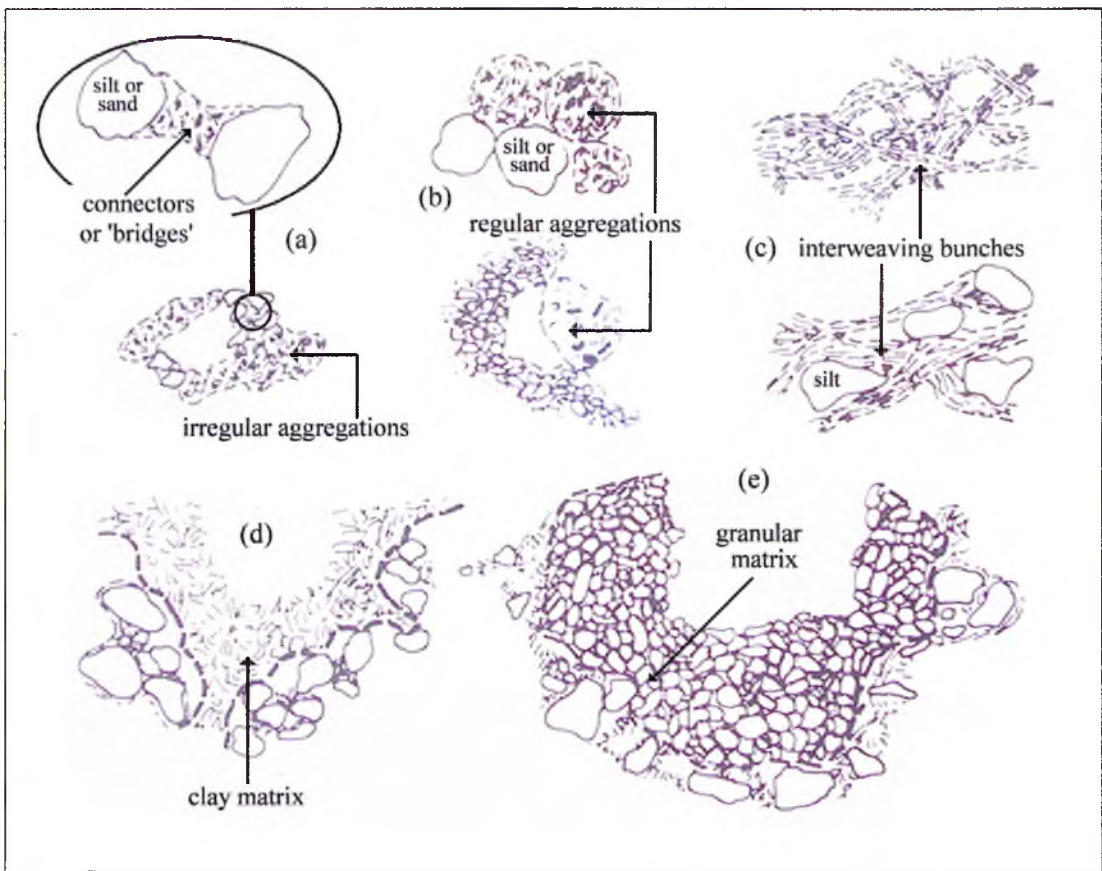


Figure 13 examples of typical particle assemblages in sub-soils (adapted from Mitchell, 1976)

In Figure 13, the example (a) illustrates how clay can form connections between granular soil particles to form bridges. It is thought that these bridges can contribute greatly to the overall cohesion within a soil and so may well pertain to the cohesion parameter (c') in Mohr-Coulomb's theory, as demonstrated by the formula for maximum shear strength (τ_f) in a soil:

$$\tau_f = c' + \sigma_n' \tan \phi' \quad \text{Equation 6}$$

Furthermore, an assemblage of irregular particle aggregations can be formed through the bonding effect of clay bridges between the granular material within a given soil structure, as shown by example (a) in Figure 13. Alternatively, as shown by the examples in (b), a soil structure may comprise a number of regular-shaped cohesive

aggregations either at the scale of granular elementary particle arrangements, or as a much larger localised agglomeration within the granular matrix.

The cohesive particle phase in some soils can become localised and oriented as interweaving strands or bunches of clay, and these can sometimes contain additional inclusions such as silt, as illustrated by example (c) in Figure 13. A typical illustration of how the clay particle matrix can surround and penetrate the granular matrix within a soil is shown by the example in (d). Where there is a localised absence of the clay particle matrix, as with example (e), the granular particle matrix exhibits an interlocking structure of non-cohesive elementary particles. This normally results in the formation of a surface defect commonly referred to as boniness, where the absence of fine-grained material leaves an open-structured appearance. Clearly, where voids exist between larger granular elementary particles that are in close contact with one another these gaps can become filled by smaller granular particles, and the gaps between these particles becomes filled by even smaller particles etc. In respect of the granular particles, the role of the clay matrix within a soil appears to be that of a cohesive binder with void-filling properties.

2.4.4.3 Pores (Voids)

As we have previously observed, pores are quite simply the voids that exist between elementary particles and/or particle assemblages. The various ways through which pores can be created within a given soil structure is illustrated by the schematic representation of pore space types shown in Figure 14.

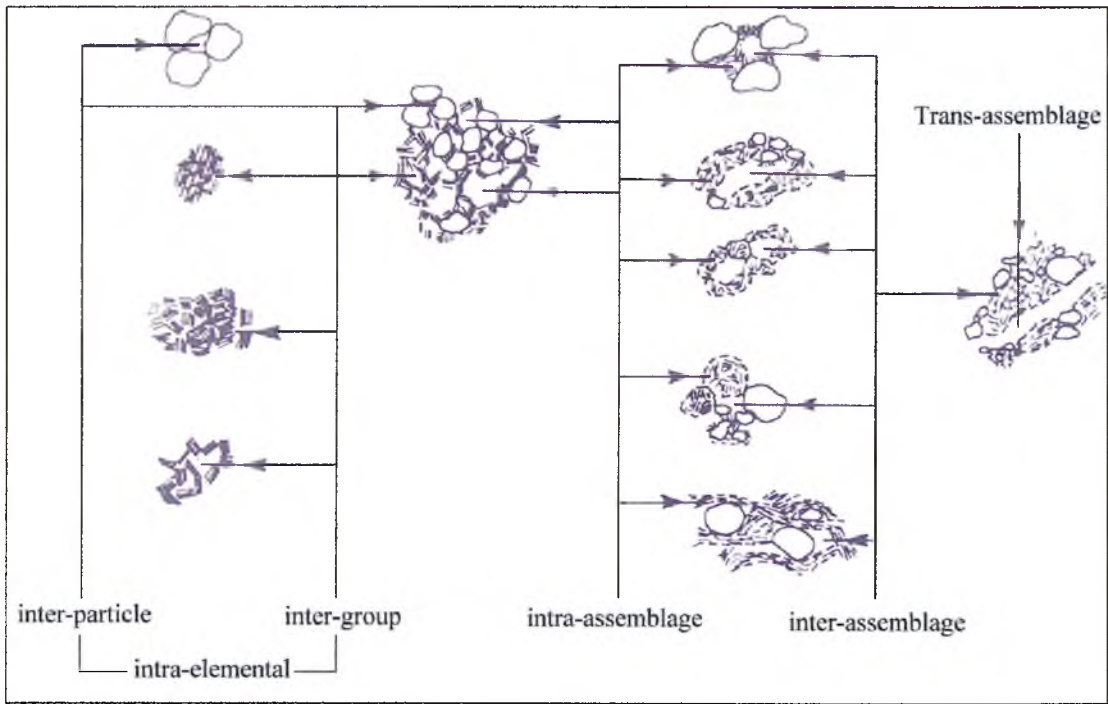


Figure 14 an illustration of the different pore spaces that can form inside sub-soils (adapted from Mitchell, 1976)

The simplest forms of intra-elemental pores are those that occur between the points of contact of granular elementary particles, e.g. silt, sand or gravel. The size of these inter-particle pores is generally greater in soils that have a correspondingly larger number of rounded granular particles (e.g. beach sand). This is due to a reduction in the angle of friction (ϕ') between soil particles, as can be seen from the example in Figure 14. Intra-elemental pore spaces also occur inside clustered groups of cohesive elementary particles such as clays. As shown by the examples above, a flocculated agglomerate of clay platelets can typically generate larger pores as part of its internal structure than a more aggregated particle association that occurs in layers.

Within the context of an assemblage, pores can sometimes form inside the matrix of the material (intra-assemblage) located between the various groups of elementary particles. Isolated pores can form between the points of contact of two or more assemblages (inter-assemblage), or they can even act as a void that creates a passage between

assemblages separating them entirely (trans-assemblage). Real-life examples of the various elemental and assemblage pore structures, as well as many of the particle associations described previously, can be identified in sub-soils using techniques such as Scanning Electron Microscopy (SEM) as shown by the example in Figure 15.

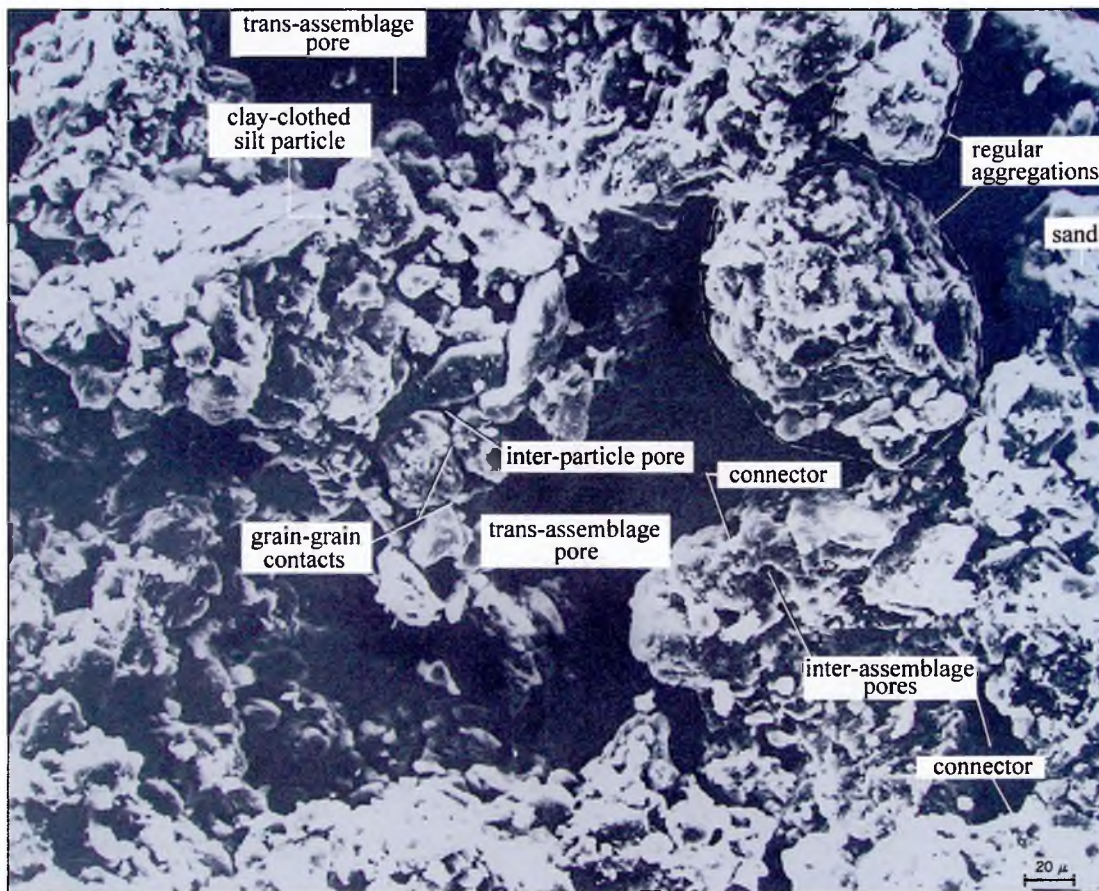


Figure 15 an SEM micrograph of the micro-soil structure in freshwater alluvial silty clay (adapted from Mitchell, 1976)

2.5 MOISTURE TRANSPORT MECHANISMS

In the previous section, we have seen the processes by which moisture can exist within porous building materials. Here we investigate the various mechanisms that can induce the moisture to move and to migrate within these materials. There are three distinctive mechanisms by which moisture can be motivated within a porous building material, each of which has an associated flow constant (Domone, 1994_c):

-
1. Flow of moisture due to a pressure differential
 2. Diffusion, i.e. the movement of water molecules under a concentration gradient
 3. Sorption due to capillary suction

Each of these mechanisms of moisture movement has been discussed in more detail in the sections below.

2.5.1 Pressure Differential

The same assumptions that are made for concrete may possibly be transferable to rammed earth materials for the purposes of saturated pressure-driven moisture ingress because the material has a similar dry density, which could indicate a typically low porosity. Both the pore size and flow rates through dense, porous building materials such as concrete have previously been observed to be sufficiently small for the flow of either a liquid or gas to be laminar (Domone, 1994_c). That is to say that the flow of moisture through the permeable pore structure is streamlined as opposed to being turbulent. Because of this, the flow of moisture can be described by Darcy's law:

The velocity of flow of a liquid through a porous medium, due to a difference in pressure, is proportional to the pressure gradient in the direction of flow
(Gove, 1993).

Therefore, in a porous building material, Darcy's law can be used to examine the rate of laminar flow in the x -direction using the following equation (Domone, 1994_c):

$$u_x = -K \frac{\partial h}{\partial x}$$

Equation 7

Where:

u_x = mean flow velocity

$\delta h/\delta x$ = gradient of pressure head

K = coefficient of permeability (e.g. m/sec)

The coefficient of permeability (K) is a constant within the formula, and its value depends upon the pore structure of the building material as well as properties of the permeating material such as viscosity and surface tension.

Measurement of the flow constant permeability is normally determined by measuring the steady-state flow rate of water through a saturated specimen under a static pressure differential. The specimen in a permeability cell is normally circular and the sides are sealed to ensure uniaxial flow. Since the fluid (water) in this case is incompressible, the pressure gradient is linear and Darcy's equation becomes (Domone, 1994_b):

$$\frac{\Delta Q}{\Delta A} = \frac{-K \cdot \Delta P}{l}$$

Equation 8

Where:

ΔQ = volumetric flow rate

ΔA = total cross-sectional area of flow perpendicular to the x -direction

ΔP = pressure head

l = flow path length

Although the bulk porosity and the permeability of a material are not necessarily related (see: Figure 11) it is known that a correction factor can be applied to concrete depending upon the water/cement ratio (Domone, 1994_b). The correction factor compensates for the reduction/increase in the level of interconnection between pores. To some degree, this may apply to cement stabilised rammed earth although the extent to which this occurs is currently unknown. It is likely that the amount and type of clay content is a large controlling factor of permeability in rammed earth, especially in relation to particle-size distribution. It is known that a water/cement ratio that is ≥ 0.55 in concrete has the effect of producing a more continuous pore system and increasing permeability. Similarly, the low water/cement ratio that is inherent to stabilised rammed earth is unlikely to be a factor that increases permeability.

2.5.2 Diffusion

The process of diffusion is one by which the particles of different solid, liquid, or gaseous substances intermingle and move from a region of higher concentration towards a region of lower concentration. This occurs most effectively in gases because they have the most dispersed concentration of particles and so are perfectly miscible with one another allowing almost uniform mixing. Consequently, the process of diffusion in liquids is a slower process than with gases, but is otherwise very similar. The process by which diffusion occurs is governed by Fick's law:

The rate of diffusion of one material into another is proportional to the negative of the gradient of the concentration of the first material (Gove, 1993).

In a porous building material, the process of diffusion in the x -direction can be defined under Fick's law by using the following equation (Domone, 1994_b):

$$P = -D \frac{\partial C}{\partial x} \quad \text{Equation 9}$$

Where:

P = transfer rate of the liquid/gas (e.g. water or water vapour) per unit area normal to the x -direction

$\delta C/\delta x$ = gradient of material concentration

D = the diffusivity constant (e.g. m^2/sec)

For any particular diffusion process, the property D can be treated as a constant although it, like the permeability coefficient K , varies according to pore size and the properties of the diffusing material, e.g. variation in water vapour concentration due to temperature. The internal pore structure of rammed earth is very narrow owing to its high density. It can vary considerably with different soil particle-size distributions and this is likely to have a marked effect on the diffusivity of the material.

The principle for experimentally testing a material in order to determine its diffusivity is essentially quite simple. The apparatus is the same as for a permeability cell. It has an inlet & outlet, and a dry sample (normally circular) with sealed edges to ensure uniaxial flow. Rather than force the liquid through the sample under a pressure differential, the diffusant (either a liquid or a gas) is introduced via the inlet and this becomes the high concentration side of the sample.

The test determines the rate at which the diffusant permeates the material and accumulates on the low concentration side of the specimen. It has previously been observed that once the diffusant has penetrated the specimen its increased accumulation on the low concentration side increases at a linear rate. In concrete, it has been found that increased diffusivity normally equates to increased permeability, and visa versa, (Domone, 1994_b) as one would perhaps expect. In rammed earth, however, the type and amount of clay present may affect both permeability and diffusivity as some types of clay are expansive and have a higher affinity with water than others. Montmorillonite and bentonite, for example, are both highly expansive clays that swell considerably upon contact with water/moisture vapour and could have the effect of reducing permeability as percolation continues.

2.5.3 Non-Saturated Flow Theory

Within the context of porous building materials, the determination of permeability (i.e. the continuity of the pore structure) is obtained by measuring the flow of water through a fully saturated specimen. This simulates the maximum theoretical rate at which moisture can flow through a given pore network under idealised conditions. Unsaturated flow theory applies to the mechanisms of moisture movement in porous building materials whose water content is non-uniform and less than saturation (Hall, 1977). Additionally, it can incorporate other external and internal forces such as gravity and capillarity respectively (Gummerson et al, 1980). When moisture ingress occurs in building materials it must first occur through non-saturated flow phenomena. Although they may later become saturated with prolonged exposure this condition is normally quite rare and so clearly non-saturated flow theory is of much greater interest in the study of moisture ingress in porous building materials.

By applying a correction factor to the coefficient of permeability (K) we can create a new term that represents the hydraulic conductivity of the material according to the moisture content at that time. This is seen in the extended Darcy equation shown below (Hall & Yau, 1987):

$$q = -K(\theta) \frac{\partial \Psi}{\partial x} \quad \text{Equation 10}$$

Where:

q = vector flow velocity

$\delta \Psi / \delta x$ = gradient of capillary potential (or suction)

$K(\theta)$ = moisture content-dependent hydraulic conductivity

The factor θ is in fact a dimensionless decimal value for the water content of a porous building material and can be calculated using the equation below (Hall, 1977):

$$\theta = (w - w_a) / (w_b - w_a) \quad 0 < \theta < 1 \quad \text{Equation 11}$$

Where:

w = gravimetrically determined moisture content

w_a = minimum moisture content (equivalent to w_h : see Fig 9)

w_b = maximum moisture content (equivalent to w_{sat} : see Fig 9)

The dimensionless water content (θ) is essentially a decimal value of the percentage water content in relation to volume fraction porosity (f). Therefore, the non-saturated moisture content of a porous material essentially becomes a reduction factor for attenuating the coefficient of permeability (K). That is to say, as the ingress of moisture

in a porous building material increases so does the hydraulic conductivity of the permeable pore spaces.

The term sorptivity (S) was introduced to unsaturated flow theory by J R Philip in 1957 (Gummerson *et al*, 1980) and was found to be a quantity that applied to any non-saturated porous material that obeyed the extended Darcy equation. It is essentially a determination of the amount of water absorption against the square root of elapsed time in a porous solid due to capillary suction, where the unit for S is $\text{mm min}^{-0.5}$. S can be experimentally determined using the Initial Rate of Suction (*IRS*) test apparatus, which is described in Chapter 4. The measurement of sorptivity, as opposed to the rate of suction, is preferred because the *IRS* data alone is a series of single-point values. S , on the other hand, is the gradient of a straight-line graph that is obtained by plotting a number of these single values over a period of time (Gummerson *et al*, 1980).

By calculating S , any errors or slight deviations between sets of data can largely be smoothed out. This methodology is suitable for any porous building material that obeys the $t^{0.5}$ law, i.e. the mass of imbibed water increases linearly per unit inflow surface area against the square root of elapsed time ($t^{0.5}$). The cumulative volume of absorbed water per unit inflow surface area (i) is first calculated thus:

$$i = m_w / A\rho_w \quad \text{Equation 12}$$

Where

m_w = the increase in mass of the sample due to water absorption, i.e. m_w

A = cross-sectional area of the inflow test face

ρ_w = the density of water (0.988 g/ml @ 20°C)

The sorptivity can then be derived using the following equation (Gummerson *et al*, 1980):

$$i = St^{0.5} \qquad \text{Equation 13}$$

S is determined simply by calculating the gradient of the slope $i/t^{0.5}$ for each of the corresponding set of values obtained in an IRS test (see: Chapter 4). When the $t^{0.5}$ law applies, S can be defined as the slope of the line produced when i is plotted against $t^{0.5}$. Consequently, the homogeneity or anisotropy of the material being tested will be reflected by the degree of linearity displayed in the line given by $i/t^{0.5}$. This degree of linearity can simply be calculated and expressed in terms of a statistical analysis tool such as linear regression (R^2 value), which gives a decimal value between 0 and 1. This is a statistical technique used to define the linearity between points on a graph. A value of 1, for example, means that the trend line between points on a graph are precisely linear, whereas a value of 0 means that they are not linear at all (e.g. a wavy line). A degree of classification for the continuity of the material's pore structure can thereby be obtained and quantified.

Unlike saturated permeability, unsaturated flow theory is sensitive to the variation in flow caused by changing water content. It is therefore possible to calculate the maximum theoretical rate at which water can be absorbed past the inflow surface of a porous building material at a known moisture content. The flow velocity (u_o) of imbibed water at the inflow face can be determined thus (Gummerson *et al*, 1980):

$$\frac{di}{dt} = u_o = \frac{1}{2}St^{-0.5} \quad \text{Equation 14}$$

and

$$iu_o = \frac{1}{2}S^2 = \text{constant}. \quad \text{Equation 15}$$

The capillary absorption of a liquid into a porous solid partly depends upon the properties of the liquid and on the microstructure of the solid (Gummerson *et al*, 1980). The controlling properties of the liquid, in this case water, are viscosity (η) and surface tension (T_s). Note that S is proportional to $(T_s/\eta)^{0.5}$, and that an intrinsic sorptivity (s) for any porous solid can therefore be calculated using (Gummerson *et al*, 1980):

$$s = S(\eta/T_s)^{0.5} \quad \text{Equation 16}$$

It is known that capillary rise is dependent on the radius of the pore as well as the liquid within the system. According to Gummerson *et al* (1980), using the volume fraction porosity (f) it is possible to determine the effective hydraulic pore radius (r) for a material as follows (Gummerson *et al*, 1980):

$$r = \frac{1}{2}(S/f)^2 \quad \text{Equation 17}$$

Obviously, the radii of pores within rammed earth vary due to the nature of the material. This is because the material comprises various soil particles with a large range of different sizes. Therefore, pore radii are chiefly a function of a soil's particle-size distribution. The effective hydraulic pore radius (r) gives an equivalent value for the

material as a whole. This is rather like an average value for a range of pore radii that are specific to a given soil type.

2.6 SUMMARY

The interactions between moisture and porous building materials are complex and numerous, but the processes can be simplified to allow the analysis of ingress mechanisms and flow mechanics. Under normal conditions the moisture content (w) of a porous building material is less than saturation. It can be determined gravimetrically and can simultaneously exist in both vapour and liquid phases. The relative concentration of each phase determines the mechanics of moisture transfer within the permeable pore space.

There are three distinct mechanisms of moisture movement in porous building materials – fully saturated flow that obeys Darcy’s law, vapour diffusion that obeys Fick’s law of diffusion, and non-saturated flow theory. The latter is the most important mechanism for this study because moisture ingress in porous building materials occurs nearly always below saturation. The extended Darcy equation allows the calculation of the parameter for moisture-content dependent hydraulic conductivity $K(\theta)$. The sorptivity (S) measures the depth of moisture penetration over time in a material that obeys the extended Darcy equation; where the mass of sorbed water per unit area (i) is proportional to the increase in the square root of elapsed time ($t^{0.5}$). The data for sorptivity can be further used to determine the surface inflow velocity (u_0) of imbibed water. Correlating sorptivity with the bulk porosity allows the calculation of a factor for the effective hydraulic radius (r) of the internal pore structure for a given material.

Rammed earth walls are dense and monolithic, and naturally protect against moisture ingress through the 'overcoat' effect. Some soil types are highly moisture resistant whereas others can suffer from significant problems of damp ingress. The application of 'impervious skin' treatments and renders are often an inappropriate design with low sustainability. The physical and chemical deleterious effects of dampness in buildings are rife and are well known to the UK construction industry. The key mechanisms of moisture ingress are capillarity and pressure differential – they are common and typically cause the greatest effect.

CHAPTER 3 - SAMPLE PREPARATION & PHYSICAL PROPERTIES

The following section discusses the techniques used for soil selection & grading, mixing & blending, and soil stabilisation using ordinary Portland cement. In addition, the production of rammed earth test cubes is described along with test methodologies for measuring their physical and engineering properties.

3.1 SOIL GRADING & PREPARATION

3.1.1 Mix Blending

The sub-soils used for rammed earth production during this research have been contrived by blending three component sub-soils of known origin and properties. The components of rammed earth material are analogous to those of concrete; the inert aggregate fraction is represented by granular soils (sand and gravel), and the binder fraction is represented by cohesive soils (silt and clay). ‘Medium’ (M) grade grit sand and 10mm pea gravel were sourced from the local supplier ‘Builder’s Centre (Chesterfield)’, and the silty-clay was obtained from the quarry owned by Rotherham Sand & Gravel Ltd. The physical appearance, texture and characteristics of these individual sub-soil components can be seen from the picture in Figure 16.



Figure 16 specimens of the silty clay, grit sand and pea gravel that were used to create the rammed earth soil mixes for this study

The process of incorporating these ingredients to form a sub-soil is comparable to a ‘giant cake mix’ (UKTV, 2003). In reality, it simply resembles a quarrying operation in reverse. Firstly, the particle-size distribution of each component soil was determined in accordance with British Standard 1377: 1990 Soils for Civil Engineering – Part 2: Classification (BSI, 1990₂). The grading of these commercially-available soils was found to be highly reliable in terms of consistency and minimal variation, making them suitable as a constant supply of materials. The technique of wet sieve analysis was used to classify the granular soil phases (i.e. sand and gravel). This was achieved by the author using the Geotechnical laboratory facilities at Sheffield Hallam University. Sedimentation was performed on the cohesive soil phases (i.e. silt and clay) by Rotherham Geotechnics Ltd.

By blending these three component soils together in varying proportions a variety of ten different mix recipes was devised, each of which conformed to the particle-size distribution parameters recommended by Houben & Guillaud (1996) of CRATerre for rammed earth (see: Figure 1). Each mix recipe was named numerically in relation to the mass (in kg) of sand, gravel, and silty clay out of a total mass of 10 kg, e.g. 523, 613, 703 etc. All of the soil components were first oven-dried to constant mass at a

temperature of 105°C. The silty clay was then pulverised into a coarse powder, using an electric paddle mixer, so that it would mix more easily with the sand and gravel. The soil was mixed in batches of 10 kg (dry mass) such that a 613 mix recipe required 6 kg sand, 1 kg gravel, and 3 kg silty clay. A 10 kg batch of mixed soil is sufficient to produce four 100mm cube samples. The soil components were first dry mixed and then a controlled amount of water was added to raise the soil to optimum moisture content. Mixing was performed using a variable speed 240V Hobart paddle mixer. This selection of recipes covered a wide range of different soil textures, and yet each conformed to the CRATerre-EAG grading parameters for suitable rammed earth soils (see: Figure 1). A typical example of a rammed earth soil is the mix recipe 523 shown in Figure 17:



Figure 17 Rammed earth soil mix recipe 523

3.1.2 Classification

The main intention of this methodology was to be able to provide a consistent source of soil material(s) where the particle-size distribution could be isolated and controlled as a single variable. By utilising the same three sources of soil components described above, and simply blending them in different proportions, variables such as mineralogy, grain shape, and clay type could be kept constant. The particle-size distribution curves for each of the ten mix recipes described above are displayed in Figure 18.

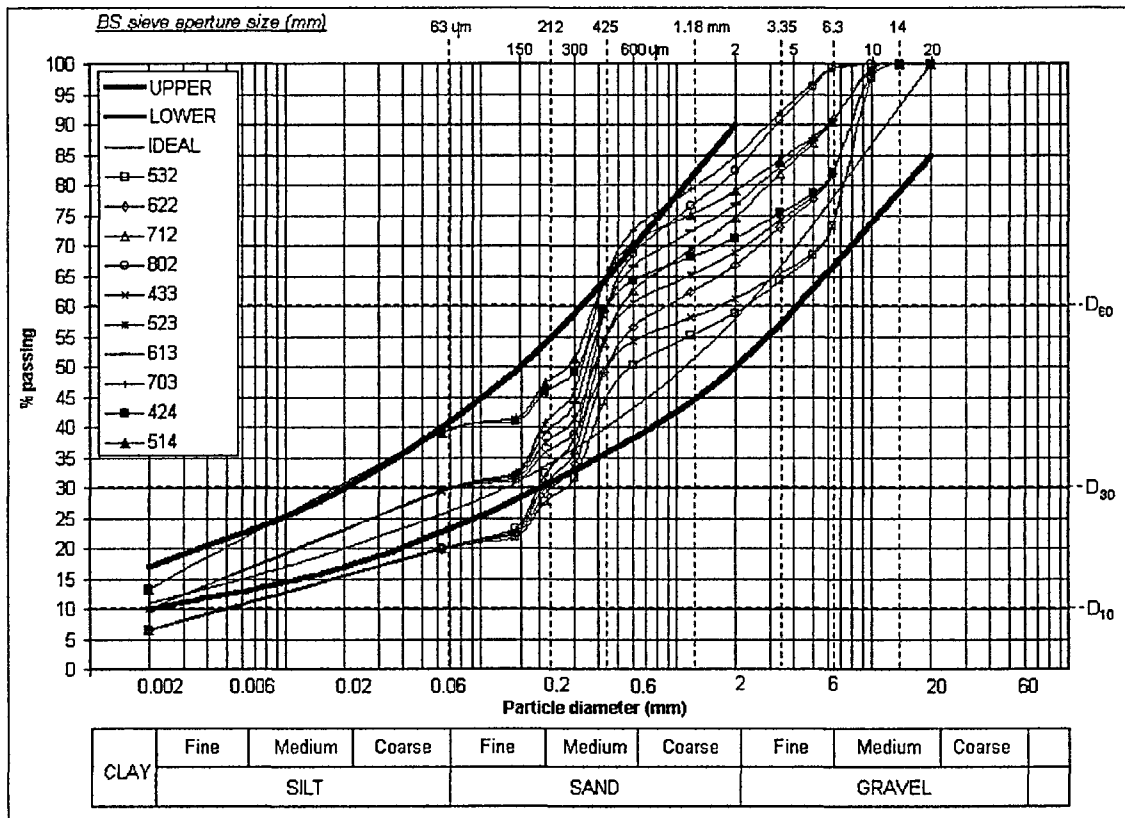


Figure 18 BS 1377 particle-size distribution chart displaying the CRATERre parameters for rammed earth soils, and the PSD curves for the ten rammed earth mix recipes

The soil mix recipes were not only chosen for their particle-size distribution but also by calculating the ratio between the clay content (CC), expressed as a proportion of the total mass, and the total specific surface area (SSA_t) of the granular particle phase. This property is referred to as the SSA_t/CC ratio. BS1377 sedimentation analysis of the silty clay showed it to have clay content (CC) of 0.33, therefore a xx2 mix recipe has a CC of 0.066, a xx3 mix has CC 0.099, and a xx4 mix has CC 0.132. The total specific surface area (SSA_t) value for each soil mix recipe was calculated using the retained mass values obtained during BS 1377 wet sieve analysis. Assuming each elemental granular soil particle to be spherical, its surface area can be simply calculated using $4\pi r^2$. The total mass retained (m_{ret}) for each particle diameter is known; therefore the SSA for a given particle diameter (e.g. 1.18mm) can be calculated and expressed in mm^2/g . The total

specific surface area (SSA_t) for a given soil mix recipe is simply the summation of the SSA value obtained for each sieve size, where:

$$SSA_t = \sum_n \left(\frac{4\pi r^2}{m_{ret}} \right) \quad \text{Equation 18}$$

The SSA_t/CC ratio, also measured in mm^2/g , simply represents the proportioning within a given soil between the surface area of the granular particles (sand & gravel) and the mass proportion of clay. Note that the SSA_t/CC ratio for each of the ten rammed earth mix recipes progressively decreases as the grading is carefully altered, as illustrated by the graph in Figure 19.

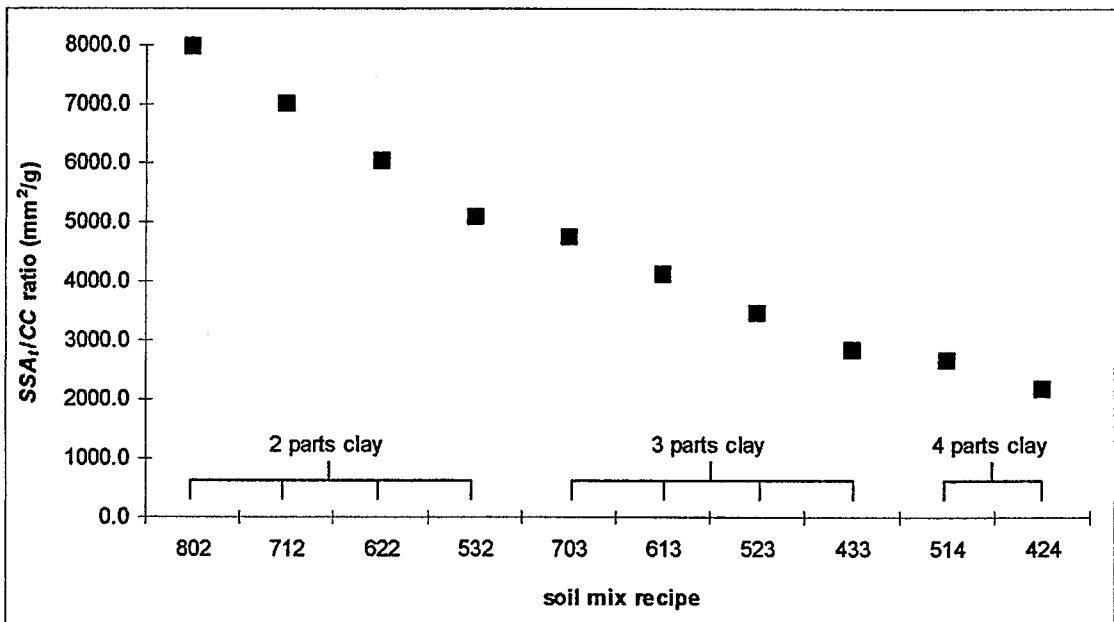


Figure 19 rammed earth mix recipes with their corresponding SSA_t/CC ratio

A further branch of investigation in this area was conducted by Benjamin Sissons (final year BSc Civil Engineering undergraduate) under the supervision of the author. The intention was to isolate the effect of the clay fraction within the mix by keeping the amount of sand and gravel constant and simply altering the clay content by small

amounts. The 613 mix recipe was selected as a start point, and from this ten new recipes were created by varying the amount of clay to ± 0.5 kg in 0.1 kg increments. This resulted in mix recipes of 61(2.5), 61(2.6), 61(2.7)...up to 61(3.5). Unfortunately, during the experimental work, problems arose with the consistency of mix blending and with the test procedure making the results from these tests inconclusive. However, this area of investigation could yield some useful data and is worthy of future research.

3.1.3 Cement Stabilisation

Three of the soil recipes discussed in the section above were chosen for a further series of testing; this time with the additional factor of cement stabilisation. The cement used for this work was Blue Circle 'Enhanced' ordinary Portland cement. The soil types were selected based upon their texture and moisture ingress performance; 433 (very good), 613 (good), and 703 (poor). The amount of cement stabilisation was calculated as a mass proportion of the total amount of dry soil, e.g. for 10 kg of dry soil, an addition of 1 kg cement would equal 10% stabilisation. In this example, the total mass of dry components for the mix then becomes 11 kg. The optimum moisture content (OMC) was always calculated as a percentage of the total mass of the dry components, i.e. including the mass of cement. This means that in an unstabilised soil with a dry mass of 10 kg, if the OMC is 8% then 800g of water must be added to the mix. If the soil is stabilised with 10% cement, then 880g of water must be added to achieve the same OMC value of 8%. A set of samples was produced for each of the three soil types using 3%, 6% and 9% cement (by mass).

3.2 CUBE SAMPLE PRODUCTION

3.2.1 Apparatus

The laboratory-based production of rammed earth samples should reflect the on-site construction technique used for making rammed earth walls (Standards New Zealand, 1998). This ensures that the test results are meaningful and can be transposed to real-life building situations. Factors such as the level of compaction and total input energy are therefore considered important. For this reason, a manual hand rammer was employed for the heavy, dynamic compaction of the soil in order to replicate rammed earth wall production. A 100mm concrete cube mould was used to ensure that the rammed earth samples conformed to standard sample production techniques for more familiar masonry materials such as concrete. The rammer was manufactured from mild steel with a solid handle, a 98 x 98mm square ramming face, and a total weight of 6.5 kg. This conforms to the specifications in New Zealand Standard NZS 4298: 1998 (Standards New Zealand, 1998) for a rammed earth hand rammer as shown in Figure 20.



Figure 20 a 6.5 kg steel hand rammer that conforms to NZS 4298: 1998

A removable guide collar attachment was fabricated in order to ensure the accurate location & entry of the hand rammer into the concrete cube mould, as shown in Figures 21 and 22.



Figure 21 (above left) hand-rammed cube sample making apparatus

Figure 22 (above right) the view inside the guide collar and cube mould assembly

The distance between the top of the mould and the top of the guide collar (i.e. the rammer drop height) is precisely 300mm. The inside of the cube mould can be painted with form oil or a proprietary release agent, as is the standard practice with formwork.

3.2.2 Compaction Procedure

NZS 4298 (Standards New Zealand, 1998) states that for rammed earth production the moisture content should never be less than 3% below OMC or more than 5% above it. This practice was strictly observed during sample production and the moisture values were intermittently observed both by gravimetric determination (i.e. oven drying & weighing) and by using the drop test as specified by NZS 4298: 1998. For each of the ten rammed earth mix recipes that were used the OMC was found to be a value ranging from between 7% and 9% moisture in relation to the dry mass of the soil. The OMC for each of the ten soils was determined in accordance with British Standard BS 1377 – Part 4: Compaction (BSI, 1990₄) using the established proctor ‘light’ compaction method.

Although the proctor method has been used to determine the OMC of each soil recipe, the nature and force of the dynamic compaction used for building rammed earth walls is quite different. For this reason, the methodology described here has been based upon the specifications for rammed earth soil compaction given by NZS 4298: 1998. The key difference between the proposed methodology, and the existing Proctor test, is that the total required energy input for compaction is not a fixed value regardless of soil type. More or less compaction can be used depending upon soil type, and the main factors controlling dry density are particle-size distribution and the corresponding optimum moisture content.

The moistened soil was placed inside the mould and compacted in three separate layers. It was discovered that between 750g and 800g of soil amounted to approximately one third the height of the cube mould when compacted. This practice ensured an additional level of standardisation in the overall process of manufacture because the three compaction layers were all the same thickness. Compaction effort was applied in accordance with NZS 4298: 1998, which states that to achieve the correct level of compaction the handle of a 6.5 kg hand rammer should make a ‘ringing’ sound when dropped from a height of 300mm onto the surface of the compacted soil. One soon becomes familiar with the sound and feel of properly compacted earth through experience. It should be noted that up until this point the fall height and number of drops is less controlled. Typically, the fall height is equal to or less than 300mm, and the total number of drops required is between 7 and 12 drops per layer. The magnitude of compactive effort for the Proctor ‘light’ methodology is calculated as being 60.8 Mg.m/m³, compared with the typical range of between 41.0 Mg.m/m³ (@ 7 drops/layer) and 70.2 Mg.m/m³ (@ 12 drops/layer) for the cube sample methodology.

A further enhancement is in ensuring the dimensional consistency of the samples that are produced. This results in more precise dry density determinations due to standardisation of sample volume. Dimensional tolerances for length, width and height are typically similar to those used for concrete blocks and fall within limits of $\pm 3\text{mm}$, although the current Australian specification relaxes the maximum variation to $\pm 7.5\text{mm}$ (Walker, 1996). This can also eliminate the need for capping of the specimen in a compressive strength test. After scraping away the compacted soil projecting above the top of the mould a small amount of moist soil was passed through a 2mm British Standard (BS 1377) sieve and sprinkled on top of the sample. This capping layer was then compacted with the hand rammer before being smoothed by a metal spatula to produce a perfectly flat surface. The resultant sample should be a perfect 100mm rammed earth cube with three even layers of compacted soil, as shown in Figure 23.



Figure 23 completed rammed earth cube samples made using the unstabilised 613 soil mix recipe

3.2.3 Catalogue of Cube Samples Produced

The cube samples were produced in batches, each containing sixteen cubes. Every specimen batch of sixteen is made using four 10 kg mix batches of soil, each providing

enough material to produce four cubes. A separate specimen batch (16 cubes) was created to represent each of the ten different rammed earth soil mix recipes in unstabilised form.

In addition, three of these soil mix recipes were selected for the additional production of cement stabilised versions. Once again, a separate specimen batch of 16 cubes was created to represent each of the three selected soil mix recipes. This time, however, a separate specimen batch (16 cubes) was created for the three different levels of cement stabilisation that were chosen: 3%, 6% and 9%.

Each of the sixteen cube samples from a given specimen batch was created for use in a specific test. The tests included compressive strength (f'_{cu}), Initial Rate of Suction (IRS) 'wick' test, and the modified Initial Surface Absorption (ISA) test. In addition to the number of cubes required for these tests an additional two cubes were produced as spares in case of accidental damage, breakage or any other unforeseen circumstances. To summarise the total number of different cube samples that were produced, and the number that were allocated to each test regime, the data in Table 1 has been presented.

Table 1 a summary of the entire scheme for rammed earth cube sample production

	Number of samples required				
	f'_{cu}	IRS	ISA	Spare	Total
Unstabilised soil type:					
532	5	6	3	2	16
622	5	6	3	2	16
712	5	6	3	2	16
812	5	6	3	2	16
433	5	6	3	2	16
523	5	6	3	2	16
613	5	6	3	2	16
703	5	6	3	2	16
424	5	6	3	2	16
514	5	6	3	2	16
Cement stabilised soil type:					
433 + 3%	5	6	3	2	16
433 + 6%	5	6	3	2	16
433 + 9%	5	6	3	2	16
613 + 3%	5	6	3	2	16
613 + 6%	5	6	3	2	16
613 + 9%	5	6	3	2	16
703 + 3%	5	6	3	2	16
703 + 6%	5	6	3	2	16
703 + 9%	5	6	3	2	16
Total number of cube samples =					304

3.2.4 Curing

The samples were stored in a sealed curing chamber for a minimum period of 28 days at a temperature of 20°C (±1°) and a relative humidity of 75% (±5%), as can be seen from the picture in Figure 24.



Figure 24 a large collection of rammed earth cube samples being stored in a curing chamber under controlled conditions

The curing chamber is a purpose-built sealed chamber with a rotating drum humidifier and digital monitoring equipment for recording the atmospheric conditions. The high relative humidity prevents the samples from drying out too quickly and so reduces the risk of shrinkage cracks occurring. When cement stabilisation was used in the samples, the high humidity in the curing chamber aids correct hydration of the cement in order to optimise its effects.

In experimental work conducted by Turner (2004), under the supervision of the author, the curing process of stabilised and unstabilised cube samples made with 433, 613 and 703 mix recipes was monitored and recorded. In the 613 mix recipe, for example, the difference between wet and dry density at 0% cement content was 151.44 kg/m^3 , whereas at 9% cement the difference was 95.85 kg/m^3 . A similar pattern was observed

for each of the three mix recipes (Turner, 2004). As the samples with no cement appear to have lost more water after curing than those with cement, it would be logical to assume that the water may simply be consumed during the cement hydration reaction.

3.3 EFFICIENCY OF PNEUMATIC COMPACTION

Commercial equipment, in the form of a pneumatic rammer connected to an air compressor, was successfully used to create three miniature rammed earth test walls made from a 613 soil mix recipe stabilised with 6% ordinary Portland cement. The purpose of this was to measure both the dimensional stability and dry density of a given rammed earth soil mix recipe when it is pneumatically compacted inside removable formwork. The intention was to determine whether or not the physical properties of the rammed earth that is produced, using this commercial building-site process, is comparable with those of the rammed earth samples that are produced using the laboratory-based cube sample production techniques described previously.

3.3.1 Equipment & Test Wall Construction

The rammer used for the construction was an Atlas Copco RAM30 sand rammer, and it was powered by a 3-phase 31cfm (@7.5 bar) Hydrovane™ Classic 05 air compressor. A picture of this equipment can be seen in Figure 25.



Figure 25 a pneumatic rammer attached to an air compressor

The soil was proportioned and mixed in exactly the same way as with the cube samples using 10 kg batches. A total amount of between six and seven 10 kg batches of soil was required to build each test wall. The entire process was performed under laboratory conditions with zero natural daylight and with the ambient climatic conditions at $20^{\circ}\text{C} \pm 1^{\circ}$ and $40\% \text{ RH} \pm 5\%$. The optimum moisture content of the soil was controlled at $8\% (\pm 1\%)$ of the total mass for the dry mix components.

The formwork was a simple, generic design made by the author using phenol-faced plywood. This was painted with Castrol release oil and held together using standard sash clamps. The internal dimensions of the formwork were 660mm wide x 300mm high x 165mm thick. In order to make sure that the test walls were portable each was constructed on top of a 19mm thick plywood base that was attached to a raised steel platform. The steel platform was of the type designed for use with a standard forklift truck. A completed miniature rammed earth test wall, including its steel base, can be seen in Figure 26.



Figure 26 a miniature rammed earth test wall built on a metal base

3.3.2 Suspended Wall Mass Determination

The mass of each miniature test wall was determined immediately after its completion and the removal of all formwork. This was basically achieved by raising the wall from the ground (including its base platform), suspending it from a calibrated load cell and then measuring its mass. The wall is built on top of a steel base that has 4x 10mm threaded steel bars attached to it. These threaded bars are installed following construction of the test wall, and are also connected to the lower section of a lifting frame. The upper section of the lifting frame is fitted with a load cell, and is placed onto the raised tangs of a forklift truck.

The upper and lower sections of the lifting frame are interconnected by a rose-bearing eyebolt that is threaded into the load cell. The rose bearing in the eye bolt allows the suspended wall to pivot and swing freely, when it is raised from the ground, thus

retaining the overall stability of the apparatus. Once the two halves of the lifting frame have been connected, the test wall and base can be raised off the ground using the forklift truck. The stress is transmitted via the load cell and so the suspended mass of the test wall (minus the weight of the base platform) can be calculated. The mass of the base platform is known because it is weighed before construction of the test wall. The overall arrangement of the suspended wall mass-measuring apparatus, when it is in operation, can be seen from the picture in Figure 27:

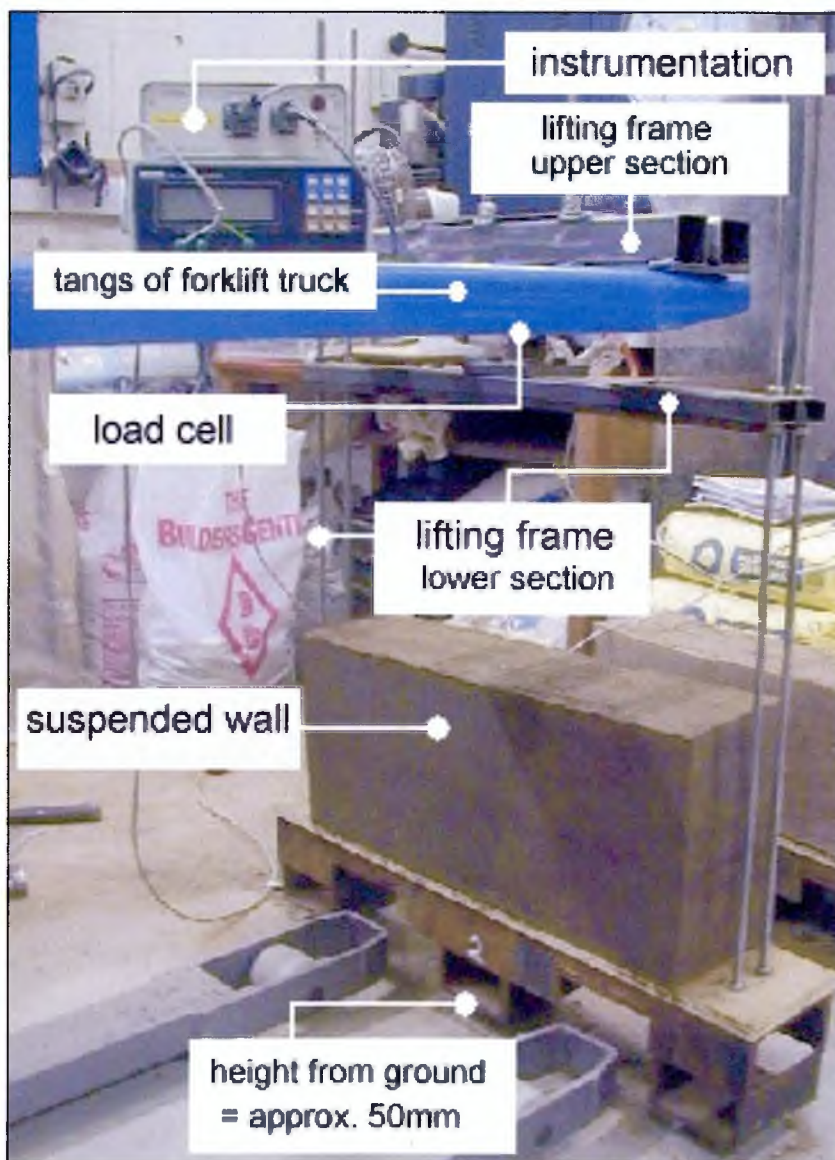


Figure 27 the SHU suspended wall mass-measuring apparatus in operation

3.3.3 Analysis of Results

The average dimensions of each wall were calculated by taking measurements across four different locations along each of the x, y, and z axes. Along the z axis (i.e. depth), for example, measurements were taken at four different points; top left, bottom left, top right, bottom right. An average value for the depth of the entire wall could then be calculated. By using this methodology to obtain average values for the width (x), height (y) and depth (z) of each test wall, the total averaged volume could then be calculated. Since the mass, volume, and moisture content of the test walls is known, then the dry density of each wall can simply be calculated by deducting the moisture content from the total mass of the wall and then dividing the total dry mass by the volume. The results for the dry density that was calculated for each test wall are shown in Table 2.

Table 2 dry density values for pneumatically compacted rammed earth walls

Pneumatically-compacted mini walls:	Dry density
Wall 1 (613 soil + 6% cement)	2075.86 kg/m ³
Wall 2 (613 soil + 6% cement)	2035.33 kg/m ³
Wall 3 (613 soil + 6% cement)	2023.66 kg/m ³
Comparison between mean values:	
Mean average – pneumatic compaction (613 soil + 6% cement)	2044.95 kg/m³
Mean average – hand rammed [cube samples] (613 soil + 6% cement)	2067.84 kg/m³

These findings appear to agree with the observations made in practice by the contractor David Easton of Rammed Earth Works CA, USA (Easton, 1996_b); hand ramming is just as effective as pneumatic ramming only slower. For a given rammed earth soil type held at optimum moisture content, with the addition of approximately 6% cement stabilisation, the variation in resultant dry density between pneumatic- and hand ramming was found to be approximately 1.1 %. A typical upper/lower limit value,

which is used in practice to ensure consistent compaction, may be a dry density variation of around 5%. Consequently, the difference observed between the dry density of rammed earth that is achieved through using either pneumatic compaction or hand ramming can most likely be assumed to be insignificant. In addition, the cube samples that were used for the experimental work described previously were compacted to the same degree as the rammed earth material in full-sized walls that have been properly constructed.

3.4 PHYSICAL PROPERTIES

3.4.1 Dry Density

The consistency of cube samples was initially assessed by means of humid density determination immediately following the production of a sample and its subsequent removal from the mould. Table 3 illustrates a typical production run of sixteen rammed earth cubes that were made with four separate batches of freshly mixed soil. On this occasion, the soil mix recipe was a 622.

Table 3 an example of the data recorded from a typical cube sample production run

Mix	Sample #	Mass at production (g)	Calculated dry mass (g) *	Batch
622	622-A	2323.0	2137.2	10 kg
622	622-B	2332.0	2145.4	↓
622	622-C	2312.9	2127.9	
622	622-D	2330.8	2144.3	
622	622-E	2308.6	2123.9	
622	622-F	2302.4	2118.2	↓
622	622-G	2332.2	2145.6	
622	622-H	2312.2	2127.2	
622	622-I	2311.2	2126.3	
622	622-J	2324.2	2138.3	↓
622	622-K	2314.0	2128.9	
622	622-L	2331.0	2144.5	
622	622-M	2315.9	2130.6	
622	622-N	2331.9	2145.3	↓
622	622-O	2327.0	2140.8	
622	622-P	2318.0	2132.6	
mean average (g) =		2320.6	2135.0	
standard deviation (g) =		10.08	9.28	
standard deviation (%) =		0.434	0.434	
Dry density variation: proctor/sample mean (g) =				14.97
Dry density variation: proctor/sample mean (%) =				0.701
<i>* Dry mass calculated using a gravimetrically-determined average moisture content of 8%</i>				

The dry density between samples is consistent with a tolerance of just 0.4%. The variation between the density of cube samples, and the density values obtained for the same material using the BS 1377 light compaction (Proctor) test, amounts to a mere 0.7%. Turner (2004) observed that for a range of 96 cube samples made using a variety of mix recipes the standard deviation for dry density is greater in mix recipes with proportionally higher gravel content. This may be because gravel particles are

comparatively large and so small changes in concentration within a mix could have a larger effect on altering dry density than would be the case for sand or silt.

The results of a separate undergraduate study by Germain (supervised by the author) indicate that for a given rammed earth mix recipe, in this case 523, the optimum moisture content is 8.4% both when the soil is unstabilised, and when it is stabilised with either 2%, 4%, 6% or 8% ordinary Portland cement by mass (Germain, 2002). In conclusion, the addition of cement through a range of typical quantities does not appear to significantly affect the optimum moisture content of the soil. Correspondingly, it was discovered that the maximum dry density of the compacted soil appears to remain consistent even with varying proportions of cement stabilisation. Using the BS 1377 proctor light compaction method, the dry density values were obtained for samples with 0%, 2%, 4%, 6%, and 8% OPC stabilisation. The average value for maximum dry density was 2061 kg/m^3 with a standard deviation of 0.10% (Germain, 2002). This data is in good agreement with the results obtained by the author using the same mix recipe: an average maximum dry density of 2112 kg/m^3 and a standard deviation of 1.1%.

After all of the unstabilised cube samples had been made, for each of the 10 soil mix recipes, the author began a second stage of cube sample production for this study. Three of the soil mix recipes were selected to be made using varying amounts of cement stabilisation. The mix designs were selected based upon contrasts in their grading. 433 is a pebbly mix with high density, 613 is a smoother cohesive mix with medium density, and 703 is a sandy mix with low density. The OMC was controlled at $8\% \pm 1\%$ in relation to the dry mix components, e.g. 8% of the total soil/cement dry mass. For each combination of variables (i.e. for a given soil type + a given cement %) sixteen cube samples were produced, as previously described for unstabilised rammed earth. Table 4

illustrates the comparison between average dry density for each soil mix with 0% (unstabilised), and with 3%, 6%, or 9% ordinary Portland cement:

Table 4 a comparison between the dry densities obtained for different rammed earth soil types with varying degrees of cement stabilisation

Average Dry Density (kg/m ³)	Soil mix recipe		
	433	613	703
Unstabilised	2170.8	2121.8	2056.1
3% cement stabilisation	2146.3	2072.6	2026.1
6% cement stabilisation	2136.6	2067.8	2019.3
9% cement stabilisation	2154.2	2067.1	2061.5
Total average (kg/m³)	2152.0	2082.3	2021.0
Standard deviation	14.5	26.4	21.1
Standard dev. %	0.7	1.3	0.8

As was previously discovered by the author and Germain (2002) using the 523 mix recipe, the dry density of all three soil mix recipes obtained here (433, 613 & 703) does not appear to be significantly affected by the addition of varying proportions of cement stabilisation. In these cases, the dry density of rammed earth for a given soil type, whether unstabilised or stabilised with up to 9% ordinary Portland cement, appears to remain constant with a standard deviation of 1.3% or less. Correspondingly, it would appear that controlling the optimum moisture content of cement stabilised rammed earth soils in relation to the total mass of dry mix components (soil + cement) is an acceptable, accurate methodology.

3.4.2 Dimensional Stability

The linear shrinkage of the rammed earth mix recipe 523 was determined in accordance with BS1377 - Part 2: Classification. Since this test only applies to the fraction of soil that passes a 425µm sieve it is unclear how meaningful the results for rammed earth

soils because it only represents between 45% and 65% of the total soil mass, depending upon which of the ten soil recipes is being tested. The level of intervention required for any of the five Atterberg limit tests, when performed on a rammed earth soil, means that obtaining a sample that is representative of the soil type as a whole is not always possible. For this reason, the test was initially applied to only one of the rammed earth soil types – the 523 mix recipe. The percentage linear shrinkage (%LS) was determined using the following formula (BSI, 1990₂):

$$\%LS = \left(1 - \frac{L_D}{L_O}\right) 100 \quad \text{Equation 19}$$

Where:

L_O = the original length of the specimen (BS 1377 shrinkage trough = 140mm ±1mm)

L_D = the length of the specimen after shrinkage

Four specimens were tested, and the amount of linear shrinkage varied from 7.56mm to 7.94mm, with an average value of 7.72mm. The linear shrinkage for the sub-425µm fraction of the 523 rammed earth mix recipe was calculated to be 5.83%. However, this value cannot be used to represent the linear shrinkage of a given rammed earth mix recipe. This is because the test requires the removal of any soil particles greater than 425µm in diameter, as described above. Since a very similar soil specimen would have to be decanted from each of the ten rammed earth soil recipes in order to perform similar tests, this avenue of experimentation was not considered beneficial and so was not explored further.

A more appropriate technique for determining the amount of shrinkage that can occur in a rammed earth sample was devised based upon BS EN 772-16 *The Determination of Dimensions of Masonry Products*. The test specimen can be produced in accordance with either light- or heavy- proctor compaction as specified in BS 1377 – Part 4. It is then extruded from the 1 litre proctor mould and cured for 7 days at $20^{\circ}\text{C} \pm 1^{\circ}$, 75% RH $\pm 5\%$. The standard dimensions for a BS 1377 Proctor mould are as follows:

Diameter (x) = 105mm ± 0.5 mm

Height (y) = 115.5mm ± 1 mm

The following test specimens were produced using this method, and the soil mix recipe used was a 523 rammed earth soil:

- $L1, L2, L3, L4$ = Proctor light compaction samples
- $H1, H2$ = Proctor heavy compaction samples
- $L1-C, L2-C$ = Proctor light compaction + 10% Ordinary Portland Cement stabilisation
- $L1-LH, L2-LH$ = Proctor light compaction + 10% Hydrated lime stabilisation

After curing, the mass of the resultant test cylinders is recorded. Since the volume of the sample is 1 litre, this can be conveniently used to calculate the total density of the specimen. The dimensions of the specimen can then be determined using a Vernier calliper to measure the height and diameter. Using typist's correction fluid the sample can be marked in such a way that the circular face is divided into quarters. The height

(y) is measured at each of these four points, as is the diameter at the top (x_1) and bottom (x_2) of the cylinder. The points of measurement have been illustrated in Figure 28.



Figure 28 an illustration of the points on a sample at which to determine the sample dimensions

Table 5 gives an example of a typical set of measurements that were recorded for a test cylinder made out of rammed earth (523 mix recipe) and compacted in accordance with the Proctor light compaction procedure in BS 1377 Part 4.

Table 5 an example of the dimensional data obtained from a typical rammed earth test specimen

Sample	Position	y (mm)	x_1 (mm)	x_2 (mm)
<i>L2</i>	1	114.22	104.76	104.38
	2	114.52	104.58	104.44
	3	115.26	104.40	104.28
	4	114.78	104.16	104.44
Avg. value =		114.70	104.48	104.39
Sample: L2 physical properties				
Mass_{dry} = 2123.9g y_{avg} = 114.70mm x_{avg} = 104.43mm				

By collating all of the values for x_{avg} and y_{avg} , in a particular sample group (e.g. L1, L2, L3 & L4), the total mean values can be calculated, i.e. mean x_{avg} and mean y_{avg} . These values represent the average reduced dimensions for a particular sample group after a period of curing. They can therefore be used in the linear shrinkage equation as the value L_D for either the x -axis or the y -axis. The corresponding values for L_O (original dimensions) can simply be taken as those of a BS 1377 proctor mould, as discussed previously. By applying the formula used to determine percentage linear shrinkage (%LS), the values for both y_{LS} and x_{LS} can be calculated. The results for each of the test specimens described previously were collated and have been presented in Table 6.

Table 6 test results for the dimensional stability assessment of rammed earth specimens

Properties	Sample			
	L	H	L-C	L-HL
Avg. Mass (g) =	2134.1	2126.8	2123.0	1992.1
Std. Dev. =	8.52	9.62	5.73	1.63
Mean y_{avg} (mm) =	114.19	113.46	114.94	114.63
Std. Dev. =	0.49	0.27	0.24	0.38
y_{LS} (%) =	1.14	1.77	0.48	0.75
Mean x_{avg} (mm) =	104.54	104.71	104.70	104.56
Std. Dev. =	0.11	0.12	0.16	0.07
x_{LS} (%) =	0.44	0.27	0.28	0.42

These results appear to show that for a given rammed earth soil mix recipe (i.e. 523), there appears to be no change in dry density between specimens prepared using either light- or heavy-Proctor compaction, nor in those with or without cement stabilisation. However, using hydrated lime stabilisation appears to have the effect of slightly lowering the maximum dry density of the rammed earth. This may be due to the higher degree of effective dispersal of clay particles that lime can induce.

The effect of both cement and hydrated lime stabilisation appears to lower the overall amount of linear shrinkage, particularly along the y -axis, when compared to unstabilised soils. However, the amount of linear shrinkage is still, in each case, much greater in the y direction (i.e. parallel to the force of compaction) than in the x direction, which is perpendicular to the force of compaction. Overall, for the rammed earth soil used in these tests, linear shrinkage is of little consequence because it typically never increases beyond 1% in any direction and in the worst case is merely 1.77%.

The high-sand content samples (e.g. 703, 712, and 802) were very stable with no visible cracking on the surfaces. However, these types of samples often appeared to exhibit small clusters that were rich in cohesive soil indicating that some pelleting of the silty clay had occurred. The mix recipes that exhibited a more pebbly texture (e.g. 532, 622, 433, 523, 613, and 424) tended to have a smoother, harder surface finish than the sandy ones for the most part. However, their surfaces often contained localised interruptions by pockets of granular soil exhibiting a pebbly, open-pored texture; a surface defect commonly referred to as 'boniness'. Samples with higher proportions of silty clay (e.g. 514) tended to display a number of visible hairline shrinkage cracks. These soils were comparatively difficult to handle and to compact, but resulted in rammed earth cubes that were very smooth and had an exceptionally hard surface finish. The visual observations referred to in this paragraph can clearly be seen from the gallery of cube sample pictures displayed in Appendix 3, where each of the ten soil mix recipes are represented.

The use of ordinary Portland cement as a soil stabiliser appeared to have a significant effect on clay flocculation in a way that is very similar to that of lime. The cement noticeably reduces, and in many cases eliminates, any tendency towards pelleting of the cohesive phases within a soil. Pelleting occurs when pockets of the cohesive soil phase (i.e. silt & clay) consolidate within the mix and will not readily blend with the granular soil phase. This can be a problem because the cohesive phase normally acts as a binder within the matrix and tends to have a significant effect on controlling moisture ingress. The positive effects of cement stabilisation in this case are to speed up the mixing process in a soil that is prone to pelleting. In addition, a more even distribution of silt & clay is achieved making the mix much more thorough.

3.4.3 Particle Density

Determination of the particle density (ρ_s) of each mix recipe was achieved by first testing each of the three mix components (gravel, sand and silty clay) using the gas jar method performed in accordance with BS 1377 - Part 2: Classification. ρ_s for the 10mm pea gravel was found to be 2.68 kg/litre, whilst for both the grit sand and silty clay ρ_s was found to be 2.65 kg/litre. Domone (1994_a) states that ρ_s for cement is typically 3.15 kg/litre.

The particle density (ρ_s) for a given mix recipe was then calculated by simply using ρ_s for the relative proportion of each soil component. The calculation of ρ_s for a 613 mix recipe with 6% cement, for example, would be:

$$\rho_s = 0.94 \cdot \left(\left(\frac{2.65}{10} \cdot 6 \right) + \left(\frac{2.68}{10} \cdot 1 \right) + \left(\frac{2.65}{10} \cdot 3 \right) \right) + (0.06 \cdot 3.15) \quad \text{Equation 20}$$

3.5 COMPRESSIVE STRENGTH

3.5.1 Apparatus & Calibration

To further test the consistency of sample production, as well as to compare rammed earth to conventional masonry materials, compressive strength testing was performed. The apparatus used for this was a Mayes SH250 compression test machine, as shown in Figure 29.

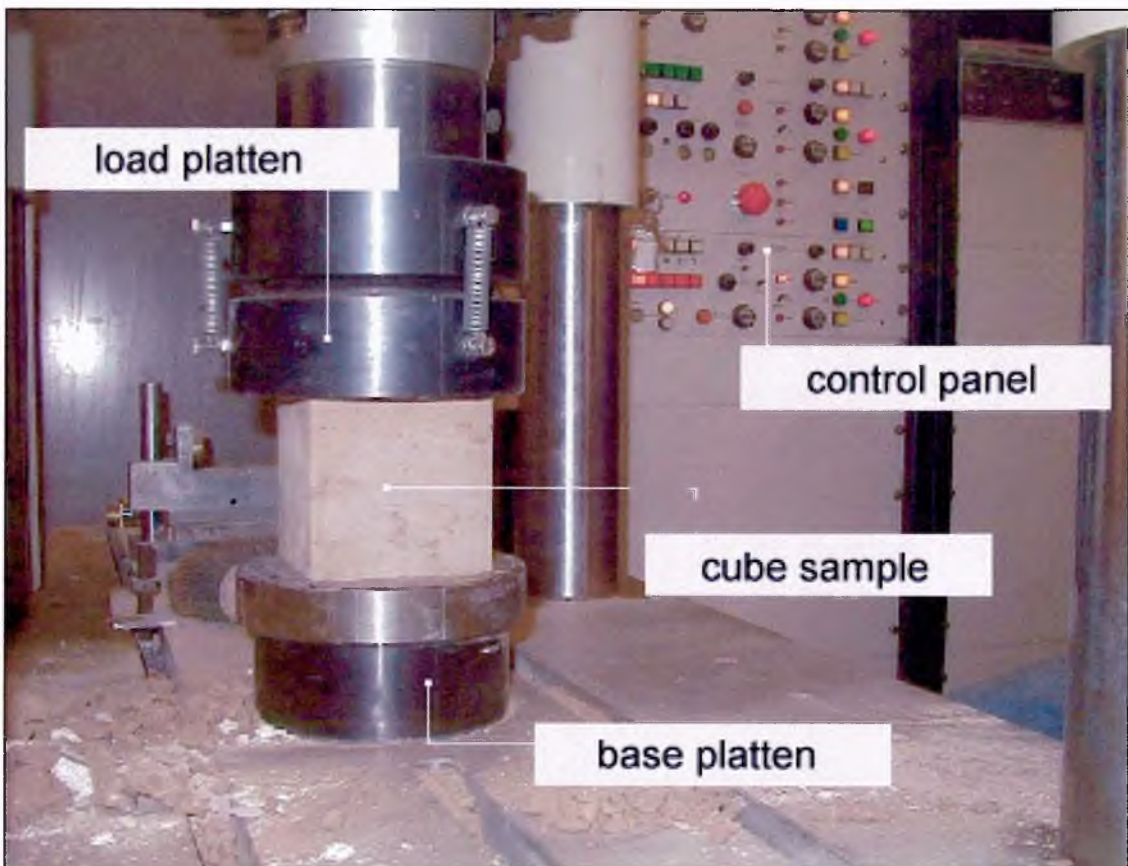


Figure 29 the Mayes SH250 compressive strength test machine

An E40 50kN load cell, of certified calibration, was placed between the load platens of the Mayes SH250. The machine was then used to apply an increasing force at a known load rate to the load cell. By comparing the stated load reading of the Mayes SH250 to the stated output of the calibrated load cell (at set time intervals) the accuracy of the test machine could be determined. Using this methodology, repeat testing of the Mayes SH250 apparatus revealed that the machine was consistently accurate to within 0.5% of the stated reading.

3.5.2 Testing Procedure

During compressive strength testing of the rammed earth cube samples, the applied load rate was set at 20kN/min. This ensured that failure of the samples occurred at a time typically between 30 and 90 seconds after the beginning of the test. This method is

consistent with standard test procedure for conventional masonry materials such as concrete and mortar. A minimum of five rammed earth cube samples is required for compressive strength testing in order to give a good representative value for a particular soil type (Standards New Zealand, 1998).

An aspect ratio correction factor of 0.7 has to be applied to the compressive stress value obtained for a cuboid sample (Standards New Zealand, 1998). This is because any sample with an aspect ratio of less than 2:1 is generally considered partially restrained by the lateral friction that exists between the load platens and the sample due to the Poisson effect (Domone, 1994_b). It is therefore assumed that this partial-restraint effect can give a falsely high reading for the unconfined compressive strength of a cube sample unless the correction factor of 0.7 is applied (CSIRO, 1987). Once the correction factor has been applied to the compressive stress data, the final value for characteristic unconfined compressive strength (f'_{cu}) is calculated using the following formula (Standards New Zealand, 1998):

$$f'_{cu} = \left(1 - 1.5 \frac{X_s}{X_a} \right) x_1 \quad \text{Equation 21}$$

Where:

X_s = standard deviation of the data series (e.g. 5 cube samples)

X_a = mean average of the data series (e.g. 5 cube samples)

x_1 = the lowest result from the series

In terms of individual sample selection, one representative cube sample was taken from each of the four production mix batches (for a given soil type) and the fifth sample was taken from a batch at random. This ensured that each soil mix batch was properly represented and acted as a measure of consistency in the soil mixing process as well as inherent variables within a given soil type.

3.5.3 Shear Plane Failure of Soil Specimens

When a rammed earth cube sample is subjected to a uniaxial compressive load it fails by exploding the sides of the cube and producing a double pyramid. This is also the most common form of failure in concrete cube samples (Domone, 1994_b) indicating similarities between the two materials. This mode of failure occurs through the development of inclined shear planes (Neville, 1986). Therefore, in the case of a rammed earth cube, we can refer to the Mohr-Coulomb theory in soil mechanics to deduce that the resistance to uniaxial compressive loading offered by the soil is related to the maximum shear strength (τ_f). As with concrete, the compressive strength of the individual granular particles (e.g. sand & gravel) is considerable, and so the specimen fails along a shear plane at the angle θ . This mode of failure is graphically illustrated by the crushed cube sample in Figure 30.



Figure 30 shear plane failure of a rammed earth specimen in an unconfined compressive strength test

In rammed earth, the maximum shear strength (τ_f) along the plane of failure is controlled by a number of physical properties within the soil structure. Firstly, the elementary soil particles are bound together by a force of cohesion (c) which represents the binding effect of the clay, cementation and other attractive forces (Barnes, 2000). Secondly, the confinement stress (σ'), that acts perpendicularly to the failure plane, restrains the impetus of movement along the shear plane (Barnes, 2000). Clearly σ' is greater in a cube sample than in a 2:1 cylindrical sample due to the partial lateral restraint caused by the Poisson effect, accounted for by the 0.7 correction factor. Finally, the angle of friction (ϕ') between elementary soil particles represents two parameters: the effect of friction between the individual soil particles, and the interlocking effect of particles with one another (Barnes, 2000). The maximum shear strength (τ_f) of the rammed earth soil is therefore calculated using equation 6.

In the case of cement-stabilised rammed earth, the bonds between elementary soil particles are enhanced and strengthened considerably by the formation of C-S-H

between the points of contact. This results in far greater values for f'_{cu} even with relatively small additions of cement, as demonstrated later in this chapter.

3.5.4 Results & Discussion: Unstabilised Rammed Earth

Only four of the ten soil mix recipes had characteristic unconfined compressive strengths (f'_{cu}), in unstabilised form, that satisfied the minimum requirement of 1.3 N/mm² specified in NZS 4298 (Standards New Zealand, 1998). The consistency of results is always impeded by the inherently significant levels of natural variation that can occur in soils. The mean average for the standard deviation of f'_{cu} was 8.73%, and the maximum recorded standard deviation in f'_{cu} was 12.8%. The graph in Figure 31 compares f'_{cu} with the maximum dry density (ρ_d) for each of the ten different soil mix recipes.

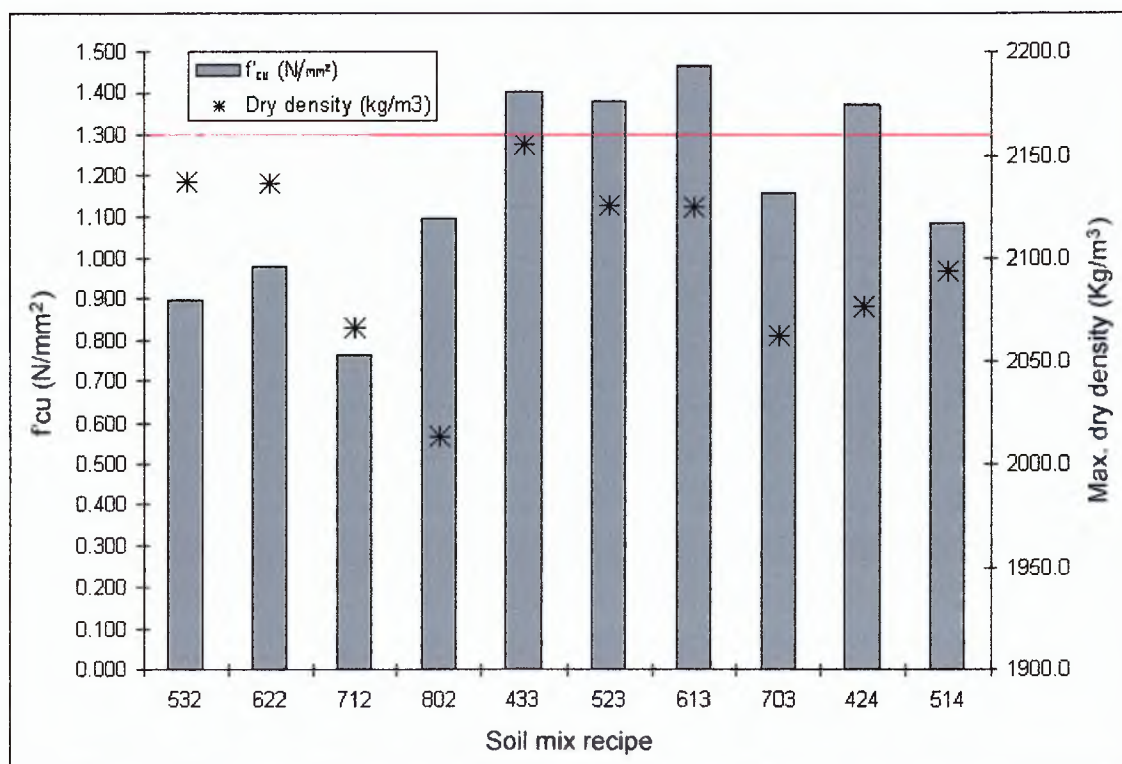


Figure 31 the relationship between f'_{cu} and ρ_d for different unstabilised soil mix recipes

It is widely accepted that, in a given soil an increase in ρ_d results in an increase in τ_f mainly because the angle of friction (ϕ') becomes greater with increased levels of compaction. Therefore, for a given soil type the maximum ρ_d is assumed to produce the maximum f'_{cu} . This is achieved by compacting the soil when it is at OMC. In the examples shown in Figure 31, however, the ten different soil mix recipes were all compacted at OMC and yet each produced a higher/lower maximum ρ_d relative to one another simply due to differences in the particle-size distribution.

The differences in maximum ρ_d between the various soil mix recipes does not appear to be directly related to f'_{cu} as there is no correlation evident from Figure 31, e.g. 532 has a similar f'_{cu} to 613, but ρ_d is very different. It is suggested that a difference in particle-size distribution can produce different values for ϕ' where the efficiency of particle packing and interlocking can vary. In addition, cohesion may alter in relation to the amount of clay, and the effectiveness of this to act as a binder could be influenced by the SSA_t of the granular soil matrix.

3.5.5 Results & Discussion: Cement-Stabilised Rammed Earth

Even a very small amount of cement stabilisation allows a given rammed earth soil to make significant gains in f'_{cu} . This general observation has been clearly illustrated by the graph in Figure 32 showing the 28-day compressive strength for three different soil mix recipes that contain varying percentage of cement stabilisation.

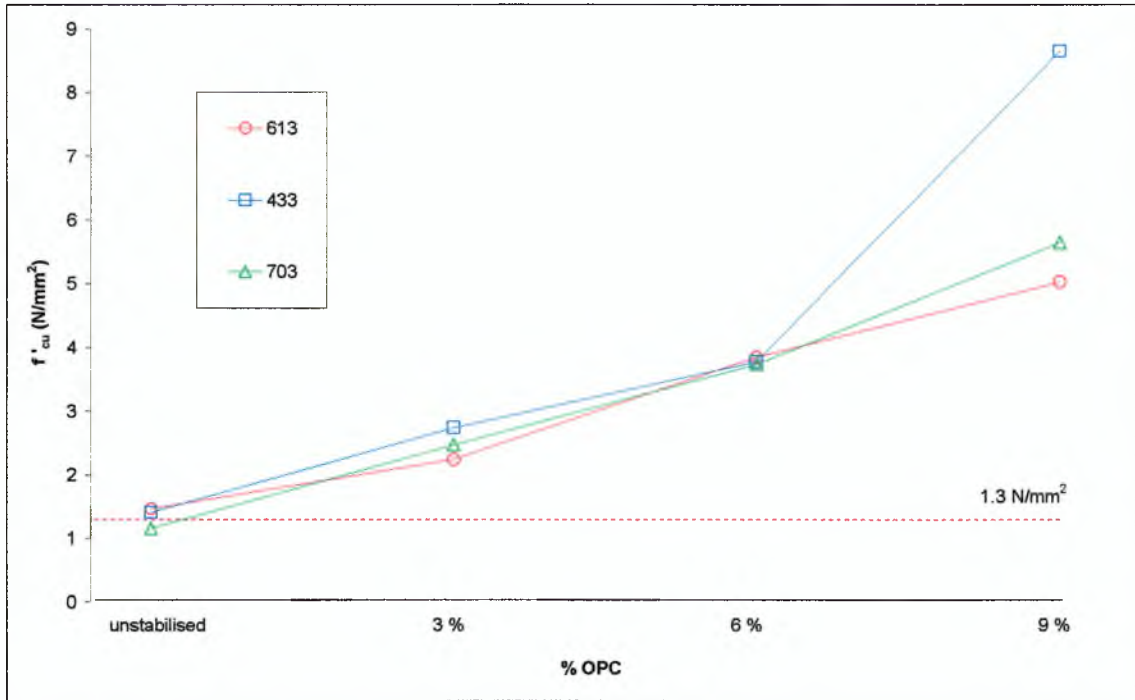


Figure 32 a comparison between the 28-day f'_{cu} for different soil mix recipes with varying percentage of cement stabilisation

The use of cement stabilisation is often considered to make rammed earth a more flexible masonry material to build with because it significantly enhances the level of durability. Cement stabilisation enables a weaker soil to be used for construction when it is not considered strong enough in unstabilised form, e.g. 703 unstabilised $f'_{cu} = 1.16$ N/mm² at 28 days. The 703 soil mix recipe can, for example, achieve a 28-day f'_{cu} of 2.47 N/mm² with the addition of just 3% cement by mass. Therefore, cement stabilisation generally increases the range of soils that are available for rammed earth construction.

Some differences have been observed between the comparative effect of varying amounts of cement stabilisation and the use of soil mix recipes that have a different particle-size distribution. These are illustrated by the graph in Figure 33.

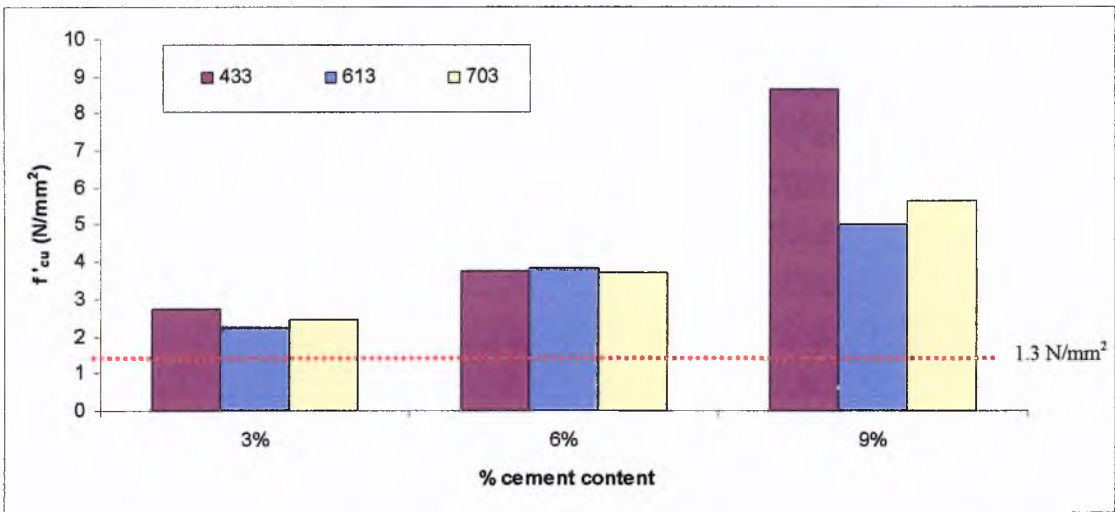


Figure 33 the relative effect of varying levels of cement stabilisation on the 28-day f'_{cu} increase in different soil mix recipes

In studies performed by CRATerre-EAG a linear relationship between f'_{cu} and % cement content was observed (Houben & Guillaud, 1996). This linear trend was also observed by one of the author's undergraduate students when comparing the 7-day f'_{cu} of a 523 mix recipe with cement content increasing from 0% up to 10% (Germain, 2002). However, as can be seen from Figure 33, the comparative effect of a given % cement content is greater for some soil types than for others. A clear exception to the linear trend is the 433 mix recipe in which f'_{cu} increased from less than 4 N/mm² at 6% OPC to more than 8.5 N/mm² at 9% OPC. It may be possible that the lower SSA_t of the 433 mix recipe is responsible for such an unusual strength increase because there are fewer points of contact between soil particles than for the other two mix recipes possibly allowing the cement to have a greater effect. However, this hypothesis would require significant further testing in order to validate it.

3.6 SUMMARY

The methodology for blending graded quarry material to specify and produce rammed earth soil mix recipes has been found to be consistent and reproducible, and it allows

the accurate control of parameters such as particle-size distribution. Unlike the Proctor method, the level of energy input used for compaction of the cube samples can be varied depending upon soil type. The technique for rammed earth cube sample production replicates commercial, on-site rammed earth wall production and satisfies the New Zealand earth building standards. The resultant cube samples have a consistent dry density that is in good agreement with the results obtained using the BS 1377: 1990 part 4 'Proctor' methods.

Commercial pneumatic compaction equipment has successfully been used to create a small number of full-scale miniature rammed earth test walls. An effective methodology for determining the mean volume and total mass of these test walls has been presented. The difference between the dry density of rammed earth that has been pneumatically compacted inside removable shuttering (i.e. on-site practice), and that of rammed earth cube samples using the methodology described above (i.e. laboratory practice), appears to be insignificant.

The difference between the maximum dry density (ρ_d) of different unstabilised rammed earth mix recipes does not appear to be directly related to the characteristic unconfined compressive strength (f'_{cu}). This is perhaps partly due to differences in the angle of friction (ϕ') between granular particles as a result of changes in the particle-size distribution. It may also be partly due to changes in the cohesion (c) caused by differences in the SSA_f/CC ratio between mix recipes. The addition of a small amount of cement gives significant increases in f'_{cu} and appears to have the greatest effect on the mix recipe with the lowest SSA_f/CC ratio. This is perhaps due to a given amount of cement having a greater localised effect in a granular matrix with lower specific surface area.

4.0 INITIAL RATE OF SUCTION (IRS)

4.1 METHODOLOGY

4.1.1 The BS3921 IRS Test

When required the total water absorption, initial rate of water absorption and unit dry density may be determined using test methods developed for concrete masonry units or fired clay bricks (Walker, 1996). The British Standard BS 3921 test for determining capillary suction of water into masonry materials is known as the initial rate of suction (IRS) test (BSI, 1985). It is a fundamentally simple test that involves placing a sample (e.g. a brick) on top of two small stands that are partially submerged (3mm deep \pm 1mm) in a large tray of water. At one-minute intervals, the brick is lifted up and the excess water is removed with a damp cloth. After having previously weighed the brick when it was dry, weighing it at this stage allows the amount of water absorbed to be determined.

The test method is essentially a gravimetric determination of absorbed water in a partially immersed porous building material (due to capillary suction) over time, the value for which is expressed in $\text{kg/m}^2 \text{ min}$. BS 3921 states that the sample is to be kept 'dry' prior to testing. Hall (1981) previously observed the cumulative absorbed mass of water (m_w) per unit area of the inflow surface, increases linearly against the square root of elapsed time ($t^{0.5}$) in fired clay bricks. Their behaviour is, therefore, in agreement with the extended Darcy equation for non-saturated flow theory described in Chapter 2.

The BS3921 IRS test is, however, of little use for materials that slake (e.g. earth materials) on contact with water. This is because the determination of imbibed water mass requires the solid mass of the porous sample to be kept constant from the beginning of the test to the end. If mass loss occurs in the sample during testing then the

amount of absorbed water cannot be calculated accurately. The BS3921 test also requires the wetted sample surface to be wiped with a damp cloth to remove excess water. This presents a large degree of operator error and a potential drying effect depending upon the type, and moisture content, of the cloth. This is not specified or elaborated upon in the BS3921 document. The testing procedure can be enhanced by maintaining a constant water temperature of 20°C ($\pm 1^\circ$) in order to ensure constant viscosity. It is recommended that the weighing operation should be completed as quickly as possible, ideally within 30 seconds (Hall & Kam-Ming, 1986).

The German standard version of the IRS test (DIN 52617) has been discussed and practised within the context of earth building materials (Minke, 2000). The main differences involve encasing the sample cube sides in fibre-reinforced polyester resin, gluing filter paper to the test face and then placing the whole sample on a submerged polyurethane foam base. However, this level of sample intervention is perhaps excessive and deviates significantly from the more ‘natural’ conditions of the BS 3921 IRS test. This is because the impermeable resin coating constricts the natural expansion of the sample when it inevitably swells due to wetting. It also restricts the displacement of air from the pore network that is naturally caused by the ingressing water. As a result of this, equilibrium between water absorption and evaporation loss at the sample surface cannot occur.

4.1.2 The IRS ‘wick’ Test

The IRS ‘wick’ test is a novel adaptation of the current BS 3921 IRS test apparatus that was devised by Hall & Djerbib (2004_a). The apparatus is clearly depicted by the diagram shown in Figure 34.

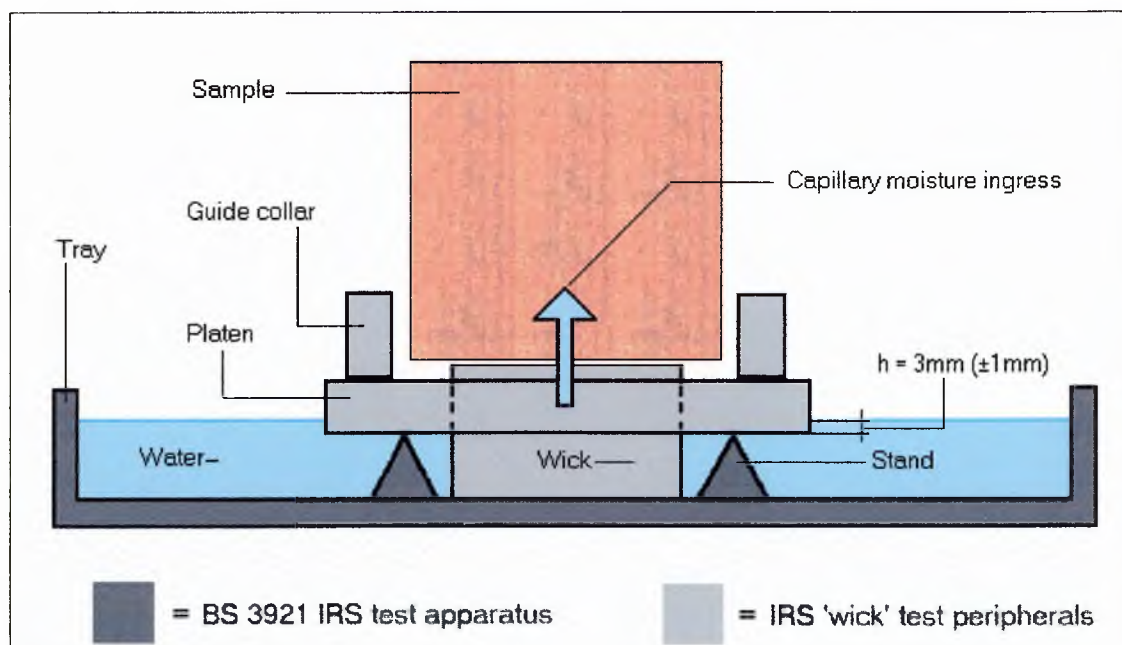


Figure 34 a diagram to illustrate the modified IRS 'wick' test

A 30mm high OasisTM 'wick', which is 80mm in diameter, acts as the point of contact between the sample and the reservoir of water. This represents free water being absorbed (by the initially dry specimen) from a saturated porous medium that offers negligible capillary resistance. According to the studies on interface phenomena performed by De Freitas, Abrantes & Crausse (1996), theoretically there should be a small degree of hydric resistance that conditions the maximum flow of moisture transmitted from the wick to the sample face being tested. However, the contact area is constant and there are no edge effects or meniscus errors to interrupt inflow-surface area calculations, as was previously the case in the BS 3921 IRS test. Therefore, where the diameter (d) of the contact area is 80mm, the inflow surface area (A) is calculated to be 5027mm^2 . This is approximately half the inflow surface area of the BS 3921 IRS test where, for a cube sample, A is equal to $10,000\text{mm}^2$.

Unstabilised earth that slakes in contact with water remains stable throughout the test and negligible mass loss occurs as the inflow surface is retained by the self-weight of

the sample acting on the solid surface of the wick. The wick itself can simply be taken out, washed and then reused such that repeatability of the test can be maintained. The various stages of a rammed earth cube sample undergoing the IRS ‘wick’ test can be seen from the pictures shown in Figure 35.

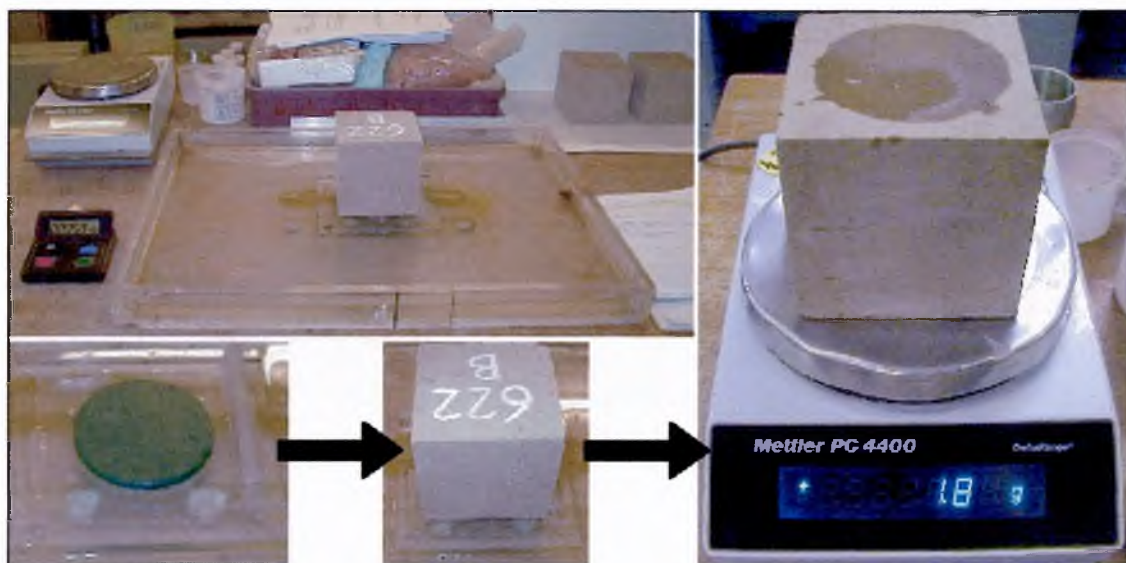


Figure 35 the various stages of the IRS ‘wick’ test in operation

4.1.2.1 Validity of IRS ‘wick’ Test

Testing was performed on vibration-compacted C30 concrete 100mm cubes and 3 types of brick; London Brick ‘Fletton’ (high porosity), London Brick ‘Dapple Light’ (medium porosity) and Engineering Brick (low porosity). Six representative samples for each of these material types were selected. The bricks were cut on a diamond bit saw to give a 100mm inflow-surface area the same as the concrete cube samples. Firstly, the IRS test was performed in accordance with BS 3921 (BSI, 1985) for a period of 5 minutes for each sample with gravimetric moisture determinations taken at 1-minute intervals. Secondly, the same samples were oven dried to constant mass and tested for a second time. For the repeat test, the same procedure was followed (as above) but was performed using the IRS ‘wick’ test apparatus. Hall (1981) previously observed that no

changes occurred in the pore structure of fired clay bricks during repeat-tests of this nature; however, it is unknown whether the same applies to concrete or cement stabilised rammed earth.

The IRS 'wick' test values for initial rate of suction were in close agreement with those obtained using the BS 3921 IRS test. Figure 36 illustrates the comparison between BS 3921 IRS and IRS 'wick' test data obtained during calibration testing.

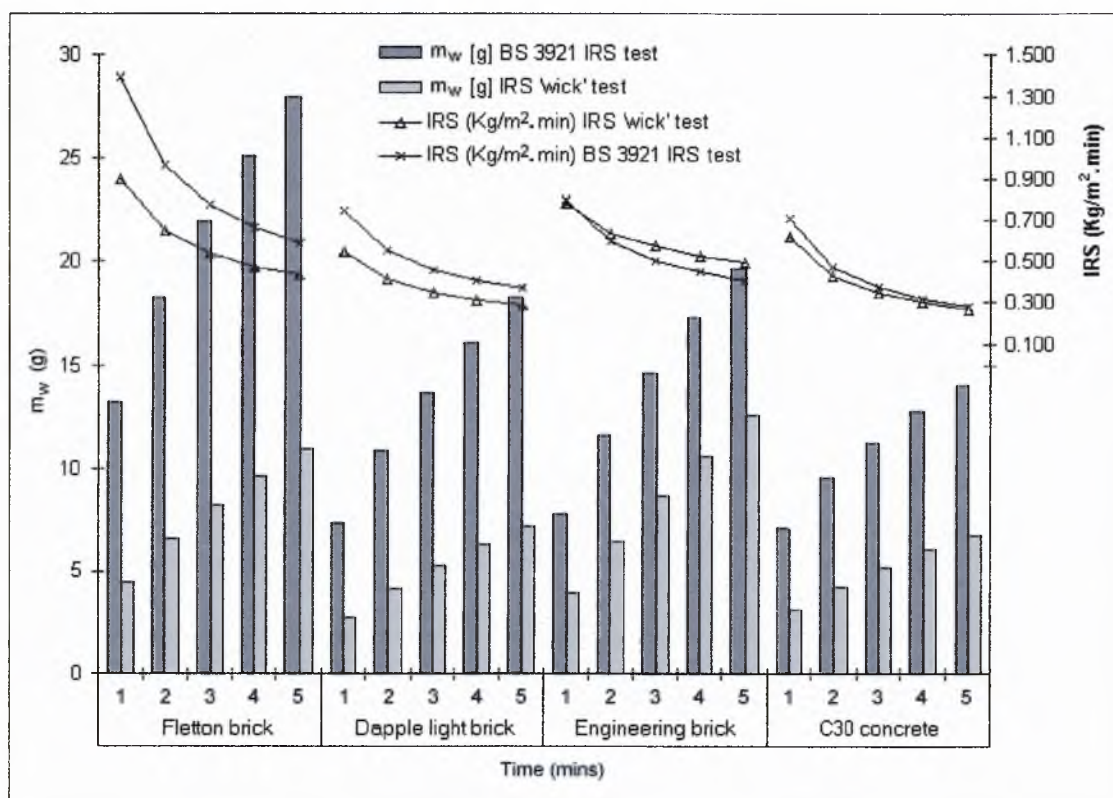


Figure 36 a comparison between the BS3921 and the IRS 'wick' test results obtained for conventional materials

Note that the actual mass of sorbed water in the 'wick' test samples is around half that of the BS 3921 IRS test samples. This is simply because the inflow-surface area of the wick is approximately half that of the BS 3921 IRS test. A good correlation is therefore indicated by a similar IRS value, which is calculated as the mass of sorbed water per

unit of inflow surface area over time. It was observed that for very porous samples a greater disparity occurred between the values obtained using the BS 3921 IRS test and those obtained using the IRS 'wick' test (see: results for Fletton and Dapple Light bricks). This may be due to the effect of hydric resistance at the wick/sample interface. This would explain why the same effect is magnified when the IRS value increases. However, rammed earth is particularly dense with a low porosity (typically lower than concrete) and so the IRS 'wick' test is considered a suitable means with which to test this material.

The variation that occurs between results for individual test specimens is significant and is an inherent problem with both the BS 3921 IRS test and the IRS 'wick' test. The average level of variation between rammed earth samples was observed to be between approximately 20% and 40%. These parameters are well within the typical variations observed in the SHU Construction Materials laboratory for numerous varieties of fired clay bricks after several thousand cycles of BS 3921 IRS testing. The degree of variation that inevitably occurs between individual test specimens may be attributed to natural variations in pore structure both within the cube and, more importantly, at the inflow face. This emphasises the myopic nature of testing individual masonry building materials at this scale when, for example, the behaviour of a construction element (e.g. a wall) cannot be defined by the performance of an individual brick. However, testing a randomly selected batch of samples can be used to give a good indication of a porous masonry materials performance in terms of moisture ingress due to capillary suction through a set of average values.

4.1.2.2 Moisture Dissipation Test

Following the performance of the IRS ‘wick’ test, the cube sample has been subjected to a standardised degree of moisture ingress for a known period of time. In order to gain additional results, an undergraduate study was performed by Turner (2004) under the supervision of the author to investigate the rate at which absorbed moisture is lost from a wetted sample. The moisture dissipation test commences immediately after the completion of an IRS ‘wick’ test for a given cube sample. Therefore, the total mass of absorbed water (m_w) at this point is known.

The cube sample is allowed to dry naturally in controlled laboratory conditions of 20°C ($\pm 1^\circ$) 40% RH ($\pm 5\%$) with the wetted face pointing upwards. The mass of the cube is recorded at 5-minute intervals for the first 30 minutes, and then at 15-minute intervals for an additional 90 minutes (Turner, 2004). The total duration of the dissipation test is 2 hours, the results of which were used to calculate the total moisture loss, cumulative rate of moisture loss, and the percentage moisture retention in relation to the initial m_w . The results from these experiments are linked with other undergraduate studies on a common theme and so the results from each study have been combined and presented in Chapter 7 - Section 7.3.2.

4.1.3 Test Procedure

The production of rammed earth cube samples using synthetically blended soils, whose particle-size distribution can accurately be specified and controlled, has previously been discussed (see: Section 3.2). Further details on the physical and mechanical properties of the 1 litre rammed earth cube samples have also been previously examined and illustrated. This method of rammed earth sample production was found to be highly

repeatable and consistent in terms of density, dimensional stability and compressive strength (see: Section 3.5).

4.1.3.1 Unstabilised Rammed Earth

All ten of the soil mix recipes that were specified previously in this chapter have been used in unstabilised form for the first stage of IRS ‘wick’ testing. Six representative samples from each of the ten soil types were used as the test specimens. Each sample was tested for a period of 5-minutes and the mass of sorbed water (m_w) was recorded at 1-minute intervals. After this testing, the samples were then allowed to dry before the IRS ‘wick’ test regime, described above, was repeated using the same samples and the same inflow-surfaces. This time, however, only three from each of the six samples (in each set) were selected for the re-testing. The samples selected from a particular soil type all had a similar IRS value, thereby eliminating the upper and lower values from the repeat-test results. Weight determinations were made at 1-minute intervals but the total test duration was extended to give values for 1, 2, 3, 4, 5, 10, 20, 30, 40, 50 & 60-minute elapsed time intervals.

4.1.3.2 Cement-Stabilised Rammed Earth

As discussed previously, three of the ten soil recipes were selected for a further series of testing in conjunction with ordinary Portland cement (OPC) stabilisation. The soil types selected were sandy (703), cohesive (613) and pebbly (433). A range of samples was produced for each soil type using 3%, 6% and 9% cement (by mass). Six representative specimens from each sample group were used for the testing. Each sample was tested using the IRS ‘wick’ test for a period of 5-minutes, and the mass of sorbed water (m_w) was recorded at 1-minute intervals.

4.2 RESULTS & DISCUSSION

4.2.1 IRS – Rammed Earth vs. Conventional Masonry Materials

Rammed earth generally has a very low initial rate of suction (IRS) compared to conventional masonry materials such as concrete and fired clay bricks, and absorbs much smaller amounts of water over a given time span. This is perhaps due to its relatively high density and resultant lower bulk porosity. This relationship has been illustrated in Table 7 where the average mass of sorbed water (m_w) for each material tested has been expressed as a percentage of the sample's dry mass during a 5-minute IRS 'wick' test.

Table 7 the average amount of sorbed water during a 5-minute IRS ‘wick’ test

Masonry type	Dry Mass _{avg} (g)	W _{avg}		St Dev (%)	w _{avg} (% of dry mass)
		Mass (g)	St Dev (g)		
London brick - Fletton	851.0	10.95	2.22	20.3	1.29
London brick - Dapple Light	923.2	7.12	1.1	15.4	0.77
Engineering brick	1316.6	12.47	4.89	39.2	0.95
C30 concrete	2165.8	6.72	0.66	9.8	0.31
Rammed earth - 532	2136.9	3.17	1.14	36.0	0.15
Rammed earth - 622	2132.0	3.37	0.75	22.2	0.16
Rammed earth - 712	2068.8	8.45	3.29	38.9	0.41
Rammed earth - 802	2030.6	15.15	4.01	26.4	0.74
Rammed earth - 433	2180.5	3.42	0.64	18.6	0.16
Rammed earth - 523	2101.3	4.22	1.27	30.1	0.20
Rammed earth - 613	2120.0	4.15	0.84	20.2	0.20
Rammed earth - 703	2058.4	5.95	2.24	37.7	0.29
Rammed earth - 424	2067.3	5.92	2.05	34.7	0.28
Rammed earth - 514	2089.0	3.12	0.67	21.6	0.15

Note that, for some materials, the mass of water absorbed (m_w) is larger than for others, whilst the percentage moisture absorption (w) is actually lower. This is because the percentage water absorption is a function of the material’s dry density (ρ_d). The 802 rammed earth soil mix recipe, for example, absorbs more than double the mass of water compared with a dapple light London brick. However, the percentage water absorption for both the brick and the rammed earth are virtually the same due to the disparity in ρ_d .

Also, note that the standard deviation for the results is in keeping with the typical level of dispersion expected for masonry materials in IRS tests (see Section 4.1.2.1). The test results are therefore suitable for comparison with one another, and may provide only an indication of the likely performance for each masonry material within the context of a construction element.

The initial rate of suction (IRS), recorded over a five-minute test period, has been illustrated in Figure 37 to show the comparison between different unstabilised rammed earth mix recipes and a selection of conventional masonry materials.

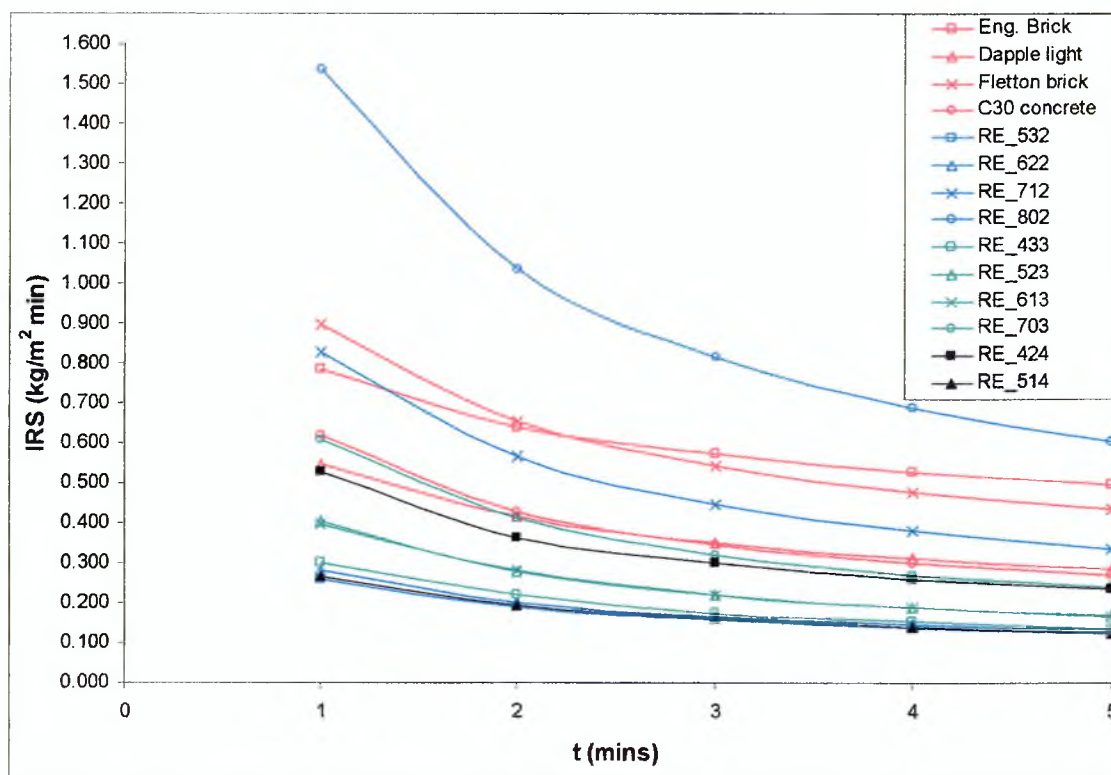


Figure 37 a comparison between the IRS ‘wick’ test results (5-minute regime) for various unstabilised rammed earth mix recipes and a small selection of conventional masonry materials

Fletton bricks and Engineering bricks have a higher initial rate of suction than every rammed earth mix recipe apart from 802. The IRS values for vibration-compacted C30

concrete appear just above those for rammed earth mix recipe 703, which is one of the high-moisture ingress examples of rammed earth. More notably the IRS curves for fired clay brick appear to be at a different gradient to those for rammed earth, whereas that of concrete is almost the same. This indicates clear similarities between the internal pore structures of concrete and rammed earth, and a disparity with those of fired clay brick.

4.2.2 IRS Testing of Unstabilised Rammed Earth

4.2.2.1 5-minute IRS ‘wick’ Test Results

The pattern in Figure 37 appears to suggest that the IRS curves for these mix recipes align themselves in three distinct bands along the y-axis. The highest of these three bands is singly represented by the 802-mix recipe, the medium range band by the 712, 703 & 424 mix recipes, and the lowest band by 523, 613, 433, 622, 532 & 514. The 802-mix recipe appears to suffer from significantly higher moisture ingress compared with the others. Within the parameters of these mix recipes, it would appear that IRS values that are equal to/below $0.4 \text{ kg/m}^2 \text{ min}$ could be classed as ‘low’ IRS, 0.4 to 0.8 are ‘medium’, and above 0.8 are ‘high’. Variations in the level of permeability between different mix recipes appear to be a function of certain parameters within the soil grading. These parameters are closely analysed and discussed in Chapter 7.

4.2.2.2 60-minute IRS ‘wick’ Test Results

The graph in Figure 38 shows the comparison between the ten unstabilised rammed earth soil types that were repeat-tested under the 60-minute IRS ‘wick’ test regime (refer: Section 4.1.3.1).

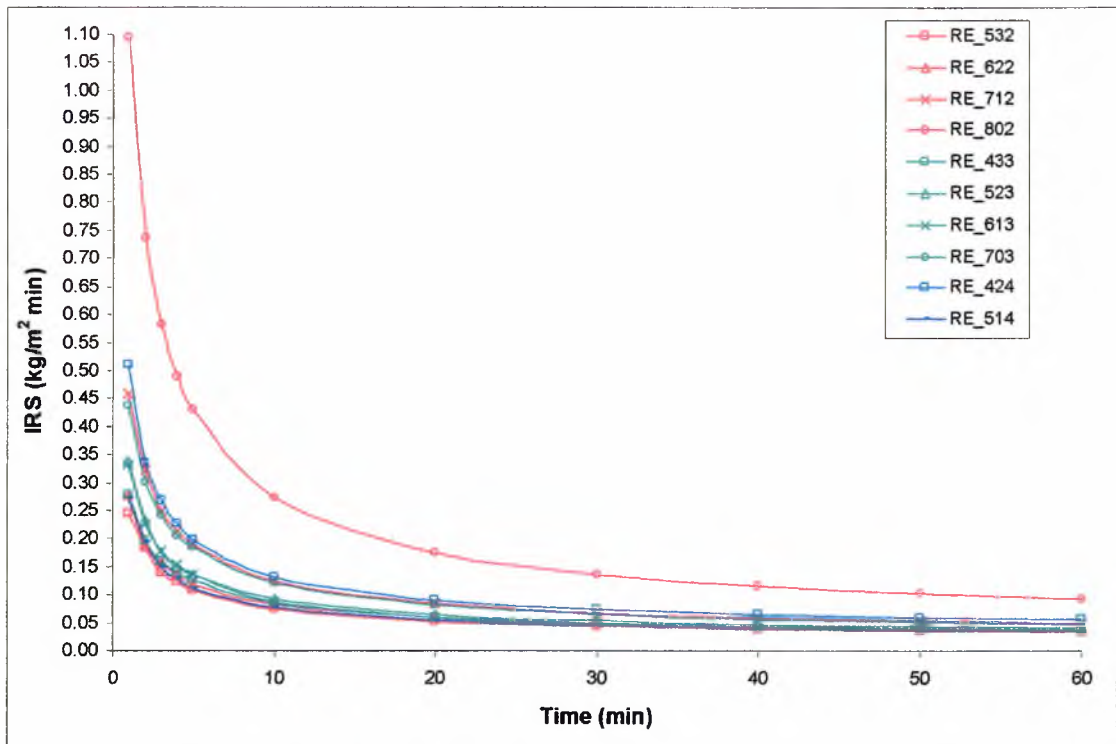


Figure 38 a comparison between the IRS of different unstabilised rammed earth mix recipes under the 60-minute (repeat) IRS ‘wick’ test regime

We can observe from the pattern in Figure 38 that the IRS results for these mix recipes appear to be displayed as an exponential curve over a 60-minute duration. In addition, the curves appear to align themselves in the same three bands (high, medium and low - refer Section 4.2.2.1 for ranges) along the y-axis as with the 5-minute test regime described above, although this time the separations between curves appear to be more clearly defined. Beyond the 10-minute point, the IRS of all samples begins to decrease significantly and by 50 to 60 minutes, all of the mix recipes are at a very similar IRS value. This pattern may be due to the 3-dimensional nature of capillary moisture migration within the samples where, after 1-hour of testing, we can observe the beginnings of a steady state between absorption and evaporation. This theory has previously been studied by Hall (1981) and is explained in more detail in the following section.

4.2.2.3 3-Dimensional Moisture Migration

It has been observed elsewhere that after approximately 3 hours of testing, m_w becomes proportional to t giving experimental confirmation of a steady state in 3-dimensional water absorption scenarios (Hall, 1981). This occurs where equilibrium is established between the mass gained from absorbed water, and the mass lost through evaporation at the exposed surfaces of the sample. The BS 3921 IRS test is a 1-dimensional case whereas the IRS 'wick' test is 3-dimensional, as illustrated by the diagram in Figure 39.

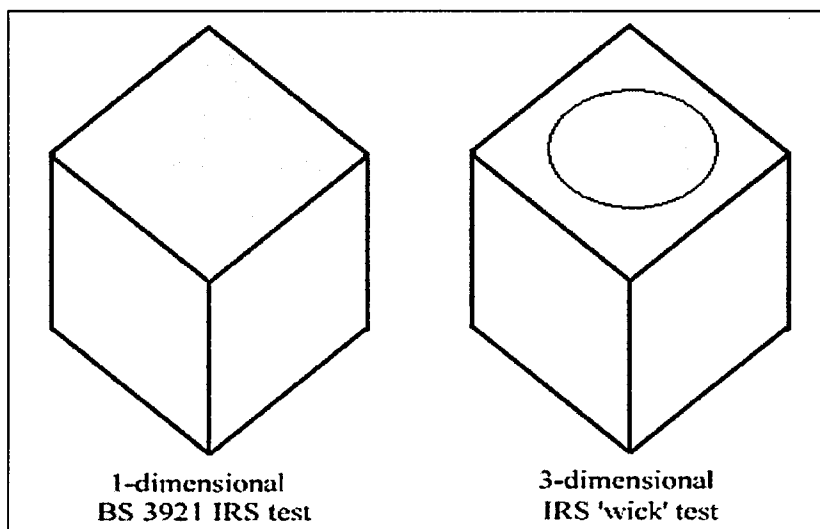


Figure 39 a comparison between the geometry of IRS test methodologies

Hall (1981) previously observed that a spherical inflow source in the centre of the specimen face provides lateral spreading of the absorbed water within the material. In the 3-dimensional case, the geometric shape for the advancing wet front of the ingressing moisture is that of an oblate hemispheroid (Hall, 1981). It is possibly a more realistic scenario than the 1-Dimensional BS 3921 IRS test for experimentally comparing the results to those obtained using full-sized test walls. It has been observed elsewhere that the absorption rate per unit source area is not independent of the source dimensions (Hall, 1981). The 80mm diameter circular inflow source on the IRS 'wick'

test should therefore be standardised for other 3-dimensional test methodologies such as the Initial Surface Absorption (ISA) test.

4.2.2.4 Repeat-testing of Inflow Surfaces

Differences were observed in the IRS of a given sample between it being tested under the 5-minute regime, and then being re-tested under the 60-minute regime. Repeat-testing unstabilised rammed earth appears to result in significantly lowering its IRS from the original value. The average variation between results, due to repeat testing, indicates an approximate decrease in IRS from as little as 5% up to as much as 44% depending upon soil type. The quantity of reduction in IRS was observed to coincide with the original IRS value of the specimen. That is to say, samples that were already prone to higher capillary moisture absorption exhibited a greater reduction in IRS following repeat testing. These observations can be seen from the results illustrated by the graph in Figure 40.

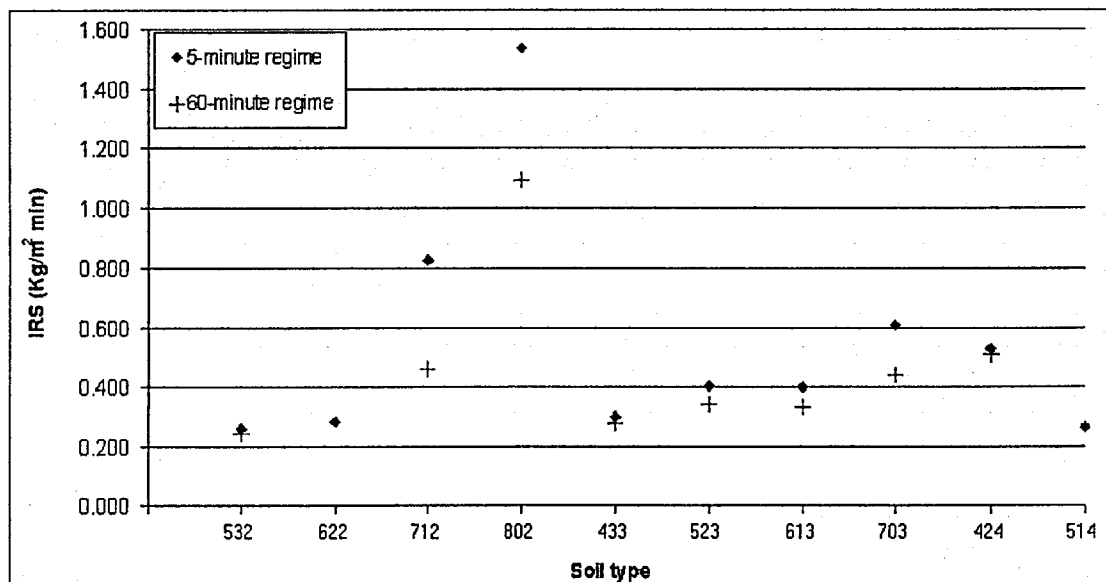


Figure 40 the variation of IRS in different rammed earth mix recipes samples due to single repeat-testing of the sample face

These trends appear to indicate that non-saturated moisture ingress in unstabilised rammed earth may change the properties of the material such that its pore structure becomes less permeable. The surface finish of the test specimens appeared to have become visibly altered following the first period of IRS ‘wick’ testing. The pore structure of a soil varies in cleanliness (Bowles, 1984) and so it may be possible for the fines within the soil to become mobilised and relocated to a different position within the soil structure due to the migration of moisture. The mobilised fines may have the effect of partially blocking passages within the pore network and reducing their permeability. It has been reported by rammed earth contractors that some rammed earth façades appear to be ‘self-healing’ when they are exposed to the effects of weathering (Dobson, 2001, *pers comm.*). The moisture-induced mobilisation and redistribution of fines along the façade may account for these observations.

4.2.2.5 The Effect of Surface Finish

The surface finish of the inflow test face seems to be critical in determining the level of moisture ingress in rammed earth. Observations suggest that this may be chiefly controlled by the particle-size distribution of the soil, and more specifically by the random location of different sized particles at the façade. Larger granular particles (e.g. gravel) appear to be responsible for the formation of small cracks and areas of boniness. These surface features may allow increased amounts of water to be imbibed. In addition, moisture ‘tracking’ may occur where the ingressing water follows the contour of large, isolated particles due to surface tension. This particular factor may be magnified on small-scale laboratory tests such as this where, for example, a piece of 14mm gravel represents over 1/8th the width of an 80mm diameter inflow surface area.

The moisture ingress in rammed earth sample faces was visually observed to be slightly greater at the compaction planes (i.e. the zones between layers of compacted soil) where the inherent degree of compaction is slightly less. This effect is analogous to that of the position of casting in a concrete specimen where the trowelled surface can be as much as twice the porosity of the bottom region, and with a greater percentage of large pores due to a lower degree of consolidation (Khatib & Mangat, 2003). Rammed earth contractors often apply the practice of carefully layering the soil inside the formwork, as opposed to tipping it in, in order to prevent the larger aggregates from accumulating at the bottom of each subsequent layer. The use of oiled shuttering may induce a smoother surface finish on the wall, although it has previously been observed in oil-formed concrete cube samples that the porosity of the sides is often greater than that of the core of the specimen and has a greater sensitivity to exposure (Khatib & Mangat, 2003).

Discretionary operator control during small-scale laboratory testing introduces factors that would not normally be present in the testing of a full-sized wall. Sample faces that were free from defects, for example, were selected for testing to reduce the variability of results and random effects as much as possible. This level of control is acceptable for small-scale laboratory testing, as the number of variables should be controlled wherever possible. However, the use of full-sized test walls would lessen these considerations and, in one sense, provide a more realistic representation of the materials performance as a building element. Conversely, the accuracy and quality control of an experiment can often decrease as the scale of the test increases.

4.2.2.6 Non-saturated Flow Theory

Previously, the $t^{0.5}$ law (detailed in Chapter 2) was only observed to be applicable to fired clay bricks for the 1-dimensional case of the BS 3921 IRS test where the inflow of sorbed water is normal to the inflow surface (Hall, 1981). Hall (1981) states that for a circular source, with 3-Dimensional lateral internal spreading, the cumulative absorption should increase more rapidly than $t^{0.5}$ for common clay bricks, however their internal pore structure is perhaps different to that of rammed earth. In contrast to these findings the results obtained here for unstabilised rammed earth show that in the case of 3-dimensional water absorption (IRS 'wick' test), when the mass of sorbed water (m_w) for a given inflow surface area is plotted against the root of elapsed time ($t^{0.5}$) the relationship is linear. The data supporting this observation has been plotted in the graph shown in Figure 41.

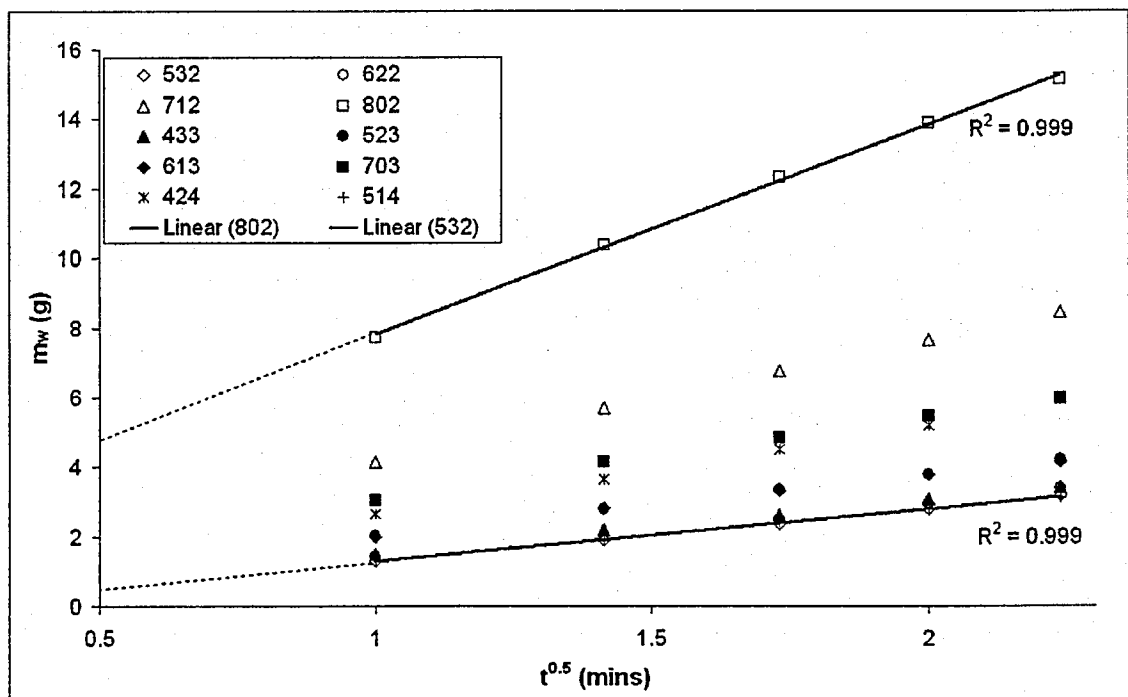


Figure 41 the relationship between the total mass of sorbed water and the square root of elapsed time for different unstabilised rammed earth mix recipes

This effect may occur because the total mass of sorbed water is considerably less for rammed earth than for conventional fired clay brick materials, and that a deviation from pure linearity in the $m_w/t^{0.5}$ relationship is not visible at these levels. The linearity of the results for unstabilised rammed earth is, nevertheless, plainly evident and may simply illustrate a difference in behaviour to fired clay bricks (refer Section 4.2.1). This difference in behaviour may logically be attributed to factors such as differences in internal pore structure and the surface tension of the material.

4.2.3 IRS Testing of Cement-Stabilised Rammed Earth (SRE)

Three rammed earth mix recipes were selected for IRS testing when stabilised with varying amounts of cement. These soil recipes were picked to represent capillary moisture ingress performance that is classed as good (433), medium (613) and poor (703). Each of the mix recipes were made using 3%, 6%, and 9% (by mass) of ordinary Portland cement (OPC), as explained in Chapter 3 - Section 3.1.3.

4.2.3.1 5-minute IRS ‘wick’ Test Results

The IRS values for these samples, illustrated by the graph in Figure 42, were all taken at the first minute interval of a 5-minute ‘wick’ test regime.

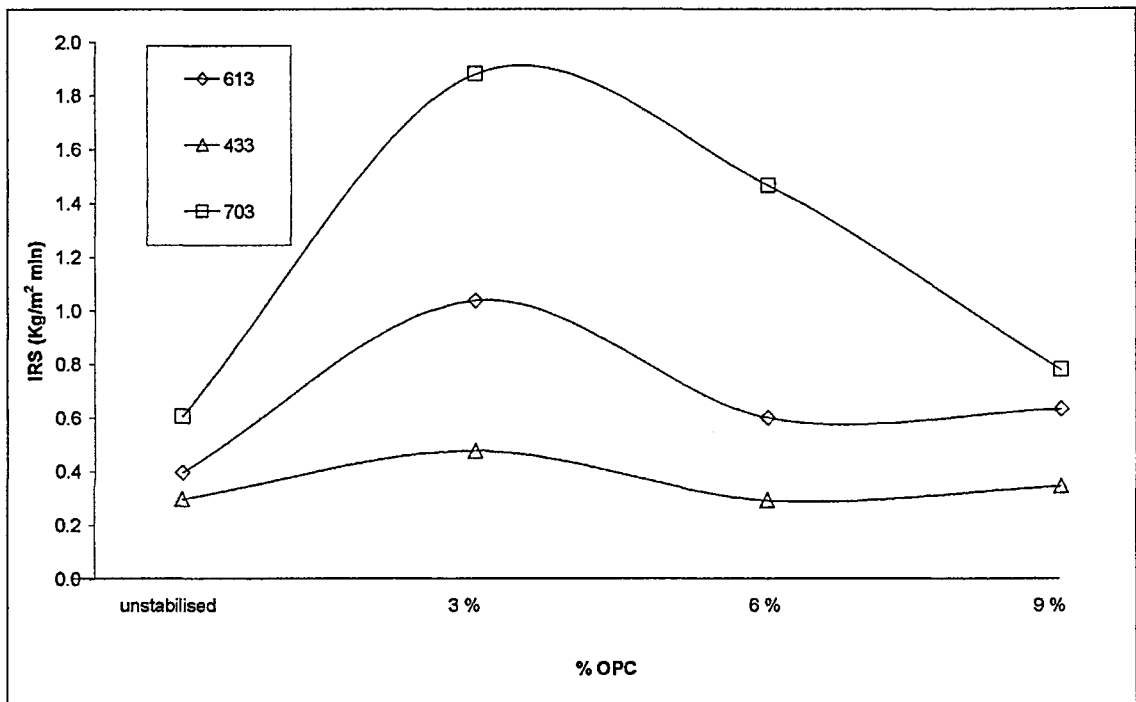


Figure 42 the relative effects of varying cement content on the 1-minute IRS value of three stabilised rammed earth mix recipes

Unlike compressive strength, the linear increase of cement content does not appear to produce linear changes in moisture ingress performance. The addition of up to 3% OPC (by mass) has a very significant effect in increasing capillary moisture ingress for each of the three soil types tested. It also appears to exacerbate this effect of increasing moisture ingress in accordance with the susceptibility of a particular mix recipe. That is to say, the level of increase in IRS for 703 soils is considerably greater than that for 433 soils. In a separate study, Walker (1996) observed that the initial rate of suction values for cement stabilised compressed earth blocks is often in excess of 1.5 kg/m²/min. In the case of the cement-stabilised mix recipes tested here, the IRS values are mostly significantly lower. This is most likely caused by differences in the soil grading and/or dry density of the materials being tested.

The continued addition of OPC beyond 3% appears to have the effect of reducing capillary moisture ingress, back towards the original level of the unstabilised mix.

According to these results, the optimum level of cement stabilisation for the ‘good’ 433 mix recipe is 6% (by mass) giving a 1-minute IRS value that is approximately the same as that for the unstabilised mix. The optimum level of cement for the ‘medium’ 613 mix is also 6%, although even at this the IRS value is significantly higher than the unstabilised mix. The optimum level of cement for the ‘poor’ 703 mix is 9%, but even at this level its IRS value is still higher than the unstabilised mix.

4.2.3.2 Clay/Cement Interaction

When cement stabilised rammed earth (SRE) is curing it can remain moist (i.e. ‘green’) for several days and so the clay bonds are not likely to be as strong as when the specimen has dried. Meanwhile, the presence of moisture at this stage will fuel the first stages of the cement hydration reaction. The cement forms strong, chemical bonds between the granular soil particles and reduces the effectiveness of clay particle assemblages (Walker, 1995). These effects combined may inhibit or retard the formation of clay bridges between the granular soil particles.

It may be the case that a small amount of cement (e.g. 3%) is enough to inhibit the formation of clay bridging and so therefore could increase the permeability of a soil. However, this small amount in itself may be unable to produce enough C-S-H to form an inter-particle structure that replaces the waterproofing effect of the clay. A further increase in cement content would produce more C-S-H and so may reduce the permeability of the soil. In theory, a more permeable soil (e.g. 703-mix recipe) would therefore require more cement than a less permeable soil (e.g. 433-mix recipe) to optimise the level of reduction in permeability.

Metakaolin (MK) is a very fine, alumina-rich powder that is highly pozzolanic but that essentially has the same oxide formation as ordinary kaolin, i.e. china clay (Khatib & Wild, 1998). The addition of MK in concretes, as a partial cement replacement additive, has been observed to produce an apparent pore-blocking effect that reduces capillary moisture ingress in concretes significantly (Khatib & Clay, 2004). The pore volume of MK/cement paste is actually higher than pure cement paste indicating that the porosity of the material is increased. However, this increase in porosity is apparently caused by densification of the C-S-H phase, and so the greater level of porosity is in the form of an increased percentage of fine pores. The creation of this finer pore structure has been referred to as a possible reason for the reduced level of capillary moisture ingress that was observed (Khatib & Clay, 2004).

4.2.3.3 Non-saturated Flow Theory

As was the case for unstabilised rammed earth, the results obtained for cement stabilised rammed earth show that when the increasing mass of sorbed water (m_w) for a given inflow surface area is plotted against the square root of elapsed time ($t^{0.5}$) the relationship is linear as can be seen from the graph in Figure 43.

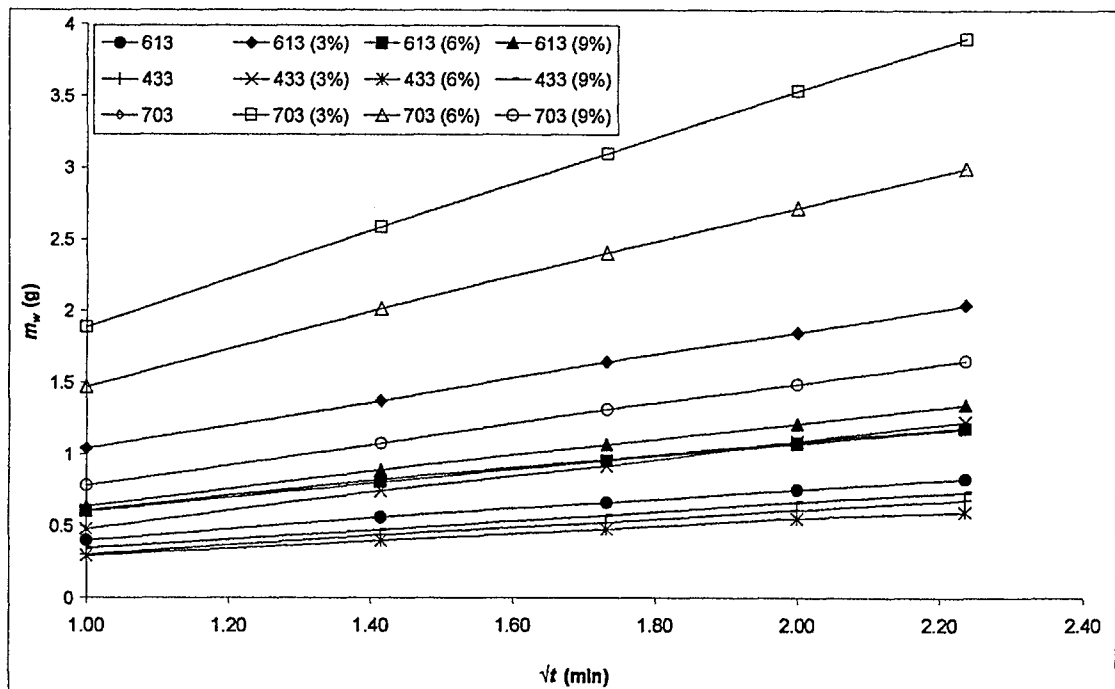


Figure 43 Relationship between mass of sorbed water and square root of elapsed time for cement stabilised rammed earth

In previous research, relating to fired clay bricks, the linear relationship between m_w and $t^{0.5}$ was found only to occur in samples where the inflow of moisture was 1-dimensional and normal to the test face. The lateral internal spreading that occurs in a 3-dimensional scenario, such as the IRS ‘wick’ test, should therefore cause m_w to increase at a much faster rate than $t^{0.5}$. In contrast to this, however, the linear increase of m_w against $t^{0.5}$ has now been observed in both unstabilised and stabilised rammed earth with varying levels of cement content.

4.3 SUMMARY

The novel IRS ‘wick’ test has been devised as a peripheral to the established BS 3921 IRS test, and is suitable for use with both unstabilised and cement-stabilised earth materials that may slake on contact with water. It produces consistent results that, for higher density materials such as concrete and rammed earth, are in good agreement with the original BS 3921 IRS test.

The IRS for rammed earth is typically much lower than conventional masonry building materials and is comparable to or better than that of vibration-compacted C30 concrete. There is a great similarity between the IRS profile over elapsed time for rammed earth and concrete indicating similarities in pore structure. The mass of absorbed water (m_w) increases linearly against the square root of elapsed time ($t^{0.5}$) in both unstabilised and stabilised rammed earth.

5.0 INITIAL SURFACE ABSORPTION (ISA)

5.1 METHODOLOGY

5.1.1 The BS 1881-208 ISA Test

The Initial Surface Absorption (ISA) test is a non-destructive methodology devised by M. Levitt in 1971 for testing concrete. It measures the absorption rate of water, which is applied under a static pressure differential, by the surface of a porous building material (e.g. concrete). It is currently accepted as a British Standard for testing concrete: BS 1881 – 208: 1996 *Testing Concrete – Recommendations for the Determination of the Initial Surface Absorption of Concrete* (BSI, 1996). Figure 44 illustrates the apparatus and configuration of the currently defined ISA test:

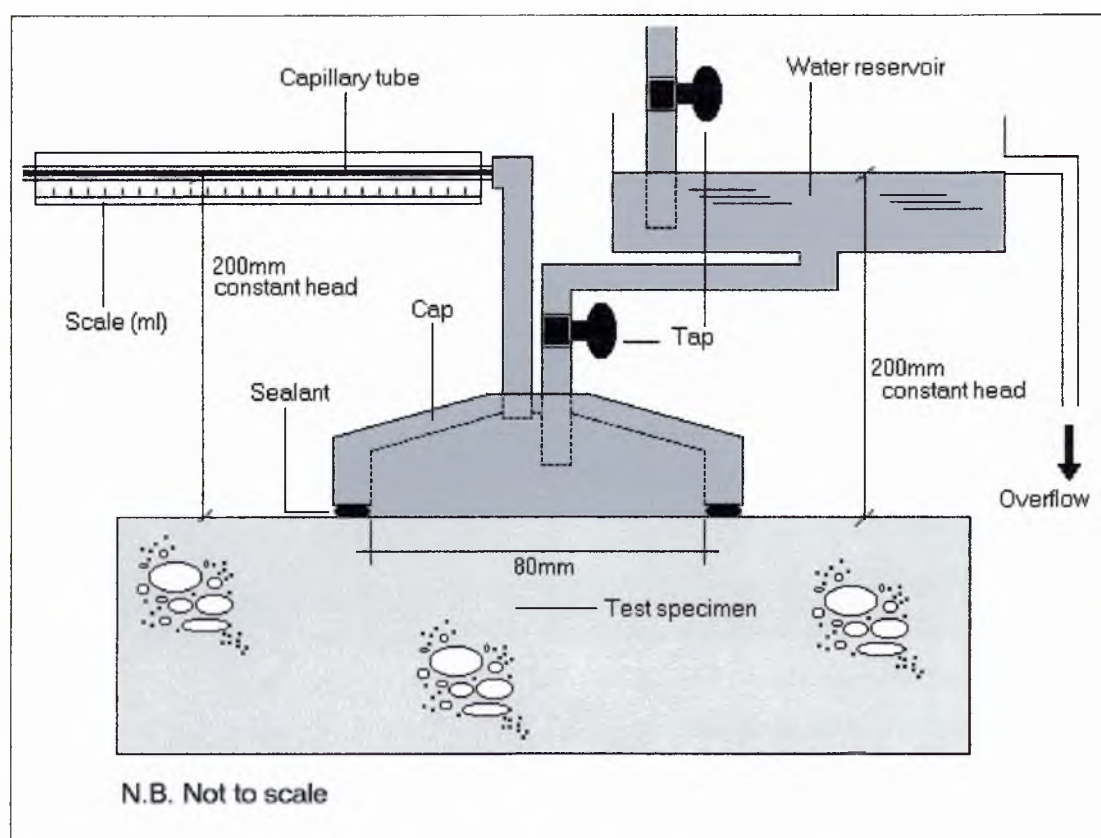


Figure 44 an illustration of the Initial Surface Absorption (ISA) test apparatus

Each specimen is subjected to static pressure-driven water from a 200mm (± 10 mm) constant head supply for a total duration of 60 minutes. Determinations of the absorption rate are made at 10-minute intervals. The procedure for measuring the absorption rate is to lower the capillary tube to a height of 200mm above the sample test face, until the tube has completely filled with water (see: Figure 44). The reservoir tap is then closed and the capillary tube is raised back to 200mm constant head. The capillary tube now temporarily acts as a finite reservoir and so the water moves along the horizontal capillary as it gets absorbed by the sample. The rate that the water is absorbed by the sample surface can be measured along the scale rule under the capillary tube and timed using a stopwatch. Since the cross-sectional area of the capillary tube is known (1mm^2) the volume of water can be calculated against the scale rule measurement, and therefore gives the absorption rate over time.

The duration of the measurement interval is typically 1 minute for rammed earth although this can be altered depending upon the magnitude of the absorption rate, as defined in BS 1881 – 208: 1996 (BSI, 1996). Following the measurement interval the reservoir tap can be re-opened to continue subjecting the sample to pressure-driven moisture penetration from the main (large) reservoir until the next 10-minute measurement interval. The water and ambient air temperatures were both maintained at a constant temperature of 20°C ($\pm 2^\circ\text{C}$), and the air was maintained at a relative humidity of 40% ($\pm 5\%$). All samples were conditioned for a minimum of 28 days in a curing chamber at 20°C ($\pm 2^\circ\text{C}$) and 75% ($\pm 5\%$) prior to testing. The unit of measurement for the initial surface absorption is $\text{ml/m}^2 \cdot \text{s}$ and therefore quantifies the mass per unit inflow surface area over time. This can easily be converted to $\text{kg/m}^2 \cdot \text{min}$ or visa versa as a means to compare data obtained from IRS ‘wick’ testing.

5.1.2 The Modified ISA Test

For the experimental work conducted in this study the author created custom-made ISA test apparatus, based on the specifications in BS 1881 – 208: 1996. It was devised to improve upon the standard ISA equipment and to make it more suitable for testing rammed earth samples. The modified ISA test apparatus, including all of the required peripherals, is shown in Figure 45.

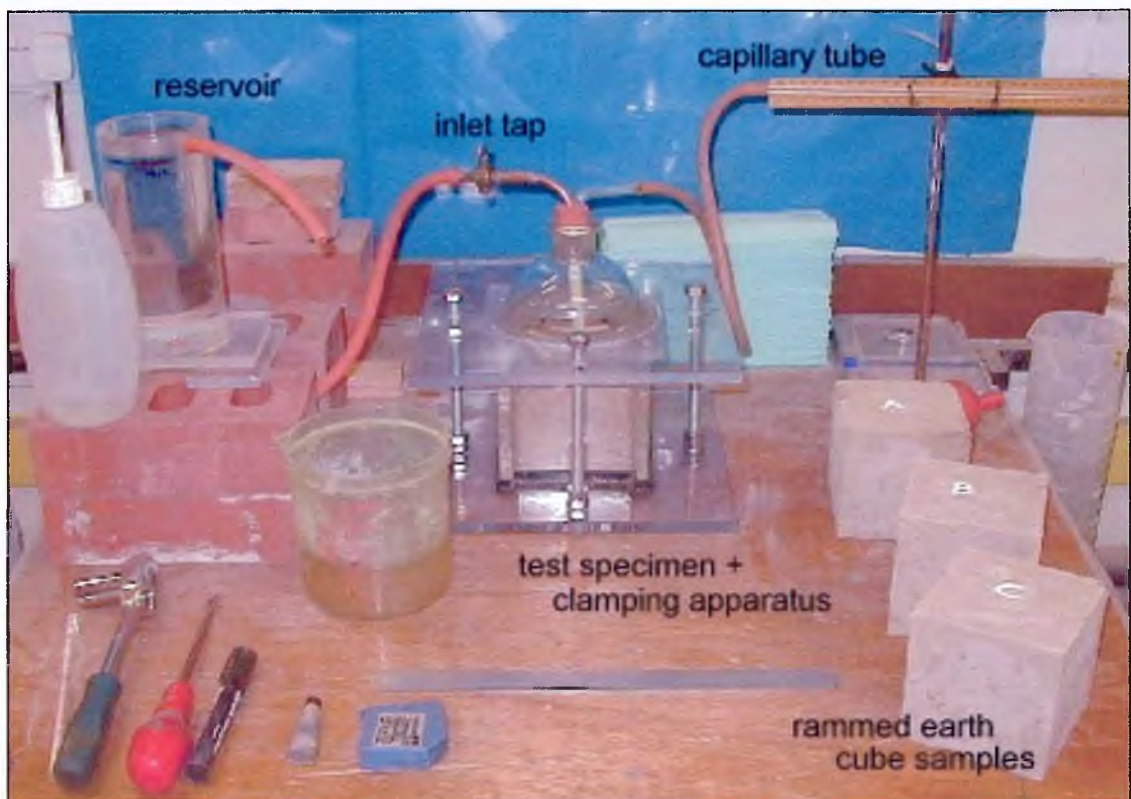


Figure 45 Modified ISA test apparatus ready for use including all peripheral equipment

The modified ISA apparatus has been designed to test 100mm cube samples through the integration of a clamping-frame assembly. The basic assembly and operation, however, is the same as the standard ISA test shown in Figure 44. The sample is held perfectly central to allow the correct location of the cap. The inflow face is circular (80mm diameter) to ensure axial symmetry of the ingressing water. This dimension was

purposefully designed to be identical to the previously defined Initial Rate of Suction (IRS) ‘wick’ test. Therefore, in a given batch of 100mm cube samples the differences in results between the rate of moisture ingress due to both capillary suction (IRS ‘wick’ test) and pressure-driven moisture (modified ISA test) can be directly compared on equal terms. The assembly of the modified ISA apparatus is depicted in Figure 46.

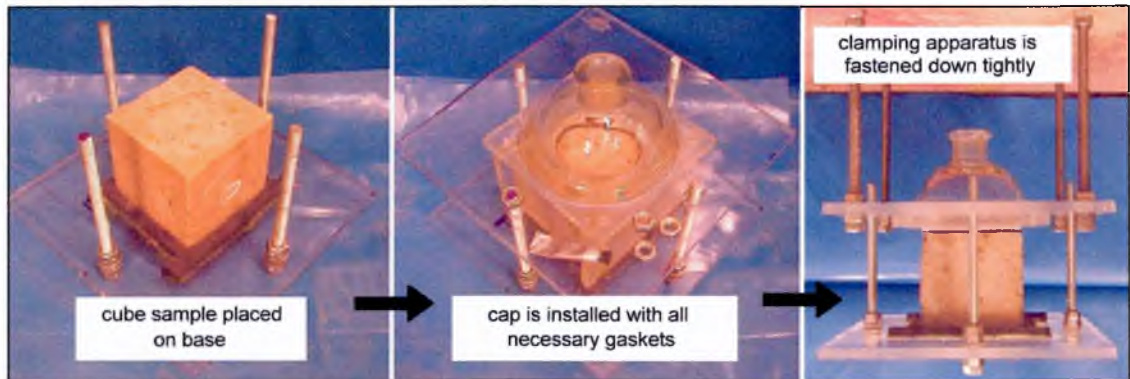


Figure 46 an illustration of the procedures for assembling the modified ISA test apparatus for use with rammed earth cube samples

An oiled neoprene gasket is used to maintain a pressure-tight seal during ISA testing (see: ‘sealant’ in Figure 44). The cap is a large transparent glass unit that doubles as an inspection dome to allow observation and photography of the surface during testing in case slaking and/or blistering of the inflow surface occur. This feature is illustrated by Figure 47, although on this occasion the sample face remains intact despite the pressure-driven moisture ingress to which it is being subjected. The reason that this particular sample does not slake under these conditions is that it was stabilised with 6% cement.

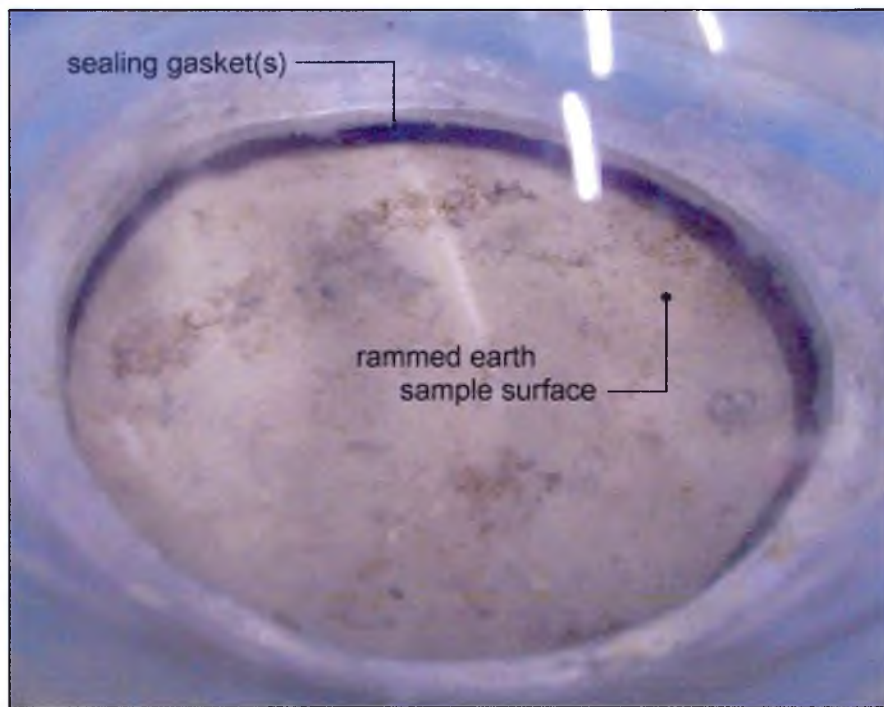


Figure 47 the view through the water-filled glass inspection dome during a modified ISA test

5.1.3 Calibration of the Modified ISA Test

The calibration, accuracy and repeatability of the modified ISA test apparatus was tested in a pilot experiment that preceded the main testing. The test specimens were solid engineering bricks (215 x 100 x 65mm) that had been cut using a diamond bit saw to give a 100 x 100 x 65mm sample. This sizing technique enables clay brick specimens to be used with apparatus that was designed for testing 100mm cube samples. A selection of three test specimens was chosen in accordance with BS 1881 – 208: 1996 (BSI, 1996). However, in order to quantify the repeatability of the test methodology each specimen was repeat-tested twice to give a total number of three tests per sample, i.e. nine tests in total. Table 8 shows the results for the calibration tests performed on engineering bricks.

Table 8 the assessment results for calibration of the modified ISA test, illustrating the suitability and repeatability of the methodology

Sample	Time (min)	Flow 1 (ml)	Flow 2 (ml)	Flow 3 (ml)	Mean flow (ml)	St dev. (ml)	ISA (ml/m ² . s)
Brick #1	10	1.45	1.40	1.48	1.44	0.0404	9.57
	20	1.15	1.10	1.14	1.13	0.0265	7.49
	30	1.00	0.96	0.99	0.98	0.0208	6.52
	40	0.88	0.87	0.92	0.89	0.0265	5.90
	50	0.86	0.82	0.85	0.84	0.0208	5.59
	60	0.77	0.77	0.80	0.78	0.0173	5.17
Brick #2	10	1.50	1.40	1.46	1.45	0.0503	9.64
	20	1.15	1.06	1.13	1.11	0.0473	7.38
	30	0.97	0.91	0.98	0.95	0.0379	6.32
	40	0.87	0.84	0.89	0.87	0.0252	5.75
	50	0.80	0.78	0.79	0.79	0.0100	5.24
	60	0.75	0.73	0.73	0.74	0.0115	4.89
Brick #3	10	1.58	1.59	1.69	1.62	0.0608	10.74
	20	1.23	1.25	1.24	1.24	0.0100	8.22
	30	1.02	1.02	1.01	1.02	0.0058	6.74
	40	0.90	0.92	0.91	0.91	0.0100	6.03
	50	0.88	0.80	0.80	0.83	0.0462	5.48
	60	0.74	0.74	0.74	0.74	0.0000	4.91

The standard deviation between repeated test results equates to a typical value of approximately $\pm 3\%$ of the average flow rate. The results obtained may therefore be assumed repeatable to these tolerances under the conditions specified for the modified ISA test.

5.1.4 Test Methodology

The conventional materials that were tested here were the same specimens as those used for the IRS 'wick' tests described previously: vibration-compacted C30 concrete 100mm cubes, and 3 types of brick; London Brick 'Fletton' (high porosity), London

Brick ‘Dapple Light’ (medium porosity) and Engineering Brick (low porosity). Three representative samples of each material type were selected. The bricks were cut on a diamond bit saw to give a 100mm test face area the same as the cube samples.

Both unstabilised and cement stabilised (3%, 6% and 9%) rammed earth cube samples were defined and produced in accordance with the methodologies and recommendations detailed previously. This involves the creation of specific rammed earth soil blend recipes, a modified 100mm concrete cube mould with removable collar attachment, and a 6.5 kg hand rammer. As before, the three soil recipes selected for testing in conjunction with ordinary Portland cement (OPC) stabilisation were classed as ‘poor’ (703), ‘good’ (613) and ‘very good’ (433), in terms of moisture ingress (see: Section 3.1.3). For the unstabilised specimens, cube samples were produced using all ten of the soil mix recipes. Three cube samples were produced to represent each of the different variables within the material.

5.2 RESULTS & DISCUSSION

The modified ISA test is an improvement on the standard test equipment in several areas and is suitable for testing both unstabilised and stabilised rammed earth 100mm cube samples. The test can be a little severe and often results in the partial destruction of unstabilised rammed earth, particularly when it is made with soil types that suffer from higher levels of moisture ingress (e.g. 703, 712, 802 etc). This may give an unfair representation of material performance for rammed earth in a relatively aggressive small-scale test scenario. The actual conditions would possibly not be quite as severe in the case of full-sized test walls. This adaptation of the Initial Surface Absorption (ISA) test provides axial symmetry of the imbibed water and has identical inflow surface

dimensions to the Initial Rate of Suction (IRS) ‘wick’ test. This means that the results for moisture ingress due to capillary suction can be directly compared with those obtained for static-pressure driven water.

According to BS 1881 – 208: 1996, the equivalent static pressure differential of 200mm (supplied by constant head) is greater than that which could reasonably be expected from natural wind-driven rain conditions in the United Kingdom (BSI, 1996). The inflow of water is vertical and therefore the force due to gravity is at maximum effect. The severity of the test is therefore representative of the materials performance in relatively extreme weather conditions for the British climate.

5.2.1 Rammed Earth vs. Conventional Masonry Materials

Under static pressure-driven conditions, fired clay bricks imbibe a much greater amount of water than concrete or unstabilised rammed earth, as illustrated by Figure 48. Note that three of the soil mix recipes (703, 712 & 802) were not durable enough, in unstabilised form, to survive the conditions of an ISA test and so the results cannot be presented.

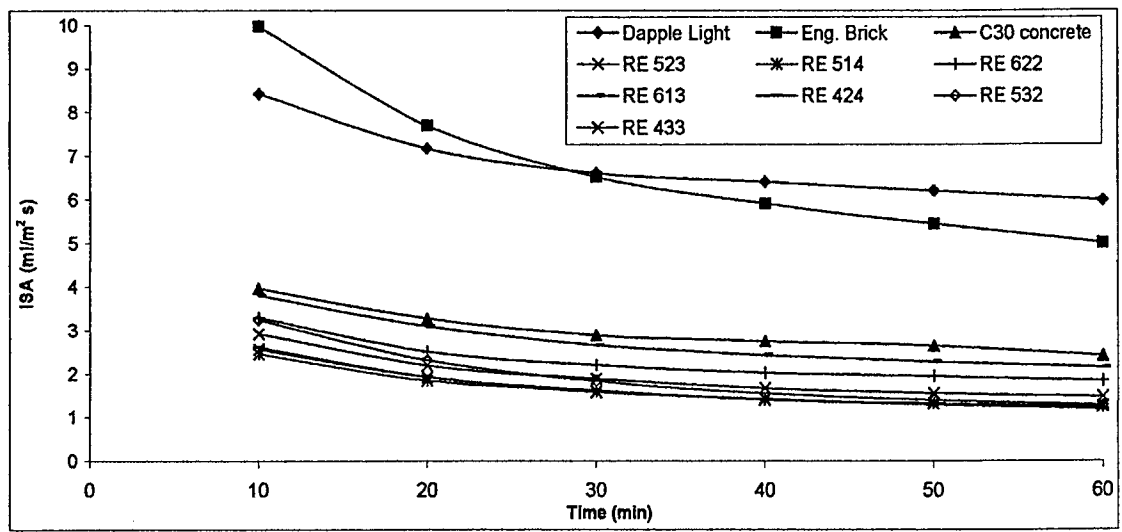


Figure 48 a comparison between the ISA rates of various conventional masonry materials and unstabilised rammed earth made with a selection of different mix recipes

Typical fired clay facing bricks absorb approximately double the amount of pressure-driven moisture than most forms of unstabilised rammed earth. However, the rate of decline in absorption over time is significantly greater in bricks than in compacted C30 concrete or unstabilised rammed earth. The profile of the ISA curve for compacted C30 concrete is remarkably similar to that of rammed earth indicating clear similarities in pore structure and non-saturated permeability. In comparative terms, most forms of unstabilised rammed earth have a lower ISA rate than vibration-compacted C30 concrete. This possibly relates to the typically low porosity of rammed earth in addition to the waterproofing effect of clay particles that can bridge the pore spaces between sand and gravel.

Both concrete and fired clay brick, of course, do not begin to slake or lose any structural integrity when they are significantly wetted, whereas unstabilised rammed earth mostly does. This is not the case, however, for rammed earth that has been stabilised with between 3% and 9% ordinary Portland cement. Cement-stabilised rammed earth can

easily survive periods of prolonged wetting and surface run-off without any slaking, erosion or loss of structural integrity.

5.2.2 ISA Testing of Unstabilised Rammed Earth

The graph in Figure 49 has a reduced y-axis in order to display the comparison between the initial surface absorption (ISA) for different unstabilised rammed earth mix recipes.

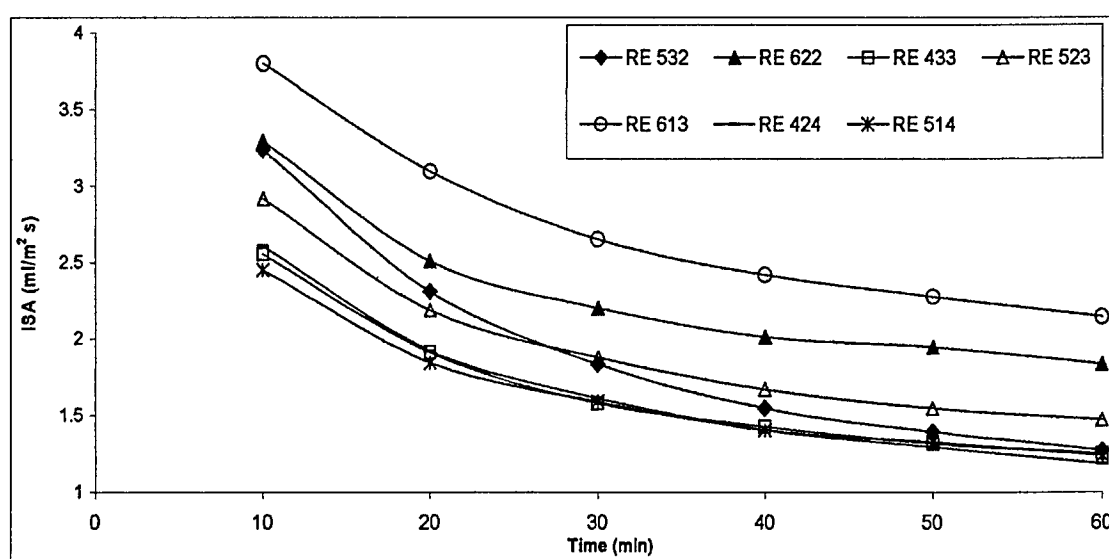


Figure 49 a direct comparison between the ISA over elapsed time for various unstabilised rammed earth samples made using different mix recipes

As previously stated, three of the unstabilised mix recipes (703, 712 & 802) were not able to survive the conditions of a 60-minute ISA test and so the results are not presented here. All three of these mix recipes have previously been observed to suffer from high levels of capillary moisture ingress in the IRS 'wick' test. They each have a relatively high SSA_i/CC ratio, which may result in lower cohesion and increased permeability. It appears that the kinetic force of the static pressure head in the ISA test was sufficient to cause disintegration of the samples made with these three mix recipes. Since these samples were unstabilised their inter-particle cohesion and granular friction

would have been reduced by the ingressing moisture, and it was within the wetted regions that failure occurred.

As we can see from Figures 50 and 51, the slaking effect upon the surface of 523-mix unstabilised rammed earth is significant after just 1 hour of exposure to pressure-driven moisture ingress.

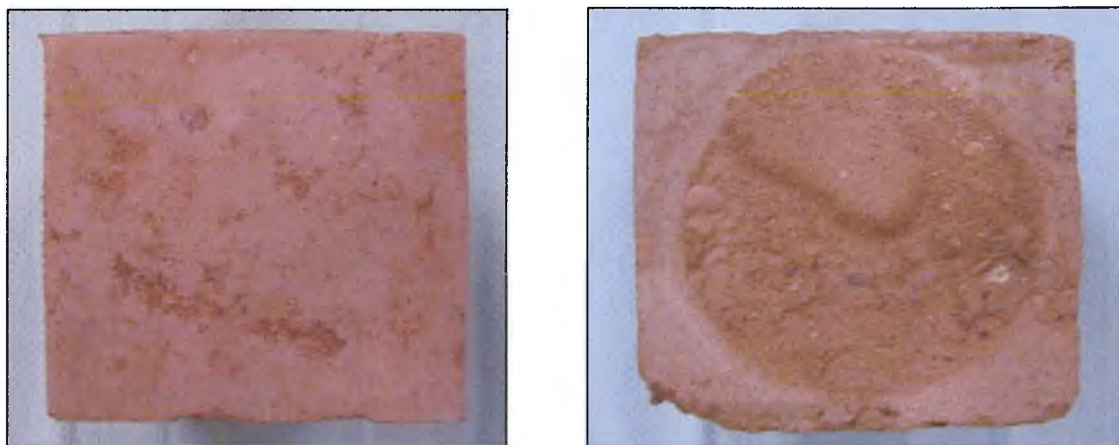


Figure 50 (above left) Unstabilised rammed earth sample face *before* ISA test

Figure 51 (above right) Slaking effect of water penetration *after* 1hr ISA test

The example shown in Figures 50 and 51 is in fact one of the better mix recipes in terms of moisture ingress performance. The picture in Figure 52 shows the loss of structural integrity that can occur in unstabilised rammed earth made from a high-moisture ingress mix recipe (e.g. 703), in less than 1 hour of exposure to pressure-driven moisture ingress.



Figure 52 (above left) Unstabilised rammed earth – structural collapse of high-moisture ingress soil types during an ISA test



Figure 53 (above right) Cement stabilised rammed earth – the same high-moisture ingress soil types do not slake or disintegrate when stabilised

The picture in Figure 53 shows that the same high-moisture ingress soil mix recipe (703) can be made resistant to the effects of moisture-induced slaking and disintegration by stabilising them with 9% ordinary Portland cement. Interestingly, the example shown in Figure 53 illustrates how the presence of cement can exacerbate the level of moisture ingress in a given mix recipe. The results of ISA testing on cement stabilised rammed earth have been presented and discussed in the following sub-section.

5.2.3 ISA Testing of Cement-Stabilised Rammed Earth

Three rammed earth soil recipes were selected for further ISA testing using varying amounts of cement stabilisation. As with the IRS ‘wick’ testing, the same three soil recipes were picked to represent capillary moisture ingress performance that is classed as good (433), medium (613) and poor (703). The sample cubes were made using 3%, 6%, and 9% (by dry mass) of ordinary Portland cement (OPC) for each of the mix recipes, as discussed in Section 3.1.3. The comparative effect of adding increasing amounts of cement to each of the three mix recipes is illustrated by the graph in Figure 54.

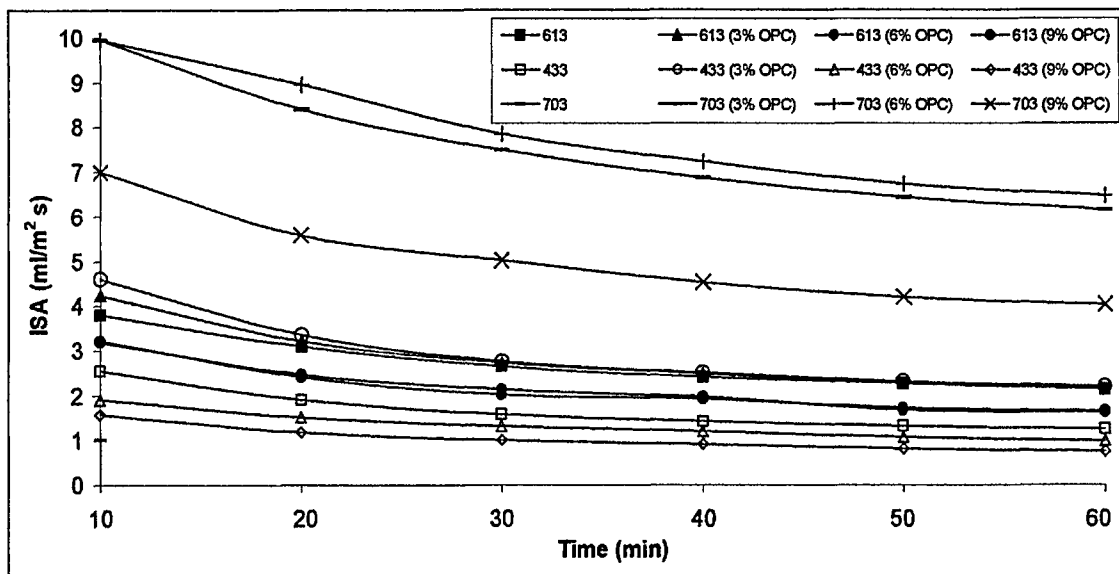


Figure 54 the comparative effect of cement content on the ISA of selected rammed earth mix recipes

The progressive rate of decline (i.e. the curvature of the graph) in the initial surface absorption (ISA) of each rammed earth mix recipe appears to have a similar gradient regardless of cement content between the values of 0% (unstabilised) and 9%. However, the magnitude of the ISA varies considerably for each mix recipe depending upon cement content. This indicates that the effect of cement stabilisation on rammed earth, in terms of its resistance to pressure-driven moisture ingress, is to alter its permeability. The way in which increasing cement content alters the ISA value of different soil types is illustrated by the graph in Figure 55.

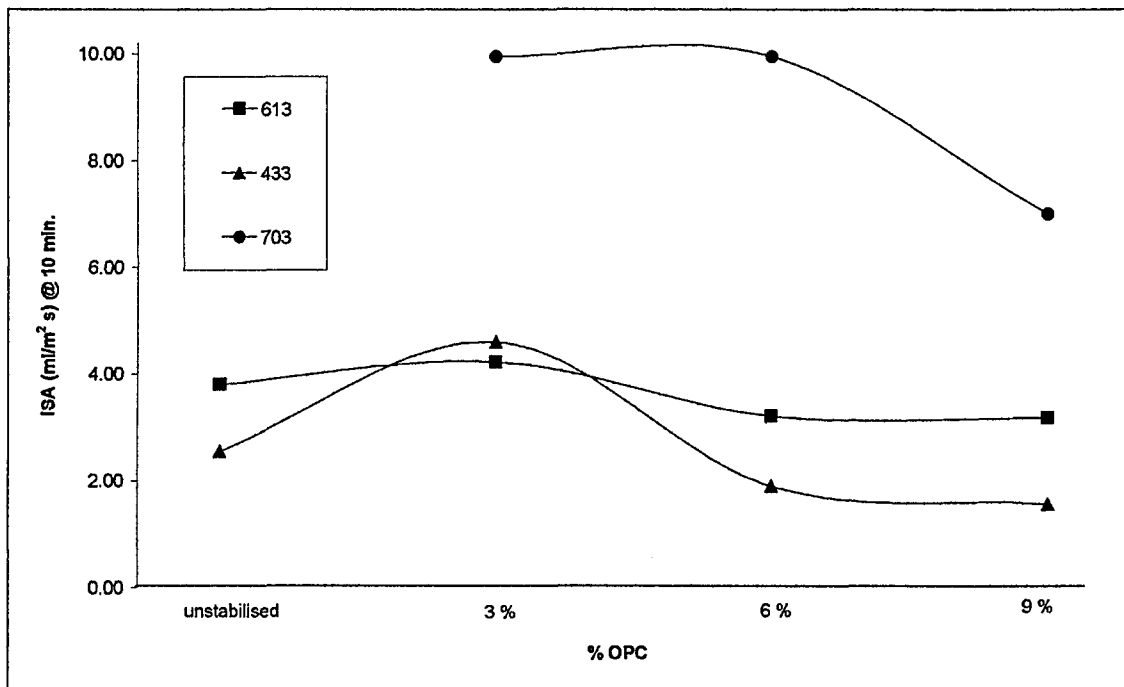


Figure 55 the effect of increasing cement stabilisation on ISA value of different rammed earth mix recipes

In each of the three mix recipes tested here (433, 613 & 703) the addition of up to 3% cement (by mass) appears to have a very significant effect in increasing pressure-driven moisture ingress. This same pattern was observed during the IRS ‘wick’ test regime using the same test specimen parameters (see: Section 4.2.3.1). The influence of this effect appears to increase in accordance with the susceptibility to moisture ingress of a given mix recipe, i.e. it is greatest for the 703 mix, and least for the 433 mix.

As with the results for capillary moisture ingress, it would appear that the optimum level of cement content for moisture ingress performance is 6% for the 433 and 613 mixes, and 9% for the 703 mix. One consistent disparity between the IRS and the ISA results appears to be that the optimum cement content of a given mix provides an IRS that is slightly above the original value, and an ISA that is slightly below it. This measurable contrast in results may be explained by the fact that cement stabilisation increases the fines content of a soil and so consequently may have the effect of narrowing the pores. It has been observed by Khatib & Clay (2004) that densification of

the C-S-H in metakaolin/cement paste can cause an increase in the level of micro porosity. It is reasonable to assume, therefore, that a similar effect may occur due to clay/cement reactions in a rammed earth soil. An effective narrowing of the internal pore structure could have the effect of increasing the capillary potential of the material whilst reducing its capacity for moisture to be propelled due to an external force, e.g. pressure differential.

5.2.4 Analysis of the ISA Test Methodology

Hall (1981) previously observed that the amount of absorbed water in an ISA test does not appear to increase linearly per unit inflow surface area against the square root of elapsed time ($t^{0.5}$). The introduction of a flow characteristic in the water caused by the static-pressure differential may partially negate the effects of surface tension that would normally cause a porous material to absorb water through capillarity. Furthermore, in order for the $t^{0.5}$ law to apply the following idealistic conditions must be wholly satisfied (Hall, 1981):

1. The material must be homogenous throughout the test region
2. The inflow of water must be normal to the test area; neither converging or diverging
3. Contact with an unlimited reservoir of water must be maintained
4. Gravitational effects must not be apparent in the absorption process

Clearly, items two and four are not well satisfied using the ISA test methodology. The inflow of water is from a circular source that diverges with axial symmetry, and the force due to gravity is at maximum effect. However, it has previously been observed that a diverging axially symmetrical water source in the IRS 'wick' test did not prevent

the occurrence of a linear relationship between $i/t^{0.5}$. It could mainly be the influence of external forces (i.e. pressure differential and/or gravity) acting upon the ingressing moisture that has the effect of inducing a more rapid, non-linear increase in $i/t^{0.5}$.

5.3 SUMMARY

The modified ISA test is a novel adaptation of the BS 1881 Initial Surface Absorption (ISA) test. It is an improvement on the standard test equipment because it provides axial symmetry of the imbibed water into the test specimen. Additional modifications make it suitable for testing rammed earth cube samples and it has identical test specimen geometry to the proposed Initial Rate of Suction (IRS) ‘wick’ test allowing fair comparisons between the respective test results.

Modified ISA test is suitable for testing unstabilised and stabilised rammed earth. Unstabilised rammed earth often loses structural integrity during testing particularly on mix recipes with a high SSA_f/CC ratio. This often resulted in test results being unobtainable and/or discarded, for some of the mix recipes. This also indicates that failure occurs due to loss of cohesion (c) between the clay and the granular particle matrix caused by wetting. The ISA of rammed earth is typically very low compared to conventional masonry building materials and is comparable to or better than that of vibration-compacted C30 concrete. The ISA typically permits significantly higher moisture ingress than the IRS for a given mix recipe.

6.0 CLIMATE SIMULATION CHAMBER

6.1 APPARATUS & METHODOLOGY

6.1.1 SHU Climatic Simulation Chamber

Sheffield Hallam University's climatic simulator was designed and built by Alan Taylor-Firth and David Flatt (Taylor-Firth & Flatt, 1991). Their aim was to investigate the performance of building materials and full-sized building elements (e.g. walls) under a wide range of simulated climatic conditions. It is the only existing prototype of its kind and remains unique in the United Kingdom. The main advantage of the climate chamber is that it represents the elusive 'middle-ground' between naturally exposed outdoor test walls and the less representative small-scale laboratory tests. Full-sized test walls can be constructed inside the climate chamber following normal trade practices, but realistic climatic effects of weather and exposure can be accurately controlled and monitored under laboratory conditions. In recent times, the climate chamber has been used mainly to study the behaviour of masonry construction elements with realistic outer and inner wall conditions (Laycock, Hetherington & Hall, 2002).

The simulator itself is composed of two separate chambers called the 'design' side and the 'climate side'. The dimensions of each chamber are 4m long, 3m wide and 2.6m in height. The normal operating temperature range is +20°C to -15°C ($\pm 5^\circ\text{C}$) depending on the internal conditions specified (Laycock, Hetherington & Hall, 2002). A schematic diagram illustrating the basic operation of the climatic simulation chamber is illustrated in Figure 56.

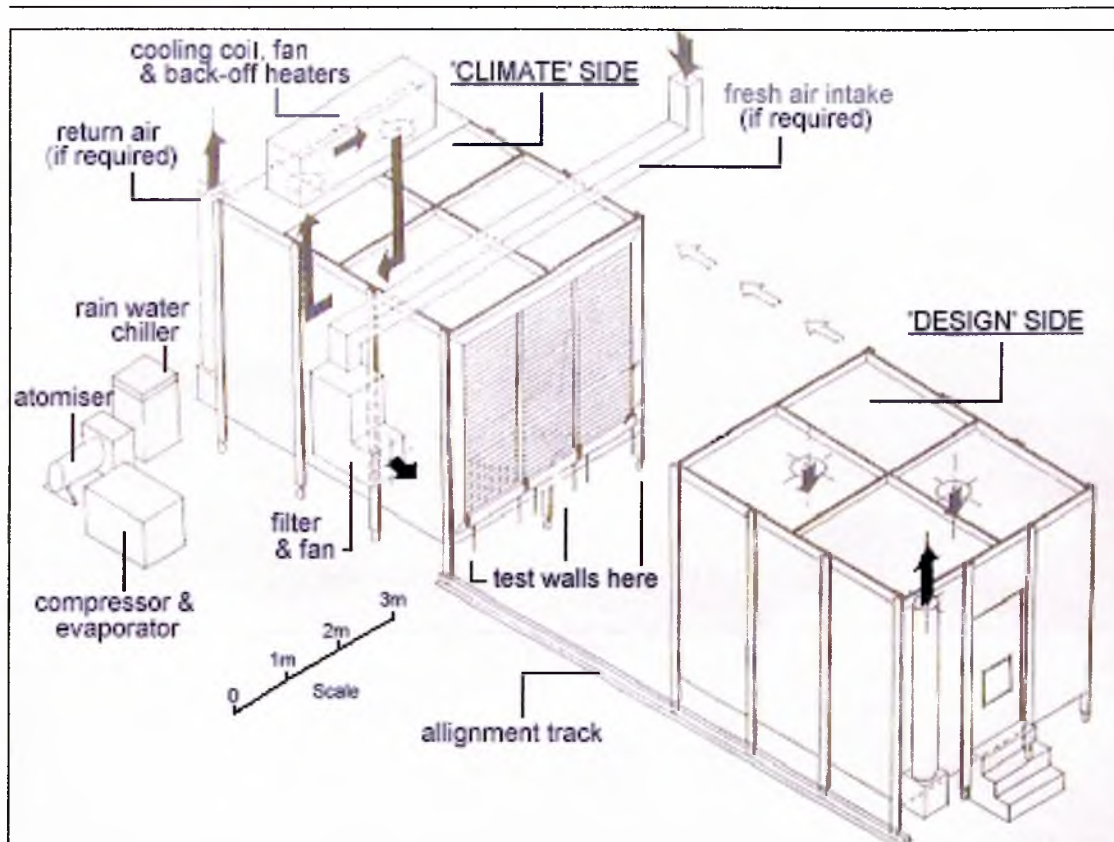


Figure 56 a schematic diagram of the SHU climatic simulation chamber (adapted: Taylor-Firth & Flatt, 1991)

6.1.1.1 The 'Design' Side

This side of the simulation chamber represents the interior conditions of a building. It has the capacity to be sealed and generate a standard temperature and relative humidity profile throughout the test regime. Alternatively, it can be left unsealed which means that the temperature and relative humidity are the same as the ambient laboratory conditions. This is the most common practice for establishing standard indoor room conditions as the laboratory is both underground and heated, thus maintaining steady conditions of $20^{\circ}\text{C} \pm 1^{\circ}$ and $40\% \text{ RH} \pm 5\%$. Using this method it has been observed that standard UK room temperature conditions can be efficiently maintained and so, in this situation, the test methodology can be simplified by eliminating the use of heating/cooling plant. However, if interior climatic conditions other than 20°C and $40\% \text{ RH}$ are required then the operator has no choice but to operate the design side under

sealed conditions and artificially control the environment with the heating/cooling plant (see: Figure 56).

6.1.1.2 The 'Climate' Side

This side of the simulation chamber creates realistic sequences of different external weather conditions that can run in a fixed mode, sequence mode, or cyclic mode. The advantage of this is that the start and finish temperatures can be specified, as well as the rates of change of other weather components such as relative humidity and/or rainfall. All of these factors can be accurately controlled under laboratory conditions.

The climate chamber also has the ability to simulate fog and rainfall. Either the rainwater can be provided via a chiller unit that specifies and controls the temperature of the rainwater, or it can simply be provided from the mains water supply. The water can be delivered via a low-pressure header tank providing accurate constant head pressure but at low volumes; this is typically used for creating rainwater run-off situations. When supplied from high-pressure (9 bar) mains water, with a needle valve in-line flow restrictor, it can be used to create high-velocity/impact rainfall to simulate storm conditions.

Relative humidity is regulated by injecting temperature controlled mist sprays that are entrained into the air flow. Depending upon the temperature this can be used to create fog-like conditions or even the very damaging phenomenon of freezing fog. To illustrate the flexibility of the simulation chamber, a few examples of the climatic conditions that can be produced include:

-
1. A fixed temperature/humidity gradient between outdoor and indoor conditions, e.g. warm & dry indoors (20°C 45% RH), cold & damp outdoors (8°C 80% RH), etc.
 2. Cyclic freeze/thaw regimes, e.g. -5°C to +5°C with 15 set points over a 24 hour overall test duration. The wall can be thawed either by raising the ambient air temperature, or by using rainfall. In the latter case, the rainwater can be pre-cooled to prevent thermal shocking of the wall façade.
 3. Static pressure-driven rainfall with specified flow rates for wall face water runoff and a simulated wind-driven pressure differential equivalent to 250 N/m² (25mm of water). The rainwater can either be trickled down the wall face at low velocity or sprayed at the wall face at high velocity. The pressure differential is equivalent to very strong winds pushing up against the outdoor face of the wall, and driving the moisture ingress towards the interior.

6.1.2 Stabilised Rammed Earth (SRE) Test Walls

Four 300mm thick SRE test walls were constructed inside the SHU climatic simulation chamber. The first step in constructing test walls for the climatic simulation chamber was to build a concrete plinth wall at the junction between the climate side and the design side. This plinth wall effectively acts as the foundations on which to build the rammed earth test walls. Figure 57 shows the building work for the concrete block plinth, which is built onto the laboratory floor.

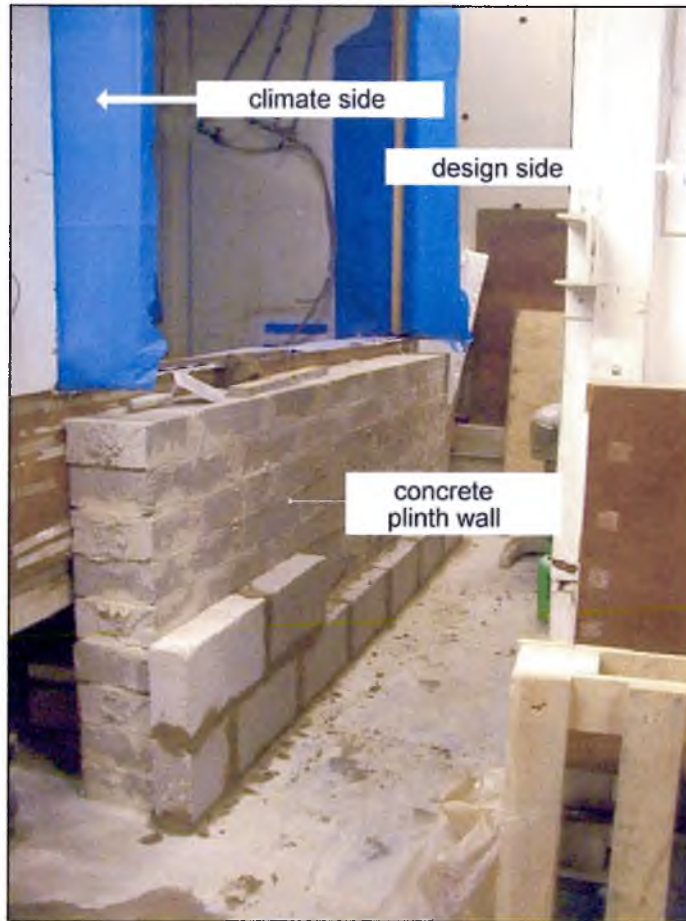


Figure 57 the concrete plinth under construction

The plinth is over 3m in length and partly exceeds the overall width of the climate chamber. In Figure 57 the climate side of the chamber is on the left of the picture whilst the design side is on the right. When the test walls have been built, the design side (which is on wheels) can be moved back into position and sealed up against the climate side, thus trapping the test walls in the middle. The diagram in Figure 58 illustrates the test wall design and cross-sectional construction detail at the foundation level.

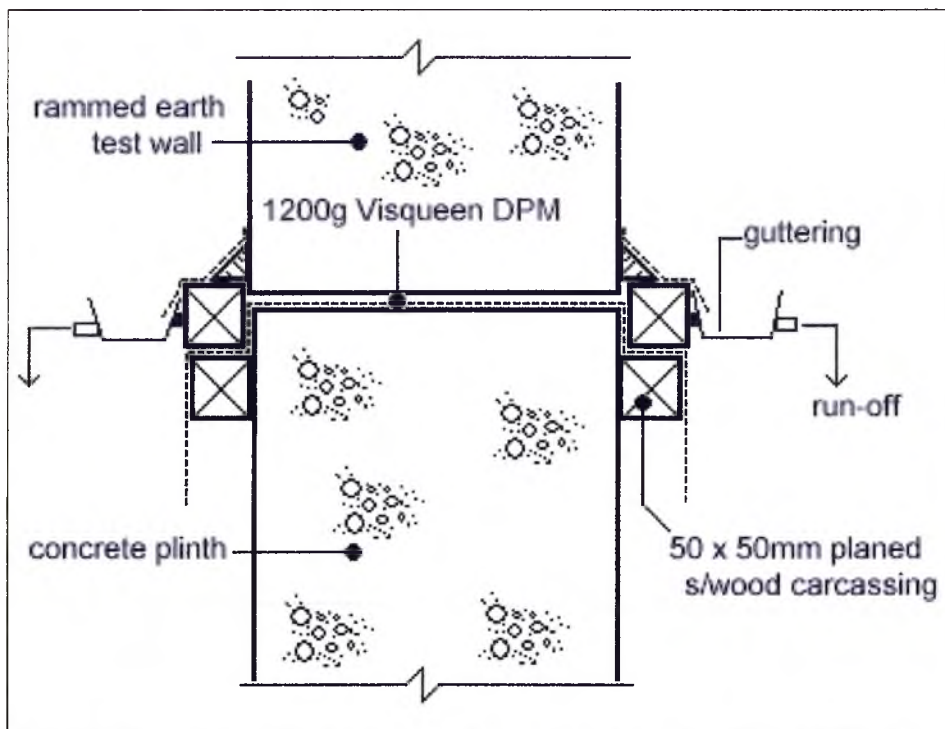


Figure 58 cross-sectional diagram of test wall construction detail at foundation level

The four test walls had to be separated from one another and this was achieved with 100mm timber stud-framed cavities that incorporated the end boards from the formwork (see: Figure 59). The end boards then become sacrificial (i.e. lost) formwork and are retained as a part of the experimental design. The stud-framed end boards were fixed to the concrete plinth at 600mm centres, as shown in Figure 59.

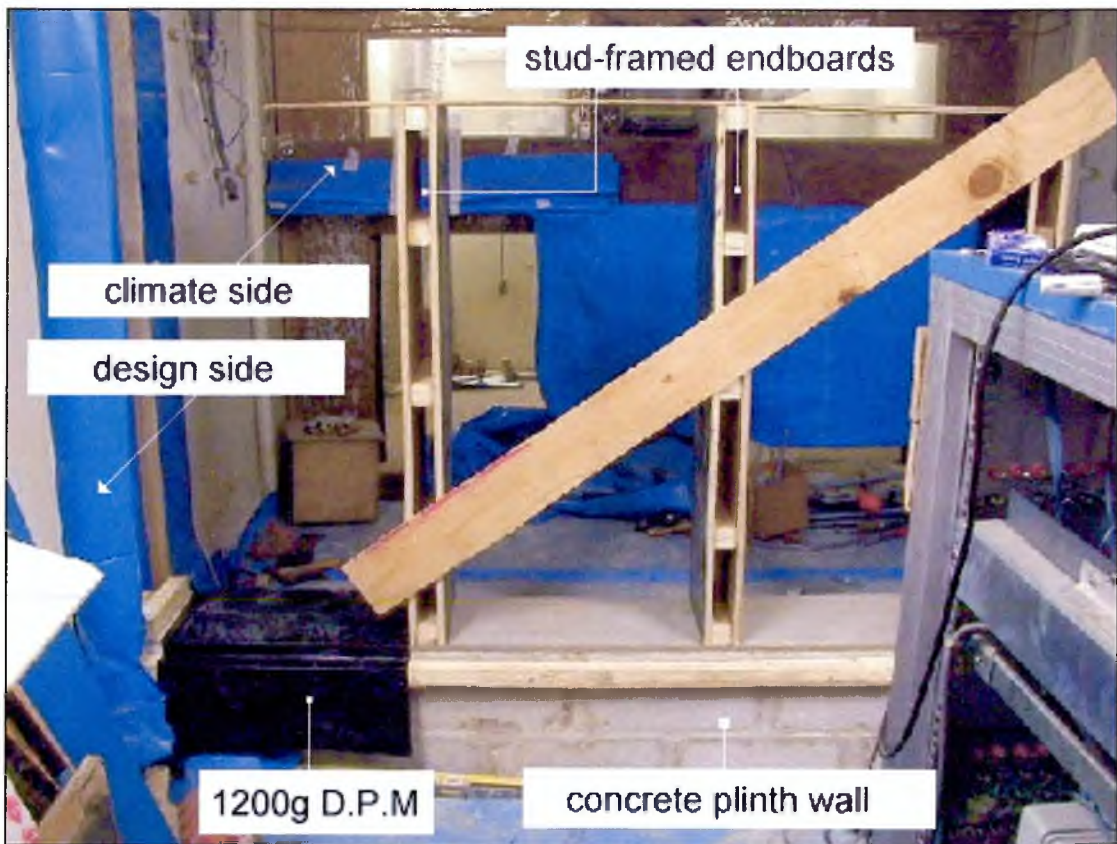


Figure 59 stud wall end boards fixed to the concrete plinth to act as spacers between test walls

By placing a sealed cavity between the test walls, the effects of sample interaction, in terms of thermal transmittance and moisture transfer, are minimised. The board faces are phenolic resin coated $\frac{3}{4}$ " formwork ply that has been caulked with silicone sealant at the joints and drill holes.

The author used a miniaturised version of David Easton's REW formwork (see: Appendix 2), and so the following components were required:

- 10 @ $\frac{3}{4}$ " BSP steel water pipe with nominal O.D. 1.04" 1500mm lengths
- 10 @ Jorgensen 'Pony' brand pipe clamps; $\frac{3}{4}$ " #50
- 10 @ 50 x 250mm rough sawn s/wood timber whalers
- 2 @ phenolic resin-faced 19mm formwork ply, 1200x1200mm

-
- 20 x tapered hardwood wedges (100mm long, 36mm wide, taper 19mm – 6mm)

The picture in Figure 60 shows how the miniature REW formwork was used in conjunction with the stud-framed end boards.



Figure 60 a miniature version of the REW formwork system that was used for the mini test walls

Mixing of the soil was performed using a 240V Hobart paddle mixer, which is the same apparatus as was used for the production of cube samples. Mix proportioning was controlled in relation to the size of the batch, which was approximately 15 kg for the soil components. An example of this is for the 613 soil recipe, where in a 15 kg batch the proportions are as follows: 9 kg zone 'M' grit sand, 1.5 kg 10mm pea gravel, and 4.5 kg silty clay. In addition to the soil, 900g of cement was added which is the

equivalent of 6% (by mass) of cement stabilisation. Finally, water was added to the dry mix components to raise the moisture content to the optimum value of 8%. This equates to 1272g of water being added to the dry mix components (soil & cement). The water is added gradually once the dry components have been thoroughly mixed together.

The soil components were not oven dried prior to mixing as it was impractical to do this for such a large quantity of soil; almost 1 ton of soil was required to make four test walls. After gravimetric determination (oven drying to constant mass) the moisture content of 10mm pea gravel was found to be insignificant when stored in the laboratory; the assumed climatic conditions being $20^{\circ}\text{C} \pm 1^{\circ}$, $40\% \text{ RH} \pm 5\%$. The sand was spread out across the laboratory floor, raked over, and then allowed to air dry under the ambient laboratory conditions. After approximately 12 hours the moisture content of the sand dropped to a level whereby it could be considered insignificant (i.e. less than 1% by mass).

The silty clay was found to have an average moisture content of 12.5%, and so where the silty clay proportion in a mix is 30% the added mass is increased from 4.5 kg to 5 kg. The inherent water content entrained into the mix (from the silty clay) reduces the additional required amount of water necessary to reach optimum moisture content. Consequently, the additional required mass of water is lowered to 772g to take into account the moisture already added from the moist silty clay. The OMC of the mix was measured and controlled during construction using the drop test as defined NZS 4298: 1998 (see: Chapter 2 - Section 2.2.4).

It was observed that the addition of the cement helps to disperse the silty clay and allows the user to mix the soil more thoroughly, especially when the soil is still moist

and cohesive. The cement used was the same as used for all other related test work; Blue Circle “Mastercrete Original” – ‘enhanced’ Portland cement.

Previously it was observed that, for a given soil type at its optimum moisture content, the technique of pneumatic compaction was found to produce rammed earth of the same density as that achieved by hand ramming (see: Chapter 3 - Section 3.3). Therefore, the technique of pneumatic compaction was employed for the rapid commercial-type production of the rammed earth test walls. The same Atlas Copco RAM 30 pneumatic rammer was used with a 3-phase Hydrovane™ Classic 05 air compressor with 31cfm free air delivery running at 7.5 bar pressure. During construction of the walls the soil was mixed in two batches at a time: 2x 15 kg batches + 6% OPC stabilisation + 8% water (OMC), as described above. The mixed soil (2 batches) was placed inside the formwork to give a loose layer of between 100 and 150 mm (4-6”). The thickness of the soil, when compacted, decreased to between approximately 50% and 70% of its original height, depending upon soil type. The process of compacting the soil inside the formwork using a pneumatic rammer is shown in Figure 61.



Figure 61 compaction of earth using Atlas Copco RAM 30 pneumatic rammer

The four 300mm thick test walls were constructed in the following order:

1. 11/3/2003: Wall #4 – 613 (good) soil with 6% OPC stabilisation
2. 12/3/2003: Wall #1 – 613 (good) soil with 6% OPC stabilisation [repeat]
3. 14/3/2003: Wall #3 – 703 (poor) soil with 6% OPC stabilisation
4. 17/3/2003: Wall #2 – 433 (very good) soil with 6% OPC stabilisation

The completed array of test walls inside the climatic simulation chamber can be seen from the picture in Figure 62.

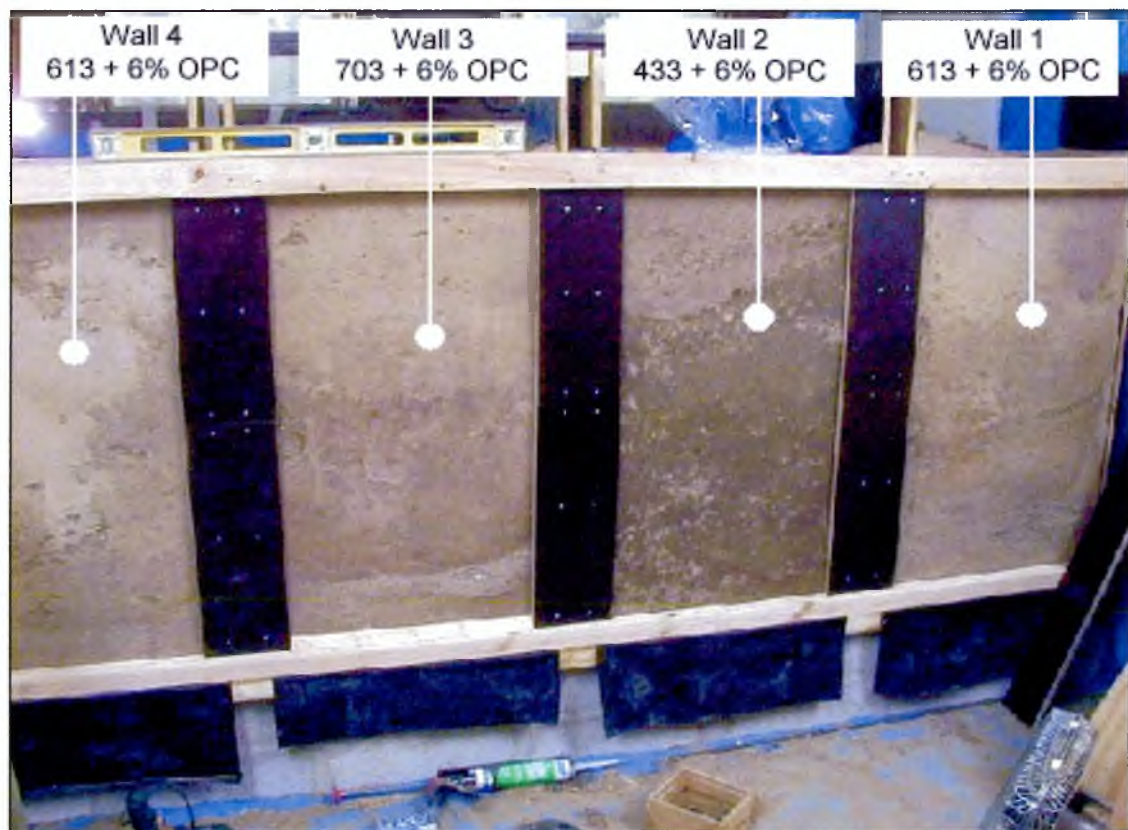


Figure 62 the four rammed earth test walls as seen from the design side of the climate chamber

Following their completion, the mini test walls were allowed to cure for a minimum period of 28 days in laboratory conditions at $22^{\circ}\text{C} \pm 1^{\circ}$ and $40\% \text{RH} \pm 5\%$. The wall edges were then overlapped and sealed with phenolic resin-faced plywood and caulked around the entire perimeter with silicone sealant. The top half of the climate chamber (the remaining height above the test walls) was completed with timber stud walling and $\frac{1}{2}$ " ply wood sheets. These were then covered with 1200g Visqueen DPM and fastened around the edges with cloth tape to seal off the climate side of the chamber. The resultant dimensions for the test face of each wall are 500mm wide, by 900mm high (0.45m^2). The result of the finishing & sealing work described here can be seen from the picture in Figure 63.

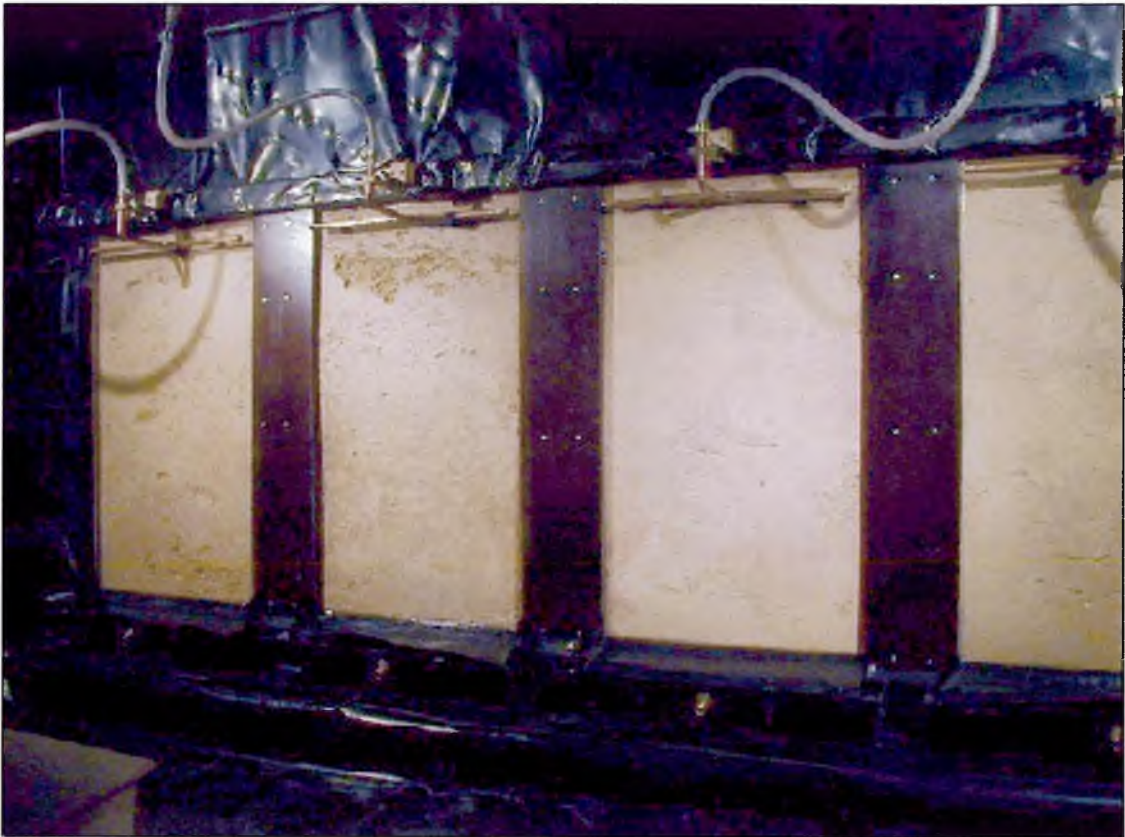


Figure 63 the mini test walls (viewed from the climate side) after being framed and sealed, with the top half of climate chamber closed off and sealed

6.1.3 Static Pressure-Driven Rainfall Simulation

The test methodologies and apparatus described in the following section are based on the specifications provided in BS 4315-2: 1970 *Methods of test for resistance to air and water penetration – permeable walling constructions (water penetration)*. The methodologies described therein have previously been incorporated into the SHU climatic simulation chamber and used successfully on a number of research and consultancy projects.

Two types of rainwater delivery systems were installed for use with the rammed earth test walls. Test run #1 employed the 15mm sparge pipe delivery system with a low-velocity constant head supply of water. Test run #2 utilised mains high-pressure water

supplying high-velocity raindrop spray nozzles. The first two test runs are explained in more detail in the following sub-sections. In both cases, the purpose of the testing was to measure the moisture absorption of each test wall and their resistance to pressure-driven moisture penetration.

6.1.3.1 Low-Pressure Sparge Pipes – Test Run #1

This system employed copper sparge pipes (1 per wall) fed by a 15mm diameter common rail. The sparge pipes themselves were manufactured from 15mm copper tube and had an array of eight holes with 0.7mm diameter in order to deliver the rainfall ‘trickle’. Each sparge pipe had a piece of skirting made from 1200g Visqueen DPM connecting the flow of water with the wall in such a way that the run-off was distributed more evenly across the face of the test wall. The picture shown in Figure 64 illustrates how the sparge pipe delivers a trickle of rainwater run-off with the aid of the skirting attachment.

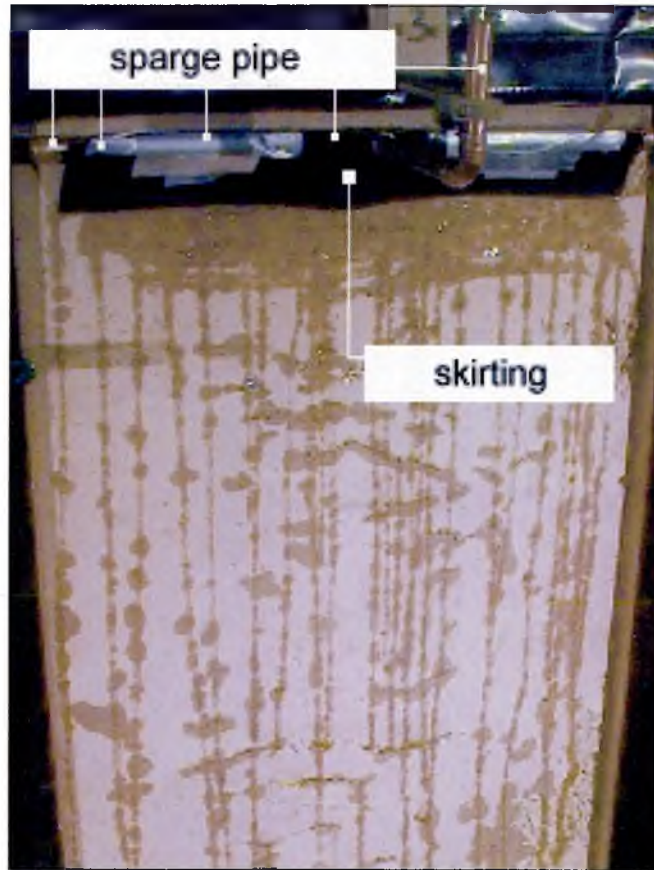


Figure 64 a 15mm sparge pipe with skirting attachment delivering rainfall run-off down the face of a mini rammed earth test wall

The water used to supply the sparge pipes was pumped from the main water reservoir of the climate chamber into a separate header tank that was positioned on the roof of the chamber itself, as shown by the picture in Figure 65.

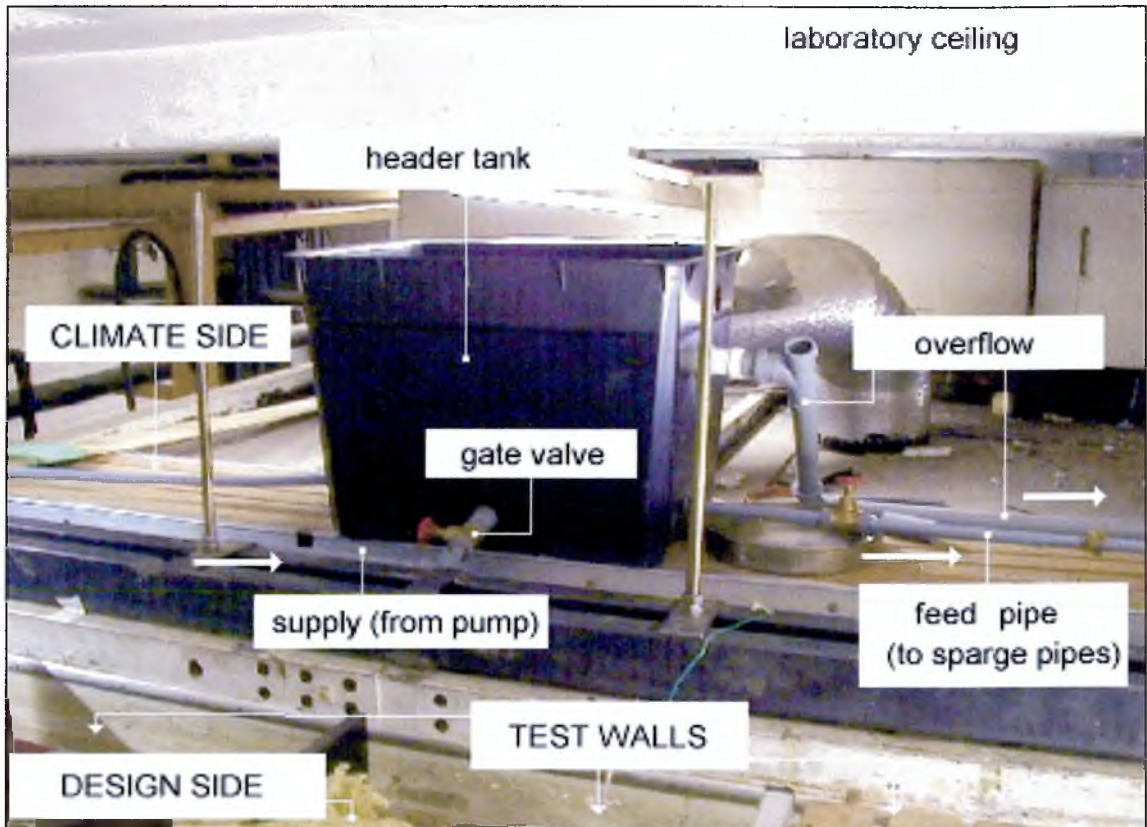


Figure 65 the header tank positioned on the roof of the climate chamber

The header tank was fitted with an overflow that returned excess water back to the reservoir. By keeping the pump running constantly a constant head of water pressure was maintained at the height of the overflow. This method was used to ensure a greater degree of accuracy in setting and maintaining the water flow rates. Between the supply of water from the header tank, and each of the four sparge pipe, was an in-line gate valve to enable the water supply to be shut off from within the climate side of the chamber. Fitted in-line after the gate valve was a 1/8" (6.7mm) BSP needle valve to act as a flow restrictor. This valve could be accurately set to regulate flow through a range between 0.2 and 2.0 litre/min. The overall configuration of this rainfall delivery system is illustrated in Figure 66.

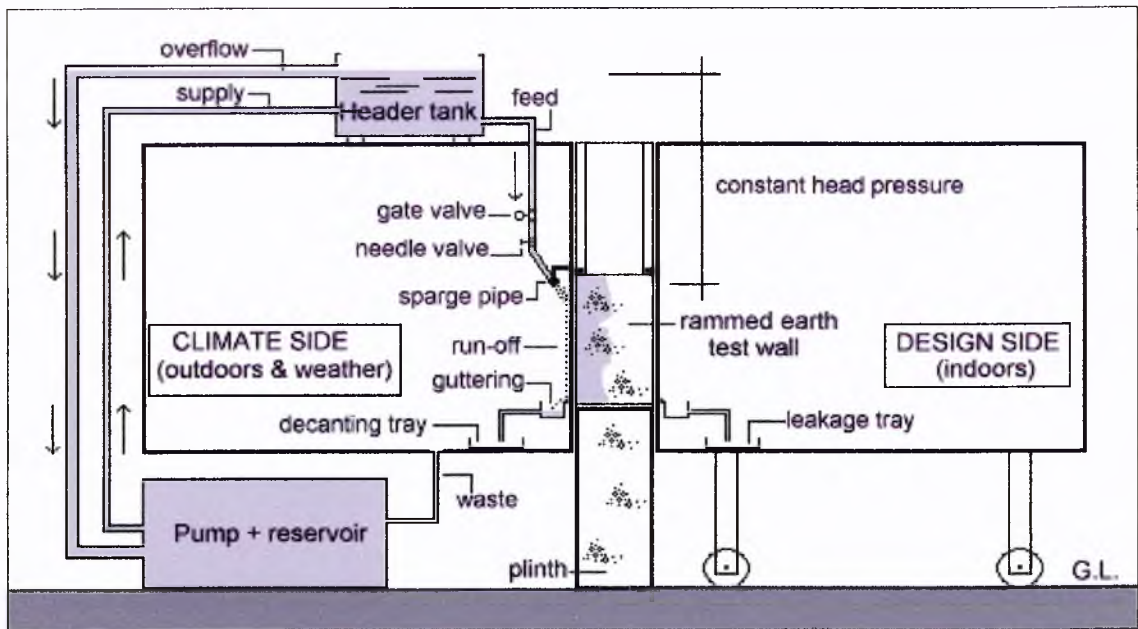


Figure 66 a schematic diagram for the constant head low-pressure water delivery system

The rainfall delivery rate was calibrated by a process that involved covering the faces of the test walls with 1200g Visqueen DPM plastic sheeting. When the water supply was activated, 100% of the run-off delivered to each wall by the sparge pipes ran down its respective face of plastic sheet. The water was collected in the guttering at the bottom of each test wall, all of which subsequently flowed through the decanting pipes and into the tray beneath it. The surface run-off was collected in the receptacle over a 1-minute period. The mass of water delivered per minute, divided by the surface area of the test wall, equals the set flow rate in $\text{g/m}^2 \text{ min}$ (or $\text{ml/m}^2 \text{ min @20}^\circ\text{C}$). The pictures shown in Figure 67 and 68 depict how the calibration and guttering systems actually worked in practice.



Figure 67 a test wall in calibration mode (above left)

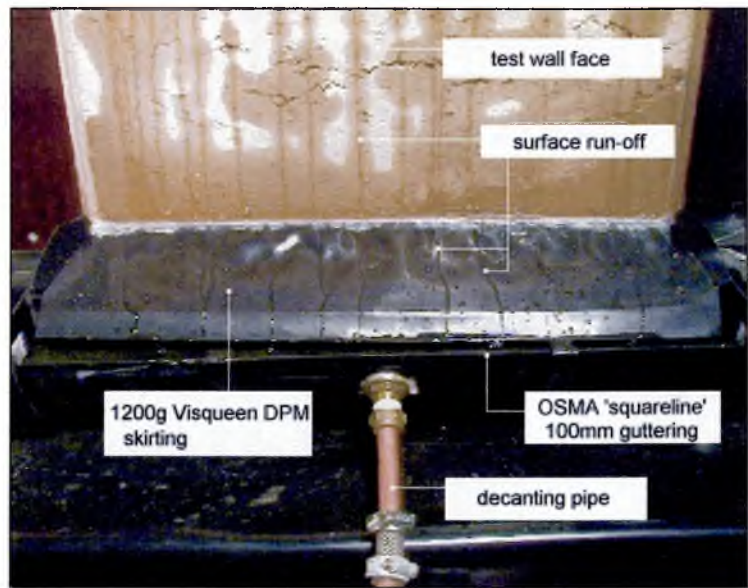


Figure 68 surface run-off collection and decantation (above right)

The outlet for each decanting pipe was positioned approximately 6mm above the base of the guttering. This is so that the guttering effectively acted as a silt trap for any solid particles that washed away from the wall surface. In order for this to work, the guttering first had to be primed (prior to the test commencing) by filling it with water until the decanting pipe overflowed the excess amount of water.

The rate of water delivery specified in BS 4315-2:1970 is 0.5 litres/m². min (BSI, 1970). Since the surface area of the rammed earth test walls is 0.45m² the required rate of water delivery equates to 225 ml/min. In reality this is a particularly low flow rate and very difficult to achieve in practice with any sort of accuracy. In addition, because of the low pressure required to achieve this flow rate the delivery pattern of the rainfall is very poor. This point is illustrated by Figure 64 where the rainwater can be observed to trickle down the wall in discreet channels.

6.1.3.2 High-Pressure Spray Nozzles – Test Run #2

The high-pressure spray nozzles used here were supplied by a company called Lechler Ltd. and had a 120° flat, fan-shaped spray pattern. The efficient distribution of water, and subsequent run-off, across the full width of the test wall face is plainly evident from the pictures shown in Figure 69.



Figure 69 Lechler 120° flat spray nozzles providing high-velocity rainfall run-off simulation

The spray nozzles were supplied by high-pressure potable mains water delivered via a large header tank from the top floor of the Sheffield Hallam University 12 storey building at a pressure of approximately 9 bar (130 psi). The in-line gate valves remained connected to act as an emergency shut off valve operated from inside the climate side of the chamber. The in-line needle valves were removed, however, and a single needle valve was used to regulate the mains water supply that fed the common rail connecting all four spray nozzles. The design for this high-pressure rainfall delivery system is illustrated in the diagram shown in Figure 70.

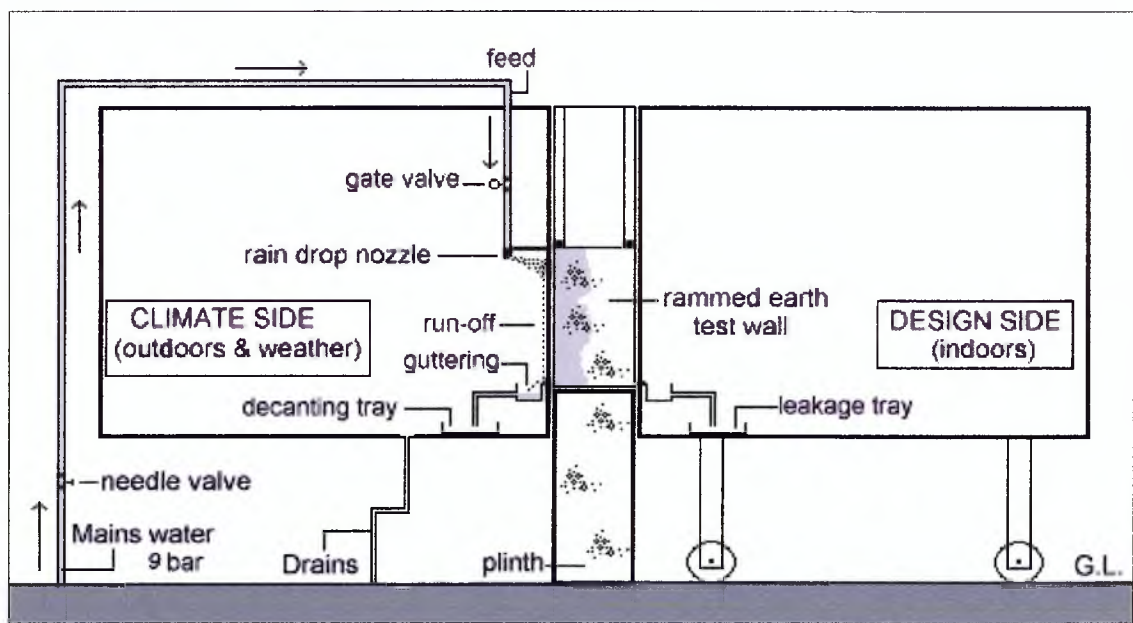


Figure 70 schematic diagram for the mains powered high-pressure water delivery system

The same process of calibration was used with this system as was used for the sparge pipe system described previously. This methodology includes covering the wall face with a removable plastic sheet such that the total amount of water delivery can be measured. On this occasion, however, the flow to each of the four spray nozzles was controlled by a single needle valve located in the mains water feed pipe, as opposed to having an individual needle valve per nozzle.

Using this method the lowest possible flow rate that can be achieved is 500ml/min (0.5 litres/min), as specified in BS 4315-2: 1970 (BSI, 1970). Unfortunately, the spray pattern is erratic at this flow rate and does not give a suitably even distribution across the wall face. Since the surface area of these particular test walls is only 0.45m² the total flow rate would need to be 225ml/min in order to fully satisfy the BS 4315-2: 1970 specified delivery rate of 0.5 Litres/m² min. It was observed that a flow rate of 650ml/min was the minimum rate at which a very good spray pattern could be achieved using this apparatus (see: Figure 69). In addition, the accuracy and consistency of this

flow rate was very good and so it was decided that this configuration should be used for the test methodology.

6.1.3.3 Test Procedure

Each test run began at 10-00am on the Monday and ran for a total of 5 days and so finishing at 10-00am on the Saturday. The first 5-day test run (Test run 1) used the low-pressure constant head supply with the 15mm diameter sparge pipes. Following a 4 week drying period, the second 5-day test run (Test run 2) began and instead used the high-pressure mains supply with flat spray nozzles. The actual test procedure that was used was identical for both types of rainwater delivery systems described above.

Approximately 30 minutes before the test was scheduled to begin (10-00am) the temporary protective sheets were placed over the test walls and the flow rate for the rainfall system was calibrated as described above. To start the test, the protective plastic sheets (used during the calibration phase) were removed, and the climate side of the chamber was pressurised to 250 N/m^2 (i.e. 25mm water, or 0.036 psi). This is the figure recommended by BS 4315-2: 1970 and is equivalent to strong winds pushing up against a wall element in the UK.

The rainfall and pressure differential is constantly maintained for a period of 6 hours, after which the pressure and rain are turned off for the total duration of an 18-hour drying out period. This first test cycle represents Day 1, where the entire test programme runs for a total of 5 days. Approximately 30 minutes before the commencement of Day 2 the temporary protective sheets were re-placed over the test walls and the flow rate for the rainfall system was calibrated as described above. At 10-00am on Day 2 the protection sheets are removed, the climate side is pressurised and

the pressure-driven rainfall phase begins once more...and so on. Figure 71 shows the test walls being subjected to the simulated pressure-driven rainfall.

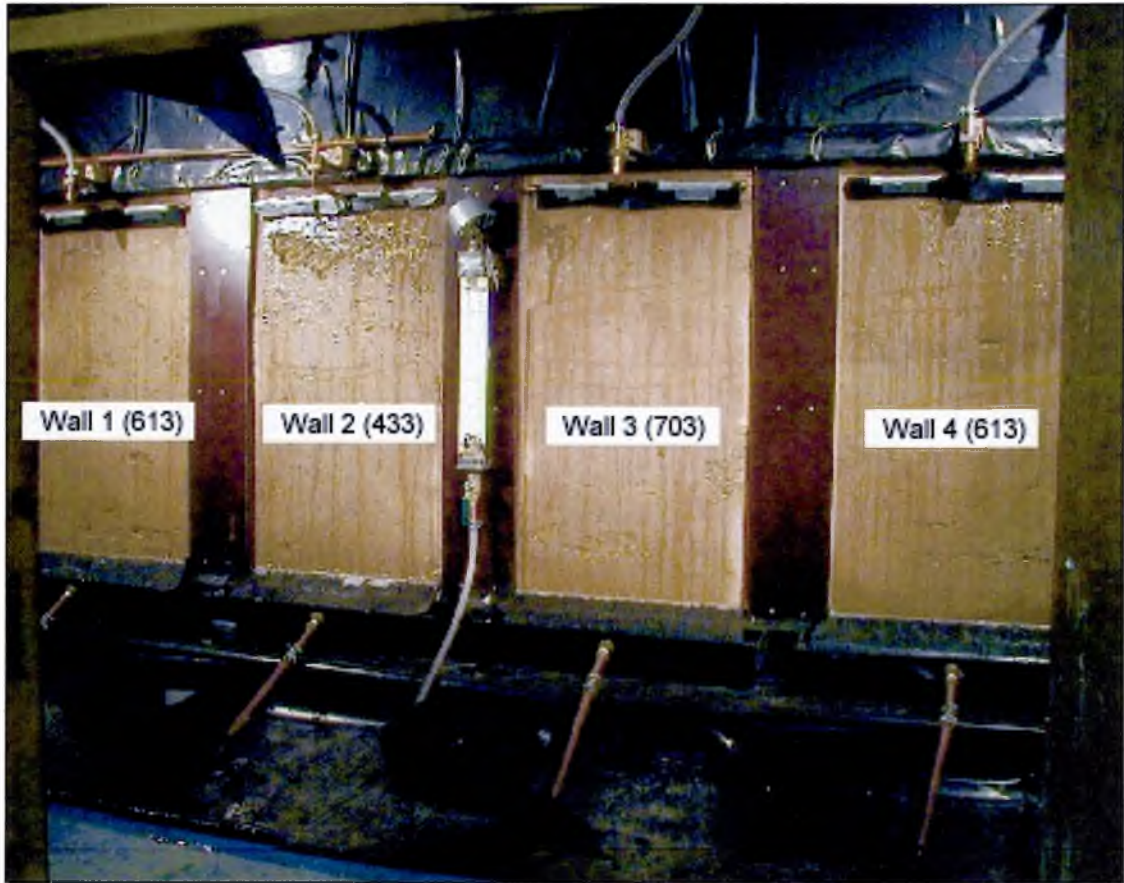


Figure 71 a view of the mini test walls from the climate side during the pressure-driven rain phase (6hr) of the test procedure using the low-pressure sparge pipe delivery system

The water run-off is collected at the following intervals after the start of each 6-hour pressurised rainfall period: 10mins, 20, 30, 40, 50, 60, 90, 120, 150, 180, 210, 240, 270, 300, 330, and 360. That is to say, the readings are taken every 10 minutes for the first hour and then every 30 minutes for the remaining five hours.

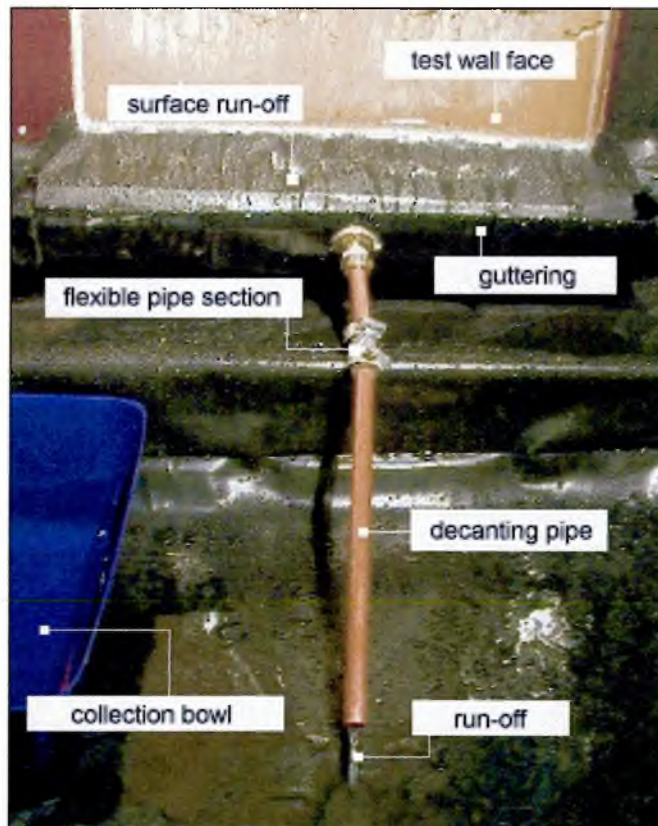


Figure 72 rainfall run-off collection device and equipment

By referring to Figure 72, one can appreciate that the water is collected following a procedure where the operator places their thumb over the end of the decanter pipe whilst simultaneously starting a stop-clock. The pipe is quickly raised at the flexible joint allowing the collection bowl to be placed underneath. The run-off is then allowed to drain into the bowl for a period of 1 minute. At the end of this time, the operator places their thumb over the end of the decanter pipe to stop the flow, and then raises it out of the collection bowl. The mass of the water can then be determined using an accurate balance. When testing all four walls, the start of each 1-minute measurement period is staggered such that after wall 1 has started, wall 2 starts three seconds later, wall 3 six seconds later, and wall 4 nine seconds later. This allows the operator a period of 3 seconds in which to move between each of the four collection bowls and either start or stop the measurement process.

The mass of water that is collected in each bowl can be calculated as an effective rate of water run-off (in $\text{ml/m}^2 \text{ min}$) for each of the four test walls. The test walls will have absorbed a varying amount of rainfall run-off water at different stages throughout the test period. One can simply deduct the amount of run-off that was collected at each time interval of the test from the actual amount of rainfall delivery recorded during calibration. Following these calculations, the amount of water absorption that occurred in each test wall, at each different time interval, can be calculated. By dividing the amount of water collected over each 1-minute measurement period by 60, one can convert the reading into an initial surface absorption (ISA) value for each wall surface, i.e. $\text{ml/m}^2 \text{ s}$.

Theoretically, the initially dry test wall(s) should absorb a relatively large amount of water during the first hour of exposure, with decreasing amounts of water absorption as the remainder of the test period proceeds. It was anticipated that factors such as the total amounts of water absorption, rate of penetration, and the rate of decreasing absorption over time will be significantly affected by the soil type of each the different rammed earth test walls.

6.1.4 Embedded Sensor Apparatus – Test Run #3

After the first and second test runs had been completed, an array of electronic sensors was retrofitted to each of the four rammed earth test walls. Three different types of sensors were installed such that the properties of temperature, relative humidity, and liquid moisture content could be monitored throughout subsequent test regimes. Each of the sensors was embedded in the wall by drilling a hole to the required depth and then carefully inserting the sensor. The sensor was positioned using a special tool made up of

a 5mm diameter metal rod with different depths marked along its length at the appropriate points.

Once in place the sensor hole was capped and sealed using a silicone-based caulking sealant. Six thermocouples were embedded at different depths in the top half of the wall, a single humidity sensor in the centre of the wall, and six wetness sensors at different depths in the bottom half of the wall. The inside face of a test wall, viewed from the design side, complete with a fitted sensor array is shown in Figure 73.

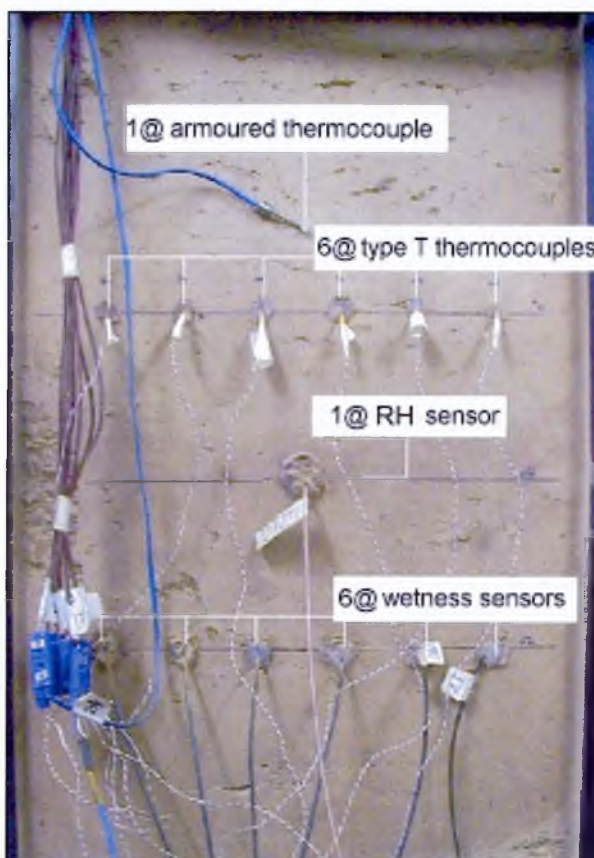


Figure 73 the design side of a test wall showing a fully fitted embedded sensor array

Once the sensors had all been embedded and correctly sealed the procedure described above in Test run 2 (high-pressure spray nozzles) was repeated here for Test run 3. However, on this occasion both the internal and surface conditions of the test walls were monitored using the newly-fitted sensor array. These were retrofitted inside holes of

either 8mm diameter (for thermocouples) or 10mm (for all other sensors) drilled using a 300mm long masonry drill bit. The probes were installed by drilling from the inside face of the test walls (design side of the chamber) to depths of 25mm, 50mm, 75mm, 100mm, 125mm, and 150mm. Unfortunately, it was decided not to risk drilling further into the wall than 150mm using the available equipment because the test face of the wall could easily have been damaged by the vibrations. Further details of the individual sensor types and the data logging system that was employed are discussed in the following sections.

6.1.4.1 Thermocouples (Temperature Sensors)

The temperature sensors used for embedment were type-T copper/constantan thermocouples from RS Components Ltd. The welded tips of the type-T thermocouples (see: Figure 74) are very delicate and so these were protected by inserting them inside hollow plastic tubing. All of the thermocouples were connected to the data loggers using special compensating cable made from the same copper/constantan wires. Armoured thermocouples (see: Figure 75) were mounted onto both the internal (design side) and external (climate side) wall faces. These were held in place using 3mm diameter threaded nylon bar and a captive nut. The nylon bar was inserted into a shallow hole drilled in the wall face and secured using adhesive. The loop of the armoured thermocouple was slid over the bar and the nut fastened on to hold it tight up against the wall façade.

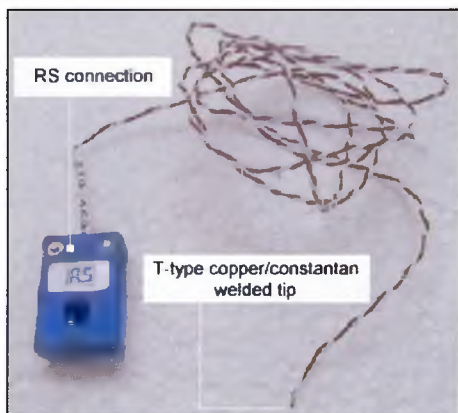


Figure 74 type-T thermocouple

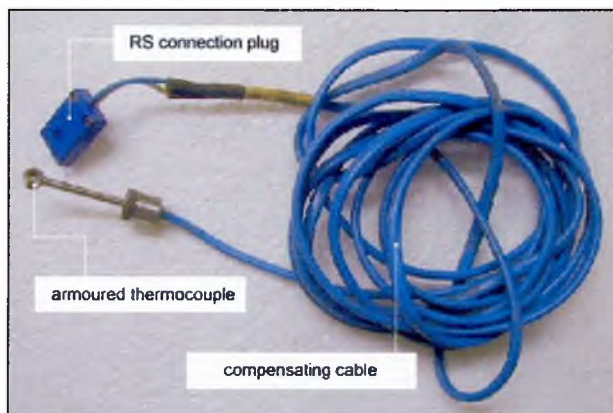


Figure 75 armoured thermocouple

The thermocouples were controlled using IMP integrated data loggers connected to a PC interface card. Using windows-based computer software the thermocouples could be calibrated using the hardware's own on-board temperature sensors. The polling rate was set to 5 minute intervals and the data was logged in the form of *.dat files that could simply be transposed for use with Microsoft Excel spreadsheet software.

6.1.4.2 Relative Humidity (RH) Probes

The sensors used here were provided by Rotronic Ltd., a company specialising in the electronic measurement of relative humidity. The sensors that they provided also contained a temperature sensing device. The sensor head was designed for being embedded and is encased in a thick, protective membrane made from PTFE (polytetrafluoroethylene) that allows the passage of moisture vapour. One of these sensors was embedded at the centre of each of the four test walls to a depth of 150mm. The picture in Figure 76 shows the combined RH & temperature sensor complete with wiring and connections.

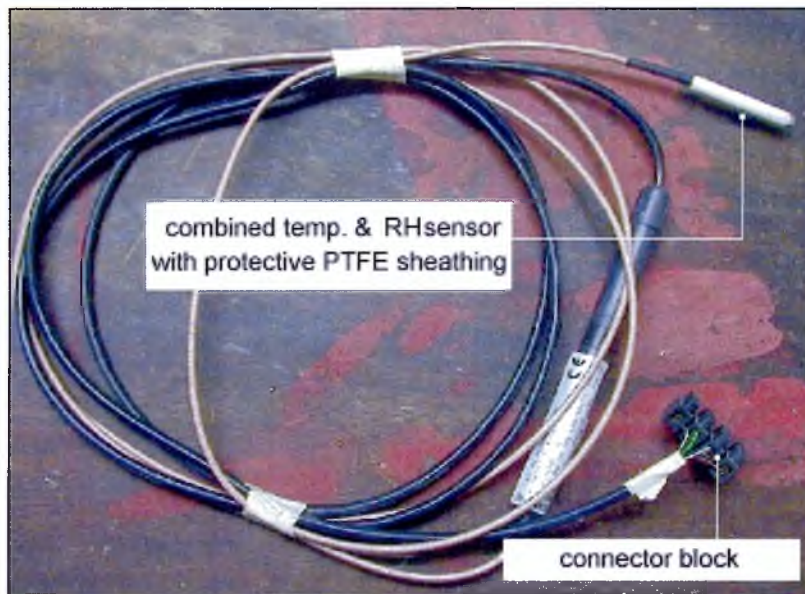


Figure 76 Rotronic relative humidity & temperature embedment probe

The sensors were energised using a 5 Volt D.C. stabilised supply. The probe connections are configured for convenience such that the output readings are decimal values between 0 and 1. On the relative humidity range the values between 0 and 1 equate to the actual humidity percentage, for example where a value of 0.34 is equal to 34% RH. On the temperature range the decimal value equates directly to degrees Celsius, for example where a reading of 0.22 is equal to 22°C. The sensor outputs were connected to the logging channels of a Solartron Orion data logger. The Solartron was then instructed to record the relative channels every 10 minutes for each 24 hour period of a given 5-day test regime.

6.1.4.3 Resistance-Type (Ω) Moisture Content Sensors

These sensors were custom-made by the author using 3 amp plastic connector blocks cut into strips of two. The probe tips were made using the gold plated pins extracted from an RS 232 computer data plug socket. Two gold pins were fastened into each connector block, as illustrated by Figure 77 and Figure 78.



Figure 77 twenty four custom-made resistance probes



Figure 78 gold-plated sensor tips

Normally the problem with resistance probes that are energised using a direct current (D.C.) is that the probe tips become polarised; i.e. one becomes the anode and the other the cathode. This can cause rapid corrosion of the probe tips, which can have a deleterious effect on sensor accuracy. By using gold plated tips the problem of probe tip corrosion due to electrolysis is minimised. The use of plastic connector plugs creates a sensor that is highly durable and that keeps the probe tips a set distance apart.

The probes are energised via a bridge circuit that is powered by a 5 volt D.C. stabilised supply. Each energised probe then outputs a precise voltage of 2.50 V when the probe tips are not in contact with any solid or liquid material. When the probe tips come into contact with such an object the voltage output drops to a value below 2.5 volts depending upon the level of electrical conductivity in the material. When immersed in potable water, for example, each of the probes gave a precise output voltage reading of 0 V. This gives a maximum and minimum reading for the sensor when the test medium is dry or saturated, i.e. 2.5 V when completely dry, and 0 V when completely saturated. The probes and bridge circuit used here have a sensitivity that is suited for measuring the changes in conductivity caused by the presence of moisture. The picture in Figure

79 shows the way in which the probes and bridge circuits, for each of the four test walls, were connected to the stabilised power supply and the Solartron data logger.

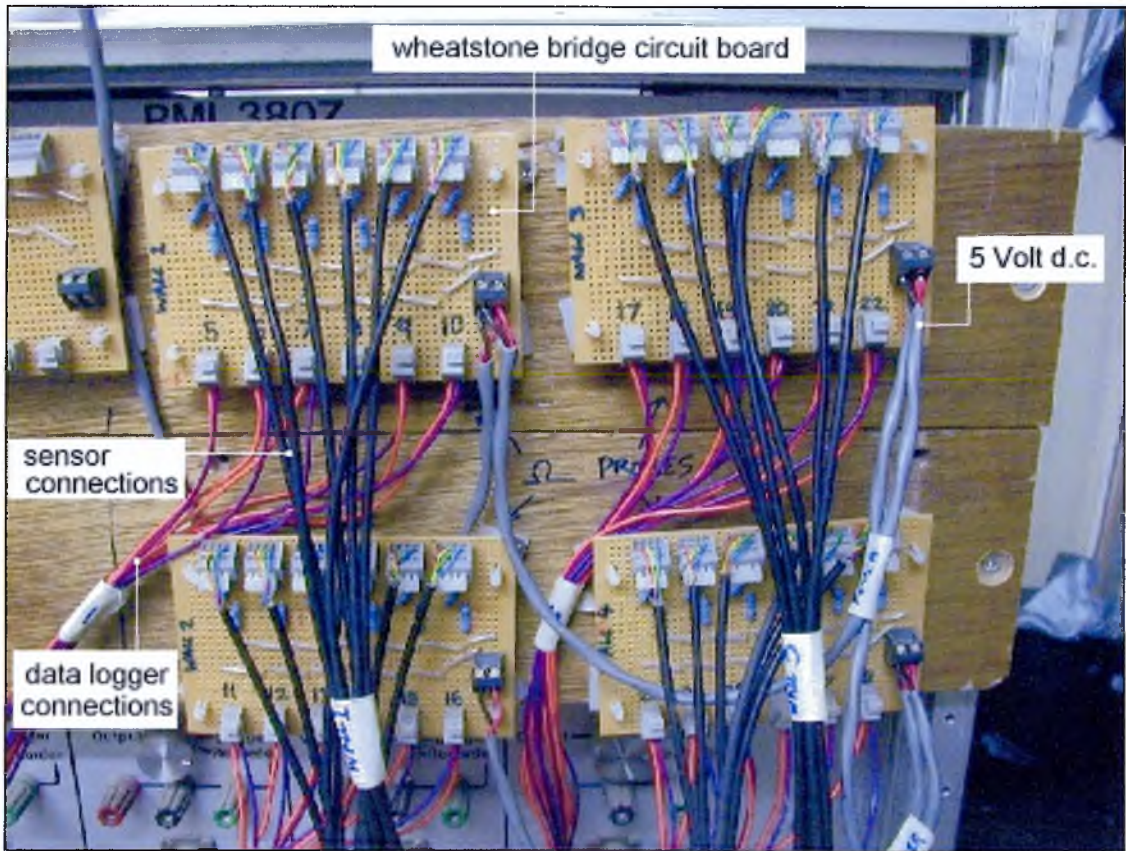


Figure 79 the bridge circuit array with sensor wiring configuration

The main disadvantage to resistance probes is that they can measure any factor that alters electrical resistance in a material, e.g. the presence of salts. In practical terms, when the probe tips were placed in a moist sponge the output voltage was approximately 1.7 volts. Since the linearity of the corresponding voltage output of the probes was not determined, the actual value of this reading could only be calculated following subsequent calibration. Calibration of the actual moisture value against voltage output (i.e. those values between the maximum and minimum) was postponed until the successful collection of data from the test walls. It was concluded that owing to

the lengthy and expensive process of full sensor calibration it would only become necessary if any data was actually obtained during the tests.

6.1.5 Fixed-Climate Differentials – Test Run #4

The effect of temperature differential has been explored further by creating various fixed temperature & humidity gradients across the test walls. This was achieved by maintaining a difference in temperature/humidity between the design side and the climate side of the chamber for a 24-hour period. All of this testing was, therefore, performed in the absence of any rainfall and/or pressure differential. The indoor (design side) conditions were maintained at $20^{\circ}\text{C} \pm 1^{\circ}$ and $40\% \text{ RH} \pm 5\%$ to represent a comfortable indoor living environment.

The outdoor conditions (climate side) were kept at a constantly high level of relative humidity: $75\% \pm 5\%$. This represents a damp outdoor environment that is typical of the inclement British weather. The entire test run (Run 4) lasted for a period of four days and included three different outdoor temperature levels. Throughout days 1 and 2 the outdoor temperature was lowered and maintained at 8°C for the entire 48 hour period. On day 3 the temperature was lowered to 0°C for the entire 24 hour period. Finally, on day 4 the temperature was lowered to -8°C for the remaining period of 24 hours. During all four days of Test run 4 (described above) the entire sensor was used for recording the performance of the test walls. As with Test run 3, the resistance wetness probes and the RH + temperature embedment sensors took readings every 10 minutes, whilst the thermocouples took readings every 5 minutes.

6.2 RESULTS & DISCUSSION

6.2.1 Test Run #1: Low-Pressure Sparge Pipes

The low-pressure sparge pipe delivery system that was used for Test Run 1 was essentially the equivalent of water run-off on the wall face caused by sustained rainfall. The applied static air pressure differential of 250 N/m^2 (25mm water) was the equivalent of strong winds pushing up against the exterior wall face and this has the effect greatly exacerbating moisture ingress. This methodology was specifically designed for the climatic simulation chamber and was based upon the recommendations in British Standard 4315-2: 1970.

The applied water delivery rate was specified as $500\text{ml/m}^2 \text{ min.}$ in accordance with BS 4315-2: 1970. This is the equivalent to 225ml per wall/min, or 13500ml per wall every hour. Since the wall surface area is 0.45m^2 (4635cm^2) a total depth of 29.1mm of rain would effectively fall on the surface of each wall every hour for a total of six hours in any 24 hour period. This gives a total of 174.6mm (approx 7") of rainfall for a given six hour test period. The applied air pressure difference of 250N/m^2 (25mm water @ 20°C) between the 'outside' and the 'inside' face of the wall is the equivalent force of strong winds constantly pushing against wall face, as opposed to the dynamic (on/off) effects of gusts and blowing.

6.2.1.1 Observations

All four test walls 'passed' the test because absolutely no signs of water penetration or leakage occurred during the entire 5-day test run. A previous study in the climate chamber involved a series of single leaf natural stone (black granite) walls built with hydraulic lime mortars, and some with the additional application of protective lime

renders. In this case the test methodology was almost identical to the one applied to the rammed earth test walls described above. Most of the stone test walls began to leak during the first six hours of exposure to these conditions, and even those protected by a render began to permit water penetration to occur after only a few days.

The flow rates of water run-off appeared to be so inconsistent that variations in the calculated absorption appeared to be masked by fluctuations in the actual rate of water delivery. As a direct result of these issues, the calculated data for water absorption in the test walls is intangible. It was concluded that this particular methodology of water delivery was perhaps only consistent enough for a test that was designed just to measure the time taken for full penetration/leakage to occur, and not to measure the rate of water absorption over time, i.e. simply a “pass” or “fail” test.

6.2.2 Test Run #2: High-Pressure Spray Nozzles

The target delivery rate was 650ml/min per wall although in practice the actual delivery rate could only be set to an approximate value of between 630- and 680ml/min per wall. Due to the high pressure in the system and the increased flow rates the average variation in the delivery rate, once it had been set, was approximately ± 40 ml/min per wall. Since the test wall(s) surface area remains at 0.45m^2 (4635cm^2) this is the equivalent to a sustained rain shower where a total of approximately 84mm (3.3”) of rain runs downwards across the face of each test wall every hour for six hours in any 24 hour period.

6.2.2.1 Analysis of Results

During the six hour daily rainfall period the water run-off from each test wall was collected and measured at regular intervals. For observation purposes the average

ambient climatic conditions of temperature & relative humidity were recorded for the climate side of the simulation chamber. Table 9, for example, shows the entire water run-off collection data for the first day (Monday) of Test Run 2.

Table 9 an example data set for water run-off collection during Test Run 2

<i>19/05/2003 Day 1 – Monday</i>		<i>Climate-side ambient conditions:</i>			
start at 10am		Avg. ambient temp. = 22.4°C			
finish at 4pm		Avg. ambient RH = 52.8 %			
Time (mins)	Water run-off collected (ml)				
	Wall 1	Wall 2	Wall 3	Wall 4	
10	638	657	658	673	
20	650	665	655	678	
30	646	657	650	663	
40	647	662	634	660	
50	653	668	657	664	
60	656	667	653	667	
90	653	681	658	702	
120	660	689	660	688	
150	650	660	659	689	
180	664	675	669	700	
210	668	682	663	695	
240	655	681	663	692	
270	665	681	671	703	
300	656	673	658	659	
330	665	671	681	697	
360	680	695	671	707	

The water run-off collection data from each of the five days was plotted against elapsed time on a graph. Even though the level of variation in water delivery had been much improved over that of Test Run 1, its effects still appeared to have a highly significant influence. The differences between the sets of data that were obtained for each of the

five different days were judged to be of little significance. A representative example of the daily water run-off collection data from Test Run 2 is shown in Figure 80.

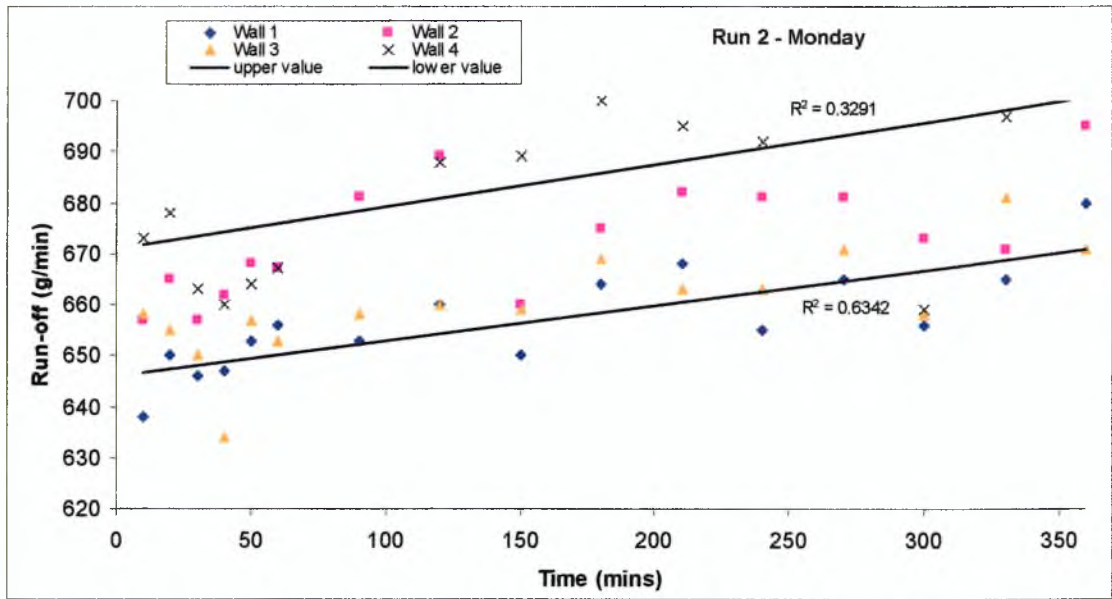


Figure 80 the water run-off collected at each time interval of Monday on Test Run 2

As one would expect, the recorded mass of collected water run-off for each of the test walls was smaller during the early stages of the test and then began to increase back towards the original delivery rate. This is because the rate of water absorption is much higher when initially dry test walls are first exposed. Over the duration of the 5-day test period the rate of water run-off appears to slowly decrease, with a degree of linearity, against the elapsed time (t) as illustrated by the graph in Figure 81.

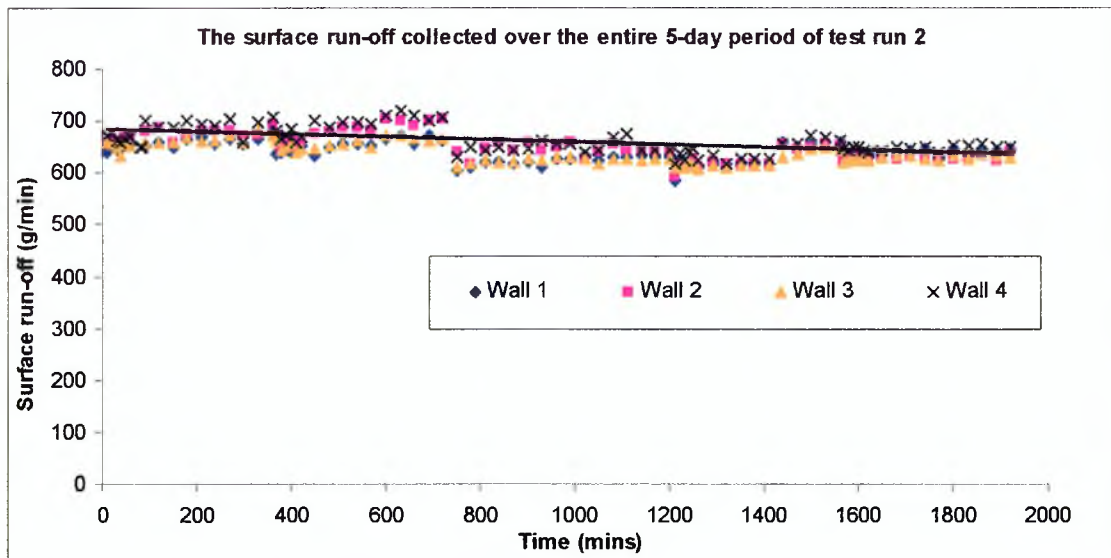


Figure 81 the rate of surface run-off water collected over the entire 5-day test period of Run 2

The run-off collected for any given test wall is typically between 600 and 700 g/min. This appears to indicate that periodic pressure-driven wetting over a 5-day regime means that the degree of moisture penetration in the walls increases in relation to the length of time of exposure.

To look at this data in isolation, however, is misleading since the delivery rates between test walls can actually vary by up to ± 40 ml/min. For each test wall, one can calculate the mean absorption rate by deducting the collected amount of water run-off, at each time interval, from the set delivery rate. The graph in Figure 82 illustrates the calculated total absorption rate for each test wall against the elapsed time for the duration of the 5-day test period.

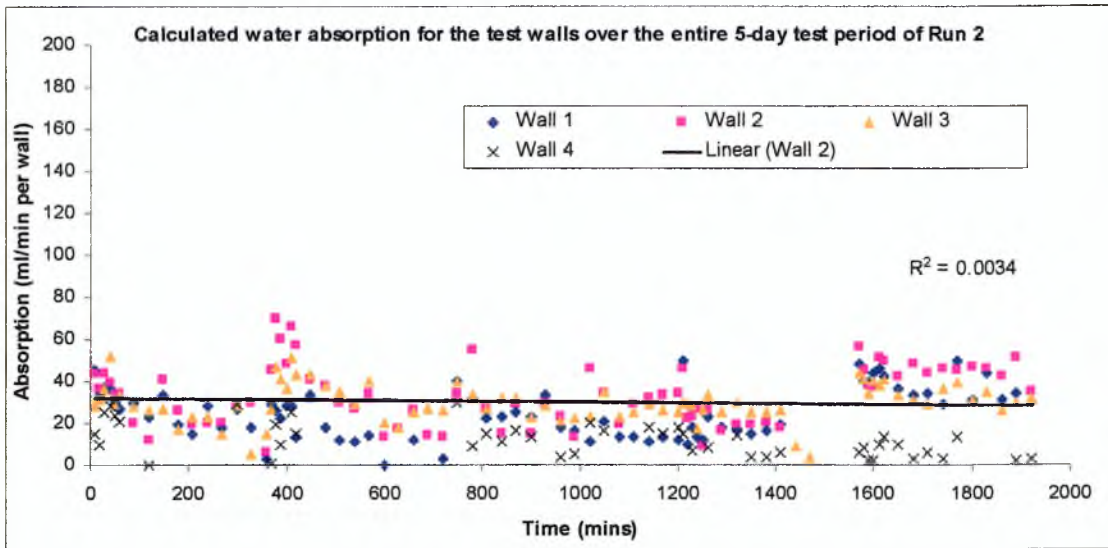


Figure 82 mean water absorption in stabilised rammed earth test walls over the entire 5-day period of Run 2

Apparently the mean absorption from surface run-off water, in any of the cement stabilised rammed earth soils used for the test walls, was very low and typically less than 80g/min per wall. However, the variation in set delivery rate is apparent once more, which accounts for the mean absorption rate sometimes being calculated as a negative value, i.e. when the run-off is recorded as being greater than the calibrated flow rate. Since the typical dry mass for one of these 300mm thick test walls is approximately 280 kg, the calculated mean water absorption only represents around 0.01% of the entire wall mass.

Since this methodology appeared to provide both the effects of static differential combined with a known quantity of surface absorption, attempts were made to calculate the rate of water absorption per unit inflow surface area, i.e. the initial surface absorption (ISA). The graph in Figure 83 shows the calculated rate of water absorption per unit inflow surface area for each of the test walls on the first day (Monday) of Test Run 2.

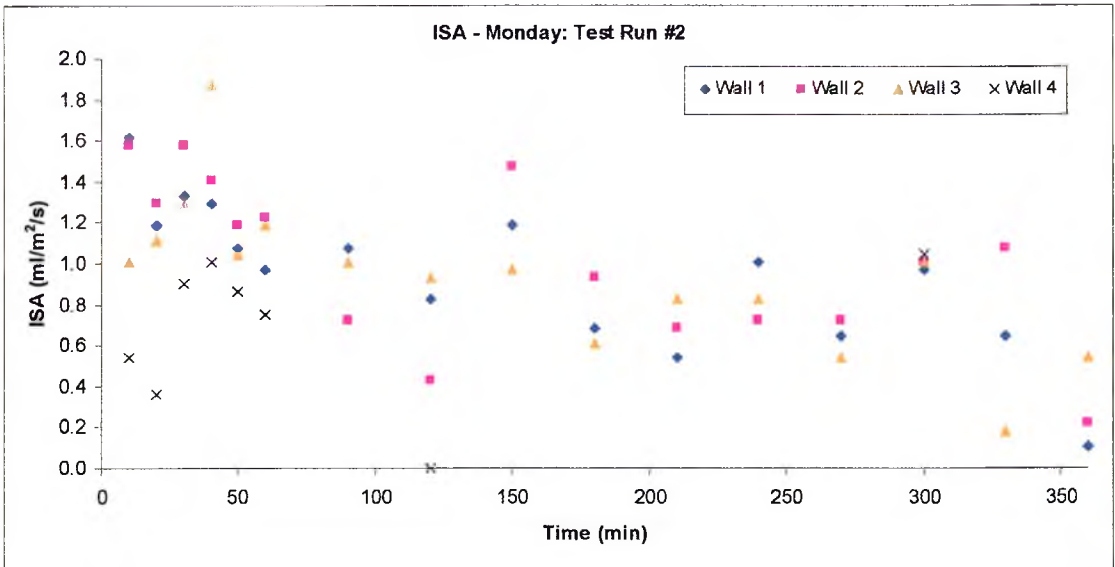


Figure 83 the calculated rate of water absorption per unit inflow surface area for each test wall on the first day of Test Run 2

The maximum rate of water absorption calculated for the test walls was less than 2.0 ml/m² sec, or 30ml/m² min and is insignificant when compared to the mass and thickness of the wall itself. Over the entire five-day test period of Run 2 there appears to be no visible pattern in the initial surface absorption of any of the test walls, as shown by the graph in Figure 84.

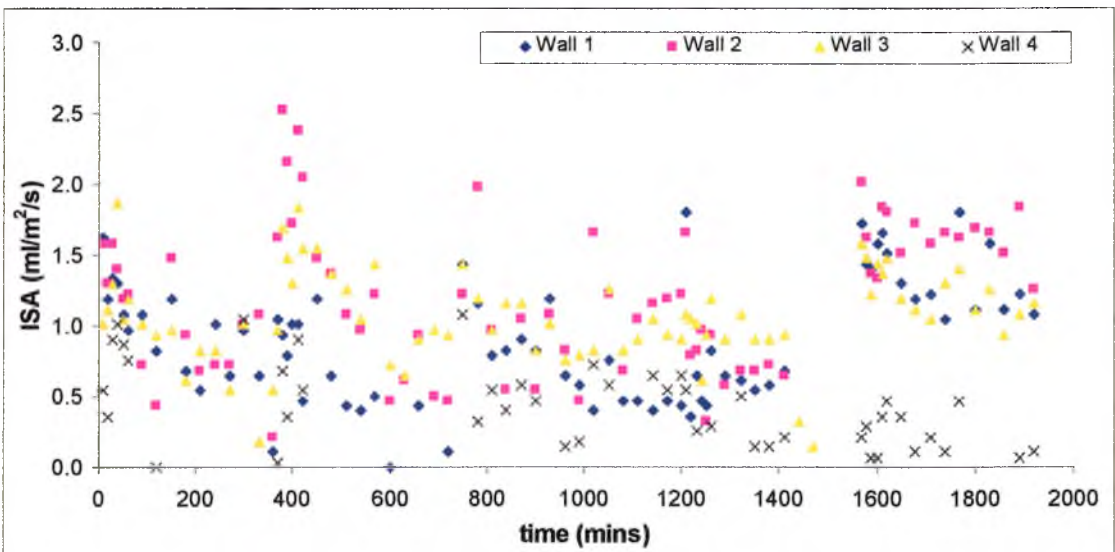


Figure 84 the initial surface absorption (ISA) for each test wall over the entire 5-day test period of Run 2

We can compare these findings with the previous experimental work involving rammed earth cube samples since this work was performed with the same soil mix recipes (433, 613, and 703). They had the same material dry density and were stabilised with the same percentage of cement (6% by mass). The graphs in Figures 85, 86 and 87 show the comparison between the ISA of rammed earth cube samples for a given mix recipe, with the ISA observed in the corresponding climate chamber test wall.

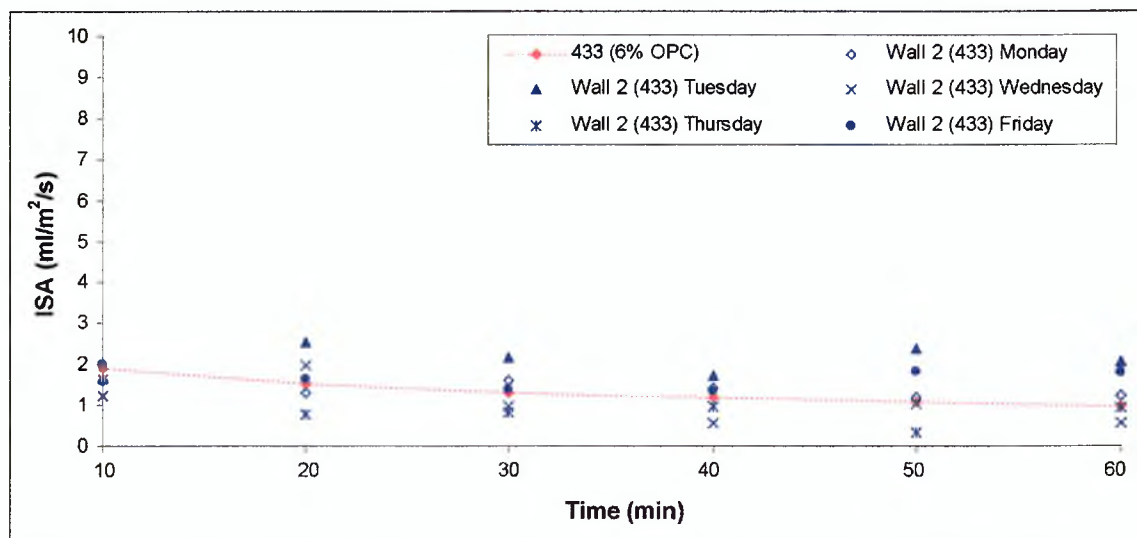


Figure 85 comparison between ISA values for cube samples and test walls - 433 mix recipe + 6% cement

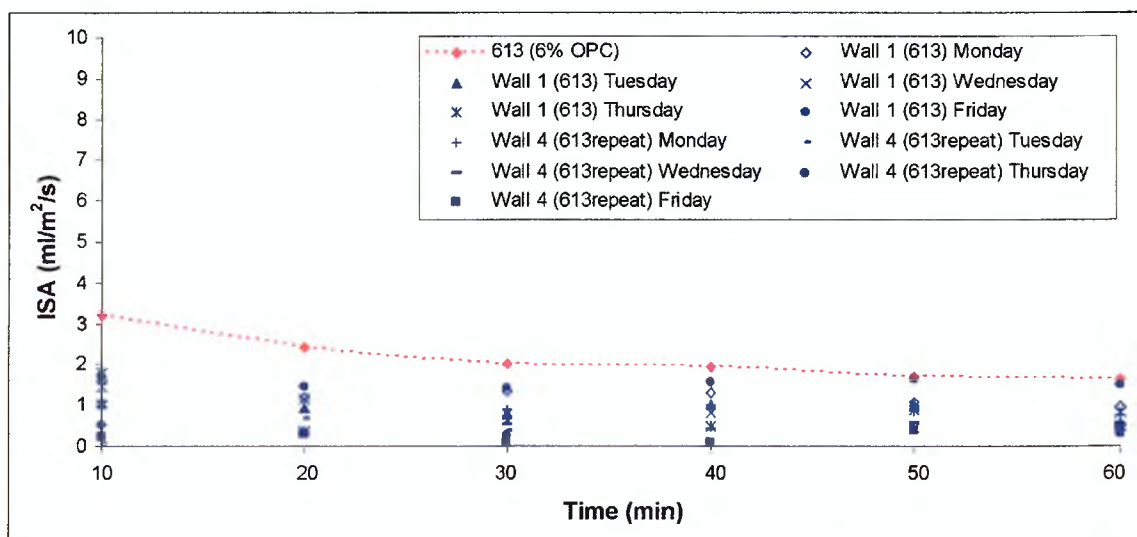


Figure 86 comparison between ISA values for cube samples and test walls - 613 mix recipe + 6% cement

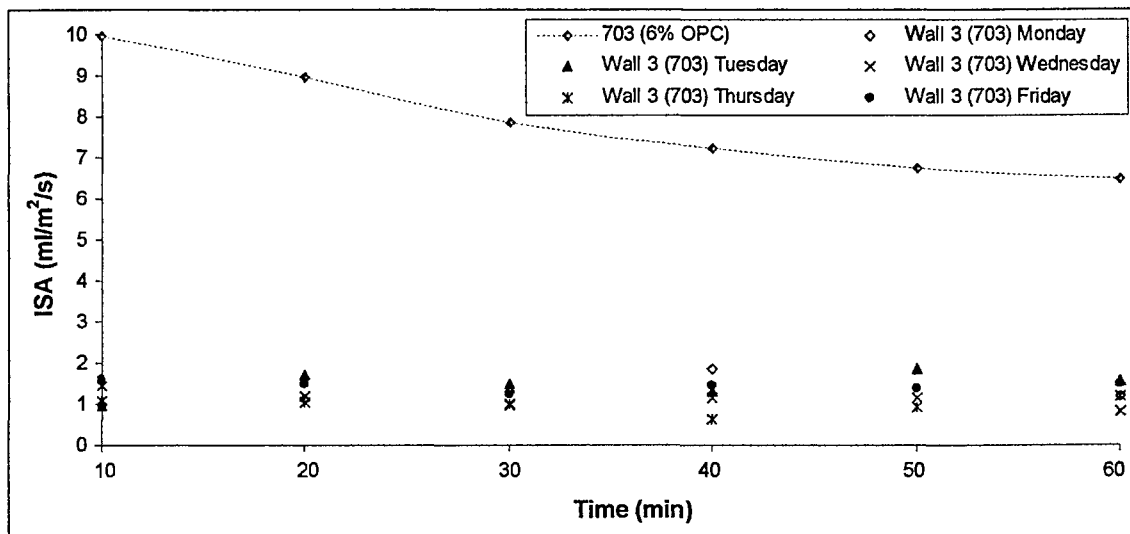


Figure 87 comparison between ISA values for cube samples and test walls - 703 mix recipe + 6% cement

We can see from the three graphs above that all of the test walls appear to have similar ISA values to one another regardless of the type of soil mix recipe or the day on which it was tested. However, the differences in ISA values for the cube samples vary greatly according to the type of soil mix recipe, as was observed previously. There is virtually no disparity between the cube sample and test wall ISA values for the 433-mix recipe. The test wall ISA values for the 613-mix recipe are significantly lower than the cube sample values, whilst the test wall ISA values for the 703-mix recipe are considerably lower than their equivalent cube sample values.

Perhaps the insignificant level of moisture ingress that occurred in the climate chamber test walls may result from the moisture source being dynamic and not static. This theory is logical since we assume that it would be harder for a porous material to absorb running water than a stationary water source. The forces of capillarity and applied pressure differential, which are working to incise absorption of the surface run-off, are perhaps working against the kinetic energy of the moving water.

The silty clay content of each test wall was kept constant, and yet the granular particle-size distribution was varied considerably by using different mix recipes. We can conclude that, for full-scale test walls under simulated rainfall conditions, the initial surface absorption of pressure-driven water run-off appears to be independent of the granular particle-size distribution in a soil. In addition, it would appear that, at this scale, the level of clay content in a soil might be the principal factor controlling the level of moisture ingress and migration. Summarily, an approximate clay content (*CC*) of 0.1 and a silt content of 0.2 can be used to produce stabilised rammed earth walls (with 6% cement) that have a very low absorption when exposed to pressure-driven water run-off.

6.2.2.2 Additional Observations

After the application of pressure-driven rainfall has begun the wall remains initially water-repellent as much of the water runs off the surface. However, the area that receives the impact of the sprayed water appears to wet up more quickly whilst some absorption of run-off water does slowly begin to occur during the first hour of exposure as shown in Figure 88.

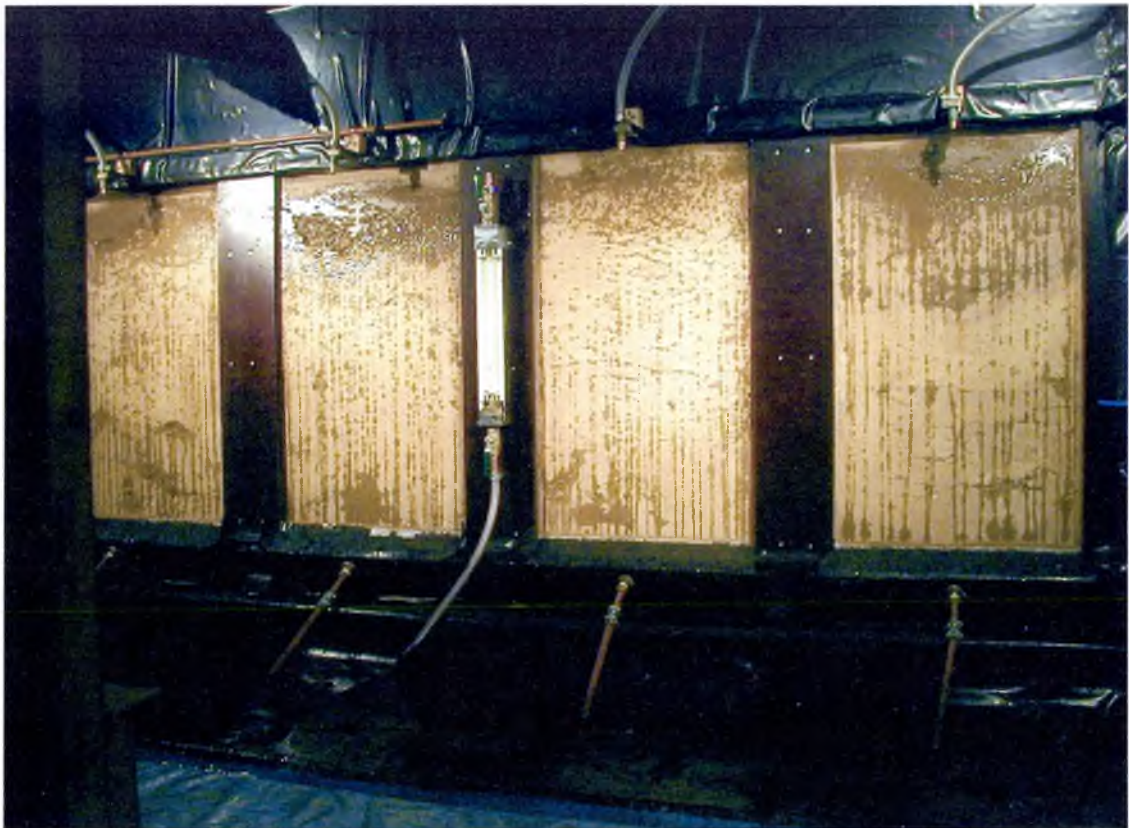


Figure 88 the initial stages of the pressure-driven rainfall applications for Test Run 2; much of the surface run-off pours down the wall face without being absorbed

After approximately two hours of prolonged exposure the test wall faces were becoming visibly wet over the majority of the exposed face. The water ran off the wetted wall surfaces producing a glass-like appearance. It appeared that only a thin outer layer of each wall actually became saturated before subsequent further moisture ingress was prevented, i.e. the 'overcoat' effect as demonstrated by Figure 89.



Figure 89 the later stages of the pressure-driven rainfall applications for Test Run 2; the test wall surfaces have become visibly wet and the ‘overcoat’ effect appears to repel further ingress

6.2.3 Test Run #3: Embedded Electronic Sensors

The same methodology for pressure-driven rainfall that was used in Run 2 was also applied in Run 3 using high-pressure spray nozzles. The target rainfall delivery rate remained at 650ml/min per wall (± 40 ml/min) and the applied static pressure differential had a force equivalent to 250N/m^2 (25mm water). The behaviour and performance of each test wall was monitored using embedded sensors.

No changes in liquid moisture content or relative humidity were detected between the depths of 150mm and 300mm (inside face) from the exposed external face. From this we can simply deduce that, under these conditions, the test walls did not leak nor did they allow the pressure-driven moisture to penetrate as far as 150mm into the wall. The

relative humidity recorded at the centre point of each test wall typically remained constant and ranged between 93% and 94%.

The observed cooling effect of the surface run-off water (approx. 15°C) upon the wall surface (approx. 22°C) was significant, and it affected the wall temperature all the way to the interior surface. The thermal behaviour for each of the test walls was observed to be very similar with no significant differences occurring between soil mix recipes. The initial temperature of both the internal and external wall faces was approximately 22°C, and the temperature of the exposed faces became lowered by the cooling effect of the water to around 4° lower (approx. 18°C) than the interior face. The core temperature of each test wall gradually dropped by up to 1.5° (approx. 20.5°C) below the interior wall face temperature during the six-hour period of exposure to rainfall. A typical example of this behaviour is illustrated by the example of wall 1 on Monday (day 1) in Figure 90.

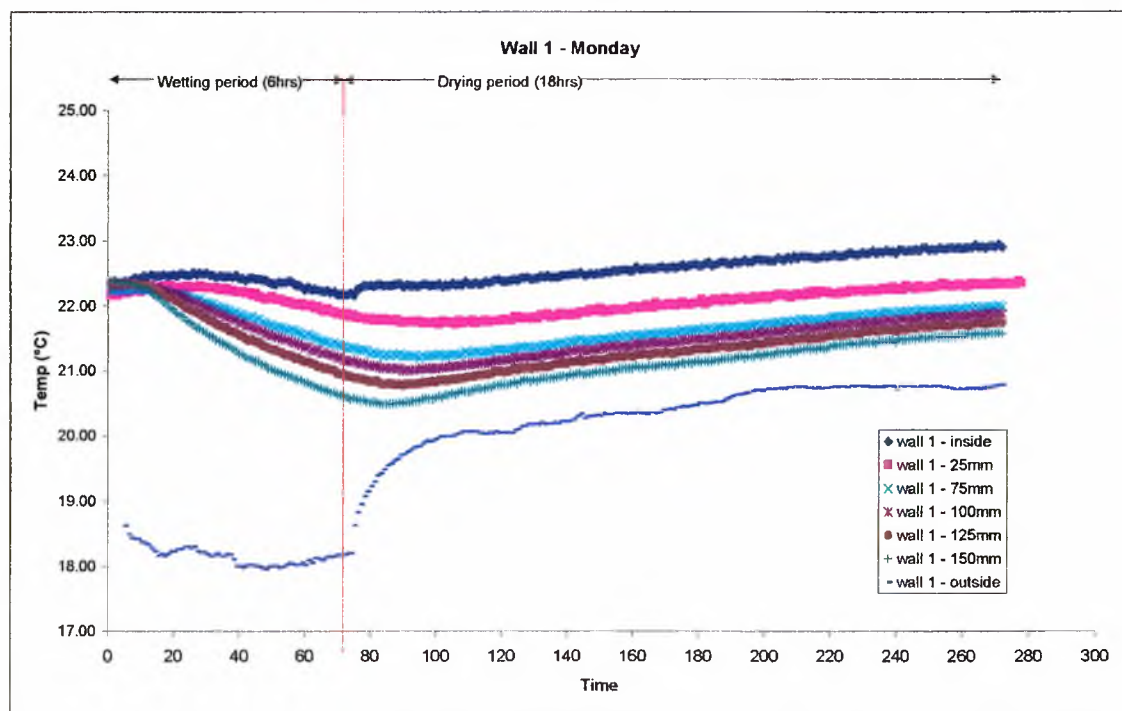


Figure 90 a typical example of a wall temperature depth profile chart for wall 1 on Monday (day 1) of Run 3

We can observe from Figure 90 that even by the end of the first day (Monday) of Run 3, the test wall had not fully recovered from the temperature fluctuations caused by the cooling effect of rainwater run-off. As one may anticipate, since the second day (Tuesday) began with another 6-hour rainfall period the cooling effects of the rainwater run-off became cumulative. This is clearly illustrated by the graph in Figure 91 where the temperature depth profile of wall 1 is displayed for the entire duration of the 5-day test Run 3.

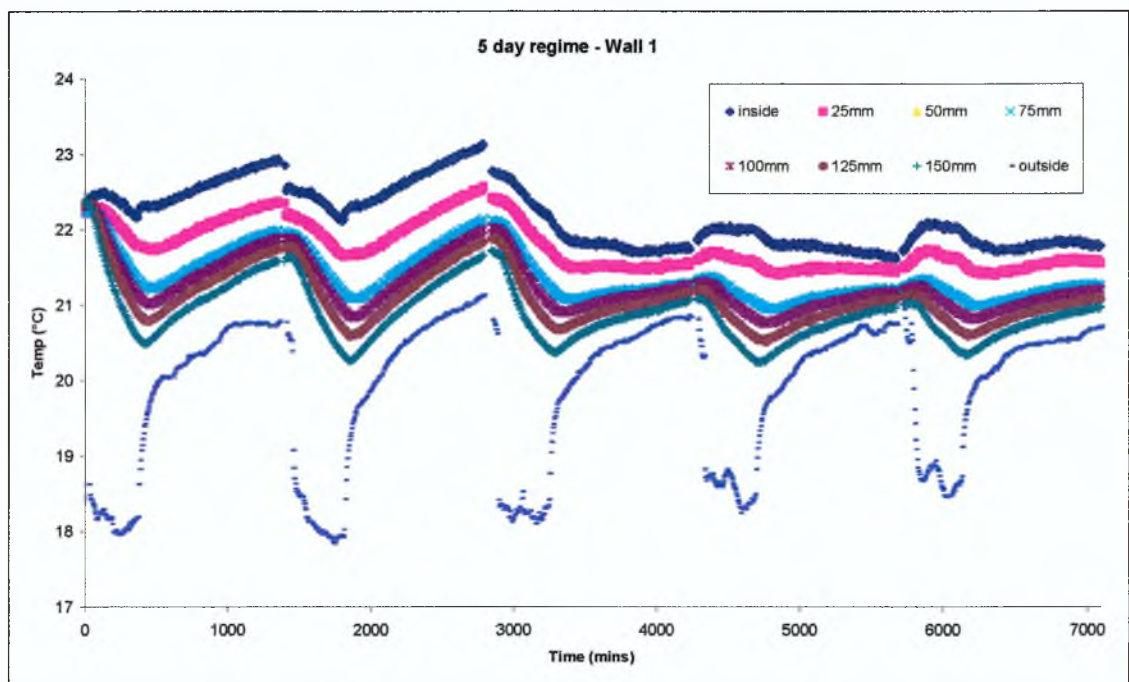


Figure 91 a typical temperature depth profile chart for wall 1 over the entire 5-day regime of Run 3.

The implications of these findings are that potential may arise for interior surface condensation or the accumulation of interstitial condensation within a stabilised rammed earth wall. This would strongly depend upon the vapour permeability of the material, the determination of which would require further research at this stage.

The difference in particle-size distribution (PSD) between mix recipes appears to have no significant effect on the temperature depth profile for each respective test wall.

However, the effect of PSD on the thermal conductivity (k) of stabilised rammed earth remains inconclusive and demands further research. The variation in particle-size distribution between rammed earth soil types alters both the dry density (ρ_d) and volume fraction porosity (f) significantly, and yet it appears not to significantly affect thermal conductivity (k) within the confines of this test regime.

6.2.4 Test Run #4: Temperature Differential

Test Run 4 was performed in order to provide additional data on the interesting effects of temperature depth profiling that were incidentally discovered during Run 3. Since the properties of heat and mass transfer in building materials are interrelated, it is anticipated that this additional data, whilst not directly relevant to this project work, may be useful in future research projects. During Run 4 no rainfall or pressure differential was applied as the aim was simply to explore the effect of static temperature differentials on the temperature depth profiles of the SRE test walls.

The interior conditions (design side) of the climate chamber were kept constant at 22°C ($\pm 1^\circ$) and 45% RH ($\pm 5\%$) in order to represent typical indoor living conditions. During days one and two the exterior (climate side) conditions were set to 8°C and 75% RH ($\pm 5\%$) in order to represent damp, cool outdoor conditions. During day three the exterior conditions were lowered to 0°C and 75% RH ($\pm 5\%$), and then on day four lowered further to -8°C and 75% RH ($\pm 5\%$) during which time snowfall began to occur.

The temperature depth profiles for each of the four test walls appeared to be remarkable similar throughout Run 4. The typical thermal performance of the test walls throughout the four-day test period can be universally represented by the example of wall 1 shown in Figure 92.

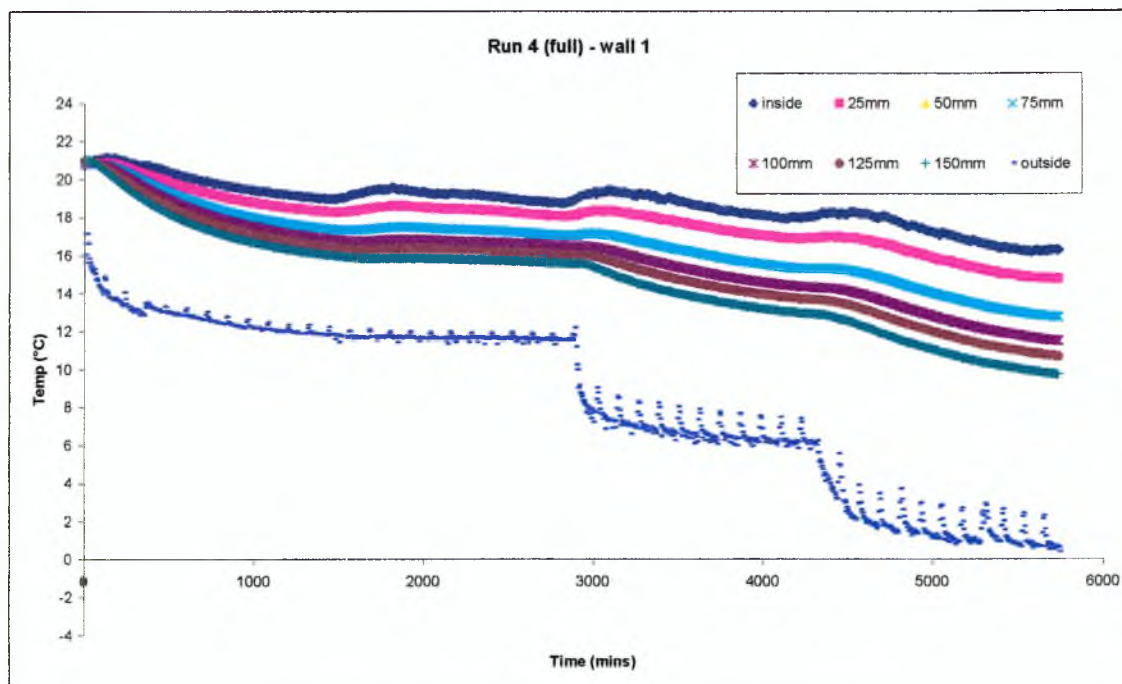


Figure 92 the temperature depth profile of wall 1 during the entire four-day test regime of Run 4

No significant changes were observed in the relative humidity or moisture content resistance probes during Run 4. This implies that no incident of interstitial condensation was generated within the location of the probes or within the confines of this test regime.

6.3 SUMMARY

The SHU climatic simulation chamber is a unique and well-established base for experimental work involving full-scale building elements, e.g. walls. A series of rammed earth test walls have successfully been constructed inside the climate chamber in a manner that conforms to established procedures and parameters for this apparatus. Test methodologies for investigating rainfall penetration with static pressure-differential have been devised based upon BS 4315-2: 1970. An array of embedded electronic

sensor apparatus has been devised for use with the rammed earth test walls in order to monitor temperature, relative humidity, and liquid moisture content.

All of the cement stabilised rammed earth test walls exceeded the SHU climatic simulation chamber rainfall penetration tests based upon BS4315-2: 1970. After five days of exposure to static pressure driven moisture ingress methodologies there was no significant occurrence of moisture penetration, wash out or erosion. Under these test conditions, the ISA is a comparatively low value that is similar for each test wall and appears to be independent of differences in the particle-size distribution between mix recipes. This indicates that the kinetic energy of the dynamic moisture source (i.e. run-off water) is sufficient to exceed the capillary potential of the wall face. However, since the silty clay content of each mix recipe was constant it may also indicate that the proportion of cohesive soil in the mix determines the ISA of a wall when it is exposed to pressure-driven rainfall. The embedded sensor array detected no significant increase in the relative humidity or liquid moisture content inside the test walls from a minimum depth of 150mm away from the exposed face.

7.0 SOIL GRADING OPTIMISATION

7.1 SORPTIVITY (S)

The experimental data used here to determine the sorptivity (S) and surface inflow velocity (u_0) of porous building materials has been derived from two separate sources:

1. Calculated using the author's experimental data investigating and comparing the ingress of moisture by capillary suction in rammed earth with that of conventional masonry materials, as discussed in Chapter 4. This data has been published in the journal paper Hall M & Djerbib Y, 2004_a, "Moisture Ingress in Rammed Earth: Part 1 – The Effect of Particle-Size Distribution on the Rate of Capillary Suction", *Construction and Building Materials*, 18 [4] pp.269-280
2. The experimental data collected by Gummerson, Hall & Hoff (1980) in a separate study of the sorptivity of conventional porous masonry materials. Their test methodology was also based on the British Standard 3921 IRS test, as was the aforementioned IRS 'wick' test.

The comparison of these independently produced sets of published data allows for the assessment of the methodology in terms of both the repeatability and the reproducibility. The results taken from Gummerson *et al* (1980) for fired clay bricks compare favourably with those obtained using the previously defined IRS 'wick' test. This proves, to some degree, that the results presented here are reproducible and that the IRS 'wick' test can be used effectively when compared to the IRS test defined in BS 3921: 1985. Experimental data on the sorptivity (S) of rammed earth has been produced and compared with that of numerous conventional building materials in Table 10. The

data represented by red italics (e.g. *123*) is that obtained by Gummerson *et al* (1980), whilst the data represented by standard text (e.g. 123) is that obtained in this study.

Table 10 the sorptivity and related properties for a variety of conventional masonry materials, unstabilised rammed earth, and cement-stabilised rammed earth

#		Sorptivity S (mm min ^{-0.5})	Intrinsic Sorptivity s (m s ^{-0.5} E ⁻⁵) *	Effective hydraulic pore radius r (nm)	Vol. frac. Porosity f
Fired clay bricks:					
1	Common brick	<i>0.995</i>	-	-	<i>0.309</i>
2	Ordinary facing brick	<i>2.470 – 2.720</i>	<i>3.742 – 4.121</i>	-	-
3	Ordinary facing brick*	<i>0.320 – 1.110</i>	<i>0.485 – 1.682</i>	-	-
4	Special quality facing brick	<i>0.830</i>	<i>1.257</i>	-	-
5	London brick – Dapple light	0.704	1.067	-	-
6	London brick – Fletton	1.033	1.565	-	-
7	Engineering brick	1.374	2.082	-	-
8	Calcium silicate brick	<i>0.890</i>	<i>1.348</i>	-	-
Concrete materials:					
1	C30 vib. comp. concrete	0.582	0.882	-	-
2	Med. concrete block	4.719	7.149	-	-
3	Concrete brick	<i>0.200</i>	<i>0.303</i>	-	-
4	Autoclaved aerated concrete block	<i>0.500 – 0.510</i>	<i>0.758 – 0.773</i>	-	-
Natural stone:					
1	Portland limestone	<i>0.300</i>	<i>0.455</i>	-	-
2	St Maximin (fine) limestone	<i>3.100</i>	<i>4.697</i>	-	-
3	Anstrude limestone	<i>0.800</i>	<i>1.212</i>	-	-
4	Kerridge sandstone	<i>0.029</i>	<i>0.044</i>	-	-
Mortars:					
1	1 cement: 3 sand	<i>0.700</i>	<i>1.061</i>	-	-
2	1 cement: 1 lime: 6 sand	<i>1.700</i>	<i>2.576</i>	-	-
3	1 cement: 3 lime: 12 sand	<i>3.300</i>	<i>5.000</i>	-	-
Plasters:					
1	Class B, type b2 gypsum building plaster***	<i>1.400 – 2.500</i>	<i>2.121 – 3.788</i>	-	-
2	Class B, type b2 gypsum building plaster	<i>2.600</i>	<i>3.939</i>	-	-
3	As above mixed with commercial hydrated lime in 2: 1 mix***	<i>3.500</i>	<i>5.303</i>	-	-

table continued on next page...

...continued

Unstabilised Rammed Earth:****					
1	532	0.301	0.456	0.619	0.196
2	622	0.312	0.473	0.631	0.196
3	712	0.692	1.048	0.885	0.221
4	802	1.201	1.819	1.125	0.237
5	433	0.307	0.465	0.647	0.184
6	523	0.350	0.530	0.654	0.205
7	613	0.344	0.521	0.655	0.200
8	703	0.466	0.706	0.721	0.224
9	424	0.525	0.795	0.775	0.219
10	514	0.287	0.435	0.583	0.211
Cement Stabilised Rammed Earth:****					
1	433 + 3% OPC	0.605	0.917	0.876	0.197
2	433 + 6% OPC	0.251	0.380	0.553	0.205
3	433 + 9% OPC	0.317	0.480	0.625	0.203
4	613 + 3% OPC	0.810	1.227	0.953	0.223
5	613 + 6% OPC	0.467	0.708	0.714	0.229
6	613 + 9% OPC	0.572	0.867	0.782	0.234
7	703 + 3% OPC	1.631	2.471	1.304	0.240
8	703 + 6% OPC	1.231	1.865	1.117	0.247
9	703 + 9% OPC	0.705	1.068	0.866	0.235
* Frost resistant to BS 3921					
** $S = s(\eta/T_s)^{0.5}$					
*** Values dependent on water content when mixed					
**** Values are derived using IRS 'wick' test					

Rammed earth generally has a very low sorptivity and is comparable (in many cases superior) to that of vibration-compacted C30 concrete. The rate of sorptivity in unstabilised rammed earth due to capillary suction is very low, ranging from 0.287 to 1.201 mm min^{-0.5} for the ten different mix recipes tested here. The range of sorptivity in cement-stabilised rammed earth is increased such that it varies from as low as 0.251 up to 1.631 mm min^{-0.5}, depending upon the mix recipe and the percentage of added cement. All of these values for rammed earth compare very favourably against fired clay bricks (0.704 to 2.720 mm min^{-0.5}), vibration-compacted C30 concrete (0.582 mm min^{-0.5}) and indeed natural stone (0.300 to 3.100 mm min^{-0.5}). A more direct, visual comparison between the range of sorptivity for rammed earth and conventional masonry materials has been illustrated by the 3-dimensional graph in Figure 93.

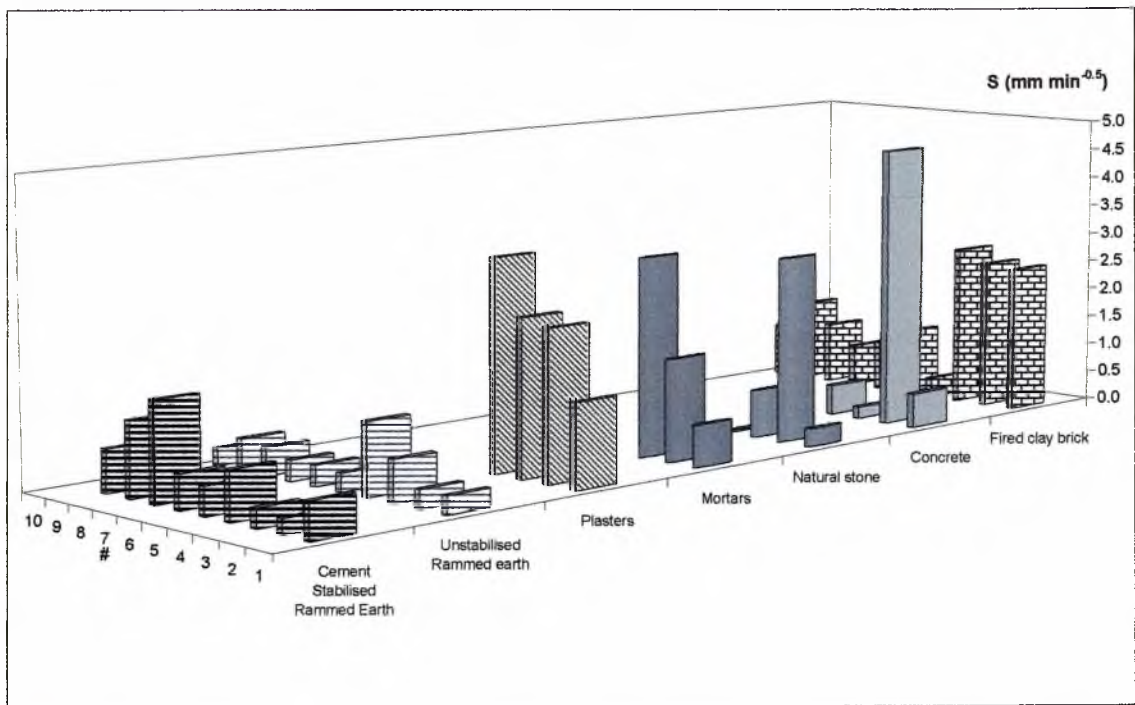


Figure 93 graphical illustration of the sorptivity (S) range for unstabilised rammed earth, cement-stabilised rammed earth and conventional masonry materials

In the case of unstabilised rammed earth, it is arguable that the key issue is not the amount of water that penetrates a wall, but the mere fact that the presence of moisture has the effect of lowering its compressive strength. However, the implications for rammed earth wall design are that if the maximum depth of water penetration that occurs for a given soil type can be quantified then this can be included in the structural design criteria. It is perhaps obvious that in developed countries such as Great Britain the level of performance that is expected from a modern building cannot normally be delivered by unstabilised rammed earth due to the climatic conditions.

For developing countries, the use of cement is often prohibitively expensive due to economic and political constraints. The correct use of cement stabilisation in rammed earth can eliminate the problem of slaking and compressive strength reduction due to moisture ingress. This occurs because the particle cohesion has been augmented by a structure of C-S-H that is not water-soluble. Direct applications for sorptivity (S) data

may relate to the minimum depth of cover required to protect electrical and plumbing conduits, and embedded steel reinforcement bar from moisture ingress and potential corrosion/safety issues.

7.2 MAXIMUM SURFACE INFLOW VELOCITY (u_o)

It has been observed during laboratory experiments that the surface finish of rammed earth appears to have a significant effect on the rate at which moisture ingress occurs. The porosity and texture of the surface of different mix recipes varied significantly from open-pored & coarse to smooth and hard. It would appear that the particle-size distribution of the rammed earth mix recipe is a significant controlling factor in determining the surface finish of rammed earth.

The maximum theoretical velocity of inflowing moisture at the surface of a specimen, that is absorbing water due to capillary suction, can be expressed as u_o (Gummerson *et al*, 1980). The value u_o decreases over time because an initially dry surface absorbs a larger volume of water per unit area (i) to begin with, and progressively less over time (t). Also, the gradient of the linear slope ($i/t^{0.5}$) represents the sorptivity (S), and so:

$$u_o = \frac{di}{dt} \quad \text{Equation 22}$$

The gradual decrease in u_o for capillary moisture ingress in different unstabilised rammed earth mix recipes has been illustrated by the graph in Figure 94.

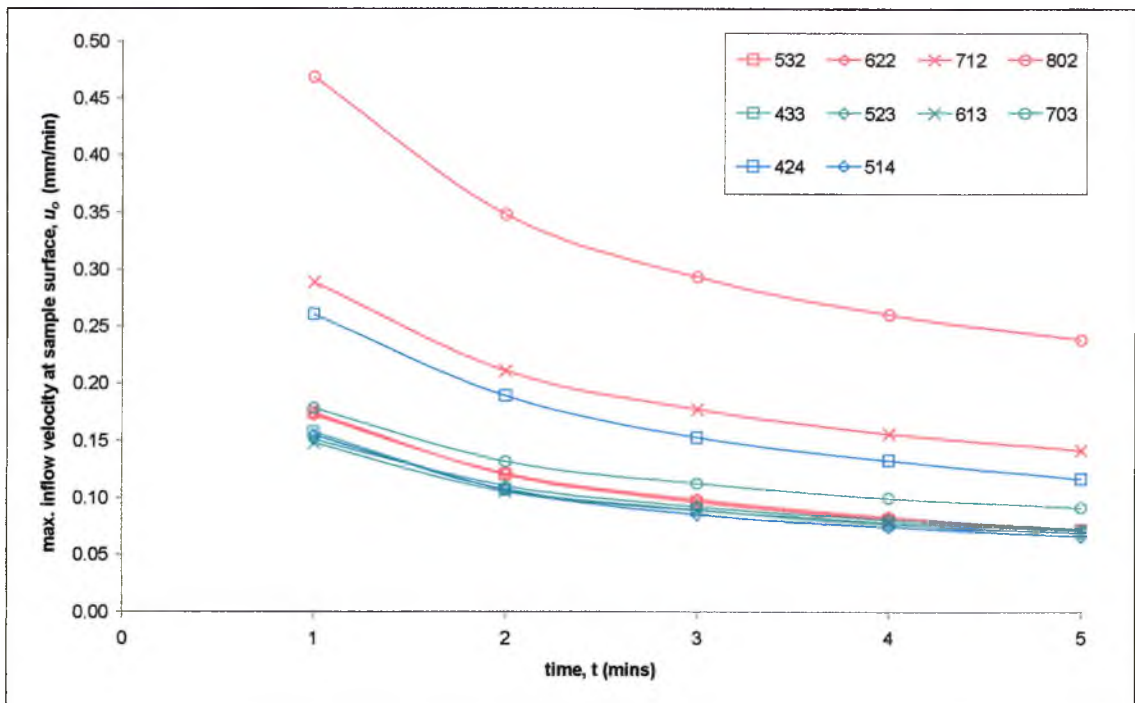


Figure 94 the surface inflow velocity (u_o) over elapsed time (t) for different unstabilised rammed earth mix recipes

The gradual decrease in surface inflow velocity (u_o) over time could be accounted for by the ‘overcoat’ effect. This occurs when the façade of a porous material effectively becomes waterlogged by the ingressing moisture and this can prevent further ingress. There appears to be a relationship between u_o and $t^{0.01}$, where the decrease in the maximum velocity of ingressing moisture (u_o) occurs linearly against $t^{0.01}$. This relationship has been illustrated by the graph in Figure 95.

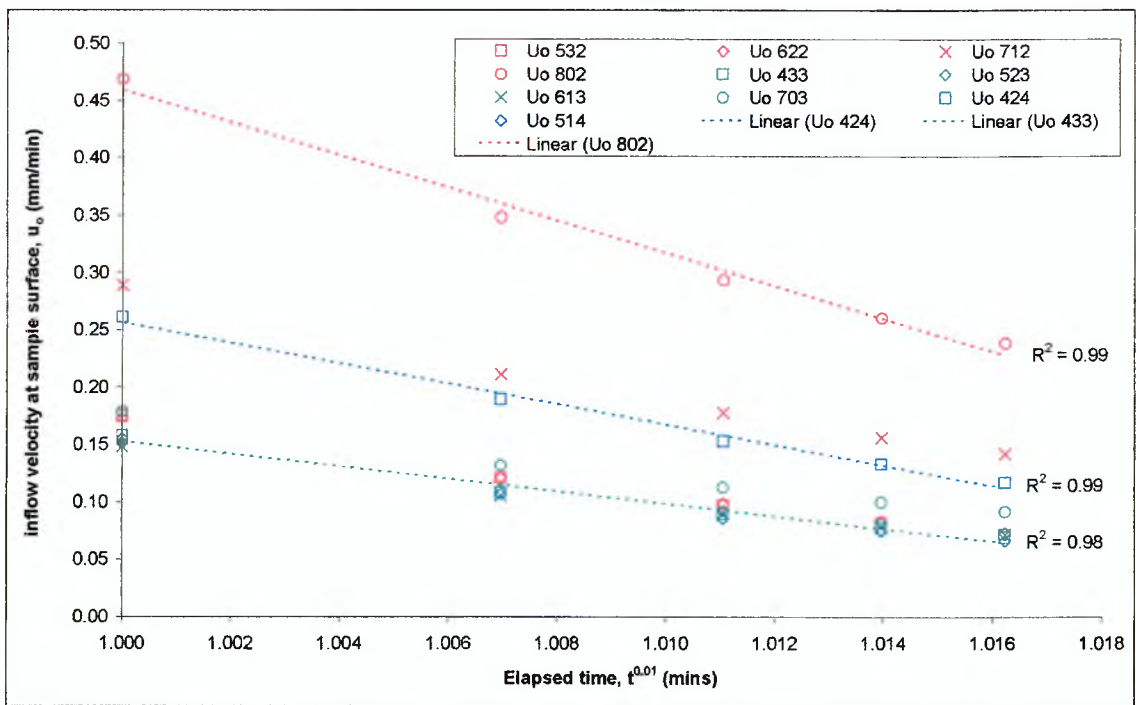


Figure 95 relationship between surface inflow velocity (u_o) and the hundredth root of elapsed time ($t^{0.01}$)

It may be possible for the gradient of the line $u_o/t^{0.01}$ to be used as a quantitative value for characterising the surface finish of a given rammed earth soil. This new value has been called the *surface receptiveness* (o), and it represents the receptiveness of the surface of rammed earth to the absorption of moisture through capillarity. The more receptive a surface is the greater will be its rate of decline in moisture inflow velocity (u_o). This is because a more receptive surface allows the internal pore structure to fill up more quickly.

A soil with a relatively high o (e.g. 802), for example, would have a receptive surface that permitted both a higher absorption rate (IRS) and a higher inflow velocity (u_o), but the rate at which water logging of the pore structure occurred would be increased and so the rate of decline in u_o is greater for these soils. A good relationship between o and r indicates that the size of the effective hydraulic pore radius of the material may be

responsible for the receptiveness of the surface to moisture ingress. This relationship has been illustrated by the graph in Figure 96.

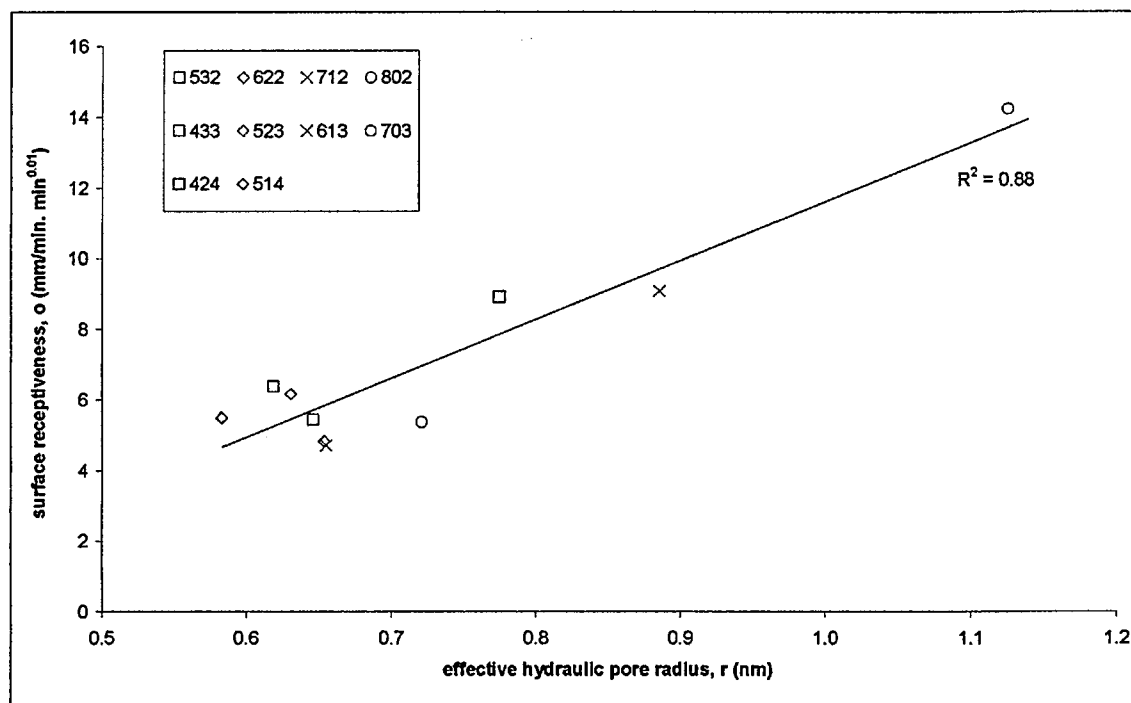


Figure 96 relationship between the effective hydraulic pore radius (r) and the surface receptiveness (o) of different unstabilised rammed earth mix recipes

We know that a soil with higher surface receptiveness (o) also has a higher IRS and u_o , and that both of these factors gradually decrease over time. The surface inflow velocity (u_o) decreases over time in tandem with the Initial Rate of Suction (IRS). This can be attributed to the ‘overcoat effect’ where the extent to which water can penetrate is reduced, essentially due to water logging of the façade pore structure.

The intrinsic sorptivity (s) of rammed earth has been calculated for each of the different soil types (see: Table 10) using equation 16. The physical properties of the imbibed liquid (water), such as surface tension (T_s) and viscosity (η), are assumed to be constant, where Sorptivity (S) depends on $(\eta/T_s)^{0.5}$ as discussed in Chapter 2 - Section 2.5.3. The

property s could perhaps be used to classify the internal pore structure of a rammed earth soil matrix. For comparison, a value of $2.1 \times 10^{-5} \text{ m}^{0.5}$ has been observed elsewhere for common fired clay bricks (Gummerson *et al*, 1980). The intrinsic sorptivity (s) values for rammed earth (see: Table 10) vary greatly according to soil type and range between 0.435 E^{-5} up to $1.819 \text{ E}^{-5} \text{ m}^{0.5}$.

7.3 SOIL GRADING OPTIMISATION THEORY

7.3.1 Total Specific Surface Area (SSA_t)

It has previously been shown that clay can bind other elementary soil particles together by forming a network of 'bridges' or connectors (see: Chapter 2 - Section 2.4.4). The author hypothesised that in a rammed earth soil, a ratio exists between the amount of clay and the SSA_t of the granular particle matrix that controls the extent of this 'bridging'. In relation to each other, for example, mix recipes with higher gravel content have a lower SSA_t , and conversely mix recipes that have more sand or fine sand have a higher SSA_t value.

From this, we can deduce that when the SSA_t of a soil increases, so must the number of points of contact between the granular soil particles. Therefore, in a rammed earth soil where the clay content is constant and known (e.g. xx3 mix recipe), if the SSA_t is increased then the number, type and effectiveness of clay bridges must decrease in relation to the granular particle matrix. This may leave more uninterrupted spaces between granular particles that could contribute towards increasing the permeability of the rammed earth. A simplified explanation of this theory has been provided by the diagrams in Figure 97.

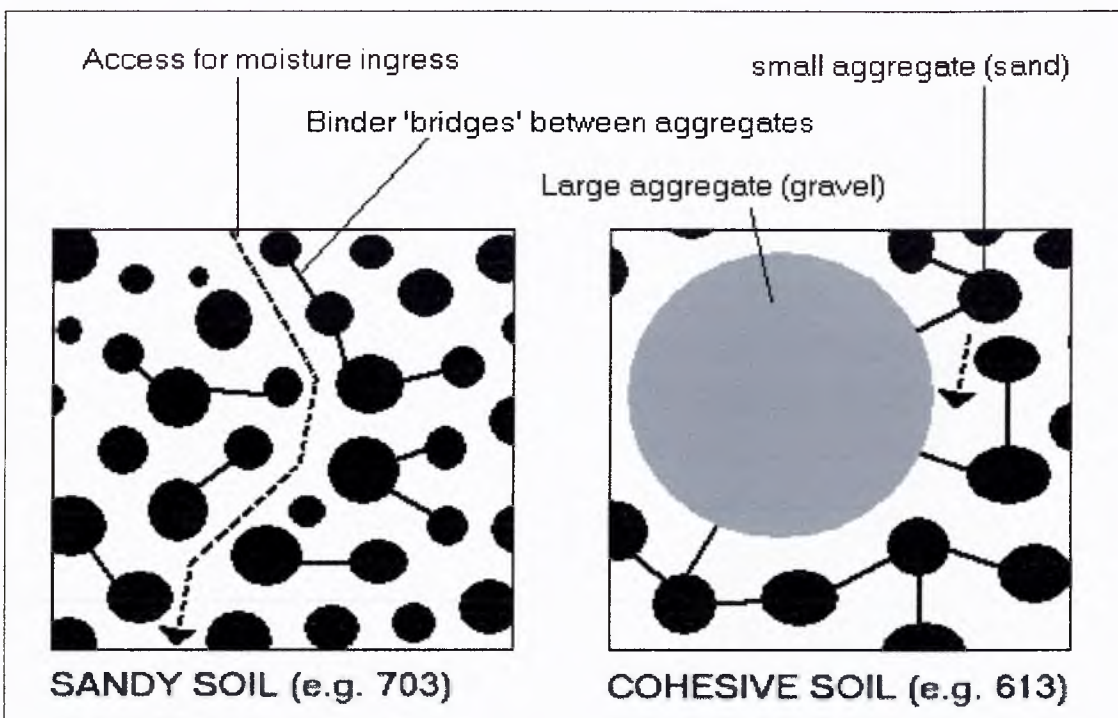


Figure 97 a graphic illustration of the total Specific Surface Area (SSA) to clay ratio theory

For the simplified examples in Figure 97, both soil mix recipes contain an identical quantity of clay which is hypothetically represented here by them having ten clay ‘bridges’ each. These clay bridges have been distributed randomly throughout the granular particle matrix. Note that the permeability of the more cohesive rammed earth mix (613) is significantly lower in comparison to the sandy soil recipe (703) due to a more effective blocking of pore spaces by the clay bridges. Quite simply, when there are a fewer number of gaps to bridge the same amount of clay has a greater effect in blocking pore spaces.

7.3.2 The 3.35 Ratio

In support of the theory in the previous section, Figure 98 and Figure 99 show an increase in average IRS value coinciding with a relative increase in the mass of particles with diameters $\leq 3.35\text{mm}$, but with a sharp decrease in the mass of particles with diameter $> 3.35\text{mm}$. This appears to indicate that, conversely, an increase in the number

of particles with a diameter $>3.35\text{mm}$ (i.e. small gravel and upwards) can give a sufficient decrease in SSA_t , such that the effectiveness of the clay is enhanced and the level of permeability is reduced.

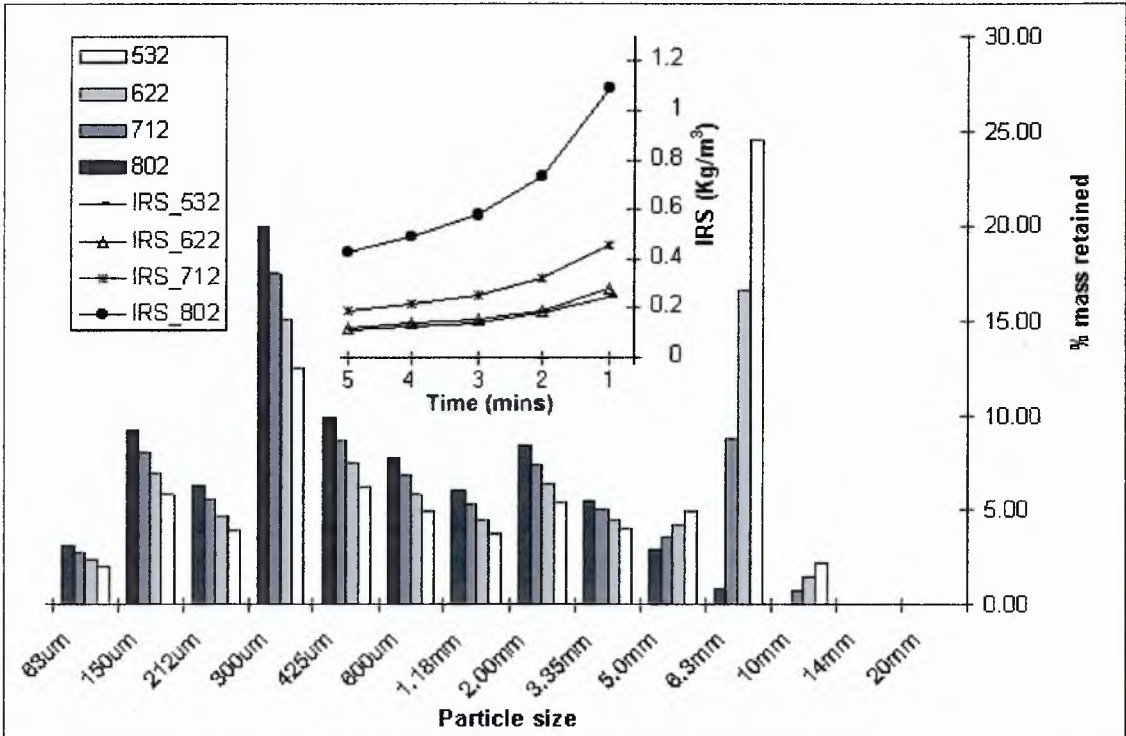


Figure 98 relationship between particle-size mass retained and the average IRS value for different unstabilised rammed earth mix recipes with a CC of 0.066 (2 parts silty clay)

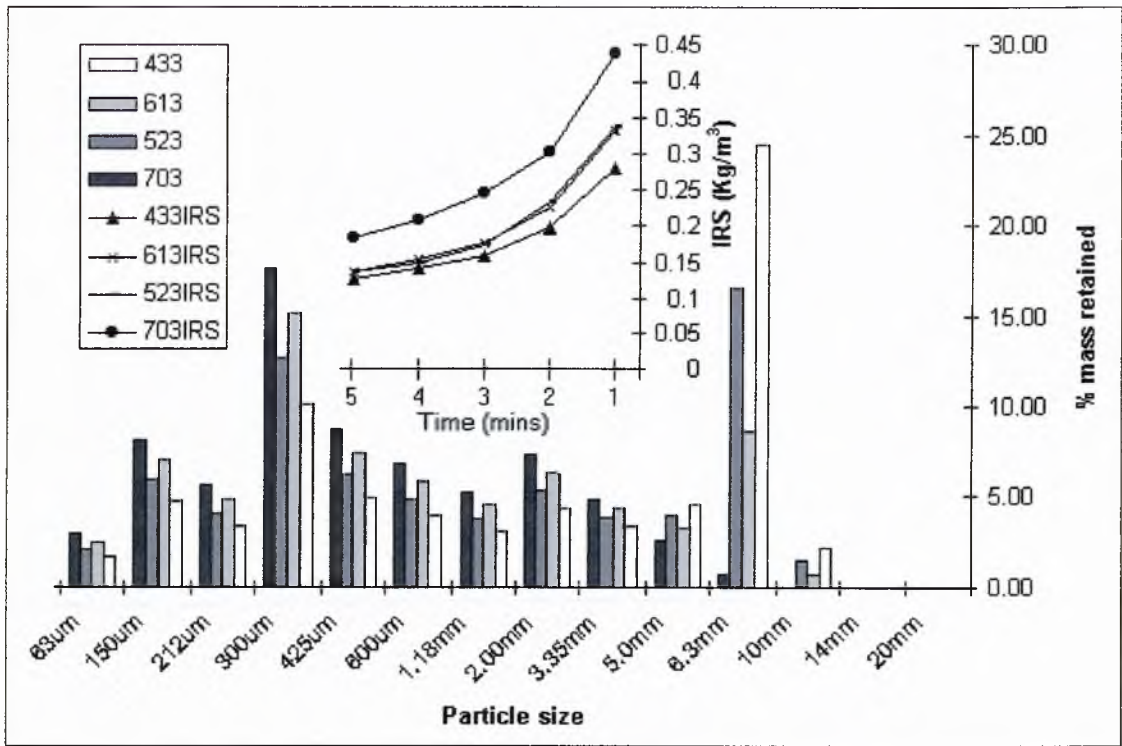


Figure 99 relationship between particle-size mass retained and the average IRS value for different unstabilised rammed earth mix recipes with a CC of 0.099 (3 parts silty clay)

Although normally we use sieve analysis to define either the percentage passing or the percentage retained for a given particle-size, here we consider the introduction of a ratio value. The ratio between the total mass retained above 3.35mm diameter divided by the total mass retained at & below 3.35mm is calculated to provide the ‘3.35 ratio’ value for a given rammed earth soil. It can be observed from Figure 100 that when the ‘3.35 ratio’ is greater than 5, the amount of water imbibed due to capillary suction increases to significant levels.

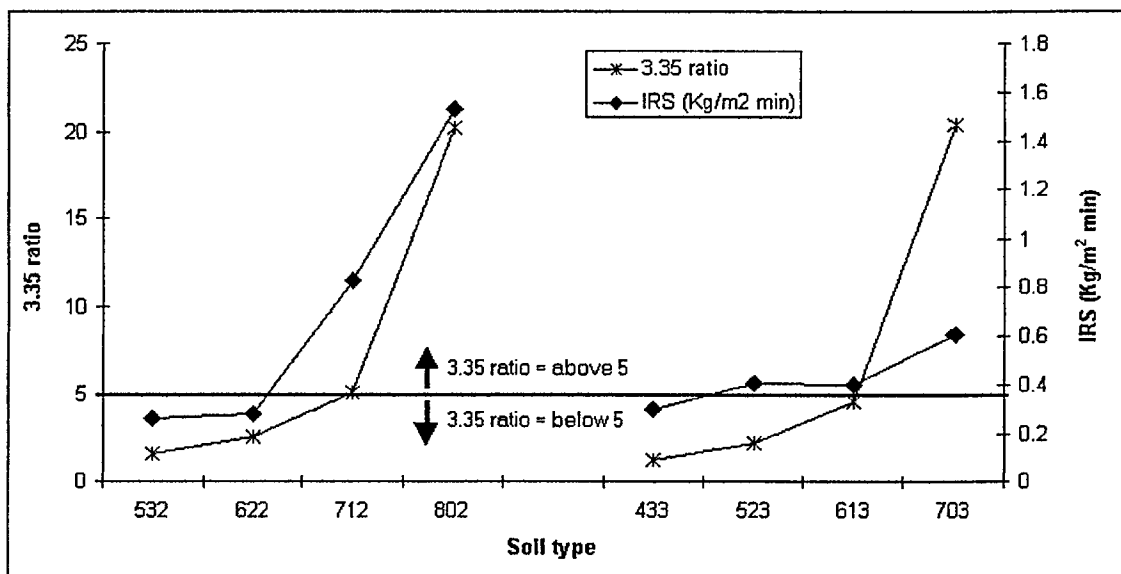


Figure 100 relationship between the IRS value and the 3.35 ratio for unstabilised rammed earth mix recipes

It may not ultimately be possible, however, to predict the moisture ingress performance of a soil based upon its particle grading due to the vast number of other variables and the ways that these can interact with one another. A more logical approach would be to determine the sorptivity (S) of a soil through experimentation and to understand the ways in which this property can be manipulated through making certain changes in the soil grading. The results from this study show that one possible way of achieving this would be to attain a 3.35 ratio of less than 5 through granular stabilisation. In the design of a building, for example, the moisture ingress of an exposed rammed earth wall could be optimised in order to reduce/eliminate the need for chemical admixtures or surface treatments.

In order to test this hypothesis for the 3.35 ratio, further experimental work was conducted via final year undergraduate projects, under the supervision of the author, using the three poorer soil mix recipes: 703, 712, and 802. A series of stabilised rammed earth (6% cement) cube samples were produced by Craven T (2004) and Turner J (2004) using the established methods and procedures detailed in Chapter 3 -

Section 3.2. Each mix recipe was produced and tested both in standard form and in modified form, which included granular stabilisation of the mix design. The modifications applied to each mix recipe have been summarised in Table 11. For each of the three mix recipes tested here this involved the addition of 10mm pea gravel, calculated as a percentage of the total dry mass of the soil, which resulted in lowering the 3.35 ratio to a value below 5.

Table 11 granular stabilisation of high moisture ingress mix recipes

Mix recipe	No. of samples	Granular stabilisation	3.35 ratio	ρ_d (kg/m ³)	f'_{cu} @ 28-days
703	8	No	20.4	2051.6	2.70
7M3	8	Yes +11% gravel	4.8	2131.0	2.33
712	8	No	5.1	2138.4	4.57
7M2	8	Yes +1% gravel	4.8	2151.4	3.80
802	8	No	20.3	2108.7	3.63
8M2	8	Yes +12% gravel	4.9	2148.9	2.95

During the first phase of testing, the samples were tested by Craven (2004) for capillary moisture ingress using the 5-minute IRS ‘wick’ test defined previously (see: Chapter 4). The volume of absorbed water per unit inflow surface area (i) was again found to increase linearly against the square root of elapsed time ($t^{0.5}$). The gradient of the straight-line $i/t^{0.5}$ was used to calculate a single value for the Sorptivity (S). The results of the tests clearly show that by lowering the 3.35 ratio to below 5, the rate of moisture ingress due to capillary suction (i.e. the sorptivity) is significantly lowered (see: Figure 101). This optimisation of the 3.35 ratio is quite simply a controlled reduction of the SSA/CC ratio. Therefore, the reduction in moisture ingress appears to be caused by an effective increase in the number and extent of clay bridges that form between granular soil particles.

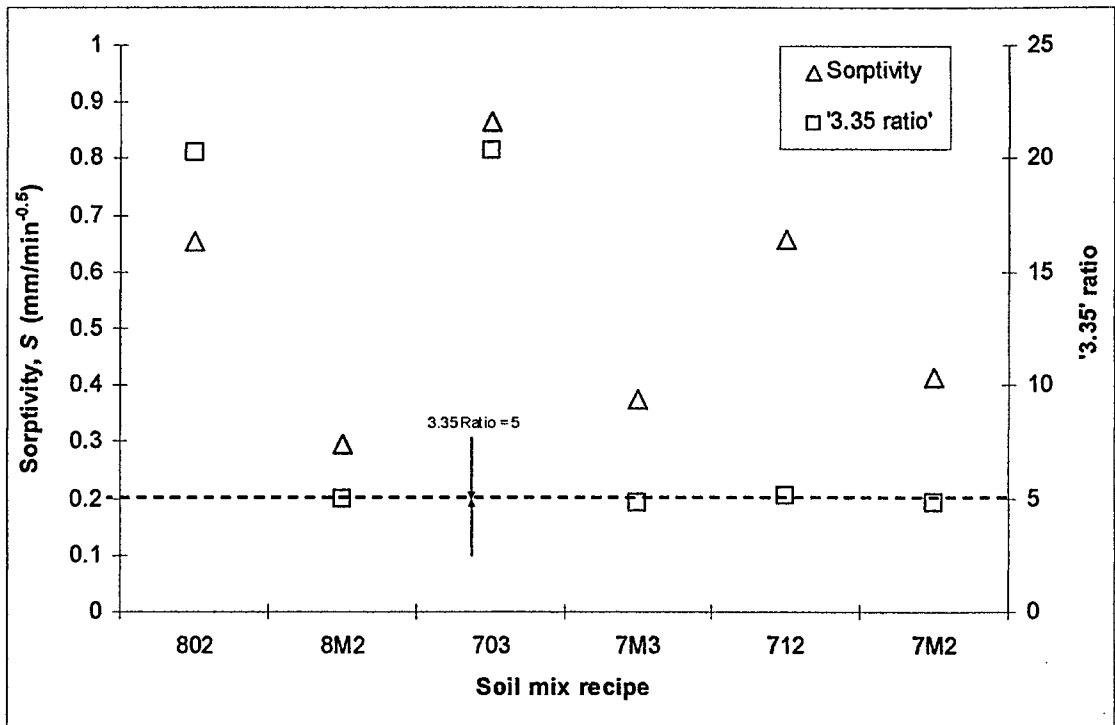


Figure 101 the relationship between 3.35 ratio and Sorptivity (S) both for poor rammed earth mix recipes and for the same recipes but with granular stabilisation enhancement

The second phase of testing was conducted by Turner (2004) following the test methodology for measuring the rate of moisture dissipation due to the effects of natural drying under laboratory conditions (see: Chapter 4 - Section 4.1.2.2). The decrease in moisture content due to evaporation (referred to here as ‘dissipation’) occurred linearly against elapsed time (t) during the 2-hour test procedure. In order to compare the moisture dissipation characteristics of one mix recipe with another, the results for mass loss were expressed as percentage moisture retention calculated in relation to the initial m_w recorded at the beginning of the drying period (see: Figure 102).

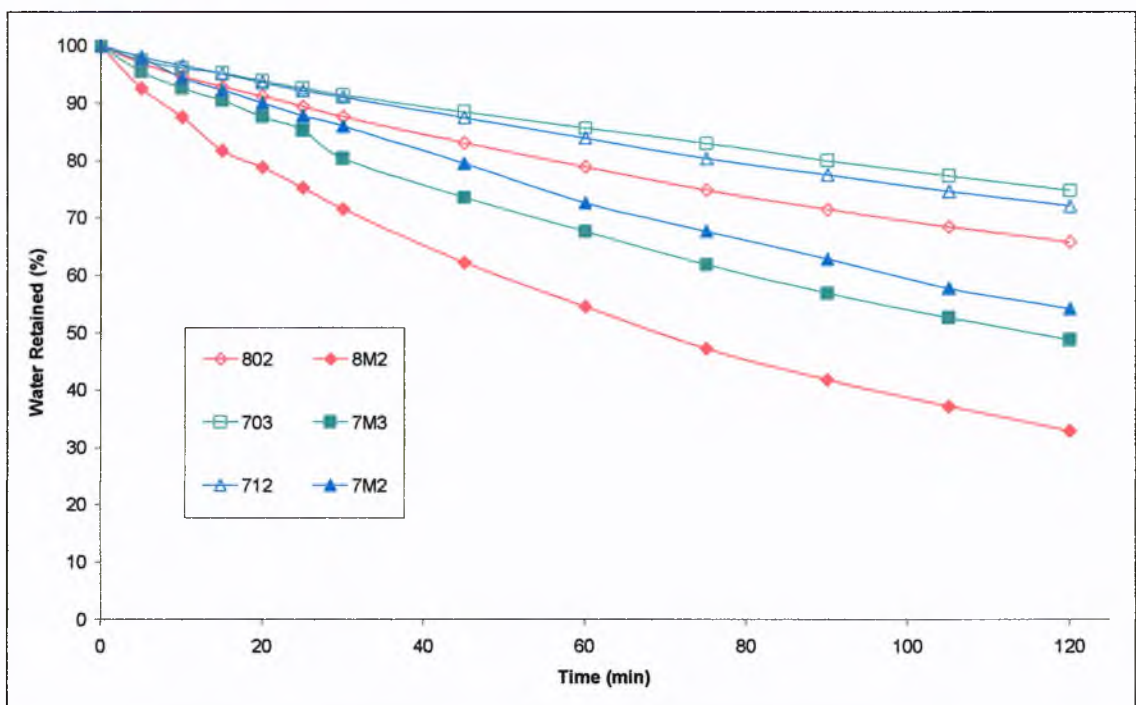


Figure 102 percentage water retained against elapsed time for both poor and modified mix recipes

The graph in Figure 102 clearly shows that when damp, stabilised rammed earth is allowed to air-dry naturally, the decrease in % water retention occurs linearly against elapsed time (t). In addition, each of the modified mix recipes exhibited significantly less moisture retention than their corresponding original mix recipe, i.e. 8M2 has less moisture retention than 802, etc. That is to say, by achieving a 3.35 ratio of less than 5 each of the three modified mix recipes has both significantly reduced capillary moisture absorption and significantly enhanced moisture dissipation through natural drying.

The enhanced level of moisture dissipation in modified mix recipes could be related to the decrease in total specific surface area (SSA_t) achieved through granular stabilisation (see: Section 7.3.1). The reduction in SSA_t may result in the absorbed water having less contact with the surfaces of soil particles causing an effective reduction in the attractive forces of surface tension between them. In simple terms, because there is less surface area to hold on to, the water has less ability to resist dissipation. It would therefore appear that a rammed earth mix recipe could be modified through granular stabilisation

to achieve a 3.35 ratio of less than 5 in order to become optimised for use in a damp climate; resisting absorption and promoting dissipation.

7.3.3 The Effective Hydraulic Pore Radius (r)

A decrease in the ratio between SSA_f/CC appears to have the overall effect of reducing non-saturated moisture ingress in rammed earth. Current theory suggests that this decrease in the permeability of both the intra-elemental and assemblage pores may be due to a reduction in their effective diameter due to the increased presence of clay ‘bridges’ inside the granular particle matrix (refer Equation 17 Section 2.5.3). We can begin to test the validity of this theory by examining the relationship between the sorptivity (S) and the volume fraction porosity (f) of the soil, as illustrated by the graph in Figure 103.

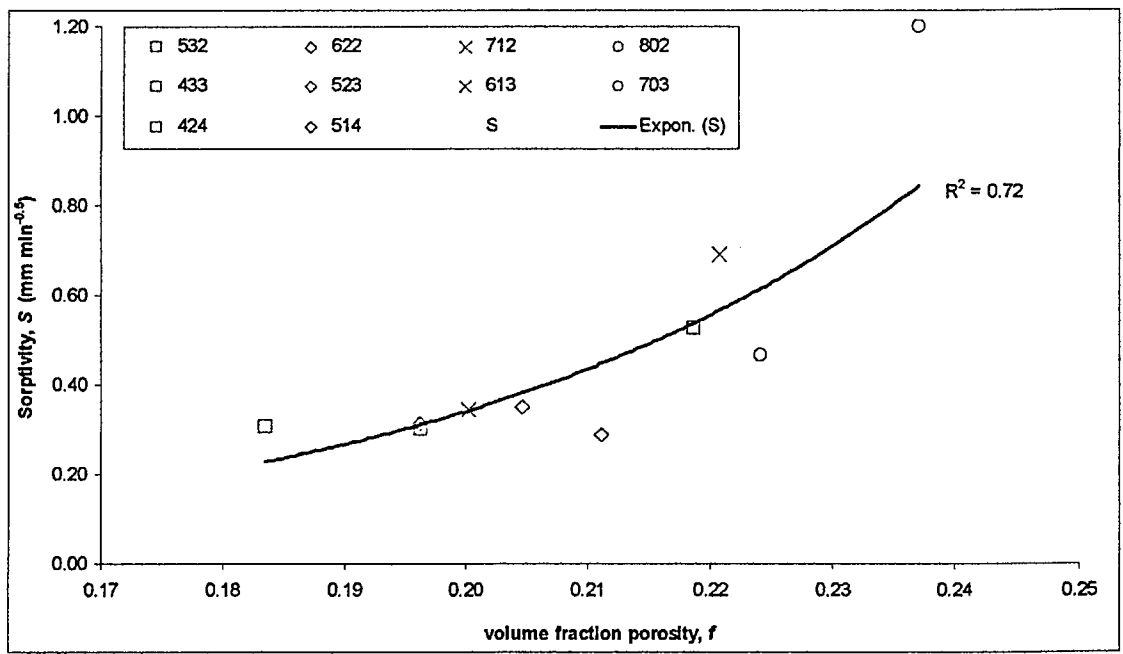


Figure 103 exponential relationship between S and f for unstabilised rammed earth mix recipes

The graph in Figure 103 appears to show some relationship between S and f for different soil mix recipes. This indicates that there is a degree of similarity between the volume fraction porosity (f) and the apparent porosity (f_{ap}). We know that many inter-elemental pore spaces occur between granular soil particles, and that these are most likely affected by particle-size distribution and the efficiency of particle packing. This may explain some similarity of variation in f and f_{ap} for the soil mix recipes used here, since their particle-size distributions are accurately varied and controlled.

However, the measure of f in itself gives no information about the tortuosity or diameter of the pores in a soil, but these are the primary factors in determining capillary potential and the coefficient of permeability. It is thought that these properties may be greatly influenced by variations in the SSA_t/CC ratio, and therefore control the sorptivity (S). We can therefore combine the volume fraction porosity (f) with the sorptivity (S) of the material to calculate an effective hydraulic pore radius (r), (refer: Chapter 2 - Section 2.5 3).

The effective hydraulic pore radius (r) for the microstructure of unstabilised rammed earth mix recipes ranged between 0.583 to 1.304 nm. In the cement stabilised rammed earth mix recipes r ranged between 0.553 and 1.304 nm (see: Table 10). Comparatively, a typical value of 1.5 nm for the effective hydraulic pore radius (r) in fired clay bricks was observed by Gummerson *et al* (1980). All of these values are generally very small and tend to indicate a high level of tortuosity and constriction in the pore structure such that moisture ingress is severely impeded. A small change in r appears to be capable of significantly altering the sorptivity (S) of different rammed earth mix recipes, both in relation to one another and in relation to conventional masonry materials.

In calculating r we may theoretically quantify the observed reduction in sorptivity (S) caused by the formation of clay bridges between the granular particles of the soil structure (refer Equation 17 Section 2.5.3). In support of this, there is a strong linear relationship between the effective hydraulic pore radius (r) and the sorptivity (S) of a given mix recipe, as illustrated by Figure 104.

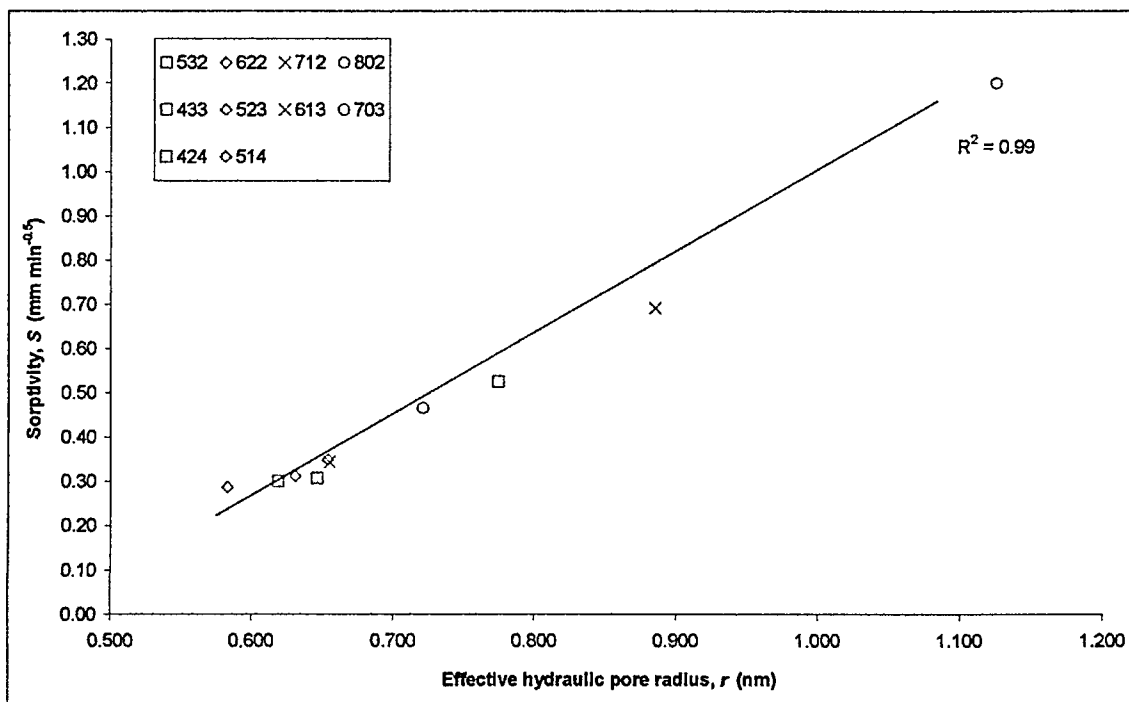


Figure 104 relationship between the effective hydraulic pore radius (r) and sorptivity (S) for unstabilised rammed earth mix recipes

We can conclude that the effective hydraulic pore radius r of a mix recipe can be manipulated by altering both the soil particle-size distribution and the SSA/CC ratio. With respect to the rammed earth mix recipes used for this study, if the value of r is less than 0.65nm then the sorptivity can be classified as ‘low’. These samples had a sorptivity (S) that was significantly lower than that of vibration-compacted C30 concrete. If the value of r is between 0.65nm and 0.7nm then the sorptivity can be classified as ‘medium’ and is approximately the equivalent to that of vibration-

compacted C30 concrete. If the value of r is greater than 0.7nm then the sorptivity can be classed as ‘high’ and is equal to or greater than that of medium/high porosity fired clay bricks. These classifications are useful for comparing rammed earth with conventional masonry materials that are generally more familiar to most people.

There is also a good relationship between S and r for cement stabilised rammed earth soils, as illustrated by the graph in Figure 105.

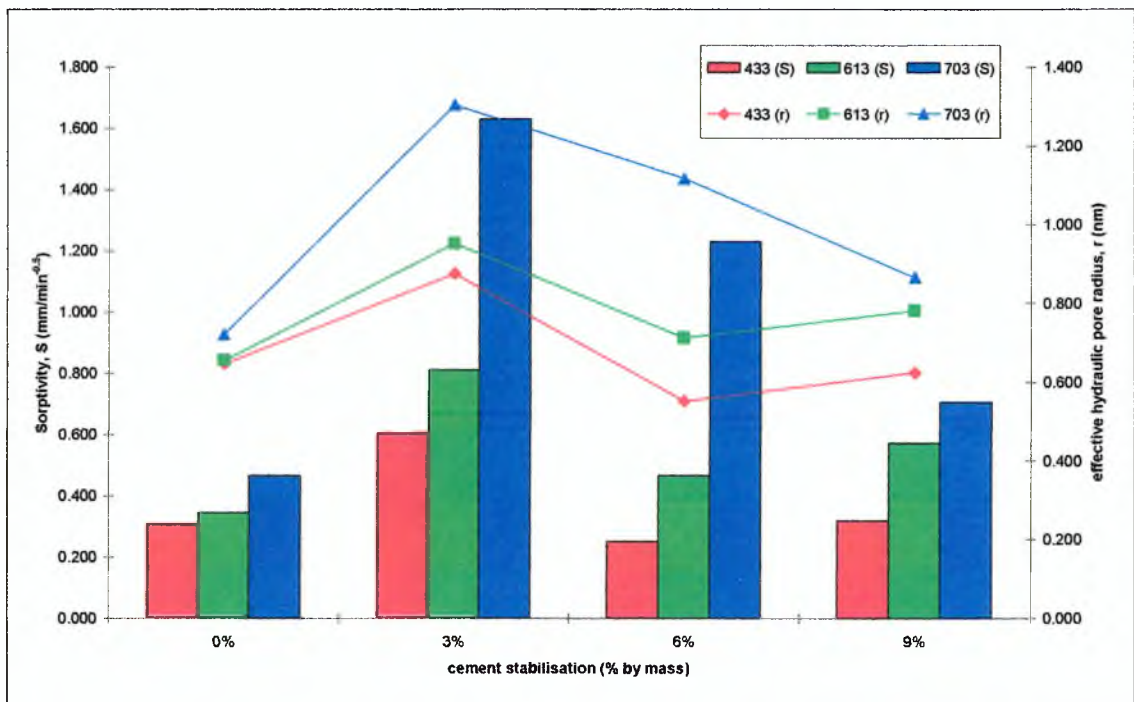


Figure 105 relationship between sorptivity (S) and the effective hydraulic pore radius (r) for different stabilised rammed earth mix recipes using varying amounts of cement

The effect of adding cement to a rammed earth mix recipe appears to be alteration in the effective hydraulic pore radius (r) of the soil pore structure. Adding 3% cement (by mass) appears to significantly increase the sorptivity (S) of all three mix recipes. Apparently, this is linked to a similarly proportionate increase in the effective hydraulic pore radius (r) of each mix recipe. The increase in r may be due to the dispersing effect

that lime/cement has on the cohesive particle matrices of some soils. This could lead to the formation of a more open-pored structure perhaps due to increased porosity in and around the clay-rich particle assemblages.

Further increases in cement content appear to have the effect of lowering the sorptivity (S) in each of the three mix recipes. It appears that the optimum cement content is 6% for the mix recipe that had an unstabilised r that is classed as low (i.e. low- r mixes), where $r < 0.65\text{nm}$, e.g. 433 mix. On low- r mixes, the S is slightly reduced when at optimum cement dosage. The optimum cement content for the medium- r mix (613), where $r = 0.65 - 0.70\text{nm}$, also appears to be 6%. On medium- r mixes, the S is slightly increased when at optimum cement content. The high- r mix (703), where $r > 0.70$, appeared to require around 9% cement in order to lower its sorptivity. On high- r mixes, the addition of cement always gives significantly increased S even at optimum percentage.

The application of cement stabilisation makes rammed earth a viable alternative masonry material for the damp UK climate because it prevents the wall from washing away in the rain and losing cohesion when it gets damp. In terms of non-saturated moisture ingress, the addition of cement can make a good soil better or a poor soil worse – the key is to optimise the soil grading.

There appears to be a strong linear relationship between the Sorptivity (S) of rammed earth and the surface receptiveness (ρ) as shown in Figure 106.

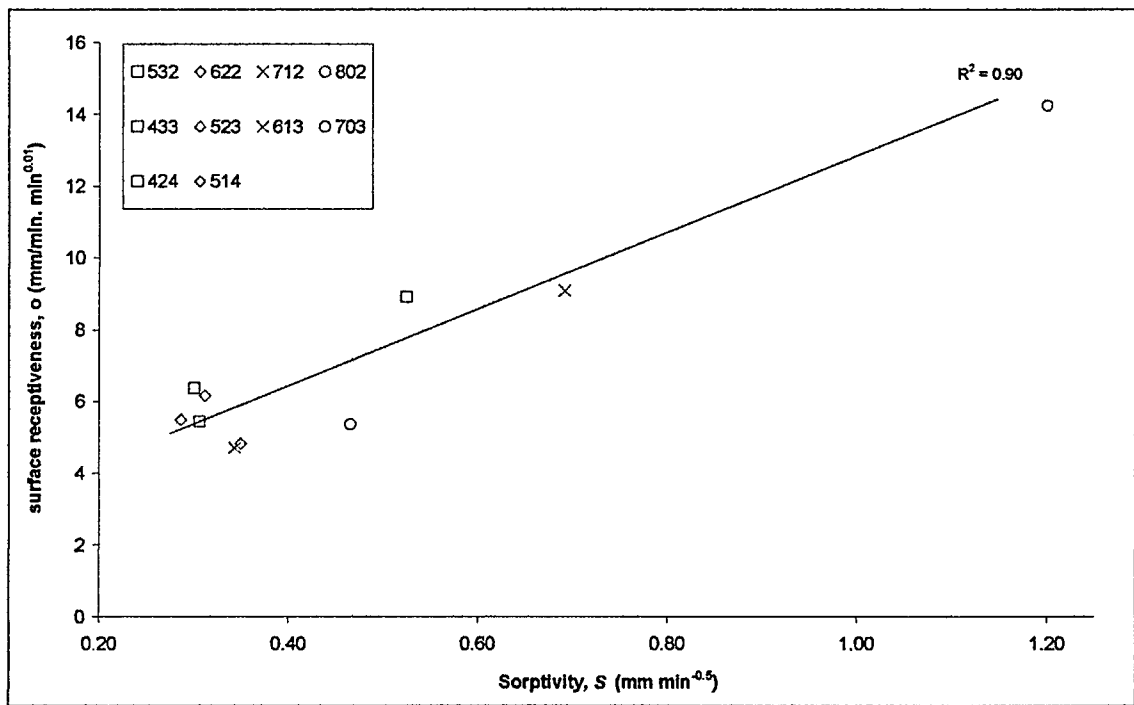


Figure 106 relationship between Sorptivity (S) and surface receptiveness (o) for unstabilised rammed earth mix recipes

This relationship appears to indicate that the receptiveness of a rammed earth surface to moisture ingress is simply related to its potential for capillary moisture ingress. This may explain why the rammed earth test walls in the climate simulation chamber displayed universally low water absorption. Since the source of moisture (i.e. surface run-off) was dynamic as opposed to static (e.g. IRS & ISA tests) the capillary suction of the rammed earth appeared to be less effective. This may be because the kinetic energy of the moving water was acting against the forces of capillary suction of the rammed earth. This would also explain the lack of discernible variation in moisture absorption between the three soil mix recipes despite their contrasting Sorptivity values.

7.4 SUMMARY

Capillary moisture ingress in rammed earth obeys the extended Darcy equation for non-saturated moisture ingress and so the slope of $i/t^{0.5}$ can be used to determine the

sorptivity (S). The surface inflow velocity (u_o) of capillary moisture ingress decreases linearly against $t^{0.01}$. The gradient of $u_o/t^{0.01}$ can be used to provide a value for the surface receptiveness (o), which describes and quantifies the surface finish of the material. The surface receptiveness (o) is positively related to the effective hydraulic pore radius (r) of the soil. When r is increased, the sorptivity (S) and surface receptiveness (o) also increase, but the rate of decline in S becomes greater due to water logging of the façade, i.e. the 'overcoat' effect.

In soils that predominantly contain granular material the majority of f is represented by the pore spaces that occur around the points of contact between elementary granular particles. Consequently the size and number of these pore spaces are determined by the particle-size distribution of the soil. However, rammed earth soils typically contain between 5 and 15% clay (i.e. $CC = 0.05$ to 0.1) and the formation of clay bridges between granular particles can alter the tortuosity and geometry of the pore structure. The pore structure of soils is dictated by the interactions between elementary particles and particle assemblages. Knowing the volume fraction porosity does not give information about the nature of the pore structure such as degree of tortuosity and pore diameters. An increase in tortuosity can significantly impede the flow of water in a vessel, whilst pore diameter controls the capillary potential and maximum volume of flow.

There is a relationship between f and S , the disparity in which appears to relate to the SSA/CC ratio of the mix recipe. The relationship can be used to calculate the effective hydraulic pore radius (r) of the soil (refer Equation 17 Section 2.5.3), which quantifies the pore structure including the effects of clay bridging. For the rammed earth mix

recipes tested in this project, r is typically very small which indicates high levels of constriction and tortuosity that exist within the pore structure. In support of these findings, a positive relationship also exists between the SSA/CC ratio and the sorptivity (S) of a mix recipe. One method for attenuating the SSA/CC ratio is to manipulate the ratio between the total mass of granular material above 3.35mm diameter, to the mass of equal to and below 3.35mm diameter – defined as the 3.35 ratio. This can be achieved in practical terms through the addition/subtraction of granular material in the mix recipe. When the 3.35 ratio is 5 or less, and the clay content is approximately 0.1, the mix recipe appears to be optimised for low sorptivity (S).

The addition of approximately 3% cement has the effect of significantly increasing sorptivity in both high- r and low- r mix recipes. This may be due to dispersal of the clay particles giving a more open-pored structure since r also increases. Generally, the further addition of cement above 3% has the effect of decreasing S and r ; this is possibly due to an increase in the presence of C-S-H. The addition of around 6% cement appears to optimise the S of low- r mix recipes and reduce it below the original value. In high- r mix recipes, the addition of up to 9% cement lowers the S but it remains at a level higher than the original value.

8.0 CONCLUSIONS & FUTURE WORK

8.1 OUTCOMES OF THE STUDY

The outcomes of this research project have been the production of a significant amount of experimental data, analysis and application of current theories. The overall conclusions that have been drawn from these outcomes have been discussed in the following three sub-sections.

- **A comprehensive understanding of the theories and factors affecting capillary and static pressure-driven moisture ingress in rammed earth materials**

The factors affecting capillary rise of moisture in rammed earth were not previously well known but can be a big problem for both new and historic buildings. The IRS ‘wick’ test is a suitable methodology for testing the rate of capillary suction in standard rammed earth cube samples. The internal pore structure of rammed earth appears to behave similarly to that of vibration-compacted concrete and a positive relationship exists between the IRS and the volume fraction porosity (f). The mass of absorbed water (m_w) increases linearly against the square root of elapsed time ($t^{0.5}$) in both unstabilised and stabilised rammed earth. Capillary ingress in rammed earth obeys the extended Darcy equation so the slope of $i/t^{0.5}$ can be used to determine the sorptivity (S). The relationship between S and f can be used to calculate the effective hydraulic pore radius (r) of the soil. This effectively quantifies the geometry and tortuosity of the pore structure including the effects of clay bridging. The r of rammed earth is typically very small which indicates high levels of constriction and tortuosity within the pore structure.

The surface inflow velocity (u_o) of capillary moisture ingress decreases linearly against $t^{0.01}$. The gradient of $u_o/t^{0.01}$ can be used to provide a value for the surface receptiveness (o), which effectively describes and quantifies the surface finish of the material. The surface receptiveness (o) is positively related to the effective hydraulic pore radius (r) of the soil. When r is increased, the sorptivity (S) and surface receptiveness (o) also increase, but the rate of decline in S becomes greater due to a more rapid water logging of the façade, i.e. the 'overcoat' effect.

- **Gaining an understanding of how to manipulate the soil grading parameters in rammed earth mix recipes in order to optimise moisture ingress resistance**

Waterproofing admixtures are expensive, difficult to mix thoroughly, are sometimes only partially effective, and are not supplied with a warranty. A correctly graded soil mix recipe can make the IRS and ISA for rammed earth significantly exceed that of vibration-compacted C30 concrete. Understanding how altering the clay content, particle-size distribution, or the SSA/CC ratio of a rammed earth mix can affect its moisture ingress performance is therefore of great practical importance. A standard procedure for blending graded quarry materials can be used to produce a variety of rammed earth soil mix recipes with accurately controlled particle-size distribution.

Knowing the volume fraction porosity (f) of a mix does not give any information about the nature of the pore structure such as the degree of tortuosity and pore diameters. A positive relationship exists between the SSA/CC ratio and the sorptivity (S) of a mix recipe. The increase in disparity between S and f appears to follow a relative decrease in the SSA/CC ratio of a mix recipe. One method for attenuating the SSA/CC ratio is to manipulate the ratio between the total mass of granular material above 3.35mm

diameter, to the mass of that below 3.35mm diameter – defined as the 3.35 ratio. This can be achieved in practical terms through the addition/subtraction of granular material in the mix recipe. When the 3.35 ratio is 5 or less, and the clay content is approximately 0.1, the mix recipe appears to be optimised for low sorptivity (S). The effective hydraulic pore radius r of a mix recipe is effectively manipulated by altering both the soil particle-size distribution and the SSA_d/CC ratio. If r is less than 0.65nm then S can be classified as ‘low’, if it is between 0.65nm and 0.7nm then S can be classified as ‘medium’, and if r is greater than 0.7nm then S can be classed as ‘high’.

The addition of approximately 3% cement has the effect of significantly increasing S in both high- r and low- r mix recipes. This may be due to dispersal of the clay particles giving a more open-pored structure since r also increases. Generally, the further addition of cement above 3% has the effect of decreasing S and r ; this is possibly due to an increase in the presence of C-S-H. The addition of around 6% cement appears to optimise the S of low- r mix recipes and reduce it below the original value. In high- r mix recipes, the addition of up to 9% cement lowers the S but it remains at a level higher than the original value.

- **Gaining a detailed understanding of the mechanics of moisture ingress in rammed earth walls when derived from different sources of exposure**

The mechanisms of moisture ingress in rammed earth can provide different outcomes depending on the nature of the water source. This is illustrated, for example, by the difference between water raining down on a wall, and water being wicked up from the bottom. The ISA of rammed earth does not obey the $t^{0.5}$ law because the effect of a pressure differential permits an accelerated rate of moisture ingress over that of

capillary suction. The climatic simulation of pressure-driven rainfall applied to stabilised rammed earth walls gives an ISA that is virtually the same for high- r and low- r mix recipes and is generally lower than that of cube samples made from the same material. The test walls should have different values for o and r , indicating that the kinetic energy of a dynamic moisture source (i.e. rainfall run-off) is greater than the combined effort of sorptivity and pressure differential. Water that is wicked up through the base of rammed earth walls can be described by the sorptivity (S) of the material, which is controlled by the effective hydraulic pore radius (r). For water that rains down on to the face of walls the motivational force of pressure differential is very great, but the absorption of rainfall run-off is very low. To summarise, rainfall penetration in rammed earth may not be a problem in most cases but capillary ingress through basal dampness or leaking water goods could be.

8.2 RECOMMENDATIONS FOR FURTHER RESEARCH

The potential for research in rammed earth construction is considerable because it is still considered an emerging field within the context of both civil engineering and building science. It is a highly topical and pertinent field of research as it relates to an alternative, sustainable building material that is currently enjoying a renaissance period throughout many of the developed countries across the world.

Following the completion of this research project, a number of avenues for further research have arisen, and these have generally been referred to in the main text of the thesis. However, the two areas of further research that are detailed in the sections below are considered to be of particular relevance and are most worthy of future study.

8.2.1 Thermal Performance of Rammed Earth Materials

The focus of this research project, in terms of materials properties, is the process of moisture transfer. The next logical step is to investigate the thermal properties of rammed earth materials made from different mix recipes and determine the variables that can control these properties. During this study, initial data from the climate simulation chamber appears to suggest that the thermal conductivity of rammed earth walls is relatively high, which supports recent research findings by CSIRO. An understanding of the heat and moisture transfer properties of rammed earth walls made from different mix recipes would arise from combining further research in this area with the existing findings of this project.

8.2.2 SEM Analysis of the Pore Structure in Rammed Earth Materials

Using Scanning Electron Microscopy (SEM) to examine the microstructure of rammed earth materials would be a new area of research that could yield a much greater understanding of moisture ingress phenomena. By looking inside the pore structure of rammed earth materials quantitative evidence could be gathered in relation to pore diameters and tortuosity. This could then be compared with the analytical work in this thesis relating to the effective hydraulic pore radius (r) of different mix recipes, and comparing the actual differences between the microstructures of low- r and high- r mixes. Analysis should be directed towards studying the differences in the pore structure in terms of types and amounts of clay bridging and any other factors that may control pore diameters or tortuosity.

REFERENCES

- asEg, 2003, *New Earth Structures*, [brochure] available: Affiliated Stabilised Earth Group, PO BOX 161, North Fremantle, 6159, Australia
- Barnes GE, 2000, *Soil Mechanics: Principles and Practice – Second Edition*, Macmillan Press Ltd., Basingstoke, UK
- Bleaklow, 2003, *Bleaklow slaked lime products*, [brochure] available: Bleaklow Industries Ltd, Hassop Av, Hassop, Bakewell, Derbyshire
- Bowles JE, 1984, *Physical and Geotechnical Properties of Soils – second edition*, McGraw-Hill International Book Company Ltd., Tokyo, Japan
- BRE, 1983, *Digest 269 - The Selection of Natural Building Stone*, Building Research Establishment, HMSO, London, pp.1-8
- Bryan AJ, 1988, “Soil/Cement as a Walling Material - II: Some Measures of Durability”, *Building and Environment* 23[4] pp.331-336
- BSI, 2000, *BS EN 772-16: 2000 Methods of Test for Masonry Units - Part 16: Determination of Dimensions*, British Standards Institute, London
- BSI, 1996, *BS 1881-208: 1996 Testing Concrete - Part 208: Recommendations for the Determination of the Initial Surface Absorption of Concrete*, British Standards Institute, London
- BSI, 1990₂, *BS 1377-2: 1990 - Soils for Civil Engineering Purposes - Part 2: Classification Tests*, British Standards Institute, London
- BSI, 1990₄, *BS 1377-4: 1990 - Soils for Civil Engineering Purposes - Part 4: Compaction Related Tests*, British Standards Institute, London
- BSI, 1985, *BS 3921: 1985 – Specifications for Clay Bricks*, British Standards Institute, London
- BSI, 1970, *BS 4315-2: 1970 – Methods of Test for Resistance to Air and Water Penetration: Part 2 – Permeable Walling Constructions (water penetration)*, British Standards Institute, London
- Camuffo D, 1995, “Physical weathering of stones”, *Science of the Total Environment* 167, Elsevier science, pp.1-14
- Concrete Society, 1988, ‘Permeability Testing of Site Concrete’, Technical Report 31, cited in Domone PL, 1994_b, *Chapter 17 - Durability of Concrete*, in *Construction Materials: Their Nature and Behaviour - Second Edition*, ed. Illston JM, E & FN Spon, London, pp.169-194
- Craven T, 2004, “A Method for Optimising the Particle-Size Distribution of Cement Stabilised Rammed Earth Soils in order to Enhance Moisture Ingress Performance”,

[BEng Civil Engineering dissertation] supervised by Djerbib Y & Hall M, Sheffield Hallam University, UK

CSIRO, 1987, *Bulletin 5: Earth Wall Construction – edition four*, Commonwealth Scientific and Industrial Research Organisation, Chatswood, Australia

De Freitas VP, Abrantes V & Crausse P, 1996, “Moisture Migration in Building Walls - Analysis of the Interface Phenomena”, *Building and Environment* 31[2] pp.99-108

Dobson S, (ramtec@bigpond.com) 1st Nov 2002, *problem*, e-mail to M Hall (m.hall@shu.ac.uk)

Dobson S, (ramtec@bigpond.com) 6th Dec 2001, *admixtures*, e-mail to M Hall (m.hall@shu.ac.uk)

Dobson S, (ramtec@bigpond.com) 16th Nov 2001, *other possibilities*, e-mail to M Hall (m.hall@shu.ac.uk)

Dobson S, (ramtec@bigpond.com) 21st Sep 2001, *soil soiling*, e-mail to M Hall (m.hall@shu.ac.uk)

Dobson, S, 2000, *Continuity of Tradition: New Earth Building*, keynote speech delivered at Terra 2000 conference, Torquay, Devon, UK

Domone PL, 1994_a, *Chapter 13 - Constituent Materials of Concrete*, in *Construction Materials: Their Nature and Behaviour - Second Edition*, ed. Illston JM, E & FN Spon, London, pp. 91-116

Domone PL, 1994_b, *Chapter 16 - Strength and Failure of Concrete*, in *Construction Materials: Their Nature and Behaviour - Second Edition*, ed. Illston JM, E & FN Spon, London, pp.169-194

Domone PL, 1994_c, *Chapter 17 - Durability of Concrete*, in *Construction Materials: Their Nature and Behaviour - Second Edition*, ed. Illston JM, E & FN Spon, London, pp.169-194

Easton D, 1996_a, *The Rammed Earth House*, The Chelsea Green Publishing Company, Vermont

Easton D, 1996_b, *The Rammed Earth Renaissance* [Video documentary] Lyceum Productions, Napa, California

Germain G, 2002, “The Effect of Ordinary Portland Cement Stabilisation on the Engineering Properties of Rammed Earth”, [undergraduate dissertation] supervised by Hall M & Djerbib Y, Sheffield Hallam University, UK

Gove PB (Ed), 1993, *Webster's Third New International Dictionary*, Könemann Verlagsgesellschaft Mbh, Cologne

Gummerson RJ, Hall C & Hoff WD, 1980, “Water Movement in Porous Building Materials - II: Hydraulic Suction and Sorptivity of Brick and Other Masonry Materials”, *Building and Environment* 15 pp.101-108

-
- Hall M, Damms P & Djerbib Y, 2004, “Stabilised Rammed Earth (SRE) and the Building Regulations (2000): Part A – Structural Stability”, *Building Engineer*, 79 [6] pp. 18-21
- Hall M & Djerbib Y, 2004_a, “Moisture Ingress in Rammed Earth: Part 1 – The Effect of Particle-Size Distribution on the Rate of Capillary Suction”, *Construction and Building Materials*, 18 [4] pp.269-280
- Hall M & Djerbib Y, 2004_b, “Rammed Earth Sample Production: Context, Recommendations and Consistency”, *Construction and Building Materials*, 18 [4] pp.281-286
- Hall M, 2002, “Rammed Earth: Traditional Methods, Modern Techniques, Sustainable Future”, *Building Engineer*, 77 [11] pp.22-24
- Hall C & Yau MHR, 1987, “Water Movement in Porous Building Materials - IX: The Water Absorption and Sorptivity of Concretes”, *Building and Environment* 22[1], pp. 77-82
- Hall C & Kam-Ming T, 1986, “Water Movement in Porous Building Materials - VII The Sorptivity of Mortars”, *Building and Environment* 21[2] pp.113-118
- Hall C, 1981, “Water Movement in Porous Building Materials - IV: The Initial Surface Absorption and the Sorptivity”, *Building and Environment* 16[3] pp.201-207
- Hall C, 1977, “Water Movement in Porous Building Materials - I: Unsaturated Flow Theory and its Applications”, *Building and Environment* 12 pp.117-125
- Heathcote KA, 1995, “Durability of Earth Wall Buildings”, *Construction and Building Materials*, 9[3] pp.185-189
- Houben H & Guillaud H, 1996, *Earth Construction: A Comprehensive Guide - second edition*, Intermediate Technology Publications, London
- Kapfinger O, 2001, *Rammed earth – Lehm und Architektur – Terra Cruda*, Birkhäuser, Basel, Switzerland
- Keable J, 1996, *Rammed Earth Structures: A Code of Practice*, Intermediate Technology Publications Ltd, London
- Kebao R, Caselli A & Kagi D, 1997, “Water Repellent Admixtures for Concrete”, conference paper presented to *Concrete 97*, Concrete Institute of Australia, Melbourne
- Khatib JM & Mangat PS, 2003, “Porosity of Cement Paste Cured at 45°C as a Function of Location Relative to Casting Position”, *Cement and Concrete Composites*, 25 pp.97-108
- Khatib JM & Wild S, 1998, “Sulphate Resistance of metakaolin Mortar”, *Cement and Concrete Research*, 28[1] pp.83-92

-
- Khatib JM & Clay RM, 2004, "Absorption Characteristics of Metakaolin Concrete", *Cement and Concrete Research*, 34, pp.19-29
- Killip IR & Cheetham DW, 1984, "The Prevention of Rain Penetration through External Walls and Joints by Means of Pressure Equalisation", *Building and Environment* 19[2] pp.81-91
- King B, 1996, *Buildings of Earth and Straw - Structural Design for Rammed Earth and Straw Bale Architecture*, Ecological Design Press, USA
- Laycock EA, Hetherington S & Hall M, 2002, "Damp Towers - Understanding and Controlling the Ingress of Driven Rain through Exposed, Solid Masonry Wall Structures", [confidential report] for *English Heritage, 23 Saville Row, London*
- Laycock EA, 1997, "Frost Degradation and Weathering of the Magnesian Limestone Building Stone of the Yorkshire Province", PhD thesis, University of Sheffield, UK
- Maniatidis V & Walker P, 2003, "A Review of Rammed Earth Construction", [report] for *DTi Partners in Innovation project 'Developing Rammed Earth for UK Housing'*, University of Bath
- Marland G, TA Boden, and RJ Andres, 2003, *Global, Regional, and National CO₂ Emissions*. In *Trends: A Compendium of Data on Global Change*. Carbon Dioxide Information Analysis Center, Oak Ridge National Laboratory, U.S. Department of Energy, Oak Ridge, Tenn., U.S.A.
- Minke G, 2000, *The Earth Construction Handbook*, WIT Press, Southampton, UK
- Mitchell JK, 1976, *Fundamentals of Soil Behaviour*, John Wiley & Sons Inc., London
- Mortensen N, 2000, "The Naturally Air Conditioned House", [online] Earth Building Research Forum, University of Technology Sydney, Australia, available via: <http://www.dab.uts.edu.au/ebi/index> [25 Mar 2004]
- Neville AM, 1986, *Properties of Concrete*, Longman Scientific & Technical, Harlow, England
- Oliver A, Douglas J & Stirling JS (Eds), 1997, *Dampness in Buildings – Second Edition*, Blackwell Science, London
- Standards New Zealand, 1998, *NZS 4298: 1998 Materials and Workmanship for Earth Buildings*, Wellington, New Zealand
- Pliny the Elder, Natural History Volume IX, Book XXXV, XLVIII (169), Loeb Classical Library, translated by H. Rackman, London: William Heinemann Ltd.
- Project Terra, 2000, *Project Terra Research Meeting - Summary Report*, [report] The Getty Conservation Institute, Los Angeles
- Rose DA, 1965, RILEM Bulletin No. 29, cited in Domone PL, 1994_b, *Chapter 17 - Durability of Concrete*, in *Construction Materials: Their Nature and Behaviour - Second Edition*, ed. Illston JM, E & FN Spon, London, pp.169-194

Sissons B, 2004, "The Effect of Clay on the Water Absorption Properties of Rammed Earth", [BSc (Hons) Civil Engineering dissertation] supervised by Djerbib Y & Hall M, Sheffield Hallam University, UK

Taylor-Firth A & Flatt DE, 2001, "Climatic Simulation and Environmental Monitoring - A Facility for Realistic Assessment of Construction Materials In-Service Performance", *Construction & Building Materials*, 5 [1], pp. 3-7.

Tuck M, 2004, "The Effect of Soil Particle-Size Distribution, Combined with Different Levels of Cement Stabilisation, on the Rate of Moisture Ingress in Rammed Earth", [BEng Civil Engineering dissertation] supervised by Djerbib Y & Hall M, Sheffield Hallam University, UK

Turner J, 2004, "Moisture Dissipation from Rammed Earth: The Effect of Stabilisers and Soil Particle-Size Distribution on the Rate of Water Dissipation", [BEng Civil Engineering dissertation] supervised by Djerbib Y & Hall M, Sheffield Hallam University, UK

UKTV, 2003, *Home Wasn't Built in a Day – Episode Guide: Episode 11*, [online] available at <http://www.uktvstyle.co.uk/WhatsOn/Index.cfm?ccs=460&cs=1644> [25th Mar 2004]

UKTV, 2003, *Home Wasn't Built in a Day: Episode 11 – 'rock solid' rammed earth*, (Television programme) BBC-commissioned series for UKTV, produced by ACP Television, June 2003

Vos BH & Tammes E, 1969, *Moisture and moisture transfer in porous materials*, [report] Report no. BI-69-96, Organisation for industrial research TNO, Institute TNO for building materials and building structures, Delft, Holland

Vos BH & Tammes E, 1968, *Flow of water in the liquid phase*, [report] Report no. B 1-68-38, Inst. TNO for building materials and building structures, Delft, Holland

Walker P & Standards Australia, 2002, *HB195: The Australian Earth Building Handbook*, Standards Australia International, Sydney

Walker P, 1996, "Specifications for Stabilised Pressed Earth Blocks", *Masonry International*, 10 [1] pp. 1-6

Walker P, 1995, "Strength, Durability and Shrinkage Characteristics of Cement Stabilised Soil Blocks", *Cement and Concrete Composites* 17[4] pp.301-310

Watson L, 1997, "Building with Earth - Not Halfbaked but Unbaked", [magazine] *Building for a Future*, UK

Weilberg Lahn, 2004, *Homepage zur Stadt Weilburg an der Lahn*, [online] available at: <http://www.weilburg-lahn.info> (follow the link to 'piseebau') [25 Mar 2004]

Williams-Ellis C, 1999, *Building in Cob, Pisé and Stabilised Earth*, Donhead Publishing Ltd., Shaftesbury, England

BIBLIOGRAPHY

Agarwil A, 1981, *Mud, Mud: The Potential of Earth-Based Materials for Third World Housing*, International Institute for Environment and Development, London

Agnew N & Avrami E, 2001, "Conservation and Continuity of Tradition: A Discussion about Earthen Architecture", [interview] with Houben H, Hurd J, and Crosby T, *The Getty Conservation Institute Newsletter* 16 [1], The Getty Conservation Institute, Los Angeles

Allaby A & Allaby M, 1990, *The Concise Oxford Dictionary of Earth Sciences*, Oxford University Press, Oxford

Alva Balderrama A & Teutonico JM, 1983, "Notes on the Manufacture of Adobe Blocks for the Restoration of Earthen Architecture", ICCROM, Rome, Italy, pp.41-54

Alva Balderrama A & Chiari G, 1995, "Protection and Conservation of Excavated Structures of Mud brick," in *Conservation on Archaeological Excavations*, Price S (ed), ICCROM, Rome, Italy, pp.101-112

Alva Balderrama A, 2001, "The Conservation of Earthen Architecture", *The Getty Conservation Institute Newsletter* 16 [1], The Getty Conservation Institute, Los Angeles

Anderson DG & Russo M, 1999, "Native Earthen Architecture in Eastern North America", *Cultural Resource Management* 22[6] pp.49-51

Arfvidsson J & Claesson J, 2000, "Isothermal Moisture Flow in Building Materials: Modelling, Measurements and Calculations Based on Kirchhoff's Potential", *Building and Environment* 35 pp.519-536

Ashurst J & Ashurst N, 1988, *Practical Building Conservation: Brick, Terracotta and Earth*, Gower Technical Press, Aldershot, England

ASTM, 1989, *ASTM D559-89 - Standard Test Measures for Wetting and Drying Compacted Soil-Cement Mixtures*, Annual Book of ASTM Standards, Vol. 04.08 pp.30-34

ASTM, 1989, *ASTM D560-89 Standard Test Methods for Freezing and Thawing Compacted Soil-Cement Mixtures*, Annual Book of ASTM Standards, Vol. 04.08 pp.35-39

ASTM, 1995, *ASTM E514-90 - Standard Test Method for Water Penetration and Leakage through Masonry*, pp.903-906

ASTM, 2000, *ASTM E1105: 2000, Standard Test Method for Field Determination of Water Penetration of Installed Exterior Windows, Skylights, Doors, and Curtain Walls, by Uniform or Cyclic Static Air Pressure Difference*

ASTM, 2001, *ASTM E2128: 2001, Standard Guide for Evaluating Water Leakage of Building Walls*, pp.1521-1555

Atkinson J, 1993, *An Introduction to the Mechanics of Soils and Foundations*, McGraw-Hill International (UK) Ltd., London

Avrami E, 1999, "Building Institutional Alliances - Project Terra", *Cultural Resource Management* 22[6] pp.14-20

Avrami E, 2001, "Project Terra", *The Getty Conservation Institute Newsletter* 16[1], The Getty Conservation Institute, Los Angeles

BBC, 1994, *Wall to Wall: Episode 1 - Back To Earth*, produced by the BBC in 1994

Berge B, 2000, *Ecology of Building Materials*, Architectural Press, Oxford

Brandsma RT, Fullen MA, Hocking TJ & Allen JR, 1999, "An X-Ray Scanning Technique to Determine Soil Macro Porosity by Chemical Mapping", *Soil & Tillage Research* 50[1] pp.95-98

Bridges EM, 1988, *World Soils - second edition*, Cambridge University Press, Cambridge, England

BSI, 1990, *BS 1377-1: 1990 - Soils for Civil Engineering Purposes - Part 1: General Requirements and Sample Preparation*, British Standards Institute, London

BSI, 1990, *BS 1377-3: 1990 - Soils for Civil Engineering Purposes - Part 3: Chemical and Electro-Chemical Tests*, British Standards Institute, London

BSI, 1990, *BS 1377-5: 1990 - Soils for Civil Engineering Purposes - Part 5: Compressibility, Permeability and Durability Tests*, British Standards Institute, London

BSI, 1990, *BS 1377-6: 1990 - Soils for Civil Engineering Purposes - Part 6: Consolidation and permeability Tests in Hydraulic Cells and with Pore Pressure Measurement*, British Standards Institute, London

BSI, 1990, *BS 1377-7: 1990 - Soils for Civil Engineering Purposes - Part 7: Shear Strength Tests (Total Stress)*, British Standards Institute, London

BSI, 1990, *BS 1377-8: 1990 - Soils for Civil Engineering Purposes - Part 8: Shear Strength Tests (Effective Stress)*, British Standards Institute, London

BSI, 1990, *BS 1377-9: 1990 - Soils for Civil Engineering Purposes - Part 9: In-Situ Tests*, British Standards Institute, London

BSI, 1998, *BS EN 772-3: 1998 Methods of Test for Masonry Units - Part 3: Determination of Net Volume and Percentage of Voids of Clay Masonry Units by Hydrostatic Weighing*, British Standards Institute, London

BSI, 1998, *BS EN 772-7: 1998 Methods of Test for Masonry Units - Part 7: Determination of Water Absorption of Clay Masonry Damp Proof Course Units by Boiling in Water*, British Standards Institute, London

-
- BSI, 2000, *BS EN 772-1: 2000 Methods of Test for Masonry Units - Part 1: Determination of Compressive Strength*, British Standards Institute, London
- BSI, 2000, *BS EN 772-2: 2000 Methods of Test for Masonry Units - Part 2: Determination of Percentage Area of Voids in Aggregate Concrete Masonry Units (by paper indentation)*, British Standards Institute, London
- BSI, 2000, *BS EN 772-11: 2000 Methods of Test for Masonry Units - Part 11: Determination of Water Absorption of Aggregate Concrete, Manufactured Stone and Natural Stone Masonry Units Due to Capillary Action and the Initial Rate of Water Absorption of Clay Masonry Units*, British Standards Institute, London
- BSI, 2000, *BS EN 772-13: 2000 Methods of Test for Masonry Units - Part 13: Determination of Net and Gross Dry Density of Masonry Units (except for natural stone)*, British Standards Institute, London
- BSI, 2000, *BS EN 772-19: 2000 Methods of Test for Masonry Units - Part 19: Determination of Moisture Expansion of Large Horizontally Perforated Clay Masonry Units*, British Standards Institute, London
- BSI, 2000, *BS EN 772-15: 2000 Methods of Test for Masonry Units - Part 15: Determination of Water Vapour Permeability of Autoclaved Aerated Concrete Masonry Units*, British Standards Institute, London
- BSI, 2000, *BS EN 772-20: 2000 Methods of Test for Masonry Units - Part 20: Determination of Flatness of Faces of Aggregate Concrete, Manufactured Stone and Natural Stone Masonry Units*, British Standards Institute, London
- BSI, 2000, *BS EN 772-18: 2000 Methods of Test for Masonry Units - Part 18: Determination of Freeze-thaw Resistance of Calcium Silicate Masonry Units*, British Standards Institute, London
- BSI, 2002, *BS EN 772-14: 2002 Methods of Test for Masonry Units - Part 14: Determination of Moisture Movement of Aggregate Concrete and Manufactured Stone Masonry Units*, British Standards Institute, London
- Bryan AJ, 1988, "Criteria for the Suitability of Soil for Cement Stabilisation", *Building and Environment* 23[4] pp.309-319
- Bryan AJ, 1988, "Soil/Cement as a Walling Material - I: Stress/Strain Properties", *Building and Environment* 23[4] pp.321-330
- Castellanos C, Descamps F & Isaura MI, 2001, "Joya de Ceren: Conservation and Management Planning for an Earthen Archaeological Site", *The Getty Conservation Institute Newsletter* 16[1], The Getty Conservation Institute, Los Angeles
- Chen Y & Chen Z, 1998, "Transfer Function Method to Calculate Moisture Absorption and Desorption in Buildings", *Building and Environment* 33[4], pp. 201-207
- Chiras DD, 2001, *The Natural House - A Complete Guide to Healthy, Energy-Efficient and Environmental Homes*, Chelsea Green Publishing Company, Vermont.

Craig JR, Vaughan DJ, & Skinner BJ, 1996, "Soil as a Resource," in Resources of the Earth - Origin, Use and Environmental Impact, Prentice-Hall International (UK) Ltd., London.

Crowley M, 1997, *Quality Control for Earth Structures*, Australian Institute of Building Papers 8, 109-118

Culpepper S, 1997, "Using Dirt and Plaster to Cast a 4,000-sq. ft. House in Two Days", *Fine Homebuilding* 107 [March], pp. 34-38

Cunningham MJ, 1992, "Moisture Diffusion due to Periodic Moisture and Temperature Boundary Conditions - An Approximate Steady Analytical Solution with Non-Constant Diffusion Coefficients", *Building and Environment* 27[3], pp. 367-377

Cunningham MJ, 1992, "Effective Penetration Depth and Effective Resistance in Moisture Transfer", *Building and Environment* 27[3], 379-386

Custance AC, 2001, "Some Remarkable Biblical Confirmations from Archaeology," 2nd edition, Doorway Publications, Ontario

Davies GC, & Bruce DM, 1998, "Effect of Environmental Relative Humidity and Damage on the Tensile Properties of Flax and Nettle Fibers", *Textile Resource Journal*, 68 [9] pp. 623-629

Davis M, 1994, *How to Make Low-Cost Building Blocks - Stabilised Soil Block Technology*, Intermediate Technology Publications, London

Deeks LK, Williams AG, Dowd JF, & Scholefield D, 1999, "Quantification of Pore Size Distribution and the Movement of Solutes Through Isolated Soil Blocks", *Geoderma* 90[1-2], 65-86

Easton D. 1996, "Using Air to Build Earth Walls", *Environmental Building News*, vol. 5, no. 5, pp. 11-12.

El Diasty R, Fazio P, & Budaiwi I, 1993, "Dynamic Modelling of Moisture Absorption and Desorption in Buildings", *Building and Environment* 28[1], 21-32

Erman A. 1894, *Life in Ancient Egypt*, Macmillan, London.

Farnsworth CB, 1999, "Earth Building Takes New Shapes", *Home Energy* 16[3] pp. 35-41 Berkeley, CA

Fathy H, 1973, *Architecture for the Poor*, The University of Chicago Press Ltd., London.

Filho RDT, Barbosa NP, & Ghavami K, 1990, "Application of Sisal and Coconut Fibres in Adobe Blocks", RILEM, France, pp. 139-149

Gayo E, De Frutos J, Palomo A, & Massa SA, 1996, "Mathematical Model Simulating the Evaporation Processes in Building Materials: Experimental Checking through Infrared Thermography", *Building and Environment* 31[5], 469-475

-
- Ghavami K, Toledo Filho RD, & Barbosa NP, 1999, "Behaviour of Composite Soil Reinforced with Natural Fibres", *Cement and Concrete Composites* 21 pp. 39-48
- Gibson S, 1993, "A House of Timber, Straw and Clay", [magazine] *Fine Homebuilding*, August/September, pp. 88-89
- Gilley JE & Finkner SC, 1985, "Estimating Soil Detachment Caused By Raindrop Impact", *Transactions of the ASAE*, pp. 140-145
- Gillott JE, 1968, *Clay in Engineering Geology*, Elsevier Publishing Company, London.
- Goodman LJ, Pama RP, Tabujara EG, Razani R, & Burian FJ, 1979, *Low-Cost Housing Technology - An East-West Perspective*, Pergamon Press Ltd., Oxford
- Greer MJA, 1996, "The Effect of Moisture Content and Composition on the Compressive Strength and Rigidity of Cob Made From Soil of the Breccia Measures near Teignmouth, Devon", [PhD thesis] University of Plymouth, UK
- Guillaud H, Joffroy T, Odul P, & CRATerre-EAG, 1995, *Compressed Earth Blocks - Volume 2: Manual of Design & Construction*, Vieweg & Sohn Verlagsgesellschaft mbH, Braunschweig, Germany
- Gummerson RJ, Hall C, & Hoff WD, 1981, "Water Movement in Porous Building Materials - III: A Sorptivity Test Procedure for Chemical Injection Damp Proofing", *Building and Environment* 16[3] pp. 193-199
- Habitat, 1986, *Characteristics of Soil Stabilisers - Fibre*, in *Earth Construction Technology - Manual on Basic Principles of Earth Application*, United Nations Centre for Human Settlements (Nairobi), Nairobi, pp. 26-28
- Hall C, & Kalimeris AN, 1982, "Water Movement in Porous Building Materials - V: Absorption and Shedding of Rain by Building Surfaces", *Building and Environment* 17[4], pp. 257-262
- Hall C, Hoff WD, & Nixon MR, 1984, "Water Movement in Porous Building Materials - VI: Evaporation and Drying in Brick and Block Materials", *Building and Environment* 19[1], pp. 13-20

Hannant DJ, 1996, "Fibre Composites - Section 2: Fibre-Reinforced Cements and Concretes," in *Construction Materials: Their Nature and Behaviour*, Second edition, (ed) J. M. Illston, ed., E & FN Spon, London, pp. 361-403.

Hannant DJ, 1999, "The Effect of Age Up To 18 Years Under Various Exposure Conditions on the Tensile Properties of a Polypropylene Fibre Reinforced Cement Composites", *Materials and Structures* 32 pp. 83-88

Harrison R, 1999, *Earth*, James & James (Science Publishers) Ltd., London

Heathcote KA, 1992, "Resistance of Earth Wall Buildings to Weathering By Wind-Driven Rain", *Australian Institute of Building Papers*, 6 pp.13-20

Heathcote KA & Piper R, 1994, "Strength of Cement Stabilised Pressed Earth Bricks with Low Cement Contents", *Journal and Proceedings - Royal Society of New South Wales*, 127 pp. 33-37

Heathcote KA & Ravindrarajah S, 2000, "Relationships Between Spray Erosion Tests and the Performance of Test Specimens in the Field", [report] University of Technology, Sydney

Heathcote KA & Moor GJ, 2000, "Durability of Cement Stabilised Earth Walls", [report] University of Technology, Sydney, Australia

Hendry AW, 2001, "Masonry Walls: Materials and Construction", *Construction and Building Materials*, 15 [8] pp.323-330

Hijazi H & Pamucku S, 1990, "Possible Re-Use of Petroleum Contaminated Soils as Construction Material", (eds) Martin JP, Cheng SC & Susavidge MN, pp. 155-170

I'Anson SJ & Hoff WD, 1986, "Water Movement in Porous Building Materials - VIII: Effects of Evaporative Drying on Height of Capillary Rise Equilibrium in Walls", *Building and Environment* 21[3/4] pp. 195-200

ICOMOS-UK, 2000, *Terra Britannica: A Celebration of Earthen Structures in Great Britain and Ireland*, James & James (Science Publishers) Ltd., London

Illston JM (Ed), 1994, *Construction Materials: Their Nature and Behaviour – second edition*, E & FN Spon, London

Intermediate Technology Development Group, 1997, "Earthquake Resistant Housing in Peru - Building in Partnership", [booklet] Intermediate Technology Publications, London

Intermediate Technology Development Group, 1999, "Nashetu-E-Maa: Building in Partnership with the Maasai", [booklet] Intermediate Technology Publications, London

Intermediate Technology Development Group, 2000, *Shelter*, [booklet] Intermediate Technology Publications, London

Intermediate Technology Development Group, 2001, *Additives to Clay - Organic Additives Derived from Natural Sources - Low-Cost Cements*, [leaflet] Intermediate Technology Publications Ltd, London

Intermediate Technology Development Group, 2001, *Mud Plasters and Renders - Low-Cost Cements*, Intermediate Technology Publications Ltd, London

James M, 1999, "A California Earthen Home", *Home Energy* 16 [3] pp. 43-45

Kezdi A, 1976, *Problems in Soil Physics*, Sociedad Mexicana de Mecanica de Suelos, Mexico

Khalili EN, 1989, "Lunar Structures Generated and Shielded with On-site Materials", *Journal of Aerospace Engineering* 2[3] pp. 1-8

Khan LE, 1973, *Shelter*, Shelter Publications, Bolinas

Klemm AJ & Klemm P, 1997, "The Effects of the Alternate Freezing and Thawing Cycles on the Pore Structure of Cementitious Composites Modified by MHEC and PVA", *Building and Environment* 32[6] pp. 509-512

Laporte R, 1993, *Mooseprints: A Holistic Home Building Guide*, [booklet] Natural House Building Center, Santa Fe, NM

Lasisi F & Osunade JA, 1984, "Effect of Grain Size on the Strength of Cubes Made from Lateritic Soils", *Building and Environment* 19[1] pp. 55-58

Lasisi F & Ogunjide AM, 1984, "Effect of Grain Size on the Strength Characteristics of Cement-Stabilised Lateritic Soils", *Building and Environment* 19[1] pp. 49-54

Ley T, 1995, "Traditional Crafts Updated: Thatching & Cob", *Structural Survey* 13[4] pp. 4-12

Ley T & Widgery M, 1997, "Devon Earth Building Association: Cob and the Building Regulations. Structural Survey", 15[1] pp. 42-49

Maso JCE, 1993, *Interfaces in Cementitious Composites*, St Edmundsbury Press, Bury St Edmunds, Suffolk

Matsumoto M, Hokoi S & Hatano M, 2001, "Model for Simulation of Freezing and Thawing Processes in Building Materials", *Building and Environment* 36 pp. 733-742

McHenry PG Jr, 1978, *Adobe: Build It Yourself*, The University of Arizona Press, Tucson, Arizona

McHenry PG Jr, 1984, *Adobe and Rammed Earth Buildings: Design and Construction*, John Wiley & Sons, Inc., New York

McHenry PG Jr, "Adobe Today", *Cultural Resource Management* 22[6] pp. 5-6

McLeister DA, 1994, "Down to Earth House: Lots of Dirt, Little Cement", *Professional Builder* 59[10] pp. 62

Mekonnen A & Hailu N, 1997, "Soil as Building Material: A Study to Improve Aggregate Stability and Compressive Strength of Earthen Materials", *Agricultural Mechanisation in Asia, Africa and Latin America* 28[3] pp. 68-71

Minke G, 1995, "Materialkennwerte Von Lehmbaustoffen", *Bauphysik*, 17 pp. 124-130

Monayem Dad, MD, 1985, "The Use of Cement Stabilised Soil for Low Cost Housing in Developing Countries", [PhD thesis] University of Newcastle Upon Tyne, UK

Morel JC, Ghavami K, & Mesbah A, 2000, "Theoretical and Experimental Analysis of Composite Soil Blocks Reinforced with Sisal Fibres Subjected to Shear", *Masonry International* 13[2] pp. 54-62

Morgan RPC, Morgan DDV, & Finney HJA, 1984, "Predictive Model for the Assessment of Soil Erosion Risk", *Journal for Agricultural Engineering Resources* 30 pp. 245-253

Standards New Zealand, 1998, *NZS 4297: 1998 Engineering Design of Earth Buildings. 1998*, Standards New Zealand, Wellington, New Zealand

Standards New Zealand, 1998, *NZS 4299: 1998 Earth Building Not Requiring Specific Design*, Standards New Zealand, Wellington, New Zealand

Ngowi AB, 1997, "Improving the Traditional Earth Construction: A Case Study of Botswana", *Construction and Building Materials* 11[1], 1-7

Norton J, 1997, *Building with Earth: A Handbook - Second edition*, Intermediate Technology Publications, London

Ogunye FO, 1997, "Rain Resistance of Stabilised Soil Blocks", [PhD thesis] University of Liverpool, UK

Ola SA. & Mbata A, 1990, "Durability of Soil-Cement for Building Purposes - Rain Erosion Resistance Test", *Construction and Building Materials* 4[4], pp. 182-187

Oliver A, 2000, *Fort Selden - Adobe Test Wall Project: Phase 1 - Final Report*, The Getty Conservation Institute, Los Angeles, USA

Olivier M, Mesbah A, El Gharbi Z, & Morel JC, 1997, "Mode Operatoire pour la Realisation D'essais de REsistance sur Blocs de Terre Comprimee", *Materials and Structures*, 30 pp. 515-517

Orlove BS, 1998, "Down to Earth: Race and Substance in the Andes", *Bulletin of Latin American Research* 17[2] pp. 207-222

Pande A, 1974, *Handbook of Moisture Determination and Control: Principles, Techniques, Applications - Volume 1*, Marcel Dekker Inc., New York

Pande A, 1975, *Handbook of Moisture Determination and Control: Principles, Techniques, Applications - Volume 2*, Marcel Dekker Inc., New York

-
- Pande A, 1975, *Handbook of Moisture Determination and Control: Principles, Techniques, Applications - Volume 3*, Marcel Dekker Inc., New York
- Pande A, 1975, *Handbook of Moisture Determination and Control: Principles, Techniques, Applications - Volume 4*, Marcel Dekker Inc., New York
- Peet TE, 1922, *Egypt and the Old Testament*, The University Press of Liverpool Ltd., Liverpool
- Pieper R, 1999, "Earthen Architecture in the Northern United States", *Cultural Resource Management* 22[6] pp. 30-33
- Project Terra, 2000, *Terra Consortium - Guidelines for Institutional Collaboration*, The Getty Conservation Institute, Los Angeles, USA
- Rahman MA, 1986, "The Potentials of Some Stabilisers for the Use of Lateritic Soil in Construction", *Building and Environment* 21[1] pp. 57-61
- Rahman MA, 1987, "A Comparative Study of the Potentials of Rice Husk Ash on Cohesive and Cohesionless Soils", *Building and Environment* 22[4] pp. 331-337
- Rahman MA, 1987, "The Potentials of Lateritic Soil-Clay and Clay-Sand Mixes in the Manufacturing of Bricks for Masonry Units", *Building and Environment* 22[4] pp. 325-330
- Ren KB & Kagi DA, 1995, "Upgrading the Durability of Mud Bricks by Impregnation", *Building and Environment* 30[3] pp. 433-440
- Richards RF, 1994, "Steady-Flux Measurements of Moisture Diffusivity in Unsaturated Porous Media", *Building and Environment* 29[4] pp. 531-535
- Rigassi V, 1995, *Compressed Earth Blocks - Volume 1: Manual of Production*, Vieweg & Sohn Verlagsgesellschaft mbH, Braunschweig, Germany
- Robertson DK, 1986, "The Performance of Adobe and Other Thermal Mass Materials in Residential Buildings", *Passive Solar Journal*, 3 [4] pp. 387-417
- Robson D, Hague J, Newman G, Jeronimidis G, & Ansell M, 1993, "Survey of Natural Materials for Use in Structural Composites as Reinforcement and Matrices", [report] The Biocomposites Centre, Bangor, Wales
- Rogers CDF & Smalley IJ, 1996, "The Adobe Reaction and the Use of Loess Mud in Construction", *Engineering Geology* 40[3-4] pp. 137-138
- Rudofsky B, 1965, *Architecture Without Architects*, The Museum of Modern Art, New York
- Schaffer RJ, 1972, *The Weathering of Natural Building Stone*, Department of Scientific & Industrial Research, London, 18
- Selvarajah S & Johnston AJ, 1994, "Water Permeation Through Cracked Single Skin Masonry", *Building and Environment* 30[1] pp. 19-28

-
- Simango DG. 1996, "Soil Stabilisation for Rural Housing", *Landwards* pp. 5-7
- Spence RJS & Cook DJ, 1983, *Building Materials in Developing Countries*, John Wiley & Sons, Brisbane
- Steele J, 1997, *An Architecture for People: The Complete Works of Hassan Fathy*, Thames & Hudson Ltd., London
- Stulz R, 1993, *Appropriate Building Materials: A Catalogue of Potential Solutions*, Intermediate Technology Publications Ltd., London
- Thayer B, 1996, "The Magic of Solar Adobe", *Solar Today*, 10 [1] pp. 18-21
- Trotman PM, 1995, "Dampness in Cob Walls", [report] Building Research Establishment, Garston, UK
- Trotman PM, 2002, *Mud Slinging at the Building Research Establishment: 80 Years of Research and Information Dissemination*, Building Research Establishment, Garston, UK
- Trulove JG & Greer NR, 2001, *Hot Dirt Cool Straw*, HBI - Harper Collins Publishers, New York
- US/ICOMOS, 1994, "Committee on Earthen Architecture. US/ICOMOS Newsletter" [10] pp. 1-22, Washington DC
- US/ICOMOS, 1995, "Specialised Committee on Earthen Architecture - US/ICOMOS Newsletter" [6] pp. 1-13 Washington DC
- Venkatarama Reddy BV & Jagadish KS, 1987, "Spray Erosion Studies on Pressed Soil Blocks", *Building and Environment* 22[2] pp. 135-140
- Venkatarama Reddy BV & Jagadish KS, 1995, "Influence of Soil Composition on the Strength and Durability of Soil-Cement Blocks", *The Indian Concrete Journal*, pp. 517-524
- Venkatarama Reddy BV & Lokras SS, 1998, "Steam-Cured Stabilised Soil Blocks for Masonry Construction", *Energy and Buildings* 29[1] pp. 29-33
- Waugh D, 1990, *Soils in Geography: An Integrated Approach*, Thomas Nelson & Sons Ltd., Surrey
- Weiner P, 1996, "Rammed-Earth Compound", *Fine Homebuilding* 101[Spring] pp. 90-94
- Whitlow R, 1995, *Basic Soil Mechanics - Third edition*, Longman Scientific & Technical, Harlow
- Wilder M, 1982, "FICON Faced Mud Walls - Appropriate Technology Walls for Housing Poor People", [report] Department of Building, Brighton Polytechnic, Brighton

Wilson MA, Hoff WD, & Hall C, 1991, "Water Movement in Porous Building Materials - X: Absorption from a Small Cylindrical Cavity", *Building and Environment* 26[2] pp. 143-152

Wilson MA, Hoff WD, & Hall C, 1994, "Water Movement in Porous Building Materials - XI: Capillary Absorption from a Hemispherical Cavity", *Building and Environment* 29[1] pp. 99-104

Wilson MA & Hoff WD, 1994, "Water Movement in Porous Building Materials - XII: Absorption from a Drilled Hole with a Hemispherical End", *Building and Environment* 29[4] pp. 537-544

Wilson MA, Hoff WD, & Hall C, 1995, "Water Movement in Porous Building Materials - XIII: Absorption into a Two-Layer Composite", *Building and Environment* 30[2] pp. 209-219

Wilson MA, Hoff WD, & Hall C, 1995, "Water Movement in Porous Building Materials - XIV: Absorption into a Two-Layer Composite ($S_A < S_B$)", *Building and Environment* 30[2] pp. 221-227

Yogananda MR & Jagadish KS, 1988, "Pozzolanic Properties of Rice Husk Ash, Burnt Clay and Red Mud", *Building and Environment* 23[4] pp. 303-308

Zhu D, Mallidi SR, & Fazio P, 1995, "Approach for Urban Driving Rain Index by Using Climatological Data Recorded at Suburban Meteorological Station", *Building and Environment* 30[2] pp. 229-236

Zumdahl SS, 1995, *Chemical Principles - Second edition*, DC Heath & Company, Lexington, USA

APPENDIX 1: THE STORY OF RAMMED EARTH

Earth construction can be loosely defined as ‘building with soil’, and for many people conjures an image of primitive housing and simplistic technology. However, nothing could be further from the truth because earth is simply one of the most fascinating and proven building materials in the world.

‘Ever since man learnt to build homes and cities around 10,000 years ago, earth has undoubtedly been one of the most widely-used construction materials in the world. There is hardly an inhabited continent, and perhaps not even a country, which does not have a heritage of buildings in unbaked earth, and even nowadays more than a third of all humanity lives in a home built of earth’,
(Houben & Guillaud, 1996).

A1.1 PAST, PRESENT & FUTURE

A1.1.1 Ancient and Historic Buildings

Perhaps the oldest recording of earth construction, as we now know it, is in chapter 5 from the book of Exodus in the old testament of the bible. After Pharaoh had declined Moses’ request to let his people go, he ordered his taskmasters to punish the Israelites by making their production of adobe (sun-dried mud bricks) all the more difficult. The traditional way of making adobe is to incorporate straw into the mud to provide additional strength and prevent the bricks from cracking.

‘Ye shall no more give the people straw to make brick, as heretofore: let them go and gather straw for themselves’ Exodus 5, verse 7 (Bible, Old Testament)

Figure 107 is taken from a painting found inside an Egyptian tomb from the 18th dynasty (1539 BC to 1295 BC); it illustrates the manufacture of sun-dried mud bricks that were used as a form of earth construction at that time, and are still used today mainly in the USA, Australia, Europe and Africa.

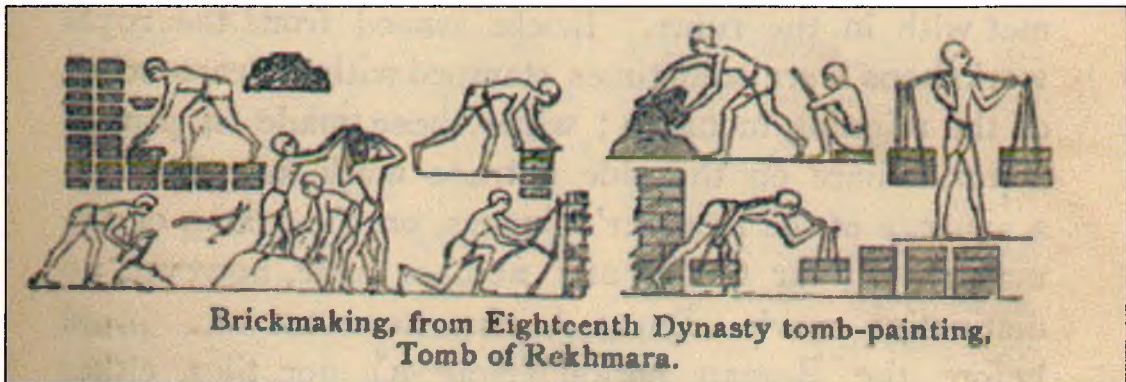


Figure 107 picture found inside an Egyptian tomb depicting the manufacture of mud bricks (courtesy: C Frederick)

According to the archaeologist Dr Charles Frederick from the University of Sheffield (*pers. comm.* 2002) surviving elements of ancient rammed earth wall construction have been discovered in many diverse locations such as settlements from Bronze Age Minoan Crete dating back approximately 3500 years. The Roman historian, Pliny the Elder, described rammed earth (or 'stuffed earth') construction during the 1st century AD in his book 'Natural History':

'Moreover, are there not in Africa and Spain walls made of earth that are called framed walls, because they are made by packing in a frame enclosed between two boards, one on each side, and so are stuffed in rather than built, and do they not last for ages, undamaged by rain, wind, and fire, and stronger than any quarry stone? Spain still sees the watchtowers of Hannibal and turrets of earth placed on the mountain ridges' (Pliny the Elder)

The Great Wall of China is over 5,000 km in length and was built between 221-214 BC by the Qin dynasty. A considerable proportion of the wall was originally built using approximately 180 billion cubic metres of rammed earth. The majority of the original wall has been replaced or over clad with alternative forms of masonry such as fired clay tiles and natural stone. Some sections of the original rammed earth wall still remain untouched and intact, and are at least 2000 years old.

Figure 108 shows the rammed earth wall that surrounds Horyuji Temple in Japan, and is thought to have been built between the dates 607 to 750 AD (Henman D, 2002, *pers. comm.*).



Figure 108 the rammed earth perimeter wall that surrounds Horyuji temple, Japan (photo: courtesy Darel Henman ©2002)

The Horyuji temple site is protected by the United Nations (UNESCO) and is Japan's first World Cultural Heritage site (Henman D, 2002, *pers. comm.*). Its very existence serves as a testament to the potential longevity and timeless appeal of rammed earth. Its extensive use across the Americas, Europe, Asia, the Middle-East and Africa have aroused a great level of interest amongst architectural conservators and archaeologists throughout the world with a keen interest in the promotion and development of earth building conservation as a science. The creation of the international Project Terra initiative is one such example of this movement, and is led by the Getty Conservation Institute (USA), CRATerre-EAG (France), and ICCROM (Italy).

Taikoubei (trans: Taikou Wall) is a lime-stabilized rammed earth wall as shown in Figures 109. The wall is connected to the main southern gate of the Sanjyusangen-Do Temple in Kyoto, Japan. It is thought to have been built around 1610 by order of Toyotomi Hideyoshi (Henman D, 2002, *pers. comm.*).



Figure 109 Taikoubei rammed earth wall – note the raised stone plinth, drainage channel and large eaves overhang on the roof (Photo: courtesy Darel Henman ©2002)

Oonerihei (trans: large rammed wall) was originally constructed somewhere between 1392 and 1466 AD for the Nishinomiya Shrine, in Hyogo-ken, Japan (see: Figure 110).



Figure 110 Oonerihei - note the degree of weathering and surface erosion on some of the wall sections is only minor for a wall that is over 500 years old (Photo: courtesy Darel Henman ©2002)

Apparently, the wall underwent a period of restoration in around 1950. In 1995, 24 out of the 62 wall sections were damaged in the Kobe earthquake and were only recently repaired. The wall panels are approximately 2.5m tall, 4m wide and 1.2m thick. It runs the entire perimeter of the shrine and its total combined length is approximately 247 metres. The soil that was available on-site was mixed in equal amounts with a new soil, of low clay content, that was imported from elsewhere in order to improve the overall soil grading (Henman D, 2002, *pers. comm.*).

The soil mix was then stabilised with lime and nigari, which is the magnesium chloride rich mineral deposits formed during the process of salt extraction from sea water.

Apparently, the use of nigari was often recorded in ancient Japanese earth building although its use has now decreased. Today, magnesium- and calcium chloride-rich products are often used in the maintenance of earthen roads as a dust suppressant and so we may hypothesise that the use of nigari may have been for the same reasons. During the construction of Ooneriheii the formwork was filled with the moist mix in layers approximately 100mm thick when loose, and then tamped down using hand rammers to a compacted thickness of about 50mm (Henman D, 2002, *pers. comm.*).

During the late 18th century a highly enthusiastic Frenchman named Francois Cointeraux 'discovered' the practice of rammed earth construction in the region surrounding Lyon. He renamed the technique as nouveau pisé, which later became known as pisé de terre. Following the ideals of the French revolution, Cointeraux adopted the dissemination of rammed earth construction as his personal mission in life and described it in a highly enthusiastic manner (Easton, 1996_a):

'a gift of Providence... a present which God has made to all people. If agriculture is the basis for all science, pisé is also the first of all the arts... Factories will multiply with pisé and commerce will flourish... One should employ this kind of building throughout the realm, for the decency of villages and the honour of the nation, to save wood, which is used in such great abundance in constructions, to avoid fires, to protect labourers from cold or excessive heat, at the same time to conserve and protect their health, and for so many other objectives, too long to list...' (cited in Easton, 1996_a)

In 1788 he founded a school in Paris specifically to promote the use of Pisé in the building industry. In 1790 and 1791 he published four advisory documents on tools,

soil, formwork and methodologies for pisé construction. These texts were translated into English and then disseminated in Great Britain (Easton, 1996_a).

Weilburg an der Lahn is a town in Germany that is noted for its relatively large number of historic rammed earth buildings. There are around 120 rammed earth houses that were built during the early- and mid-eighteenth century (Weilburg Lahn, 2004), a few examples of which are shown in Figure 111.



Figure 111 (above left) a typical selection of 19th century rammed earth buildings on Bahnhofstraße, Weilburg an der Lahn, Germany (Photo: courtesy Weilberg Lahn, 2004)

Figure 112 (above right) a seven storey rammed earth building on Heinallee, Weilburg an der Lahn, Germany that is around 150 years old (Photo: courtesy Weilberg Lahn, 2004)

The seven storey rammed earth building shown in Figure 112 was built in the early 19th century with no steel reinforcement, and yet today it is still fully intact and occupied (Weilberg Lahn, 2004). It appears somewhat ironic that so many modern steel-reinforced concrete structures of a similar type are often disused, demolished or incapable of surviving under similar climatic conditions without extensive problems relating to carbonation, spalling and structural defects after just 30 years of life. It would most likely be profitable for the modern construction industry to rediscover what the western world knew about building multi-storey rammed earth structures in the 1800s that it does not know today.

In a recent study, it has been observed that rammed earth (or pisé) construction has been practised in Great Britain for well over 200 years (Maniatidis & Walker, 2003). Throughout the nineteenth century, a significant number of rammed earth and rammed chalk buildings were built in Wessex. Following the Great War (WWI: 1914 – 1918) a series of experimental rammed earth houses were built in Amesbury, Wiltshire (Maniatidis & Walker, 2003). In addition, there are also approximately one hundred 19th century rammed chalk buildings in Andover, Winchester, and several other towns and villages in Hampshire. These are mainly residential properties although some have been converted to schools and other public buildings. An example of one of these buildings is shown in Figure 113 and it incorporates both load bearing and non-load bearing walls, both internally and externally (Maniatidis & Walker, 2003).



Figure 113 five storey rammed chalk building in Winchester, Hampshire (Photo: courtesy Maniatidis & Walker © 2003)

A1.1.2 The Modern Rammed Earth Renaissance

Rammed earth can be used to construct all masonry elements on typical construction projects from small houses to low-rise commercial buildings, from a simple outbuilding to an entire television studio complex. The longevity of the material is essentially proven in the continued existence of the numerous historic structures described above. Easton (1996_a) believes that *'the time is right for the renaissance of earthen architecture...The word "earth" - and all that connotes - has become once more a central concept for ourselves and for our civilisation'*.

The market for modern rammed earth construction is growing rapidly in many parts of the world; none more so than in Western Australia where in some towns it accounts for up to 20% of the entire new build market. This revival began in 1976 with the construction of a small rammed earth building at the Cape Mentelle winery. The interest

that this generated was largely due to the energy crisis of the 70s, growing environmental consciousness, and the high cost of borrowing money (CSIRO, 1987). Following the destruction of numerous 'conventional' buildings due to cyclone Tracy, there was the strong desire for the rapid construction of low energy, cost effective buildings that were substantial and durable. Clearly, buildings made from earth can boast excellent sustainability credentials combined with good thermal and acoustic properties. However, it is their cost effectiveness, when compared with other masonry materials, which has allowed earth buildings to compete strongly with conventional buildings both in Australia and elsewhere (Dobson, 2000).

Figure 114 shows the Thomas Moore Roman Catholic Church at Margaret River in Western Australia. This was one of the earliest modern rammed earth buildings to be constructed in Australia, and it helped to create a public awareness of the material, which resulted in the subsequent production of many other local buildings (Hall, 2002).



Figure 114 Thomas Moore R.C. church (Photo: courtesy RAMTEC Pty Ltd. ©2002)

Figure 115 shows a rammed earth rural retreat featuring passive solar design – the large, carefully oriented fenestration provides light and warmth, whilst the thermal mass of the walls evens out daytime/night-time temperature fluctuations providing a pleasant living environment (Hall, 2002).



Figure 115 a passive solar design rammed earth house (Photo: courtesy RAMTEC Pty Ltd. ©2002)

Figure 116 shows a rammed earth holiday home at Broome in Western Australia utilising wide verandas, and design for cross-flow ventilation making this home ideal for living in the tropics (Hall, 2002).



Figure 116 a rammed earth holiday home in the tropical setting of Broome, Western Australia (Photo: courtesy RAMTEC Pty Ltd ©2002)

Renewed interest in earth construction in the United Kingdom has previously been led by organisations such as the Centre for Earthen Architecture at Plymouth University, in conjunction with English Heritage, as well as some research by the Building Research Establishment (BRE) procured by Historic Scotland. Earth materials are perhaps still regarded by some as a material that belongs in the past, many types of which are studied by architectural conservators. Cob buildings, for example, are indigenous to Devon and despite the renewed level of interest in cob as a modern, sustainable material it is still perhaps mostly associated with old-fashioned, thatch cottages. In contrast to this, rammed earth has proven itself to be a highly flexible modern masonry material that can be used to create a wide variety of forms from the crisp, clean lines of modern contemporary architecture to the rustic, earthy textures more suited to a rural dwelling.

In order to support and encourage this growth of interest in modern rammed earth construction, consumer confidence in the material still needs to be significantly enhanced. During the revival period that has taken place throughout Great Britain over the past ten years or so there have been a relatively small number of modern rammed earth projects aimed at attempting to reintroduce it to the property market. A Government-funded 'Partners in Innovation' research project is presently being investigated on behalf of the Department for Trade & Industry (DTi) by Bath University and a number of other parties. Its theme is 'developing rammed earth construction for UK housing' and its general aim is to respond to the increased interest and demand described above. In terms of output, this project has recently produced an international review of rammed earth construction and contains a detailed list of almost all known rammed earth buildings, both historic and modern, that can be found in Great Britain.

In 1999 the In-situ Rammed Earth Company Ltd. built long sections of non-load bearing, unstabilised rammed earth as part of the visitors centre building at the well-known Eden Project in Cornwall. During the same year the Woodley Park Centre for Sports & Arts, Lancashire was built from a combination of unstabilised and cement stabilised rammed earth by John Renwick (Partnership for Natural Building Design) with advice from In-situ Rammed Earth Ltd). The AtEIC (Autonomous Environmental Information Centre) building was built in 2000 from a combination of unstabilised and lime stabilised rammed earth at the Centre for Alternative Technology (Wales) whose purpose, as an organisation, is to promote and disseminate sustainable technologies.

More recently, the knowledge and experience of Australia's largest rammed earth organisation – the Affiliated Stabilised Earth Group (asEg) - has been brought to Great

Britain by Bill Swaney who founded Earth Structures (Europe) Ltd. They use a patented recipe of stabilised rammed earth soil grading with the addition of a small amount of cement and moisture-repellent admixtures. In 2001, the company built a high-quality stables outbuilding for an historic listed building called The Manor in Northamptonshire, England as shown in Figure 117.



Figure 117 stables at The Manor in Northamptonshire, built by Earth Structures (Europe) Ltd. (2001)

Perhaps the most recent addition to Britain's stock of modern rammed earth structures is the Brimington bowls pavilion built in July 2003 at Chesterfield, Derbyshire (see: Figure 118). It was constructed as a collaborative project between Matthew Hall (the author) and Chesterfield Borough Council, Derbyshire. The building was completed in October 2003 and will be used as a local community facility for local people. The building measures approximately 12m x 5m and the walls are made from (6%) cement-stabilised rammed earth. It is the first public building in Great Britain to be made from

stabilised rammed earth that is fully accepted without concessions under the 2002 Building Regulations.



Figure 118 Brimington bowls pavilion at Chesterfield, Derbyshire - built by Matthew Hall and Chesterfield Borough Council (July 2003)

The construction of this building was unique in that all 17.5 cubic metres of the load bearing rammed earth walls were constructed within a continuous 24-hour period, in addition to installation of the wall plate, roof trusses and roofing membrane. The aim of this was to satisfy the challenge laid down by a television company commissioned by the BBC to make a programme called 'Home wasn't built in a day'. The programme was first aired on the channel UK Style on October 24th 2003. This episode on rammed earth was part of a series of fifteen different challenges, each aimed at proving the fact that modern ideas on sustainable construction techniques can be a quick, cost effective alternative to bricks and mortar.

'The exciting fact is, unlike the primitive earth shelters of...our prehistoric ancestors, today's earth buildings can be as refined as we care to make them' (Easton, 1996_a).

A1.1.3 The Future for Rammed Earth in Great Britain

The DTi funded project, run by Bath University, aims to compile its guidelines regarding the suitability of rammed earth construction for the UK housing market by 2004. It is their intention to be able to publish an advisory document on their findings and collective opinions. As many experts and specialists agree, the large amount of knowledge and experience of Australian and American rammed earth builders cannot simply be transferred without alteration to the British market, although we can benefit greatly from it. The skills and knowledge relating to construction technology and materials are, to some degree, interchangeable. However, if rammed earth is to be accepted as a viable alternative to more conventional masonry materials such as bricks and concrete blocks then an understanding of how to ensure that it conforms to the current Building Regulations is essential. The benefits and limitations of the material must be known and understood such that local authority planning departments are willing to accept rammed earth structures and feel confident to comment on (and criticise) design proposals that incorporate rammed earth.

New and innovative ideas that have gained support in the UK construction industry are often architect-led and rammed earth appears to be no exception. Since the creative spirit and conceptual works of a building design usually come from the architect this is a natural state of affairs. However, the support of rammed earth construction from architects and environmentalists may not be enough. In this sense, a technical manual

that is aimed at structural/civil engineers would be highly beneficial and could instigate the formation of project teams that are capable of working together on a rammed earth building with equal confidence.

A1.2 WHY BUILD WITH EARTH?

Building with earth is incredibly logical to the extent that it is all too often overlooked as a viable alternative to conventional building materials. Indeed, it is ironic that we refer to materials such as concrete blocks as ‘conventional’ when earth is by far the oldest, most established and most prolific building material in the world. The raw material is free, abundant, and of course highly ubiquitous. It can be used to quickly and easily construct a highly desirable property in a short space of time, but that could potentially last for generations. If and when the building outlasts its useful existence it can be demolished and the soil from the walls can return to the site from which it came with little or no environmental impact. This process of creation, use & demolition is analogous to a natural cycle; the same soil from a demolished earth building can be extracted and re-used to make another building, and the cycle continues.

A1.2.1 Government Incentives

Many of the Governments in western countries, including Great Britain, are placing an increased emphasis on the importance of promoting sustainable building and reducing carbon-based emissions, e.g. carbon dioxide. Rhetorical discussion suggests that the British Government plan to introduce a ‘carbon tax’ that is imposed on those responsible for the environmentally harmful output of, for example, carbon dioxide emissions. The amount of taxation is thought to be indexed to the amount of CO₂ output

that the party is responsible for. Since the production of cement is thought to account for approximately 5% of all global CO₂ emissions (Marland *et al*, 2003) the introduction of a carbon tax could potentially make the use of cement prohibitively expensive. The economic impetus for masonry materials that require little or no cement content may therefore enjoy a renewed and sustained interest from the construction industry. Masonry techniques such as bricks & mortar may become even more expensive when one considers the high level of carbon taxation a fired clay brick manufacturer may be forced to endure as recompense for their vast consumption of fossil fuels and carbon emissions.

Many local authorities are so committed to promoting sustainable development that they actually provide grants and incentives for individuals or groups actively willing to pursue a project in this field. A good example of this occurred in February 2003 when Chesterfield Borough Council joined forces with the author (Matthew Hall, Sheffield Hallam University) to form a collaborative partnership promoting the use of rammed earth as a viable, sustainable alternative to conventional masonry wall-building techniques. This venture initially generated a great deal of enthusiasm and received its first grant of £50,000-00 for the construction of a rammed earth bowling pavilion/community centre facility at Brimington in Chesterfield, Derbyshire.

A1.2.2 Environmental Qualities

Rammed earth has many excellent environmental qualities that make it very attractive to clients, contractors and professionals alike. Materials such as bricks and concrete blocks are produced through a lengthy process of manufacture. Both brick and cement manufacture involve a process of firing at high temperatures of up to 1400°C, which

presently demands the non-sustainable consumption of fossil fuels. In stark contrast to this, the embodied energy of unfired materials such as rammed earth has been calculated to be approximately 1/700th that of fired clay bricks (Dobson, 2000). Many established contractors actually quote a figure of 376 MJ/m³ for the embodied energy content of their cement stabilised rammed earth walls (asEg, 2003). This helps them to emphasise their commitment to the principles of sustainable development to the client.

During transportation, fired clay bricks are typically packaged in pallets of four hundred with the addition of significant quantities of plastic wrapping before being carried on a lorry to one of the numerous distribution centres and builder's yards found throughout the country. In contrast to this, a source of soil that is suitable for rammed earth construction can potentially be located on the building site, and can be extracted during the process of excavating for the building's foundations. If the indigenous soil is unsuitable, however, then alternative sources include local quarry waste material, soils excavated from nearby building sites (e.g. for foundations), or even recycled bricks and concrete from demolitions. Not only do the reduced transportation costs of rammed earth make environmental benefits, but also significant economic benefits. The raw material (sub-soil) is essentially free if available on-site, and the minimal cost of quarry waste materials as an alternative means that we have the opportunity, in rammed earth, to convert a waste bi-product into a sustainable building material.

A1.2.3 Contractors

The current level of expertise and experience created in Australia over approximately the past 25 years began when the first modern rammed earth building was constructed

in 1976 during the energy crisis. Contractors can use relatively low-skilled labour for much of the process of rammed earth construction due to the simple nature of the technique and the fact that it is easily learned by most able-bodied people. Modern rammed earth formwork systems are often unique (or patented) and can be highly programmable such that they are flexible towards almost any architectural designs that incorporate low- and medium-rise masonry walls. In Great Britain, where there is a lack of experience and proven examples of rammed earth construction, the total economic cost of using rammed earth has been estimated to be almost the same as that of conventional brick & block by the Technical Services Officer for Chesterfield Borough Council (Huskinson D, 2003, *pers. comm.*). Where trades such as bricklaying enjoy a long-standing proliferation, as is the case in Great Britain, it appears to be difficult to break the single-minded, inflexible approach towards rammed earth that is so commonly encountered throughout the housing market and construction industry in general.

Indeed, it is the cost-effectiveness of rammed earth when compared with other masonry materials that has allowed earth buildings to compete strongly against 'conventional' building techniques both in Australia and elsewhere (Dobson, 2000). Successful organisations such as the Affiliated Stabilised Earth Group (asEg) demonstrate that one of their three-man crews can produce between 15 and 20m² of rammed earth wall (at 300mm thickness) per day, and the walls for a standard home can take just 7 to 10 days to complete (asEg, 2003). The speed of construction they can achieve, and the associated economic advantages this brings, are clearly impressive.

Some contractors admit that rammed earth is not always the cheapest option for building walls. However, they often emphasise the fact that it can be short-sighted to economise on one of the most visible and structurally important aspects of a building, particularly when the entire wall components only account for around 12% to 15% of the total project costs. Since rammed earth is still relatively non-established in a construction industry that is geared towards using bricks and concrete blocks for its masonry materials, it is most likely that the costs of rammed earth wall construction will only decrease significantly if assisted by further gains in experience and advances in the technology.

A1.2.4 Physical Properties

Rammed earth walls are free-standing and can be used for load bearing or non-load bearing applications. They are typically between 300 and 600mm thick and are a monolithically constructed mass wall material with a typical dry density of between 1800 and 2200 kg/m³. According to the official Standards New Zealand document NZS 4298; rammed earth should have a minimum characteristic unconfined compressive strength (f'_{cu}) of 1.3 N/mm² (Standards New Zealand, 1998). It is worth noting that although this value is low when compared to brick and concrete, the typical downward thrust of a single storey house is only of the order 0.1 N/mm² (Houben & Guillaud, 1996). The semi-approved CSIRO document Bulletin 5 edition 4 states that the value f'_{cu} should be a minimum of 2 N/mm² (CSIRO, 1987). Many Australian contractors specify that the compressive strength of their cement-stabilised rammed earth walls range from 2 N/mm² up to 10 N/mm² (asEg, 2003).

The Building Code of Australia 1996 (BCA 96) references sections of CSIRO Bulletin 5 Earth Wall Construction – fourth edition as ‘*deemed-to-satisfy structural requirements*’ (asEg, 2003). There are currently no official documents providing technical specifications for rammed earth that are recognised by the Building Regulations 2002 for England & Wales. However, the Brimington bowling pavilion set a precedent through the planning & building control department of Chesterfield Borough Council who accepted the use of cement-stabilised rammed earth (SRE) under the Building Regulations (2000) Part A: Structural Stability with a minimum characteristic unconfined compressive strength of 3.5 N/mm^2 (Hall, Damms & Djerbib, 2004).

Earth is, of course, a non-combustible material and in this way is much the same as any other form of masonry. Many of the established rammed earth contractors in Australia have had fire resistance testing performed and have been quoted as reporting a 4-hour fire rating for a 300mm thick wall (asEg, 2003). Rammed earth also has excellent acoustic qualities and has very low sound transmittance creating a very solid, safe feeling within the building (UK Style website, 2003).

A1.2.5 Thermal Properties

Along with the industrial revolution came the belief in man that his technology could effectively conquer and control nature. Thankfully, this previous lack of interest in the utilisation of natural systems and sources of energy is diminishing as more people become aware of sustainable alternatives such as solar- and wind power (Mortensen, 2000). The shortsighted decision to produce energy through the combustion of fossil fuels was often one of economics, and so it is perhaps ironic that the ‘real’ price for

fossil fuels was hidden until our discovery of their impact on the natural environment in terms of pollution and global warming (Mortensen, 2000).

The conventional way of maintaining a warm living environment in a home is effectively to seal the interior space from the outside influences of nature. In terms of thermal comfort, this is conventionally achieved using an insulative material that works to prevent the passage (or escape) of heat energy. The interior of the building is then heated or cooled artificially, and the air within the building is used as the heat energy transfer medium. The artificial heating/cooling is achieved through the use of man-made systems that consume energy. The insulation is there to prevent the heat from escaping to the cold outdoors, or to prevent the warm outdoors from heating up the cooled interior, respectively.

Due to the massive nature and high density of rammed earth walls, they are noted for having very poor insulation. However, they do have very high thermal mass; a property that is responsible for a phenomenon sometimes termed the ‘thermal flywheel’ effect, and which works in the opposite way to insulation. Rather than prevent the passage of heat energy, thermal mass walls will readily absorb it and they have the capacity to store it rather like a battery. This is particularly useful in parts of the world such as Western Australia where it is very hot during the daytime, and can sometimes get much colder in the evenings. On a warm day, the interior of the building is kept cool as the heat is absorbed by the thermal mass of the walls. When the temperature drops at night, the heat energy stored within the walls re-radiates into the house interior. This thermal ‘time lag’ can last for between 6 to 8 hours in a 300mm thick rammed earth wall, and a typical thermal mass capacity has been calculated as 1673 KL/m³K (asEg, 2003).

In a building that has been designed to maximise passive solar energy gains, thermal mass walls can offer significant reductions in heating/cooling costs and can reduce energy consumption by harnessing free solar energy during the day, storing it in the walls, and then reradiating it at night when the temperature drops. In a colder or more temperate climate such as the UK, a passive solar design building with rammed earth walls should have the addition of insulation towards the outside face of the walls, or even in the form of exterior over cladding that incorporates insulation. This design allows the use of larger fenestration on the southern elevations to maximise solar gains, whilst the thermal mass of the walls absorbs and stores the heat generated inside the building. This can prevent overheating during the daytime, and can prevent the heat from simply escaping back through the windows at night. The exterior insulation keeps the warmth inside the building whilst still permitting the energy-saving benefits of the thermal mass walls to operate. A building design of this nature is normally complemented through the use of an energy efficient interior heating system and insulative window blinds, because the solar energy gains cannot always be relied upon in this climate.

The human body is often observed to be much healthier when it is warmed by absorbing radiant heat energy as opposed to being placed inside a ‘stuffy’ environment in which the air is artificially heated. This is most obvious in employees who work within an air-conditioned office and who frequently suffer from respiratory problems and tiredness due to the low humidity and lack of natural air ventilation. In a conventionally designed building with cavity insulation, significant decreases in efficiency are experienced when the heated air can leak out and escape through gaps in doors and windows etc. This is

because the air is used as a transfer medium for the heat energy, hence the term ‘paying to heat the draft’.

The walls of a thermal mass building are different because they effectively act like a giant storage heater producing radiant heat. Since they can absorb and make use of free solar energy, the occupiers can benefit from reduced heating bills. This also works in reverse to cool a building interior where the thermal mass walls can absorb excess heat. The combined effect of these properties is the aforementioned ‘thermal flywheel’ principle; the mass walls act as a buffer against changes in the outdoor climate and help to regulate the indoor climate at optimum comfort levels. This means that natural ventilation can potentially be utilised more effectively in thermal mass buildings because the air is not used as the energy transfer medium. In addition to acting like a thermal sponge, earth walls also regulate humidity inside a building by absorbing/desorbing moisture vapour in much the same way as with thermal energy. A healthy, comfortable living environment is perhaps the most renowned and noticeable characteristic of living in an earth building.

A1.2.6 What Happens when it Rains?

This is perhaps the most common question that is raised by the sceptic in relation to earth buildings. Throughout history, and even up to the present day, the stone-like properties and endurance qualities of rammed earth have been noted as one of its greatest attributes. Given the absence of mechanical damage it has long been recognised that water absorbed into porous building materials is the greatest threat to the durability of construction materials in the United Kingdom (Bryan, 1988). Rammed earth is porous, as are many masonry construction materials, and as such the absorption and

desorption of moisture and its subsequent movement lie at the root of a number of engineering problems in construction technology such as water penetration (Hall, 1977).

The main factor in the durability of an earth wall is the durability of the component elements themselves, and for this reason most building code requirements relate to tests on individual components or wall samples in isolation from their final position in the wall (Heathcote, 1995). In spite of the potentially high levels of durability rammed earth can achieve, its susceptibility to moisture-related issues are still perhaps its greatest weakness.

This area of concern is the focus of much current research where there is a fundamental question: how can we measure, predict & control the moisture ingress and moisture-related durability of earth materials? As our understanding increases it may be possible to determine and select optimum soil types and/or mix recipes in order to achieve the production of a highly durable, optimum-quality rammed earth product that is repeatable and that could lend itself to some degree of standardisation.

Many conventional tests that are used on other building materials have been adopted for soil construction without modification (Houben & Guillaud, 1996) and so the results obtained in a laboratory often represent earth materials unfairly and do not always agree with the observations made in building practice. The present methods of testing earth wall samples vary from country to country and are not based on the evaluation of field performance under a wide range of weather conditions (Heathcote, 1995).

APPENDIX 2 - CONSTRUCTION TECHNIQUES

A2.1 FORMWORK

A2.1.1 Gantry-Type Formwork

In North African countries such as Morocco the technique of rammed earth (or pisé) is still confined to rural areas and so mostly the traditional methods of formwork are still used (Mouyal D, 2003, *pers. comm.*). The most common arrangement that we see in traditional formwork is the gantry-type that uses thin timber planks as the side shutters supported at close centres (approx 650 to 700mm) by full height vertical posts. These posts are normally thick-sectioned timber that are anchored at the base and then tied at the tops using a tensile member to effectively construct a gantry arrangement. In its simplest form the tensile member can be a rope that prevents the shutters from spreading apart during compaction. Other more sophisticated variations of this method include the use of timber braces or threaded steel bars to brace the vertical posts. Modern day use of the gantry-type formwork continues and many more advanced and variant forms of the system have been observed to be in use by contractors in the USA and in Europe. The Chinese use a type of formwork that is based on the gantry system but instead of using sawn timber they use natural, stripped lumber poles for the side shutters giving the wall façade a unique, ribbed texture as shown in Figure 119.



Figure 119 traditional style of gantry-type formwork employed by the Chinese (Photo: courtesy C Frederick, 2002)

A2.1.2 Modern Proprietary Concrete Shuttering

Many of the modern rammed earth contractors in developed countries tend to use modular formwork that has often originated from the integrated systems developed by specialist manufacturers for the concrete industry. One such example of this generic, modular formwork is the interlocking modular panel system called U-form, marketed for hiring purposes in the UK by A-Plant Acrow.

The U-form 'modules' are strong and lightweight, and are available in a variety of sizes ranging from 600x600mm up to 2400x600mm. Through the use of special clips the panels are interlocking vertically and horizontally, and the shutter sides are retained through the use of snap ties. These are sacrificial steel ties that pass through the finished wall, and the protruding ends can simply be snapped off after construction of the wall.

The depth of the point at which the ties snap back inside the wall can be specified, e.g. 25mm, 40mm, or 50mm. Special U-form modules include 90° corner forms, ‘T’ junction forms, and column forms. The forms can even be arranged to construct a battered wall with a slope of up to 7°.

A2.1.3 Australian Formwork - Stabilform™

A similar design to the commonly-available modular formwork systems is the Australian style that has been patented by the Affiliated Stabilised Earth Group (asEg) as Stabilform™. Unlike most of the more traditional methods, this modern system does not progress in the horizontal direction where the first lift of rammed earth wall sections are completed the perimeter of the building, then the second lift etc. The Stabilform™ system, and its many variants, operate whereby the end boards are full height for a given wall section and the shutter sides are used to climb one on top of the other as they are filled and rammed. The walls are therefore constructed as a series of full-height rammed earth panels that interlock through a tongue & groove mechanism that is cast into the wall ends. The use of Stabilform can be seen in Figure 120 showing the construction of the stables in Northamptonshire by Earth Structures (Europe) Ltd, a member of asEg.



Figure 120 Stabilform™ being used by Earth Structures (Europe) Ltd. to construct the stables building in Northamptonshire (Photo: courtesy Maniatidis & Walker, 2003)

The advantage of progressing vertically and building each panel at a time is that the end boards can be set plumb and each lift of rammed earth is in line with the one below to give a perfectly aligned wall section. The climbing shutter sides are normally 600mm high and are used in a variety of different lengths such as 1500mm, 2400mm etc. The shutter sides are usually made from phenolic resin-coated plywood but some contractors are now using nylon shutters instead because it is more durable and will not chip like plywood. The side shutters interlock with a tongue & groove-type mechanism and are held flush to one another using scaffold poles in a similar manner to most propriety brands of concrete formwork, e.g. Acrow U-form. Standard form ties are used in the form of 2@ roll-threaded steel bars at the top and bottom of each formwork section

spaced at approximately 600mm centres. Special adaptations of this formwork can enable the creation of corners and T-sections.

A2.1.4 REW Formwork

David Easton is the owner of the contractor firm Rammed Earth Works based in Napa, California (USA) and through experience has devised the unique system of REW formwork. As with U-form and Stabilform it is a programmable, modular system but that uses standard sized plywood sheets for the side shutters. As a result of this the formwork modules are based on units of 2440mm (8') long by 1220mm (4') high when the sheets are oriented horizontally, and so a standard wall height of 2.4 metres is achieved in just two lifts of formwork. The higher priced special-order sizes of ply, such as 3000mm (10') x 1220mm (4'), can be used for increased productivity on longer wall sections.

As with the Australian system (Stabilform), REW formwork is mostly used to progress vertically with full-height end boards and produce interlocking wall panels. The form ties are horizontally spaced at centres of up to 2.4 metres because the side shutters are stiffened by extra wide walers of 50 x 250mm (2x10") rough sawn planks. This allows much more room inside the formwork for trade's people to operate, and for the placement of services and/or steel reinforcement. Special adaptations of this formwork can enable the creation of corners and T-sections. Alternatively the ply sheets can be oriented vertically and stiffened with 50x100mm (2x4") stud work such that the forms can interlock and create continuous, eaves height formwork for the entire building. This necessitates the use of more timber and extra long rammers but can be cost effective where site access is limited or where a fast-track build programme is required.

A variation of REW formwork was devised by the author for the Brimington bowls pavilion project in Chesterfield. This enabled the formwork and ramming teams to operate simultaneously such that the 24-hour challenge for constructing a building could be met. Full sheets of 3000x1220mm and 2440x1220mm 19mm thick sheathing plywood were oriented horizontally for the side shutters, with 225x75mm wide whalers. The end boards were full height 19mm plywood with 40x100mm stiffening battens attached to the rear face. The whalers rest on top of the tie bars and the end boards are shimmed with hardwood wedges against the tie bars to set for plumb (see Figure 121).



Figure 121 the modified REW formwork that was used on the 24-hour challenge build for the Brimington bowls pavilion (Photo: courtesy M. Heseltine ©2003)

This design enabled the form setters to work their way around the perimeter of the building erecting the first lift (1220mm high) of shuttering, whilst they were being followed by the ramming teams who began to fill the forms as soon as they were ready.

By the time the first forms had been filled the second lift of shuttering was already being erected and the ramming teams began to chase the form setters around the building perimeter once more. This fast-track system enabled the first ramming team to start work within 30 minutes of the form setters beginning their task. This method of formwork design was effective during the 24-hour challenge build and may be suited to future fast-track construction schemes as it was easily capable of keeping up with the mixing & ramming production rate of approximately 1.16m³/hour that was achieved on the day.

A2.2 MIXING AND BLENDING

The soil should be thoroughly dry mixed before use to ensure good consistency of the specified particle-size distribution within the mix. This is essential for quality control of the finished product and to produce the required strength and durability of the wall. Storage and mixing of the soil normally takes place on the ground due to the large volume of material under consideration. The mixing area should be free from litter and any other foreign material that may accidentally be picked up and incorporated into the mix.

A2.2.1 Mixing Techniques

Mixing with a shovel is still the most common method in poorer countries, and sometimes this is done on a tarpaulin so that the entire mix can be turned over to ensure thorough consistency. This method is generally acceptable where labour is plentiful and cheap, and where time constraints are not quite so competitive. Mechanical mixing techniques are used almost without exception in modern rammed earth construction to

increase the speed, volume and consistency of the mixing operations. In the western world, mechanisation of the mixing process is an absolute must in order to make it commercially competitive.

In Australia a very common technique is to use a skid steer loader (e.g. Bobcat or similar) to mix the soil. The bobcat operator drives the machine very fast into the loose pile of soil and takes a scoop of the material. This is then tipped and scraped a few times using the front bucket in order to thoroughly mix the soil. Any cement, chemical admixtures or additional water is usually added at this stage. This mixing technique requires a skilled machine operator. It can be very quick and normally minimises the required amount of manual labour for the mixing process. It is a technique that is well suited for mixing a dry, loose material such as quarry waste but would be unsuitable for a cohesive or sticky mix as it is not a particularly thorough methodology. The main advantage to this technique is the speed & manoeuvrability of the skid steer loader. This machine is often the favoured method of delivering the mixed soil to the formwork, as was the case during the Brimington bowls pavilion project (see Figure 122)



Figure 122 skid steer loader delivering a fresh mix of rammed earth to the formwork on the Brimington bowls pavilion project (Photo: courtesy Brimington Bowls Club 2003)

The forced-action paddle mixer (or screed mixer) is another favourite of some rammed earth contractors because it gives exceptional mix quality and consistency for all types of soil, whether they are cohesive or granular. The main disadvantages to this type of equipment are that it is quite slow, expensive to buy, and it cannot easily be manoeuvred on site. It is possible to hire plant such as this but in Britain they are relatively difficult to obtain and the typical cost of hire is quite high. They tend to be specialist mixing machines that are used by screeding contractors and tend not to produce very large volumes of material for each mix batch. A typical example of a forced action paddle mixer is shown in Figure 123, although much larger versions are also available.



Figure 123 typical forced action paddle mixer (Photo: courtesy Refina Ltd. ©2003)

The garden/field cultivator is a very fast, cheap alternative to the two methods described above and can be used in conjunction with the Bobcat method. Petrol/diesel engine cultivators, often described by the trade name Rotavator, are very thorough at mixing soil as they are designed to produce a tilth that is suitable for sowing seeds. They can be used either as a hand driven machine in their own right, or as a larger tractor-mounted version connected to the engine through a power take-off (PTO) connection on the gearbox. The Rotavator appears to be the preferred mixing method of the contractor Rammed Earth Works, who have experimented with numerous techniques including concrete batch plants, tractor buckets and numerous other devices. A 1m wide tractor mounted tiller, as shown in Figure 124, can be a good choice for the rapid, thorough mixing large amounts of earth.



Figure 124 tractor-mounted tillers can mix large amounts of rammed earth soil very quickly (Photo: courtesy J Tingle ©2003)

A large, hand-operated diesel Rotavator is also very quick and is more manoeuvrable in smaller spaces than a tractor mixer. It mixes more thoroughly than the tractor and so is more suited to cohesive/sticky mixes but can only be used effectively on much smaller batch sizes. It can be more labour intensive and tiring to use than the tractor so fatigue can easily become a factor. Figure 125 illustrates how a hand operated Rotavator can be used for rammed earth mix batches.



Figure 125 small, rapid batch mixing with a diesel-engine Rotavator

A2.2.2 Compaction

The tools that are used for dynamically compacting rammed earth are usually either hand rammers, pneumatic ramming equipment powered by an air compressor, or a combination of the two. Some European contractors prefer to use vibrating plates although these are not capable of achieving the same level of compacted density as a rammer. Martin Rauch, from the Austrian Lehm-Ton-Erde rammed earth contractor company, has also used a sheep's foot roller compactor with apparent levels of success (Kapfinger, 2001).

Hand ramming is the traditional method for producing rammed earth and it is estimated that around 99% of all rammed earth buildings across the world were built by hand ramming (Easton, 1996_a). Hand ramming the earth is slow and tedious, but it is extremely cheap and requires very few skills to operate. Pneumatic rammers are several

times quicker than hand rammers but are more expensive and require regular maintenance and skilled labour to operate.

A2.2.2.1 Hand Rammers

Typically these consist of a head and a handle, and are generally available in a variety of different materials and different shapes and sizes. The handle is usually between 1.5m and 1.8m in length and may be either metal or wooden. Metal handles, if hollow, can be filled with varying amounts of sand to modify the weight and therefore the compaction potential of the rammer, depending upon the size of the operator (Keable, 1996). Keable suggests that the entire rammer should weigh ideally between 5 and 10 kg and should be dropped from a height of around 300mm with 'moderate' force. The head should typically be square with dimensions of between 80 and 120 mm per side. According to NZS 4298 the rammer should have a steel head and the total rammer weight should be 6.5 kg (Standards New Zealand, 1998).

A2.2.2.2 Pneumatic Rammers

These are made by a variety of manufacturers and are driven by compressed air. The ramming face is usually circular and varies between 75 and 150mm in diameter. These devices have the advantage of reducing the amount of labour input needed and significantly increasing the rate of production, as can be appreciated from the images in Figure 126.



Figure 126 high-production pneumatic ramming on the Brimington bowls pavilion project (photo: courtesy M Heseltine ©2003)

The pneumatic rammer is quite different from a pneumatic tamper that uses a short, vibration-like stroke to compress loose material in narrow spaces. The preferred device is essentially a sand rammer of the kind formerly used in foundries to compress sand into moulds for casting metal. Examples of these types of rammers include the Ingersol-Rand 316L (popular in Australia), MacDonald T5 (now obsolete), Atlas Copco RAM35a, RAM30 (now obsolete), RAM20, and the Jet sand rammer. They are normally identified by their long stroke and their rapid piston-like ‘lift & drop’ ramming effort.

The author’s Atlas Copco RAM30, for example, has a 150mm diameter steel ramming head and rams with a 350mm stroke at a frequency of approximately 4 hits per second. This is ideal for rapid compaction of rammed earth material because the long stroke is very efficient at forcing the air out of the loose soil and achieving maximum density (at optimum moisture content) in a short space of time. A short-stroke (approx. $\leq 150\text{mm}$),

high frequency tamper, for example, is typically only capable of achieving a maximum dry density of around 1850 kg/m^3 (e.g. Trelawny pole scabbler with ramming attachment) compared to the 2250 kg/m^3 that is easily achievable using the Atlas Copco RAM30 sand rammer.

It has been reported that the effectiveness of pneumatic ramming, in terms of its ability to compact the soil, is actually no greater than that of thorough hand ramming (Easton, 1996_b). The real advantage of pneumatic ramming is in its ability to make rammed earth commercially competitive with conventional masonry materials in terms of production speed and project costs.

A2.2.2.3 Form Filling

When soil is being placed inside the formwork it should be carefully placed with a shovel in even layers that have an un-compacted thickness of between 100mm and 150mm. Following ramming/compaction, this layer will compress to a thickness of approximately 50-70mm (Keable, 1996) depending upon soil type. The earth should be systematically rammed starting from one end and by constantly moving the rammer in a circular motion such that an even compactive effort is applied. Some rammed earth builders prefer to ram along the perimeter of the forms first followed by a pass down the middle, and then repeat the procedure (Easton, 1996_a). Once the entire layer has been properly compacted the rammer should produce a 'ringing' sound and cause the formwork to reverberate as the force is transmitted through the dense wall mass and into the side shutters. The next 100-150mm layer is then shovelled in on top of the compacted layer and the process continues.

The shuttering can actually be removed as soon as the compaction is finished. During this process the side shutters must be slid away from the wall as opposed to being pulled away from them. This is to break any suction between the moist wall face and the shutters, and it avoids soil being pulled out of the wall face leaving unsightly cavities in the finished façade. It is often better practice to leave the formwork in place for approximately 12 to 24 hours to allow the wall to gain a little strength; both from a safety perspective and to reduce the risk of damage to ‘green’ walls that are still soft. This practice is recommended in the current Australian Code of Practice for earth construction (Walker & Standards Australia, 2002).

If dry, untreated ply wood is used then the recommended initial curing time (12 – 24 hours) can allow the wood to absorb moisture from the walls and the side shutters are much easier to remove with less chance of pull out (Dobson, 2002). This is good practice on soils that are prone to sticking, although it can also give very good results for all types of soils and the cost of 19mm sheathing ply wood is relatively cheap at around £15-00 per 2440x1220mm sheet). Since rammed earth is a ‘dry’ trade, when compared to concrete, the formwork only requires brushing before it is fully reusable. It is possible to use phenolic-faced ply (i.e. the type used for architectural concrete shuttering) but this requires the application of a releasing agent, e.g. Castrol form oil. This can give a very smooth glass-like finish to some rammed earth soils but the risk of pull out is increased on cohesive soils. Oiled forms can sometimes be harder to work with (and in) because the oil is slippery and can attract dirt. The phenolic-faced 19mm plywood is very durable and weather resistant but expensive at around £40-00 per 2440x1220mm sheet.

A2.2.3 Lintels, Wall Plates and Fixings

Conventional lintels can be incorporated in rammed earth walls in much the same way as with any mass-construction masonry wall. Lintels can be made from reinforced concrete (in-situ or pre-cast), steel, timber, or as a continuous bond beam/wall plate. A 300mm minimum bearing depth is required in order to eliminate the possibility of shear failure in the wall edges, and the lintel width should be the same as the wall width, i.e. 300mm (Hall, Damms & Djerbib, 2004). For the Brimington Bowls Pavilion project a 150x150 timber wall plate was specified in order to minimise the requirements of lintels in the construction and to speed up the build process.

The wall plate was anchored to the inner face of the rammed earth wall and braced in accordance with Appendix B of BS 5268 Part 3 of the timber design code (Hall, Damms & Djerbib, 2004). The fastening was achieved by using steel wall ties fixed onto the rammed earth using standard masonry nails, although it is also possible to use either chemical or expanding-head through bolts anchored straight through the top of the wall. A cross-sectional wall detail at eaves level from the Brimington Bowls Pavilion is illustrated in Figure 127, which demonstrates a method of lintel and wall plate design that conforms with the Building Regulations (2000) Part A: Structural Stability (Hall, Damms & Djerbib, 2004).

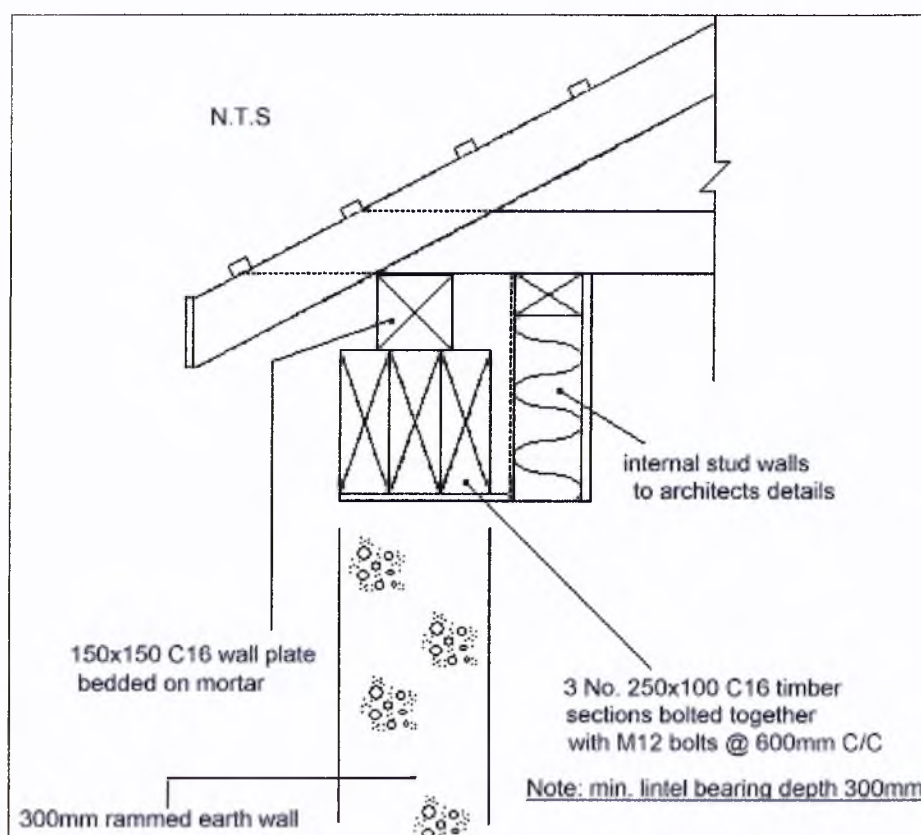


Figure 127 construction detail for the lintel and wallplate of the Brimington bowls pavilion (Drawing: courtesy Hall, Damms & Djerbib, 2004)

Fixing positive to rammed earth walls is possible, for example, using epoxy resins and threaded steel bars. This technique allows heavy items, such as floors in a two-storey building, to simply be bolted to the walls (asEg, 2002). Units such as door frames and window frames can be anchored to the wall using standard plastic wall plugs (e.g. Rawl plugs) or expanding-head impact fasteners (e.g. Fisher fixings). A properly constructed rammed earth wall can be drilled using hammer action drills equipped with standard masonry drill bits. Alternatively, it is possible to cast (or ram) carefully positioned timber elements inside the rammed earth walls to act as an anchor point for fastening shelves and pictures.

The steel channel used to support a veranda on the west elevation of the Brimington Bowling pavilion was secured to the rammed earth walls using 'Chem-fix' epoxy resin bolts. The channel was drilled in place and the rammed earth walls were then drilled using a masonry bit. The epoxy resin bolts were then fixed into the wall as shown in Figure 128.

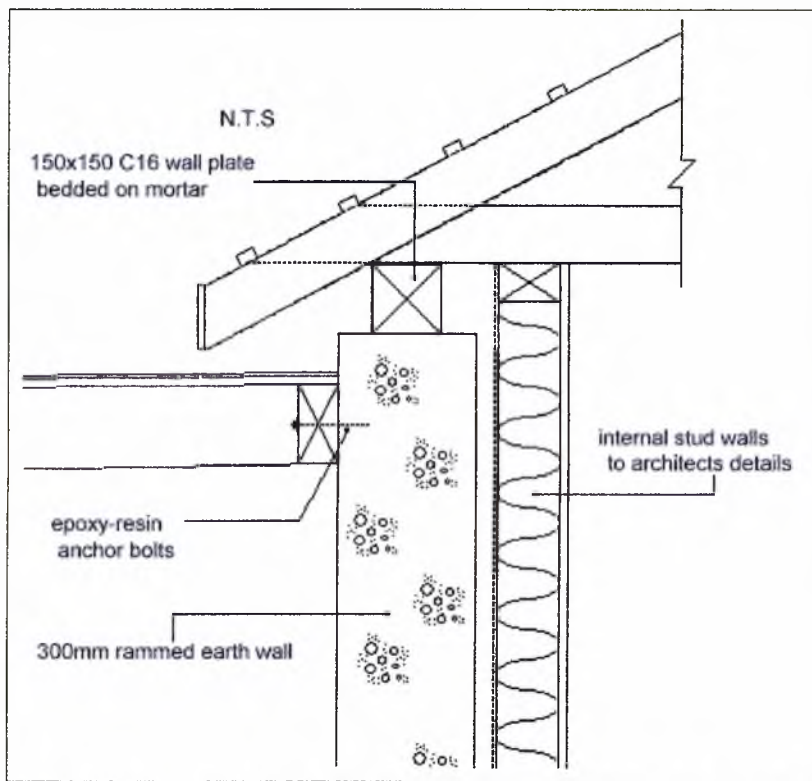


Figure 128 construction detail for horizontal positive fixing of veranda

APPENDIX 3: CUBE SAMPLES GALLERY

The following pictures are taken of unstabilised rammed earth cube samples made from different mix recipes. The number on the cube sample refers to the mix recipe (e.g. 532) and the letter simply corresponds to the sample ID that can range from A to P. Note that the surface finish and porosity of the material visibly alters between different mix recipes.







